12-2014

AN INTEGRATED SYSTEMS ENGINEERING METHODOLOGY FOR DESIGN OF VEHICLE HANDLING DYNAMICS

Mandar Hazare
Clemson University, mhazare@clemson.edu

AN INTEGRATED SYSTEMS ENGINEERING METHODOLOGY FOR DESIGN OF VEHICLE HANDLING DYNAMICS

A Dissertation
Presented to
the Graduate School of
Clemson University

In Partial Fulfillment
of the Requirements for the Degree
Doctor of Philosophy
Automotive Engineering

---

by
Mandar A Hazare
December 2014

Accepted by:
Dr. P. Venhovens, Committee Chair
Dr. E. Law
Dr. T. Rhyne
Dr. I. Haque

ABSTRACT

The primary objective of this research is to develop an integrated system engineering methodology for the conceptual design of vehicle handling dynamics early on in the product development process. A systems engineering-based simulation framework is developed that connects subjective, customer-relevant handling expectations and manufacturers' brand attributes to higher-level objective vehicle engineering targets and consequently breaks these targets down into subsystem-level requirements and component-level design specifications. Such an integrated systems engineering approach will guide the engineering development process and provide insight into the compromises involved in the vehicle-handling layout, ultimately saving product development time and costs and helping to achieve a higher level of product maturity early on in the design phase.

The proposed simulation-based design methodology for the conceptual design of vehicle handling characteristics is implemented using decomposition-based Analytical Target Cascading (ATC) techniques and evolutionary, multi-objective optimization algorithms coupled within the systems engineering framework. The framework is utilized in a two-layer optimization schedule. The first layer is used to derive subsystem-level requirements from overall vehicle-level targets. These subsystem-level requirements are passed on as targets to the second layer of optimization, and the second layer derives component-level specifications from the subsystem-level requirements obtained from the first step. The second layer optimization utilizes component-level design variables and

analysis models to minimize the difference between the targets transferred from the vehicle level and responses generated from the component-level analysis. An iterative loop is set up with an objective to minimize the target/response consistency constraints (i.e., the targets at the vehicle level are constantly rebalanced to achieve a consistent and feasible solution). Genetic Algorithms (GAs) are used at each layer of the framework.

This work has contributed towards development of a unique approach to integrate market research into the vehicle handling design process. The framework developed for this dissertation uses Original Equipment Manufacturer's (OEM's) brand essence information derived from market research for the derivation and balancing of vehicle-level targets, and guides the chassis design direction using relative brand attribute weights.

Other contributions from this research include development of empirical relationships between key customer-relevant vehicle handling attributes selected from market survey and the various scenarios and objective metrics of vehicle handling, development of a goal programming based approach for the selection of the best solution from a set of Pareto-optimal solutions obtained from genetic algorithms and development of *Vehicle Handling Bandwidth Diagrams.*

DEDICATION

I would like to dedicate this dissertation to my parents, Arun and Chanda Hazare, and my sister, Shraddha Hazare. This research could not have been possible without their love, support, and patience. The many sacrifices they made to allow me to pursue this degree will be forever appreciated.

ACKNOWLEDGMENTS

I would like to express my immense gratitude to my doctoral advisor, Dr. Paul Venhovens, for his advice and support throughout my research. Dr. Venhovens has been an inspirational mentor, and his technical expertise and inputs were invaluable for this research. During my tenure as a doctoral student, Dr. Venhovens provided me with several opportunities to get involved in state-of-the-art vehicle dynamics projects and present my research findings at different conferences across the globe. His guidance and support has undoubtedly contributed to both my personal and professional development.

I would also like to acknowledge Dr. Law for his support during the initial phases of my research here at Clemson University. Dr. Law's course on Vehicle Dynamics laid the foundations of knowledge on which this work is based. I have always enjoyed the discussions we had, and I sincerely appreciate his mentoring during the beginning of my career as a graduate student.

I am very grateful to my committee members, Drs. Imtiaz Haque and Timothy Rhyne, for their review of and input on my research. The time that each of the committee members provided to meet and review the research proposal, dissertation, and defense is greatly appreciated.

TABLE OF CONTENTS

Table of Contents (Continued)

Page

LIST OF TABLES

Table Page

List of Tables (Continued)

Tables Page

LIST OF FIGURES

Figure Page

List of Figures (Continued)

Figure Page

List of Figures (Continued)

Figure Page

List of Figures (Continued)

Figure Page

List of Figures (Continued)

Figure Page

List of Figures (Continued)

Figure Page

CHAPTER ONE

INTRODUCTION

The lifecycle of a typical vehicle development project can be described by four key phases—namely, *Strategy Determination*, *Vehicle Definition*, *Concept Development* and *Series Development*—as shown in Figure 1. The strategy phase is characterized by market analyses, determination of opportunities, product-planning resulting into decisions on which vehicles to bring into the market within a 5-7 year time frame with predetermined unique selling propositions. The decisions in the strategy phase are driven by both internal brand specific considerations and external factors such as market developments, economic situations and mega, meso and macro trends. In the definition phase, the project's target vision and business objectives are aligned and finalized, the technical and the economic feasibility of the project is evaluated, higher-level, architecture-based decisions are made, and targets are defined. These targets are defined considering the *voice of the customers*, *voice of the company* and *voice of the legislators*.

The definition phase is followed by the concept development phase (involving on average 50-200 engineers), where engineers and designers work together to formulate concepts that can meet the higher-level targets set in the definition phase. An important milestone, *target agreement*, marks the end of the concept development phase. Once all the targets are finalized and agreed upon between the different teams (i.e., chassis, powertrain, packaging, etc.), the series development phase begins. In the series development phase, elaborate design, build and test procedures are applied (involving on

average 500-1,000 engineers) per vehicle project to realize and manufacture the finalized concept. A typical vehicle development project cycle (from strategy to start-of-production) takes around 60 months.

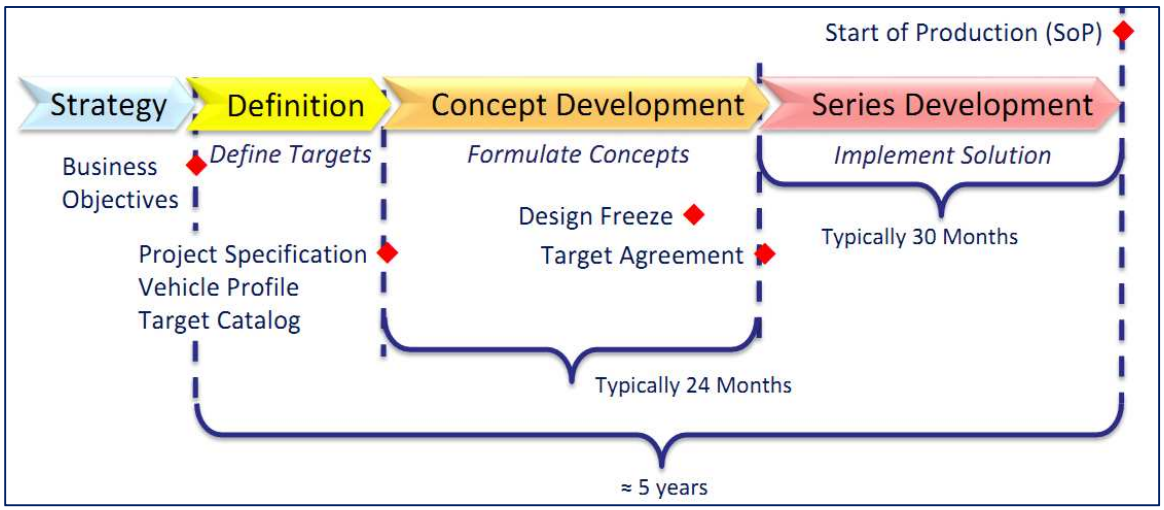

Figure 1. Typical Lifecycle for a Vehicle Development Process [1].

The concept development phase is often regarded as the most creative and the most challenging part of the vehicle development process. Design freedom is at its maximum at the beginning of the concept phase, which gives the engineers and designers the opportunity to develop the most innovative concepts. The concepts, ideas, and changes implemented during this phase can be managed much more economically with fewer resources than changes implemented later during the series development program where the design degree of freedom is limited and product changes are costly. Therefor it is desirable to increase product maturity early on in the concept development phase for cost and project timing reasons. Furthermore, automotive manufacturers aim to reduce the overall duration of the concept (and series) development phase to keep up with the

ever-changing market and customer needs and expectations. Figure 2 shows the interrelationships between design freedom, design maturity, and development cost during the concept design phase.

Some of the key challenges faced by the automotive manufacturers during the concept development phase are:

- Several vehicle functions (such as fuel economy, ride, handling, acoustics, safety, etc.) are competing with each other in terms of functional performance, cost, weight, and design space. Balancing the trade-offs in alignment with the brand identity and customer expectations needs to be carried out systematically during the entire concept development phase up until the target agreement milestone.
- In general, the automotive industry lacks systematic conceptual design tools and methods that can assist the development and quantification of vehicle-level targets and support the process of decision-making and trade-off management.
- Traditionally, these phases often rely on “trial-and-error” or “test-and-tune” methods and may use extensive physical testing of design prototypes, which is time consuming and expensive.
- The factors described above may cause low initial product maturity in the conceptual design phase and may result in expensive changes implemented later in the series product development phase if not all trade-offs were understood or resolved.

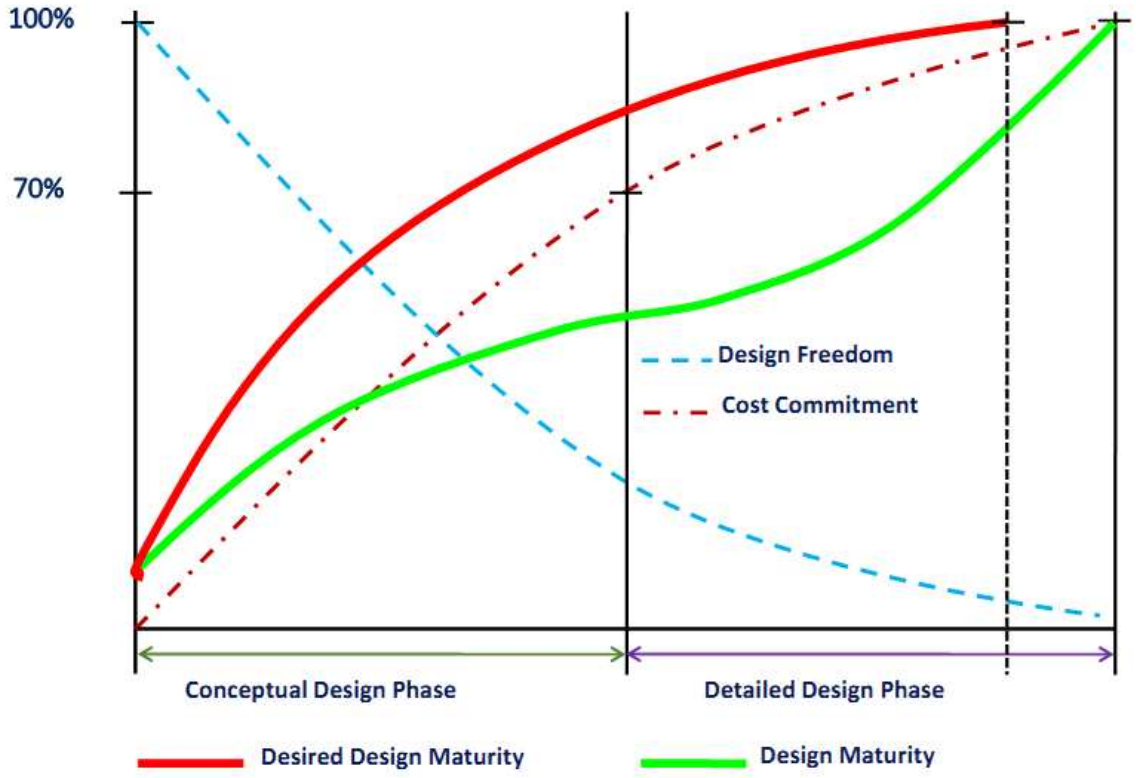

Figure 2. Traditional Vehicle Design Process Challenges [2].

The overall focus of this thesis is to develop processes, methodologies, and tools that can support conceptual engineering during the early vehicle development phase with objectives to:

- Reduce concept development time,
- Increase early design maturity,
- Resolve trade-offs and balance solutions in a systematic manner, and
- Save time, money, and personnel resources.

In the early stage of the definition phase, high-level vehicle attributes can be depicted by means of a so-called vehicle specific DNA spider/radar diagram, as shown in

Figure 3. It allows for a visual representation of important vehicle attributes and also show the relative importance of the attributes (higher importance is outwards on the spider diagram). In this thesis, vehicle handling, one of the key aspect of the overall vehicle DNA is researched in its totality.

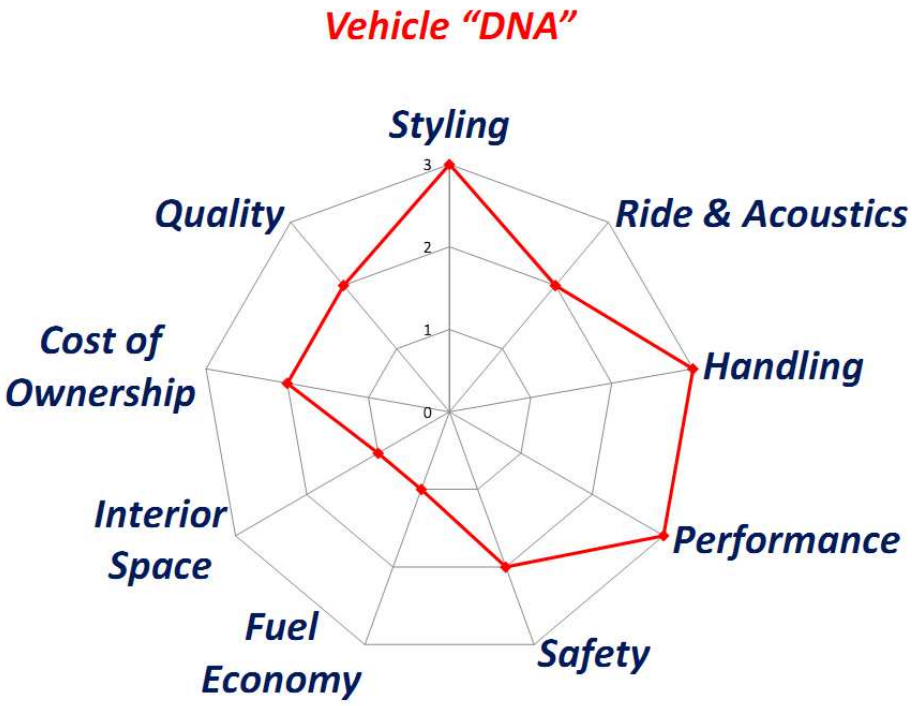

Figure 3. Spider Diagram of typical Customer Relevant Vehicle Attributes.

1.1 Motivation

The handling characteristics of road vehicles are one of the important attributes that define a major part of the vehicle's unique selling propositions (USPs). For vehicle manufacturers with a specific focus on driving dynamics offering an exceptional or enjoyable driving experience, on-road vehicle handling is an important attribute of the strategic brand "DNA". Vehicle handling can be broadly defined as the interaction between driver, vehicle, and environment, which takes place during the transportation of peoples and goods [3]. It is an indicator of the driver's ease of controlling a vehicle's chassis motions.

The domain of vehicle handling engineering focuses on the development and application of methods to qualify and quantify the directional behavior of the chassis during different driving maneuvers. The study of handling dynamics involves understanding the controllability and stability of the vehicle and is closely associated with the driver's subjective perception of the interactions with the vehicle. The engineering process of tuning the vehicle's handling dynamics is a challenging task due to the multitude of competing design requirements and parameters. Some of the key challenges involved in the process are:

- It is difficult to capture and understand the voice of the customer (i.e., interpret the driver's expectations/perception of the vehicle's handling behavior) and translate these expectations into meaningful objective metrics to be used in the vehicle product development process.

- It is challenging to find a unified chassis setup that meets the expectations of various segments of drivers interested in the same vehicle. Drivers of different age group, such as young enthusiast and aging drivers, might have different expectations regarding handling behavior for one-and-the-same vehicles.
- Different aspects of vehicle handling—such as steady-state handling, transient handling, straight-line stability, parking, and emergency handling—are often in conflict with one another.
- The vehicle's handling properties by themselves as part of the overall band essence (Figure 3), are often in conflict with competing properties, such as ride comfort, acoustic comfort, or passive safety.
- Trial-and-error approaches to find the best compromise can lead to suboptimal solutions, resulting in increased product cost and weight and the prolongation of product development time.

To address the challenges above, it is important to establish a transparent and systematic approach towards handling dynamics design ensuring that the final product meets customer expectations and cost, weight and design space targets. Most vehicle manufacturers follow their own set of unique, proprietary methods to design the vehicle's handling characteristics. Current best practice design methods are characterized by:

- Benchmarking competitor vehicles to develop vehicle-level targets and component design specifications. Competitive benchmarking can lead to products with performance levels that exceed customer expectations and may lead to

unnecessary engineering effort, higher product costs and/or weight, and potentially product performance that might not be perceived by the end-user (strategic overkill).

- Relying heavily on the application of physical prototypes during the initial development phase. Early-stage vehicle prototypes are very expensive, not infinitely tunable (such as the setup of static and dynamic body-in-white stiffness), and frequently of insufficient build quality to address competing vehicle properties such as acoustics.
- Focusing on physical testing of prototypes. Repetitive physical testing can be time-consuming and costly.
- Practicing “trial-and-error” and “test-and-tune” philosophies, which can be time-consuming if not supported by sufficient system behavior knowledge. This approach can also lead to an oversight of conflicting design objectives, resulting in a sub-optimal final setup.
- Implementation of expensive design changes later on in the vehicle development process, especially if the interaction with and dependency of the handling on other vehicle properties and design parameters is not properly understood.

1.2 Research Questions and Hypotheses

The following research questions and hypotheses are posed based the challenges associated with the conceptual design of vehicle handling early on in the product development process:

Q1: What is the best strategy to effectively address the challenges associated with the systematic design of vehicle handling characteristics connecting/balancing end-user expectation with component-level design specifications during the concept development phase?

H1: A systems engineering approach implemented using a simulation-based framework can be used to address the challenges associated with the conceptual design of vehicle handling characteristics. A systems engineering approach will provide a comprehensive, multi-level, step-by-step, and top-down methodology that will link customer expectations to the final chassis components' specifications and the validation of recommended design configurations.

Q2: What is the best strategy to ensure that the manufacturers' brand attributes are considered and are used as differentiating factors during the concept development phase?

H2: A systems engineering based framework which can accept inputs from market research at the beginning of the product development process can be a very effective strategy. Market research specifically aimed towards understanding end-user preferences

and expectations can give valuable insights regarding manufacturer's brand essence. Such market research can help understand customer's perception of a particular brand in comparison to the other brands and can provide unique ways to emphasize certain attributes or support trading off between different conflicting attributes. An intelligent systems engineering based framework should be able accept inputs from such market research and use this information for creation of vehicle-level targets, and as a trade-off strategy during the decision-making process.

Q3: What is the best strategy to accelerate the vehicle handling dynamics design process during the concept development phase?

H3: A simulation-based framework based on a hybrid set of lower-order parametric models (i.e., physics-based, knowledge-based, or surrogate) can be used to accelerate the vehicle handling dynamics design process. Computationally efficient models with appropriate levels of accuracy can be used to effectively connect, evaluate and optimize vehicle, sub-system, and component-level targets. Multiple design iterations of the vehicle concepts can be efficiently evaluated using a simulation-based approach.

Q4: What is the best strategy to efficiently resolve trade-offs and balance competing vehicle handling requirements?

H4: The interaction between various conflicting requirements and scenarios of vehicle handling can be best balanced using a simulation-based optimization framework with easy-to-characterize, computationally inexpensive, and transparent vehicle handling and

chassis design models. These models should be able to capture the various aspects of vehicle handling with reasonable accuracy and allow for interaction and integration with common parameters in a common development environment for the most common driving scenarios. These models can then be linked to each other through a multi-objective and multi-scenario optimization scheme. The use of stochastic optimization algorithms coupled with design-of-experiments and sensitivity analyses can help engineers better understand the trade-offs and compromises involved in the chassis design process and will help in the final design selection procedure.

Q5: What is the best strategy to implement the systems engineering approach during the concept development phase to ensure a consistent and concurrent chassis design solution?

H5: A system engineering approach for the conceptual design of vehicle handling characteristics can be best implemented using a combination of a simulation-based, multi-objective optimization framework and decomposition-based, Analytical Target Cascading (ATC) techniques [4]. ATC is an effective hierarchical, multi-level, and optimization-based design technique. It applies a decomposition approach in which the overall system is split into several subsystems, which are then solved independently and coordinated via target and response consistency constraints [5].

1.3 Research Objective

The primary objective of this research is to develop an integrated system engineering methodology for the conceptual design of vehicle handling dynamics early on in the product development process. A systems engineering-based simulation framework is developed that connects subjective, customer-relevant handling expectations and manufacturers' brand attributes to higher-level objective vehicle engineering targets and consequently breaks these targets down into subsystem-level requirements and component-level design specifications. Such an integrated systems engineering approach will guide the engineering development process and provide insight into the compromises involved in the vehicle-handling layout, ultimately saving product development time and costs and helping to achieve a higher level of product maturity early on in the design phase.

The proposed simulation-based design methodology for the conceptual design of vehicle handling characteristics is developed using decomposition-based Analytical Target Cascading (ATC) [4, 5] techniques and evolutionary, multi-objective optimization algorithms [6] coupled within the systems engineering framework.

1.4 Organization of the Thesis

A brief overview of the subsequent chapters of this thesis is provided in this section.

In Chapter Two, a general overview of the existing literature in the area of vehicle handling design is presented. The literature review covers two fundamental aspects related to the development of a systematic handling design methodology. The first aspect deals with derivation of vehicle handling targets using drivers' expectations, preferences, and requirements, and the second aspect deals with the methods that derive vehicles' sub-system-level requirements and component-level design specifications to meet desired vehicle handling targets. The literature review is followed by a research gap analysis to identify the opportunities/gaps in the area of vehicle handling design.

In Chapter Three, the fundamental principles of systems engineering are discussed and the theoretical framework of the proposed handling design methodology is presented. A systematic five step systems engineering based methodology for design of vehicle handling characteristics is described in details.

Chapter Four presents the implementation details of the proposed vehicle handling design methodology. This chapter describes the key building blocks required for successful implementation. The building blocks include description of a method to integrate market research into the vehicle handling design process, development of empirical relationships between customer relevant handling attributes and handling

objective metrics, description of the vehicle handling models, and development of the ATC based optimization framework.

Chapter Five describes six different case studies demonstrating the applications of the proposed handling design methodology for systematically designing the vehicle handling characteristics. Finally, Chapter Six summarizes the conclusions and contributions from this research, and discusses future research topics and directions.

CHAPTER TWO

BACKGROUND

In this chapter, a general overview of the existing literature in the area of vehicle handling design is presented. The literature review is followed by a research gap analysis to identify the opportunities/gaps in the area of vehicle handling design.

2.1 Literature Review

The roots of vehicle handling design theory can be traced to the mid-1950s, when the first comprehensive understanding of both the theory and practice of the automobile's linear handling response was introduced [3]. Since that time, the field of vehicle handling dynamics design has greatly developed, with a plethora of research activities in almost all areas of vehicle handling, including: the explanation of non-linear limit handling behavior, use of computer simulations, complex multi-body models, specialized handling measurement devices, vehicle characterization test rigs, application of active control systems, etc. It should be noted that even with these significant advances in the field of vehicle handling and the objectification of handling characteristics, subjective vehicle testing by trained test drivers still dominates the final chassis setup and sign-off process.

It is important to have a well-defined systematic methodology regarding the design of vehicle handling characteristics. The two fundamental aspects for developing this systematic methodology are:

1. Methods that derive vehicle handling targets using drivers' expectations, preferences, and requirements (i.e., understanding the voice of the customer) and

2. Methods that derive vehicles' sub-system-level requirements and component-level design specifications to meet desired vehicle handling targets.

Methods to derive vehicle handling targets based on driver's expectations, preferences, and requirements.

One of the most important challenges in the product development associated with vehicle handling is the derivation of quantifiable vehicle handling targets using drivers' preferences of vehicle handling. There are two fundamentally different directions that current vehicle manufacturers follow in this respect:

1. *Testing of physical vehicles using highly trained professional test engineers to derive targets*. This approach requires the development of objective handling metrics and conducting correlation analyses between subjective evaluation and objective measurement of vehicle handling attributes.

2. *Simulation based analyses to derive targets*. This approach relies on simulation-based methods and requires synthesized vehicle dynamics and driver models to predict and evaluate the model-based driver's perception of vehicle handling quality.

The first approach relies heavily on the physical testing of vehicles using highly trained test engineers. The subjective test driver's feedback is used as the principal source

to assess vehicle-handling quality and fine-tune the chassis setup. Vehicle testing can be conducted either in an open-loop or closed-loop manner. Open-loop testing aims at accurately quantifying the vehicle's response through repeatability (such as a step-steer test maneuver, or J-turn, at a given speed of travel and with a fixed or predetermined steering wheel input). The subjective assessment of the vehicle's behavior by the test driver is then correlated to the vehicle's measured responses, using data acquisition systems. Bergman [7, 8] used subjective ratings to evaluate vehicle response during a step-steer maneuver. He found that subjective ratings during a step-steer maneuver could be correlated to a vehicle's yaw velocity gain and TB value (where TB value is defined as the product of yaw rate peak response time and steady-state side-slip angle). He identified a relationship between subjective rating and vehicle response through the following equation:

$$Y = 5.056 - 3.28*(X1) + 94.3*(X2) - 229.6*(X2)^2 \quad (1)$$

where: X1 = TB value, X2 = Yaw velocity gain, Y = Subjective rating.

Studies of a similar nature exist in the literature (Weir and DiMarco [9], Mimuro [10], King and Crolla [11], Xia [12], Chen [13]). These studies focus on the development of relationships between vehicle response metrics from open-loop test maneuvers and subjective assessments by expert test drivers.

An alternative method of assessing the vehicle's response is by testing it during closed-loop handling maneuvers. Closed-loop maneuvers, also referred to as task performance tests, are used to quantify driver-vehicle interaction during task specific maneuvers that require the driver to follow a pre-defined driving course, such as double-lane change or slalom. The performance metric here is the speed at which the driver can negotiate the course without any tracking errors. These tests can quantify a driver's response performing the task and thus give a good understanding of driver-vehicle interaction. The biggest challenge with closed-loop testing is that the driver cannot be directly separated from the vehicle in terms of performance assessment. Hence, it becomes difficult to quantify the vehicle's performance independently of the driver. An alternative approach in this area is to identify the relationships between closed-loop performances, drivers' subjective assessment, and vehicle response characteristics from open-loop maneuvers. Lincke, et al. [14] correlated the subjective ranking of eight unskilled drivers during a severe double-lane change maneuver (at 100 km/h) with several open-loop handling performance metrics (e.g., yaw rate natural frequency, and damping ratio) from step-steer maneuver at 0.4 g (at 100 km/h). They found that, vehicles with higher yaw rate natural frequency were rated better during the double-lane change maneuver. Lincke et al. also found that for vehicles with the same yaw rate natural frequencies, the one with an apparently lower damping ratio (and shorter response times) was more preferable for drivers. The authors concluded that vehicle response rate (e.g., yaw rate natural frequency, and response times) have a greater influence on assessment by the drivers than vehicle damping. Good [15] provides a comprehensive summary of

studies that aimed to find relationships between closed-loop performance, driver's subjective opinions, and vehicle response characteristics from open-loop maneuvers.

The most important limitation to this approach of using physical testing with professional test engineers lies in its assumption that the expectations of non-expert target customers can be sufficiently described by professional test drivers. Setting of vehicle targets purely based on this approach can potentially lead to over-engineering the vehicle thereby achieving performance levels that go beyond the scope of the normal driver's needs/desires and/or perception range. Additionally, this approach does not provide a strategy for including manufacturer's brand essence information during the target setting process.

The second exploratory approach in the area of subjective driver preference of vehicle handling quality relies heavily on vehicle handling simulations. This approach is based on a simulated driver model in conjunction with a simulated vehicle dynamics model. The adaptive parameters of the driver model are used as an indicator for the handling quality of the vehicle. McRuer [16], Venhovens and Hazare [17], Horiuchi [18] and Abe [19] have presented initial work in this area. According to McRuer et al. [16], drivers adapt their driving control in such a way that they maintain nearly constant closed-loop driver-vehicle system performance. More specifically, drivers adjust their dynamic control performance to achieve an invariant form of driver-vehicle forward loop transfer function, such that it resembles a gain, time delay, and integrator in the region of the crossover frequency. Drivers adjust their gains and apply a lead-lag equalization

strategy to maintain an invariant form of open-loop transfer function which satisfies the criteria for a stable control system. The gains and lead time-constants are indicators of the driver's perception of handling quality. A range or level of gains exists that are perceived as "enjoyable" by the driver. Driver gains that are too high or too low lead to degraded perceptions of handling quality. Similarly, the generation of "excessive" lead will degrade the perception of good handling. Venhovens and Hazare [17] elaborate on the hypothesis that, if ideal gains and lead time-constants can be quantified for a particular customer and vehicle segment, vehicle dynamics behavior can be tuned accordingly to meet customer expectations.

Although this method seems very attractive, development of simulation models, which can realistically capture human driver behavior during all the complex driving scenarios, and can adapt themselves to represent the different customer segments is very challenging by itself. These models need to be thoroughly validated before they can be used for the target setting and product development process. The uncertainty associated with the human driver simulation model has somewhat restricted this approach.

Methods to systematically derive vehicle subsystem-level requirements and component-level design specifications to achieve vehicle-level handling targets.

A key area of research in vehicle handling engineering is the development of methods that systematically derive vehicle subsystem-level requirements and component-level design specifications to achieve desired vehicle handling targets satisfying the drivers' expectations regarding vehicle handling. The use of mathematical optimization strategies is probably one of the most promising approaches to analytically solving this problem.

Several researchers have used optimization strategies to derive vehicle subsystem-level specifications from desired vehicle-level targets. For example, Hagaic et al. [20] uses Genetic Algorithms (GA) to solve vehicle handling design problem and compares the results obtained from using Genetic Algorithms against other optimization methods such as Monte-Carlo [21, 22] and Simulated Annealing [23]. In these studies [20, 21, 23] the authors have used an eight-DOF vehicle dynamics model with 24 subcomponent-level design variables simulated for three different transient handling maneuvers—step steer, single sinusoidal steer and double lane change—while evaluating 22 different performance metrics. Similar work from Miano et al. [24] presents a multi-objective, GA-based approach for the selection of front and rear cornering tire stiffness during a step-steer maneuver using both linear and non-linear analytical vehicle handling models.

Schuller et al., [25] uses a GA based approach coupled with utility functions [26] to optimize vehicle handling performance. Utility functions serve as a method for

selection a preferred design solution from a set of Pareto-optimal [6] solutions resultant from GA-based optimization schemes. Benedetti et al. [27] applies concepts of fuzzy optimality as a *posteriori* selection rule for selection of the best solution from a set of non-dominated Pareto-optimal solutions while dealing with multi-objective optimization of a racing car's tire-suspension system.

Most of the genetic algorithm based optimization research described above is restricted towards analysis of transient handling behavior of the vehicle. It does not consider trade-offs and conflicts among the various handling performance requirements of a driver, for example, sportiness vs. safety or agility vs. comfort. None of the work described above has developed a systematic strategy to include customers' preference by using strategic set brand attributes during the final selection of chassis design configuration.

Gobbi et al. [29] uses a *Global Approximation* approach for optimization of the vehicle's dynamic behavior. In this approach, a physical model is used to establish the relationship (i.e., global approximation) between design parameters and performance indices, for a number of feasible combinations of the design parameters. The original, physical vehicle model is then substituted by a purely mathematical model, which is used in the iterative optimization procedure. In their research, the authors used Artificial Neural Networks (ANN) to develop an approximation model. Genetic algorithms perform the computation of the Pareto-optimal solution set. Gobbi et al. uses ANN to optimize 12 design variables—mostly suspension subsystem parameters—during 41

different driving scenarios. Guarneri et al. [30] uses a similar global approximation approach with Recurrent Neural Networks (RNN) for the optimization of tire-suspension dynamic systems.

Global approximation methods such as ANN, RNN, and Response Surfaces (RS) tend to reduce numerical simulation time dramatically and enable efficient implementation of optimization methods. The main drawback of this approach is that the use of global approximations often result in black-box models that do not provide any insight into the physical behavior of systems and hence makes the chassis design process in-transparent.

Other research in this area focuses on the derivation of vehicle component-level specifications using non-linear, multi-body simulations and optimization methods. Choi et al. [31] uses an automated routine coupling Adams/Car [32] and PIAnO [33] for the optimization of suspension tuning parameters (i.e., bushing stiffness curves, suspension hard points, springs, and dampers) in order to adjust the suspension system's kinematic and compliance characteristics and tune the handling performance of the vehicle. Choi et al. uses a global approximation method called the Progressive Quadratic Response Surface Modeling (PQRSM) built into built into the automated optimization tool PIAnO.

Li, L., et al. [34] use a detailed multi-body vehicle dynamics model with non-linear suspension bushings and lower control-arm flexibility for the optimization of suspension elastomeric bushing compliance in order to improve vehicle ride, handling, and durability performance. Li, L., et al. uses the Adams software model for vehicle

dynamics analysis coupled with another automated tool FEMFAT for durability and fatigue life analysis. The optimization is performed using another commercially available software: iSIGHT. A combination of Simulated Annealing and Programming Quadratic Line Search methods is used for optimization in this work.

Similar work in this area using multi-body simulation software was conducted by Li, M., et al. [35] and Mehdi et al. [36]. Li, M., et al. [35] uses a multi-body dynamics vehicle model (e.g., in Adams/Car) in conjunction with a commercially available optimization tool, Adams/Insight, for the optimization of vehicle handling performance during step-steer, double lane change, steady state circle, and on-center handling tests. In this research, the authors use a sensitivity analysis to identify the most relevant suspension-kinematic parameters and then use them for the optimization process. Mehdi et al. [36] uses a multi-body simulation model (e.g., in Adams/Car) to optimize steering system geometry by using a GA-based approach in order to improve the vehicle's handling performance during step steer and constant-circle test maneuvers. Mehdi et al. [36] also uses a sensitivity analysis to eliminate insignificant design parameters.

As described above, most of the previous research on deriving component-level specifications has resorted in the use of commercially available multi-body simulation software tools coupled with automated optimization routines. These multi-body simulations tools often require detailed parameter specifications before they can be reliably used for any analyses and optimization. These detailed parameter specifications are not available in concept development phase and hence, this method not suitable for

preliminary concept design. The use of multi-body software packages coupled with automated optimization tools can be regarded as a form of All-in-One (AiO) optimization where the component-level specifications are linked with vehicle-level targets without adequate consideration of the subsystem requirements. AiO optimization methods for vehicle handling design are often computationally expensive.

Fujita et al. [37] discusses the design optimization of a multi-link suspension for desired handling, straight-line stability and ride comfort using a generic algorithm with link geometry, spring-damper coefficients, and stabilizer stiffness as the design variables. This research proposes an Interpretive Structural Modeling (ISM)-based, systematic structurization procedure for the hierarchical arrangement of the handling design problem, which is particularly useful in formulating the optimization problem in a mathematically appropriate form. Although, this research describes the importance of a well-defined structural approach, it still use a combination of vehicle-level and subsystem-level targets as their objective functions to optimize for component-level specifications. It does not discuss implementation of a truly structured system where vehicle-, subsystem- and component-level targets are cascaded and derived in a systematic manner.

Another interesting optimization technique, which can potentially be used for systematically achieving and balancing vehicle handling properties, is Analytical Target Cascading (ATC). ATC applies a decomposition approach in which the overall system is split into subsystems, which are solved independently and coordinated via target-

response consistency constraints [4]. Kim at al. demonstrates the use of this technique for the optimization of ride—natural frequencies of body hop, wheel hop, and body pitch—and handling—understeer gradient—targets using a simplistic, half-car ride and single-track handling models. Separate suspension and tire design models are used at the subsystem level. The suspension system model optimizes coil spring geometry while achieving suspension stiffness targets, and the tire model optimizes tire pressures while achieving the tire's vertical and cornering stiffness targets. Guarneri et al. [38] compares the traditional All-in-One (AiO) optimization problem formulation with concepts of Analytical Target Cascading (ATC) while using a generic algorithm to optimize ride comfort and road holding and designing the geometry of the spring and damper unit.

Most of the literature on ATC comes from the field of advanced optimization research and is focused towards techniques for efficient implementation of the ATC approach. The case studies described in the literature are mostly based on simple theoretical problems demonstrating the application of ATC methodology. None of the research in the past has attempted to comprehensively solve the handling design problem using the ATC framework.

2.2 Research Opportunities (Gaps) from Literature Review

While reviewing the current state-of-the-art literature in the area of vehicle handling dynamics design, four key challenges/gaps can be identified:

- A Need for an Integrated, Systematic Approach to Vehicle Handling Design.

The literature review showed that researchers have used optimization techniques for vehicle handling design. The work to date lacks an approach which links the Original Equipment Manufacturer's (OEM's) brand DNA characteristics and customer expectations to the vehicle's objective handling targets and subsequent subsystem requirements and component-level specifications. None of the research to date uses and distinguishes between the target vehicle's brand essences.

The most significant contribution in the area of design of vehicle handling characteristics have been made by Haque [20, 21, 22, 25, 39] and Gobbi [26, 27, 28, 29, 30, 40]. Most of their work has been focused on determination of chassis subsystem-level design requirements for handling design and explores the most effective optimization technique for solving the handling design problem. The development of component-level specifications via the use of subsystem-level requirements was not addressed. None of the work to date applies a systematic, top-down system engineering approach towards vehicle handling dynamics design.

- A Need for Comprehensive Strategy that can Account for Trade-Offs in Vehicle Handling Design and can assist in the Decisions-Making Process while Section of the Final Chassis Configuration.

Vehicle handling in a broader sense comprises of several domains, for example, steady-state handling, transient handling, on-center handling, emergency handling, disturbance sensitivity, straight-line stability, and others. The different domains are related to vehicle handling performance requirements of a driver during different scenarios of vehicle operation. Each of these individual handling domains must be described by multiple objective functions in order to understand vehicle handling dynamics. Several of these domains and performance requirements are often in conflict with each other which makes vehicle handling design a multi-objective, multi-scenario optimization problem.

Researchers in the past have used multi-objective optimization techniques (for example, genetic algorithms) for solving the handling optimization problem. The key challenge that still remains is to identify a strategy that can enable efficient selection of the best design choice from a set of Pareto-optimal chassis design solutions resulting from genetic algorithms.

An effective vehicle handling design strategy needs to work systematically by first resolving trade-offs, finding compromises and identifying sensitivities involved between all the different aspects of vehicle handling and then use this information to guide the chassis engineer during the selection of the best design solution. The strategy

must provide ways to include customer expectations and brand essence information during the final design selection process.

- A Need for Less Complex and Detailed Vehicle Handling Models to be used in the Optimization Framework for Conceptual Design.

Research conducted so far has focused on a variety of vehicle handling models (i.e., analytical, differential equations-based, multi-body dynamics, global approximations, neural network, etc.) to study vehicle handling dynamics behavior. Often, these models are too complex to be used during the early stage concept development, as they require highly detailed mathematical relationships and component specifications as part of the simulation models. Often these detailed model information is not available in the early stage conceptual phase.

Often models available as a part of commercially available software packages are used in the design process. These commercially available packages often operate as complex, *black-box* models and do not provide any insight into the descriptive language of the model make-up. This can make the design process less transparent for the chassis engineer. Therefore, there is a need for simplified first-order physics based vehicle-handling models that can capture the most main aspects of vehicle handling. These models require working with reasonable accuracy and allowing for interaction and integration via the use of common design parameters in a common mathematical environment.

- A Need for a Comprehensive Optimization Framework for Vehicle Handling Design Characteristics.

Vehicle handling design is a multi-objective, multi-scenario optimization problem. The optimization strategy to solve this handling design problem must be implemented in a systematic, multi-level framework that can account for realistic constraints associated with subsystem and component-level design.

The analytical formulations required to accurately describe vehicle handling behavior are often non-linear, discontinuous, and multi-modal; hence, they require the use of stochastic search algorithms for optimization. The challenge comprises of setting up an optimization framework that can account for all these complex requirements, achieve maximum computational efficiency, and be effective for application during the concept development phase.

Researchers in the past have often highlighted the computational and time expenses associated with optimization processes. Several studies from the literature have used elaborate time-domain simulations to evaluate the handling design objective, which adds to the complexity of the problem with regard to the required resources (time, money). In order for the optimization process to be readily available for the chassis development engineer during the conceptual design phase, the process should be focused around first-order vehicle handling objectives and a limited amount of concept critical design variables. There is a need to develop a vehicle handling design optimization framework based on first-order approximation physical-based and surrogate models that

is accurate enough to capture the higher-order underlying physics to a reasonable accuracy.

Past research in this domain often applies an All-in-One (AiO) approach for optimization. In an AiO approach, top-level design targets (i.e., customer relevant full-vehicle-level targets) are linked directly to the lowest level (i.e., component-level specifications) via the use of extremely detailed, multi-body simulation models. Hence, the traditional AiO optimization approach increases computational complexity and makes the chassis design process less transparent. Therefore, this approach is not usable during the conceptual vehicle design phase.

CHAPTER THREE

PROPOSED RESEARCH

In this chapter, the fundamental principles of systems engineering are discussed and some of the challenges associated with the successful implementation of a systems engineering process are described. The theoretical framework of the proposed handling design methodology is presented with a systematic five step systems engineering based methodology for design of vehicle handling characteristics.

3.1 Systems Engineering Approach

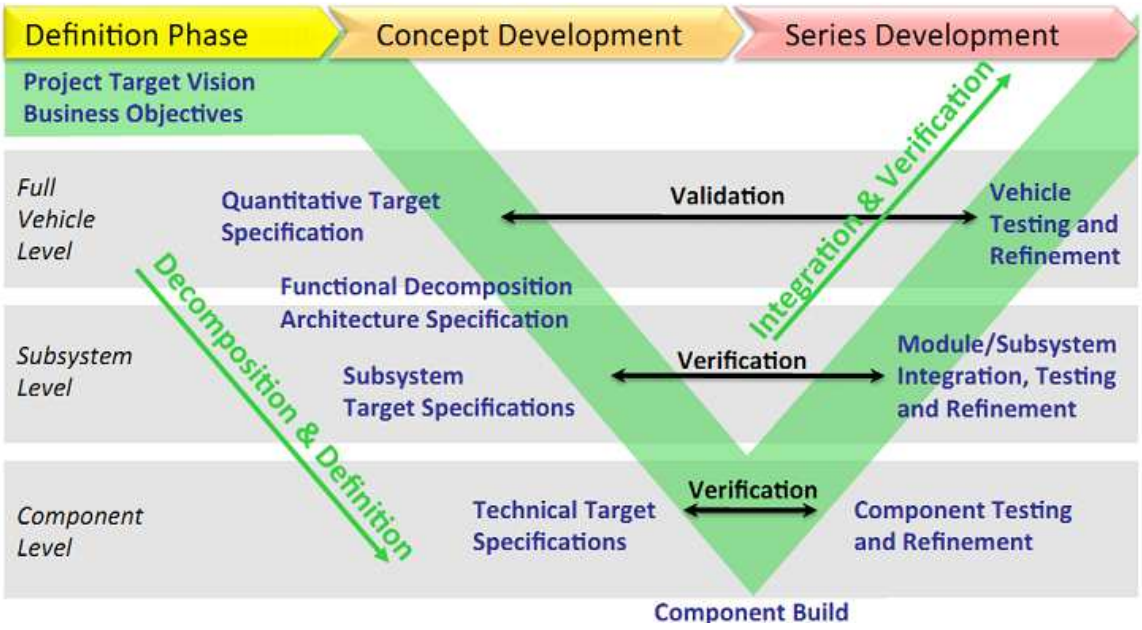

Figure 4. Systems Engineering Process "V" Diagram [1].

A systems engineering process evolves around a comprehensive, sequential, top-down approach for the successful realization of complex systems. According to the International Council of Systems Engineering (INCOSE), systems engineering seeks to

focus on the definition of customer needs and requirements early in the development process and subsequently proceed with design synthesis and systems validation. The systems engineering process inputs focus primarily on the stakeholder's (i.e., the customer, legislator, manufacturer) needs, objectives, expectations, requirements, project target visions, and business objectives. These process inputs are used to derive system-level, functional, and performance targets, which are then realized by the systematic development of subsystem-level requirements and component-level specifications. The systems engineering approach is often described with a "V" diagram, shown in Figure 4. The left-hand side of the "V" diagram deals with decomposition and definition of requirements, the bottom with product design using the defined requirements, and the right with the integration and verification of the requirements through testing [41].

Successful implementation of a systems engineering methodology for the design and development of complexly engineered systems is in itself challenging. It is often not straightforward to systematically decompose and define the requirements and specifications for the different design and development levels due to "build-in" system trade-offs and competing properties. Furthermore, the implementation methodology must be concurrent and consistent (concurrent here implies that the individual tasks at different levels are carried out separately in parallel, and consistent implies that the key interactions among different design tasks are identified, observed, and enforced until the concurrent design process results in a final product [4]).

An approach to assuring concurrency and consistency is the use of a decomposition-based target cascading methodology [4]. In a decomposition-based target cascading methodology, the entire complex problem is partitioned or decomposed into smaller and simpler problems. A decomposition-based approach helps to better understand and explore the compromises and trade-offs involved between the different subsystems and hence provides valuable insights for the system engineer. Once the system is decomposed, the *targets*, or specifications for top levels, are identified first. These *targets* are propagated, or cascaded, systematically to the rest of the system (i.e., the subsystems and smaller components. The actual design tasks are executed locally at subsystem and component level, and interaction with the rest of the system is revisited only when a target cannot be met. This often leads to an iterative target cascading process. When the design decisions can be modeled analytically, the process can be formalized as a multi-level optimization problem referred to as Analytical Target Cascading (ATC) [4, 5].

In this research, a simulation based design methodology for the conceptual design of vehicle handling characteristics is developed using a decomposition-based target cascading process and systems engineering principles.

3.2 Systems Engineering Methodology for Conceptual Design of Vehicle Handling Dynamics

A systems engineering approach applied as part of the product conception always begin with understanding the customer's expectations for a particular product so that the final product is designed to meet the end-user's expectations as best as possible. Equally important for the product developer is to understand the company's brand essence and realize how the product under development should be designed to align with the brand essence of the company to ensure consistency in the message and product experience. Translating these general ideas to vehicle handling design requires a target-setting process in alignment with the essence of the vehicle's brand and a target realization/tracking process that assures that higher-level customer expectations are met during the various stages of the vehicle development process.

As part of the process, customer requirements are cascaded step-by-step from high-level vehicle targets to subsystem-level requirements and component-level specifications. The targets, requirements, and specifications must be validated at each step during the product engineering and build phase as part of the multiple design review processes. Various steps for the specific application of conceptual design of vehicle handling characteristics are described below.

- **Step 1:** Define driving maneuvers and qualitative metrics of vehicle handling based on correlative analyses between customers' handling expectations, brand DNA targets, and objective metrics.
- **Step 2:** Quantify handling metrics.

- **Step 3:** Develop a set of knowledge-based, lower-order models as the basis for engineering design optimization.
- **Step 4:** Develop and apply a multi-objective, multi-scenario optimization framework to drive product design.
- **Step 5:** Validate and verify recommended design configurations to ensure customer satisfaction.

Step 1: Define driving maneuvers and qualitative metrics of vehicle handling based on correlative analyses between customers' handling expectations, brand DNA targets, and objective metrics.

The first step is to understand the customer's relevant vehicle handling expectations. The average consumer often describes handling highly subjectively with attributes such as "fun to drive," "sporty," or "safe". Translation of these subjective attributes into the engineering domain is a big challenge in itself. Customers with different lifestyles and backgrounds (i.e., age groups, income levels, and hobbies) might have very different expectations with respect to vehicle handling behavior, which makes the qualification and quantification of customers' vehicle handling requirements even more difficult.

A possible approach to understanding customer's handling expectations is based on the use of marketing research and clinics to better understand the product characteristics and features desirable for customers. Clinics, driving events, and marketing surveys aimed at understanding end-user preferences and expectations of

vehicle handling can be used as the first step in the vehicle dynamics development program.

Customer handling expectations should be defined and quantified with respect to the various scenarios of vehicle handling. This step requires the development of statistically relevant correlations between customer expectations and qualitative objective metrics, which can then be used by chassis engineers for the development of vehicle handling targets used in the product design phase. Table 1 shows the qualitative overview of vehicle-handling domains associated with different, everyday driving tasks. As part of the systems engineering process, each scenario should be quantified with objective metrics that captures the driver's assessment of vehicle handling behavior.

Table 1. Vehicle Handling Domains and Objective Metrics.

Handling Domains	Description of Handling Domains	Handling Objective Metrics
Steady State Handling	Scenarios of constant speed; constant steer angles with vehicle turning along a constant radius of curvature	Understeer gradient, yaw rate gain, roll gain, side-slip angle gain
Transient Handling	Scenarios of changing yaw velocity, side-slip velocity, and path curvature; represents vehicle's response during dynamic situations (i.e., turn-entry and turn-exit); evaluated with metrics: agility, responsiveness and damping	Yaw rate time constant, lateral acceleration phase lag, yaw rate damping ratio, roll angle overshoot, roll angle response time
Steering Feedback (Off-Center)	Steering system response, described in terms of steering-wheel torque feedback, of vehicle during normal driving scenarios	Steering torque feel (torque vs. angle, torque vs. lateral acceleration gradient)
On-Center Steering	Steering system response during straight-line driving at highway speeds	Steering torque time lag (vs. steering angle) at low lateral accelerations and low steering frequencies
Emergency (Limit) Handling	Vehicle's response during critical maneuvers such as obstacle avoidance	Yaw stability, roll stability
Parking	Ease of vehicle maneuverability during low-speed, high-steer angle maneuvers	Static parking torque, turn circle diameter, lock-to-lock steering turns
Coupled Dynamics	Vehicle's directional stability in scenarios where cornering is coupled with other dynamic motions such as braking or acceleration	Yaw rate increment
Road Adaptability	Handling behavior of vehicle on different road surfaces (i.e., rough roads, bumps, or low friction surfaces).	Yaw rate increment
Straight-Line Stability	Pull and drift behavior of vehicle (i.e., tendency of vehicle to deviate from intended path during straight-line cruising, acceleration, and braking scenarios); vehicle's response during acceleration and braking on split-mu surfaces.	Pitch gradient, straight-line stability index
Disturbance Sensitivity	Vehicle's straight-line performance in presence of external environmental disturbances such as winds, road crown, and road roughness.	Yaw moment sensitivity

In this research, all handling scenarios described in Table 1 contribute to the total objective vehicle handling DNA of a vehicle (see Figure 5). It is important to note that there are dependencies and trade-offs among the different aspects of vehicle handling. For example, designing a vehicle for stability during emergency handling usually results in an understeered vehicle that customers may perceive as less agile and sporty during normal driving scenarios. Making a vehicle more agile, and thus oversteered, can result in a vehicle setup that is more nervous with regard to straight-line stability. Making a vehicle easier to turn using a low steering ratio leads to high steering effort and torque during parking.

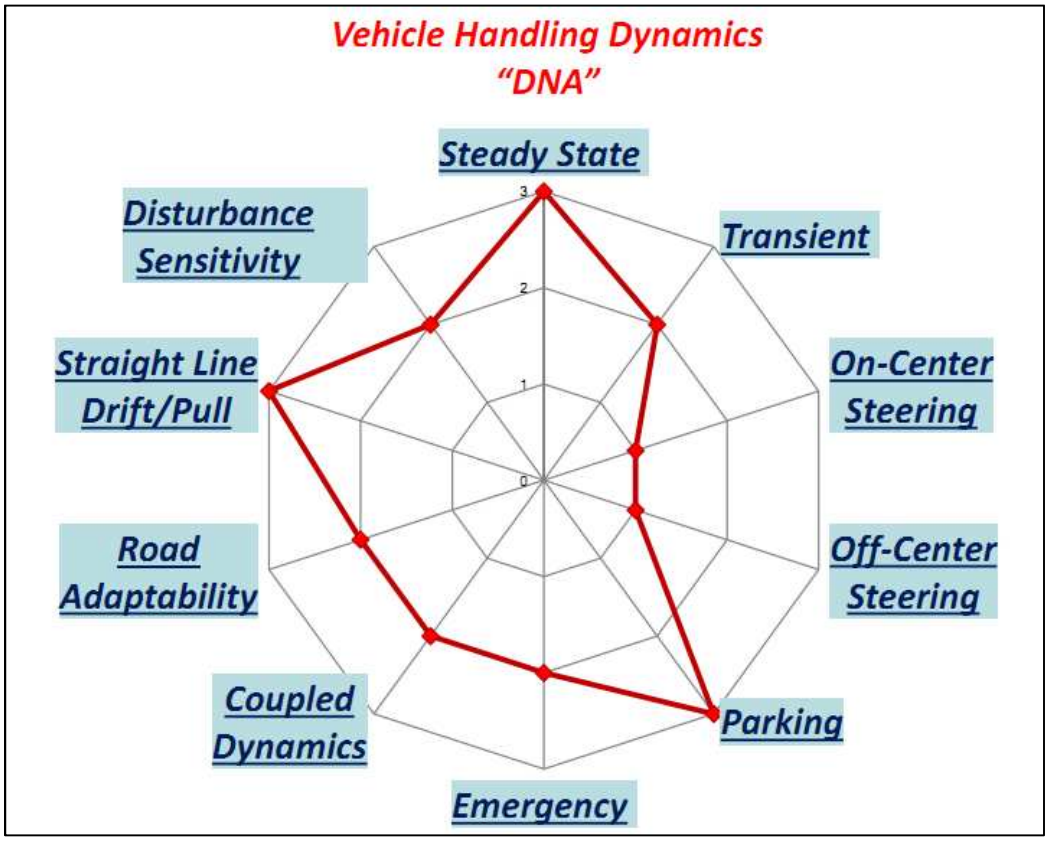

Figure 5. Typical Vehicle Handling DNA.

Step 2: Quantify handling metrics.

Once the various vehicle-handling scenarios and objective metrics associated with different everyday driving tasks are identified, the next step is to quantify objective metrics with realistic numbers. These metrics can then be used in the product development process.

There are three traditionally different approaches for quantifying objective handling related metrics:

1. *Physical testing of vehicles using highly trained professional test engineers*. The subjective feedback of trained test engineers using qualitative engineering descriptions such as "progressive handling," "predictable behavior," "cornering traction," "overall grip," "direct steering response," etc. correlates with objective responses measured by sensors installed on the vehicle. This approach assumes that the non-expert target customer's expectations can be sufficiently described by expert test engineers' subjective judgments. This approach, although most widely used within the industry, can lead to over-engineered products tuned for expert professional test engineers/drivers instead of "normal" end-users.
2. *Simulation-based strategies*. This approach relies on simulation methods and requires synthesized vehicle dynamics and driver models to predict and assess the driver's perception of vehicle handling dynamics. A simulated driver model is used in conjunction with a vehicle dynamics model, and the adaptive parameters of the driver model are used as indicators of the vehicle's handling quality.

According to McRuer et al. [16], drivers adapt their driving control in such a way that they maintain near-constant closed-loop driver-vehicle system performance. The gains and lead time-constants are indicators of the driver's perception of handling quality. A range of gains exists that are perceived as enjoyable by the driver. Gains that are too high (perceived as "twitchy" by customers) or too low ("sluggish") lead to degraded perception of handling quality. Although this method seems very attractive, uncertainty associated with the human driver simulation model has restricted this approach.

3. *Clinics and analytic research.* This approach isolates the driver's preferences and perceptions of particular vehicles and brands by conduction-driven events with non-expert target consumers to help manufacturers understand customer expectations and preferences. Drivers' preferences are then correlated with objective metrics using statistical tools (i.e., regression and correlation techniques). These objective metrics can be derived from vehicle responses measured during physical testing of the vehicles or by the use of simulated vehicle dynamics models.

The quantification of vehicle handling objectives with realistic targets requires understanding both the brand essence and brand DNA weights. The brand essence closely relates to the customer's perception of a particular brand in comparison to the other brands; for example, the customer might perceive a certain brand to be "sportier" or more "comfortable" than another brand. Brand DNA weights provide a way to realistically

account for trade-offs between different conflicting attributes (i.e., sportiness vs. comfort) relevant to the customer while emphasizing certain attribute more than others.

Step 3: Develop a Set of Knowledge-Based Lower-Order Models as the Basis for Engineering Design Optimization.

The next step is to develop suitable vehicle handling models (physics-based, knowledge-based), which can capture and connect the different vehicle handling scenarios and metrics (described in Step 1). These "hybrid" lower-order models with appropriate amount of complexity must be able to simulate vehicle behavior at each level (vehicle, sub-system and component). Since these models will be used in an iterative optimization framework (Step 4) it is important to ensure that the models are easy to characterize, computationally in-expensive, transparent and insightful for the chassis designers.

Note that there are several highly complex vehicle dynamics models available (as part of commercially available software packages). These commercially available handling packages/models are often not suitable during the vehicle concept development phase. Firstly, the detailed vehicle handling software packages (such as multi-body dynamics simulation tools) requires building elaborate models with detailed component specifications that are generally not available during the initial stages of the conceptual vehicle design, secondly, having highly non-linear and complex models make the simulation (and numerical optimization) process very computationally expensive, and thirdly, some commercially available simulation tools are of a black-box nature which

means that the chassis engineer has no clear insight into the descriptive language of the model make-up and models of such nature often do not allow access to model parameters by 3rd party optimization routines.

Step 4: Develop and Apply a Multi-Objective, Multi-Scenario Optimization Framework to Drive Product Design.

Systematically following Steps 1 and 2 will lead towards the development of quantifiable engineering metrics that correlate to customers' vehicle handling expectations. As described in Step 1, to comprehensively describe customers' vehicle handling requirements, a variety of scenarios and corresponding objective metrics are needed. These objective handling metrics can be analytically computed using vehicle handling models developed in Step 3.

Step 4 requires the availability of a multi-scenario, multi-objective optimization framework to balance competing customer relevant vehicle handling requirements; that will drive the product design development and optimization. This optimization framework will account for the interaction between various aspects of vehicle handling and supports developing chassis subsystem- and component-level design specifications with respect to realistic design constraints. The framework is applied in two consecutive steps: in the first step, objective vehicle-level handling targets derived from customer handling expectations are translated into subsystem-level engineering requirements and balanced against various competing design objectives using an optimization method. In the second step, the subsystem-level requirements are translated into component-level

design specifications where an optimization algorithm searches for the best set of design parameters.

In this research, Genetic Algorithms (GAs) [6], a type of stochastic optimization method is used at each level. As the vehicle handling design process is complex and possibly multi-modal in nature, the use of stochastic optimization approaches will ensure that the final optimal solution is not restricted to a local minimum as with traditional gradient-based optimization methods. The optimization framework has been implemented using a decomposition-based Analytical Target Cascading (ATC) methodology [4, 5]. ATC is an effective hierarchical multi-level optimization-based design methodology; it applies a decomposition approach wherein the overall system is split into subsystems, which are then solved independently and coordinated via target-response consistency constraints [4, 5].

The chassis design problem can be decomposed into a meaningful subsystem-level - such as suspension, steering and tires - and component-level - such as kinematics and bushing compliances - design problem. The desired vehicle-level targets are cascaded systematically to lower levels (i.e., subsystems) and components are rebalanced upwards based on lower-level designs. Analytical models for subsystems and components are identified and tied together in the optimization framework. An iterative optimization scheme has been established, which aims at reducing the discrepancy between targets (from higher levels) and responses (from lower levels) in order to achieve a consistent, optimized chassis design solution with respect to constraints at the subsystem and

component levels. Figure 6 shows the overall target cascading flow diagram proposed in this research.

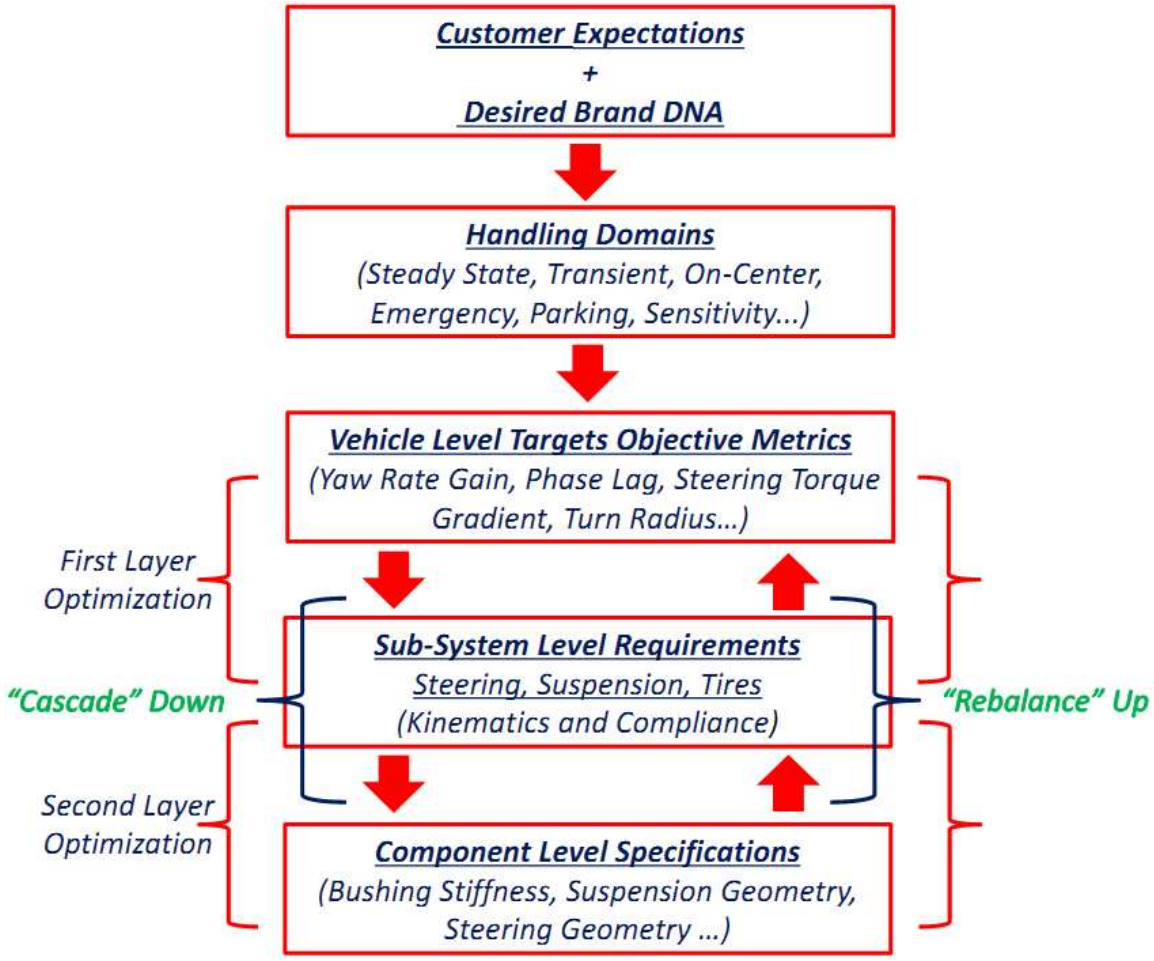

Figure 6. Target Cascading Flow Diagram.

Step 5: Validate and Verify Recommended Design Configurations to ensure Customer Satisfaction

In a typical system engineering process, the derived subsystem-level and component-level specifications are validated by physically building and testing systems at each level. (Refer to the right-hand side of the "V" diagram shown in Figure 4). The upward process ensures that the final product meets all desired vehicle level targets and end-user expectations.

For the conceptual design of vehicle handling dynamics described in this research, it is recommended that the validation process be performed virtually - potentially with higher-order, higher-quality simulation models. The component design specifications derived using the optimization framework (Step 4) can be used to characterize commercially available higher-order simulation tools, which usually have a higher degree of correlation with real vehicle behavior. For example, the suspension pick-up points generated from the optimization algorithm can be used to characterize a multi-body simulation model, which can then be used to simulate the kinematics and compliance behavior validate suspension subsystem targets, such as the compliance steer of an entire axle. The simulation models can also be used to simulate different vehicle handling scenarios to ensure that vehicle-level targets derived during Step 2 are achieved. Real world testing with physical prototypes can be used to complete the validation process.

CHAPTER FOUR

IMPLEMENTATION OF THE PROPOSED RESEARCH METHODOLOGY

In this chapter, the key building blocks required for successful implementation of the proposed systems engineering methodology for vehicle handling design are described in details. The building blocks include description of a method to integrate aggregated market research data into the vehicle handling design process, development of empirical relationships between customer relevant handling attributes and handling objective metrics, description of the vehicle handling models, and development of the ATC based optimization framework. These building blocks are the basis of all the simulation results described within the case studies in Chapter Five.

4.1 Integrating Market Research in the Vehicle Handling Design Process.

A systems engineering approach applied as part of the conceptual product design phase always begins with understanding the customer's expectations for a particular product to support the product development to meet the end-user's expectations as best as possible. Equally important for the product developer is to understand the company's brand essence and realize how the product under development should be designed to align with the attributes of the brand essence to ensure consistency in the message and product experience. Translating these general ideas to vehicle handling design requires a target-setting process in alignment with the essence of the vehicle's brand and a target realization/tracking process that assures that higher-level customer expectations are met during the various stages of the vehicle development process.

One of the key outcomes of this research is a systematic method to include customer expectations and manufacturer brand essence information into the product development process. In this thesis, market research from AutoPacific [42] is used to create an understanding of the customers' vehicle satisfaction with regard to various product attributes. The AutoPacific 2013 New Vehicle Satisfactory Survey used consists of around 56,000 responses from consumers who purchased a new vehicle within six months of filling out the survey (questionnaire). The survey captures new vehicle owners' satisfaction with their purchases with respect to different vehicle attributes. Around 50 % of the participants were "Baby Boomers" (age 50-64), 19 % were from the "Silent" Generation (age 69-94), 18 % were from Generation 'X' (age 37-48), 11% were from Generation 'Y' (age 36-24) and 1 % was from Generation "Z" (age 23-16).

Figure 7 shows sample results from the survey for five brands—Volvo, BMW, Toyota, Lexus, and MINI. The results in Figure 7 are based on the AutoPacific survey in which the customers' were asked to rate their vehicle's image with respect to pre-defined product attributes on the scale of 1 to 5. An absolute rating of 1 meant that the attribute *did not apply* to their vehicle, a rating of 3 implied that the attribute was *somewhat applicable* to their vehicle, and a rating of 5 implied that the attribute was *completely applicable* to their vehicle. The data with absolute ratings was normalized with the average of all vehicles in the 2013 AutoPacific Database (56,000 samples). The normalized data is presented in Figure 7, where the zero value indicates the average, and a positive (or negative) value indicates percentage above (or below) average.

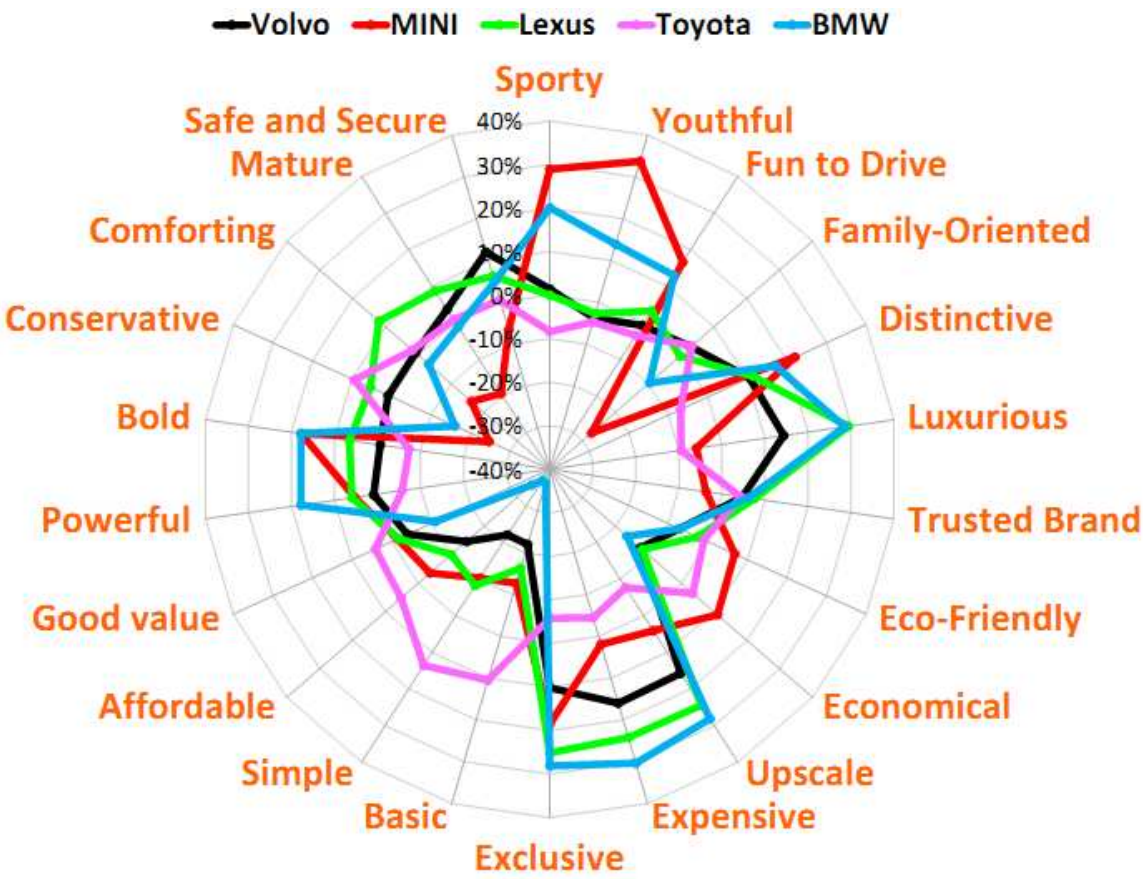

Figure 7. Customer Derived Brand Image Perception. Source: AutoPacific 2013 New Vehicle Satisfactory Survey.

Results from the survey are very intuitive to understand, for example, customers perceive MINI to be *Sporty, Youthful, Fun-to-Drive, Distinctive,* and *Bold.* Both BMW and Lexus are perceived to be *Upscale, Expensive, Exclusive, and Luxurious*. The survey indicates that BMW is ahead of its competitors with respect to *Sporty* and *Fun-to-Drive* attributes whereas Lexus leads the market with respect to *Comfort*. Volvo is considered to be a leader in *Safety (Safe and Secure)*. Toyota is perceived to be a relatively balanced brand and is regarded as *Simple, Affordable, Basic, and Good Value*.

The next step in this research was to create an understanding how the customers' satisfaction is related to vehicle handling attributes. From the survey, four key attributes related to vehicle handling behavior—*Sporty, Fun-to-Drive, Safety,* and *Comfort*—were selected to develop a mathematical relationship between customer's satisfaction and objective metrics of vehicle handling.

Figure 8 shows a comparison of vehicle handling attributes among five manufactures—Volvo, Toyota, BMW, Lexus, and MINI. From Figure 8, it can be seen that the customers perceive MINI high with respect to *Sporty* and *Fun-to-Drive* attributes, Volvo is considered as the high in terms of *Safety,* and Lexus is considered high with respect to *Comfort*. BMW is among the leaders with respect to *Sporty*, *Fun-to-Drive*, *and Safety* but is slightly comprised with respect to *Comfort.* Toyota, on the other hand, is a balanced mainstream brand; it does not excel in any specific attribute and is generally regarded as *Safe* and *Comfortable.*

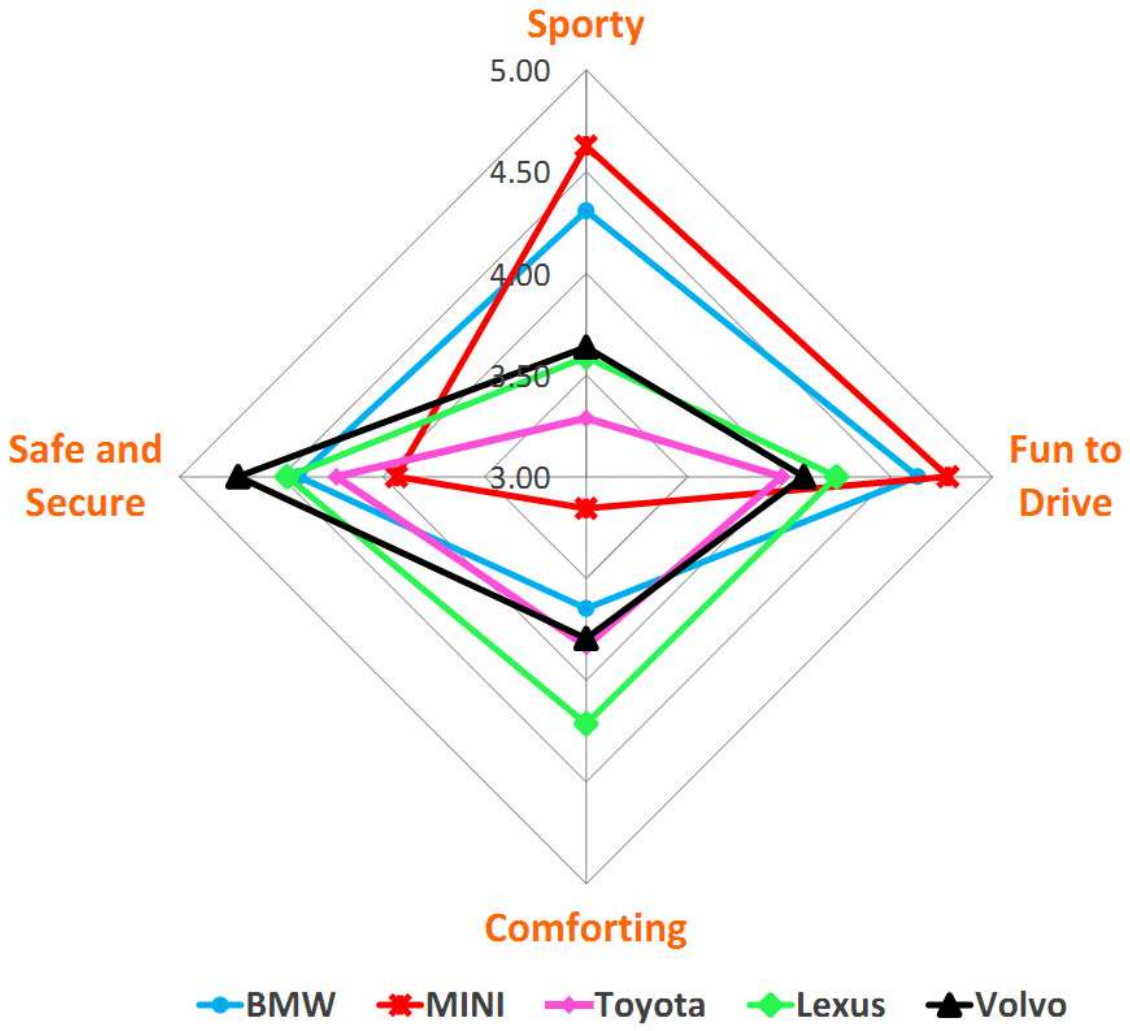

Figure 8. Comparison of Vehicle Handling Attributes for Five different Manufacturers Source: AutoPacific 2013 New Vehicle Satisfactory Survey (Rating Scale: 1 = Does not Apply, 3 = Applies Somewhat, 5 = Applies Completely).

Note that the AutoPacific survey database relates to customers' satisfaction with the vehicle features and perception of the vehicle's brand attributes. With some limitations this information can be used to represent the vehicle manufacturer's strategic direction of the brand (which is normally not publicized). If the perceived brand image

and intended strategic brand identity do not align, this approach cannot be used to "reverse engineer" the essence of the brand.

Another important piece of information that can be synthesized from the AutoPacific market data is the relative importance of the individual brand attributes (comparable to genetic instructions of living organisms), which form the makeup of the brand (comparable to the DNA information of living organisms). The so-called *Brand DNA weights* provide a way to represent the relative importance of different (often conflicting) brand attributes relevant to the consumer (i.e., sportiness vs. comfort). For example, from the survey it can be derived that the customers' perceive the BMW brand to be 10.3% more *Sporty*, 8.9% more *Fun to Drive*, 0.7% more *Comfortable*, and 9.2% more *Safe* than a reference brand (like e.g. Mazda). The relative importance of the attributes can be normalized for each brand to determine the *brand DNA weights*. For example, the BMW *brand DNA weights* are 25.3 % for *Sporty*, 27.2 % for *Fun-to-Drive*, 21.5 % for *Comfort* and 26% for *Safety*. Note that the sum of the *brand DNA weights* is equal to 100%. The quantification of vehicle handling objectives with realistic targets requires the understanding of both brand essence and *brand DNA weights*.

Table 2 shows the absolute ratings and various brand attribute for Volvo, Toyota, BMW, Lexus, and MINI from the AutoPacific 2013 New Vehicle Satisfactory Survey. Table 3 shows the *brand DNA weights* derived from market data and gives insight into the relative importance for the different brand attributes. For the data shown in Tables 2 and 3, Mazda is considered as the Reference Brand.

Table 2. Perceived Brand Attribute Rating Results from Market Data (Rating Scale: 1 = Does not Apply, 3 = Applies Somewhat, 5 = Applies Completely).

Absolute Rating					% Difference from Reference Brand			
Brands	Sporty	Fun to Drive	Comforting	Safe and Secure	Sporty	Fun to Drive	Comforting	Safe and Secure
BMW	4.31	4.63	3.65	4.42	10.3	8.9	0.7	9.2
MINI	4.63	4.78	3.16	3.93	18.4	12.4	-12.9	-2.8
Toyota	3.29	3.96	3.83	4.23	-15.8	-6.9	5.8	4.6
Lexus	3.59	4.23	4.21	4.47	-8.1	-0.5	16.3	10.6
Volvo	3.64	4.07	3.80	4.71	-6.9	-4.3	4.7	16.6
Reference	3.91	4.25	3.62	4.04	0.00	0.00	0.00	0.00

Table 3. Brand Attribute Weights (derived) from Market Data.

Brand Attribute Weights – Relative Importance					
Brands	Sporty	Fun to Drive	Comforting	Safe and Secure	Sum
BMW	0.253	0.272	0.215	0.260	1.000
MINI	0.280	0.290	0.191	0.239	1.000
Toyota	0.215	0.259	0.250	0.276	1.000
Lexus	0.218	0.256	0.255	0.271	1.000
Volvo	0.224	0.251	0.234	0.291	1.000
Reference	0.247	0.269	0.229	0.255	1.000

The results shown in Tables 2 and 3 are used extensively in the optimization procedure developed for this thesis. Specifically, Table 2 is used for incorporating the balance of different vehicle brand attributes in the vehicle handling optimization process and Table 3 is used for guiding the design direction of the chassis based on relative brand attributes weights.

4.2 Description of Vehicle Handling Domains and Metrics.

Vehicle handling behavior can be comprehensively described by the different domains of vehicle handling. These domains are formulated considering the vehicle handling performance requirements of a driver during different scenarios of vehicle operation: steady-state handling, transient handling, steering system feedback (which includes on-center and off-center steering performance), emergency or limit handling, parking, coupled dynamic cornering describing scenarios such as acceleration/braking while cornering, handling adaptability on different road surfaces, straight-line stability, drift/pull behavior during constant speed coasting, and disturbance sensitivity describing vehicles response to external agents such as side-winds, road roughness and road crown. The different domains of vehicle handling were described earlier in this thesis in Table 1. Table 4 shows an overview of objective metrics defined for each domain. The different domains of vehicle handling are described in more detail in Appendix A.

Table 4. Overview of Vehicle Handling Objective Metrics.

Handling Domains	Handling Objective Metrics	Description of Metrics	Units
Steady-State Handling	Understeer Gradient	Expressed as the gradient of steering wheel angle and lateral acceleration response.	deg/G
	Yaw Rate Gain	Expressed as the sensitivity of heading angle response change per unit steering wheel angle.	1/sec
	Side-Slip Angle Gain	Expressed as the sensitivity of side-slip angle response to lateral acceleration.	deg/G
	Roll Angle Gain	Expressed as the sensitivity of roll angle response to lateral acceleration.	deg/G

Transient Handling	Yaw Rate Time Constant	Expressed as the inverse of the frequency at which the phase of the yaw rate transfer functions equals -45 degrees.	ms
	Yaw Rate Damping Ratio	Expressed as the ratio of steady-state value and peak value of yaw rate from the yaw rate transfer function.	-
	Lateral Acceleration Phase Lag	Expressed as the phase lag of lateral acceleration from lateral acceleration vs. steering wheel angle transfer functions at 1 Hz.	deg
	Roll Angle Overshoot	Expressed as the ratio of the difference between the peak and steady-state values and steady-state value of the roll angle response.	%
Steering Feedback	Steering Torque Gain	Expressed as the gradient of steering torque and steering wheel angle input.	Nm/deg
	Steering Torque Feel	Expressed as the gradient of steering torque and lateral acceleration response.	Nm/G
On-Center	Steering Torque Time Lag	Expressed as the phase lag of steering torque from steering torque vs. steering wheel angle transfer function at 0.2 Hz.	ms
Parking	Lock-to-Lock Steering Rotations	Expressed as the maximum number of steering wheel rotations required for 360 degrees of steering wheel motion.	-
	Turning Circle Diameter	Expressed as the diameter (wheel-to-wheel) of the smallest circular turn that the vehicle is capable of making.	m
	Parking Static Torque	Expressed as the magnitude of static steering wheel torque during low speed maneuvering.	Nm
Disturbance Sensitivity	Yaw Moment Sensitivity	Expressed as degree of yaw angle response per unit yaw moment disturbance input.	Deg/KN-m-sec
Coupled Dynamics	Yaw Rate Increment	Expressed as the percentage increase in yaw rate while accelerating out of a corner.	%
Road Adaptability	Yaw Rate Increment	Expressed as the percentage increase in yaw rate after cornering on single bump.	%

Straight-Line Stability	Straight-Line Stability Index	Expressed as the measure of vehicle's tendency to develop a destabilizing yaw moment while reacting to un-balanced longitudinal and lateral force inputs. Lower value of this indicates higher straight-line stability.	Nm/N
	Pitch Gradient	Expressed as the sensitivity of pitching motion per unit lateral acceleration.	Deg/G
Emergency Handling (Roll Stability)	Static Stability Factor	Expressed as the ratio of half-track width to center of gravity height.	-

4.3 Establishing Empirical Relationships between Objective Handling Attributes and Perceived Brand Qualities.

In this section, the four key customer-relevant band attributes—*Sporty, Fun-to-Drive, Safety,* and *Comfort*—will be associated to the various objective handling metrics.

Table 5 shows the relationships proposed to associate brand attributes with objective handling metrics. These relationships were developed through empirical studies that correlate objective handling metrics with brand image ratings from market surveys using four passenger cars—the MINI, Ford Focus, Mazda RX8, and Mazda Miata—and two pickup trucks—the Ford F-150 and Toyota Tundra as case studies.

From Table 5, it is can be seen that the *Sportiness* of a vehicle is associated with four fundamental aspects: 1) a neutral steer response during steady-state cornering scenarios, 2) agile vehicle behavior during transient cornering situations, 3) good road feel via steering torque feedback through the steering system, and 4) reaction to driver inputs during coupled dynamics cornering scenarios (i.e., high yaw rate changes while accelerating out of a corner).

While analyzing the handling behavior of the 6 case study vehicles, it was found that the *Fun-to-Drive* attribute is a subset of *Sportiness* however with metrics that are most obvious for a casual driver. A *Fun-to-Drive* vehicle would be the one, which is most intuitive and enjoyable for a casual driver during nominal day-to-day driving.

Table 5. Brand Attributes and Objective Handling Metrics.

Brand Attributes	Objective Handling Metrics
Sporty 5 Metrics to be Maximized and 8 Metrics to be Minimized	Higher Yaw Rate Gain, Higher Steering Torque Gain, Higher Steering Torque Feel, Higher Damping Ratio, Higher Yaw Rate Increment (Acceleration-in-Turn).
	Lower Understeer Gradient, Lower Side-Slip Gain, Lower Roll Gain, Lower Pitch Gradient, Lower On-Center Lag, Lower Yaw Rate Time Constant, Lower Lateral Acceleration Phase Lag, Lower Roll Angle Overshoot.
Fun-to-Drive 2 Metrics to be Maximized and 6 Metrics to be Minimized	Higher Yaw Rate Damping Ratio, Higher Steering Torque Feel.
	Low Side-Slip Gain, Lower Roll Gain, Lower Pitch Gradient, Lower On-Center Lag, Lower Time Constant, Lower Lateral Acceleration Phase Lag.
Safety 2 Metrics to be Maximized and 4 Metrics to be Minimized	High Understeer Gradient (Yaw Stability), Higher Static Stability Factor (Roll Stability) Higher Straight-Line Stability (Lower Straight-Line Stability Index).
	Lower Yaw Rate Increment (Accelerating in Turn), Lower Yaw Rate Increment (Rough Road Cornering), Lower Roll Angle Overshoot.
Comfort 2 Metrics to be Maximized and 6 Metrics to be Minimized	Higher Side Wind Stability (Lower Yaw Moment Disturbance), Higher Yaw Rate Time Constant, Higher On-Center Delay.
	Lower Steering Torque Gain, Lower Steering Torque Feel, Lower Parking Torque, Lower Lock-to-Lock Steering Turns, Lower Turn Circle Diameter.

Vehicle *Safety* is related to the yaw, roll and straight-line stability of the vehicle. *Safety* is also associated with the vehicle's directional performance during coupled dynamics cornering and rough road cornering. A *Safe* vehicle will have a tendency to minimize any changes in yaw rate while negotiating scenarios such as accelerating out of a turn or cornering on curbs and rough roads. It can be inferred that *Sportiness* and *Safety* are often in conflict with each other.

Vehicle *Comfort* is associated with factors such as low steering torque workload, ease of maneuverability during low speed scenarios, and low sensitivity to side-wind disturbances. Apart from these factors, it was found that vehicle *Comfort* is also associated with responsiveness of the vehicle. Specifically, vehicles that are not very agile were found to be the ones, which were most comfortable for the customers. As in the case of *Safety*, *Comfort* also seems to have several trade-offs with *Sportiness.*

Using the empirically derived associations described in Table 5, a mathematical associating scheme has been developed for further use in this research. The mathematical relationships are described here using an example of a sporty rear wheel drive coupe. Table 6 illustrates the objective handling characteristics of this example vehicle, and Figure 9 shows a relative performance spider diagram depicting brand-related handling attributes for the example vehicle.

Table 6. Handling Performance Metrics for an Example Vehicle.

Handling Domains	Objective Handling Metrics	Unit	Example Vehicle (RWD)
Steady-State Handling (v=80 km/h)	Understeer Gradient	deg/G	1.197
	Yaw Rate Gain	1/sec	0.307
	Side-Slip Angle Gain	deg/G	-1.34
	Roll Angle Gain	deg/G	3.57
Transient Handling (v=80 km/h)	Yaw Rate Time Constant	ms	105
	Yaw Rate Damping Ratio	-	0.918
	Lateral Acceleration Phase Lag	deg	-43.4
	Roll Angle Overshoot	%	8.0
Steering Feedback (v=80 km/h)	Steering Torque Gain (per Steering Angle)	Nm/deg	0.308
	Steering Torque Feel (per Lateral Acceleration)	Nm/G	25.4
On-Center (v=80 km/h)	Steering Torque Time Lag (@ 0.2 Hz)	ms	63
Parking	Lock-to-Lock Steering Rotations	-	3.2
	Turning Circle Diameter	m	10.47
	Parking Static Torque	Nm	10.3
Disturbance Sensitivity (v=80 km/h)	Yaw Moment Sensitivity	deg/KN m-sec	2.301
Coupled Dynamics (v=80 km/h)	Yaw Rate Increment (Acceleration out of Turn)	%	3.54
Road Adaptability (v=80 km/h)	Yaw Rate Increment (Cornering on Rough Roads)	%	-1.95
Straight-Line Stability	Straight-Line Stability Index	Nm/N	1.518
	Pitch Gradient	deg/G	1.79
Emergency Handling (Roll Stability)	Static Stability Factor	-	1.499
	NHTSA Stars	-	5

Figure 9 is based on empirical associations shown in Table 5. These correlations have been developed such that a higher value of a metric on the spider diagram represents an improvement of the attribute. The first step in developing the mathematical association is to calculate the normalized values of the vehicle handling objective metrics. The normalized values are calculated by dividing each objective handling metric by values for a reference vehicle. The next step involves either addition or subtraction of the normalized metrics, depending upon whether they need to be maximized or minimized (to achieve an improvement of the metric), to calculate the relevant handling attribute based on associations shown in Table 5.

$$Handling\ Attribute = \frac{Sum\left[\left(Normalized\ Metrics\right)_{TO\ BE\ MAXIMIZED} - \left(Normalized\ Metrics\right)_{TO\ BE\ MINIMIZED}\right]}{Total\ Number\ of\ Metrics} \quad (2)$$

Assuming that the reference vehicle used for the normalization step is the same as the example vehicle shown in Table 6, all of the values of normalized metrics in this case will be one. Therefore, for this example vehicle,

Sporty = (+5 – 8)/13 = -0.231

Fun to Drive = (+2 – 6)/8 = -0.500

Safety = (+2 – 4)/6 = -0.334

Comfort= (+2 – 6)/8= -0.500

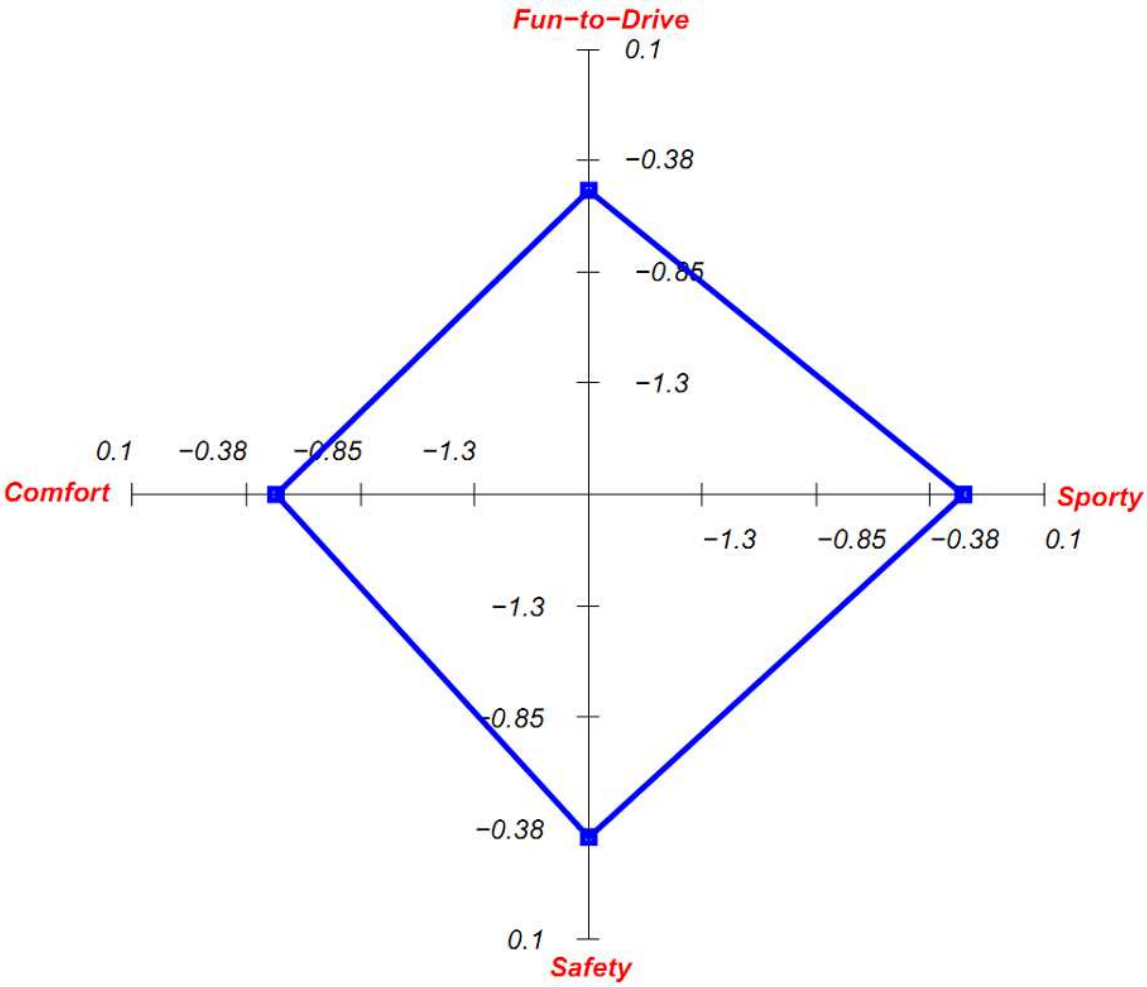

Figure 9. Handling Attribute Spider Diagram for Example Vehicle. A higher value (outwards on the diagram) indicates an improvement.

4.4 Vehicle Handling Models.

The vehicle handling models developed for this research need to be relevant for the conceptual phase of the product development processes and computational efficient when used in an iterative optimization framework. It is important to define model that do not require detailed engineering drawing and component specification since such parameters are not yet available in a conceptual design phase. Therefore the model complexity needs to reflect 1^{st} order effects of the vehicle handling phenomena to be investigated and relevant to the conceptual phase of the vehicle definition. The models need to be parametric (describing physical subsystem and component properties) such that design relevant parameters can be tuned.

The vehicle-handling model used in this thesis is based on a three Degrees of Freedom (DOF) model with roll, yaw, and lateral motions as the three degrees of freedom. This is coupled with a steering system model, which adds another DOF and accounts for steering system compliance between the road wheel and steering wheel.

The tire force model is based on Pacejka's Magic Formulae [43] and includes a simple transient tire side force model extension based on a first-order lag using the tire's relaxation length as the time constant. The influence of steering system compliance, suspension kinematics and compliance, weight transfer due to the height of the center of gravity, roll stiffness, and centrifugal forces are included in the tire force calculations using effective axle cornering characteristics [43]. The effective cornering characteristics include tire properties based on Pacejka's Magic Formulae and incorporate tire force

dependency on slip angle and vertical load to provide mechanisms for combined cornering and braking with tire force saturation. The elasto-kinematic characteristics of the suspension are modeled by using the suspension compliance matrix formulations described by Knapczyk [44].

A detailed description of vehicle dynamics models used in this research can be found in Appendix B.

Model Validation

The comprehensive vehicle handling model used in this research has been validated using physical test data from various vehicles. Figure 10, Figure 11 and Figure 12 show the validation results for a constant speed step steer maneuver performed with a sporty, RWD coupe (1991 Mazda Miata). Additional model validation results for a FWD sporty hatchback and a pick-up truck are shown in Appendix C.

Model Validation: Mazda Miata (Step Steer, Lateral Acceleration = 0.4 G's, Speed = 80.5 km/h)

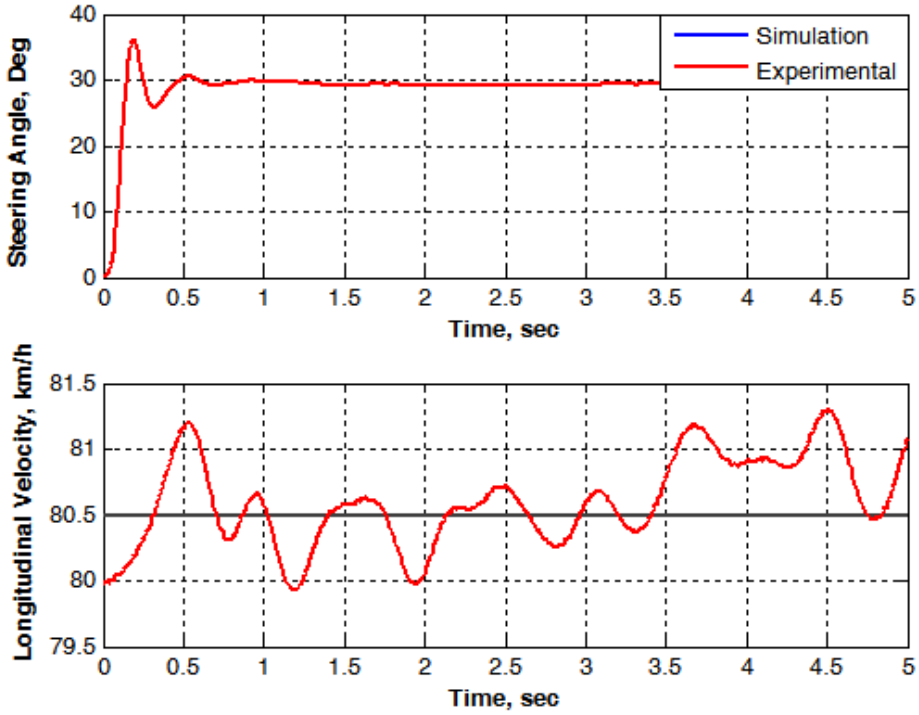

Figure 10. Steering Wheel Angle and Vehicle Speed Input for Model Validation.

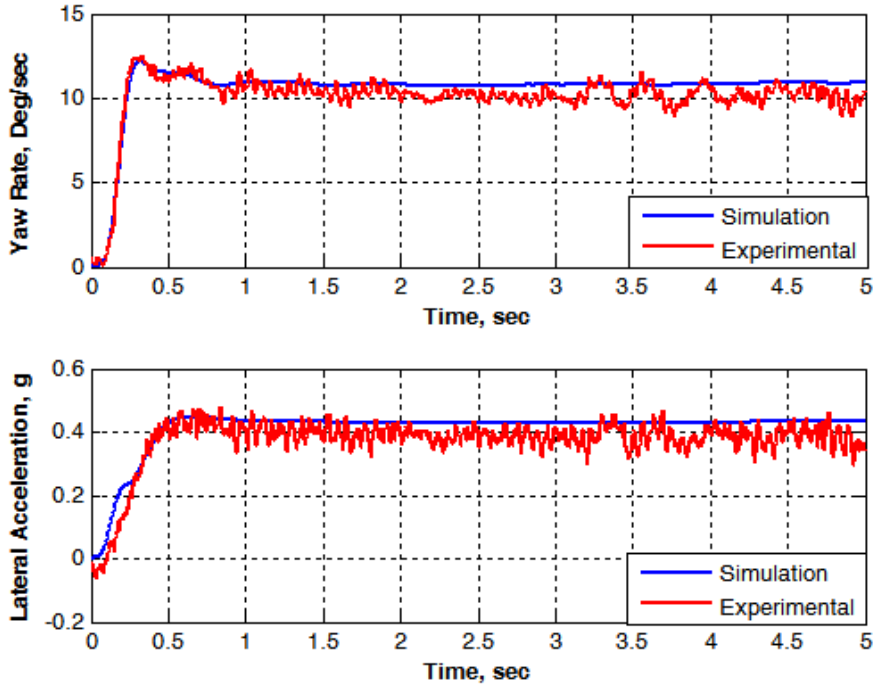

Figure 11. Comparison of Yaw Rate and Lateral Acceleration for Model Validation.

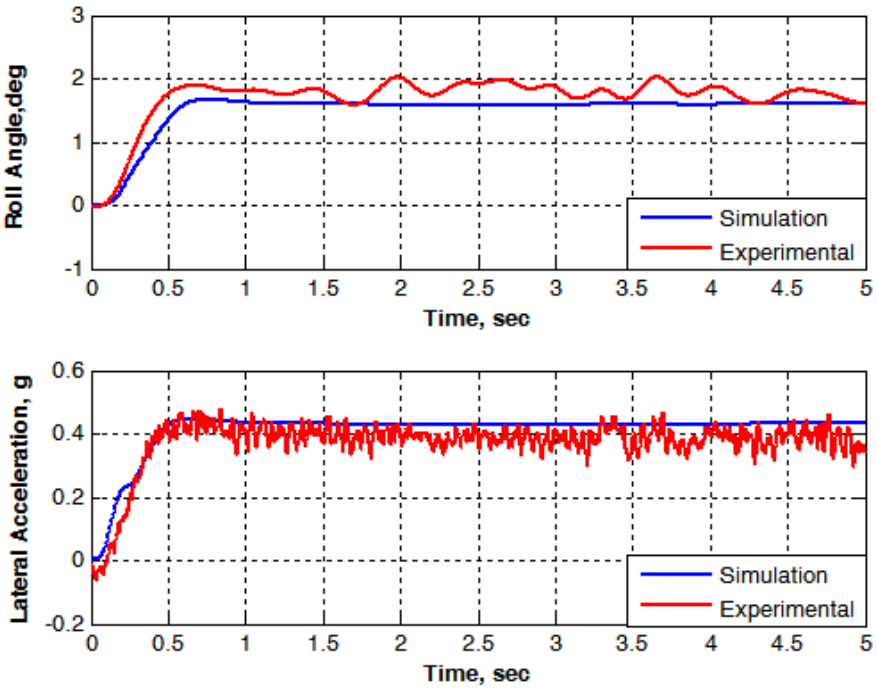

Figure 12. Comparison of Roll Angle and Lateral Acceleration for Model Validation.

4.5 Optimization Framework.

A multi-scenario, multi-objective optimization framework has been developed in this research for optimization and balancing of the customer relevant vehicle handling metrics.

The implementation of a true system engineering based optimization framework necessitates that the targets, requirements and specifications for the different design and development levels are systematically decomposed, defined and coordinated with each other during the optimization process. It is equally important to ensure transparency, accuracy, and computational efficiency in the coordination process. As described earlier on this thesis, one of the most important challenges of a systems engineering methodology is the development of such a framework, which can assure concurrency and consistency during its implementation. In this research, the optimization framework is developed using a decomposition-based, Analytical Target Cascading (ATC) [4, 5] methodology. ATC is an effective hierarchical multi-level optimization-based design methodology. It applies a decomposition approach wherein the overall system is split into subsystems; these subsystems are then solved independently and coordinated via target-response consistency constraints [4, 5].

The ATC optimization framework developed for this research works in a two-layer optimization schedule. Genetic Algorithms (GA) [6], a type of evolutionary optimization algorithms, are used at each layer of the framework.

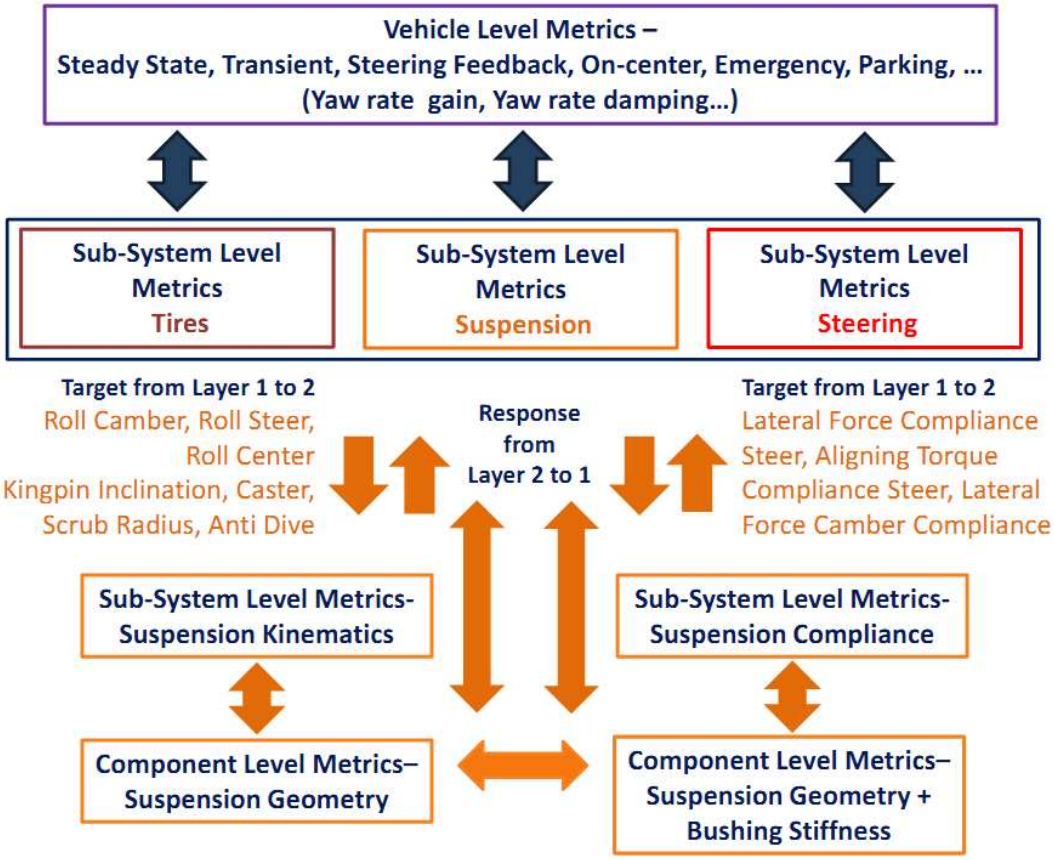

Figure 13. Analytical Target Cascading Flow Diagram for Vehicle Handling Dynamics.

The first layer is used to derive subsystem-level requirements from overall vehicle-level targets. These subsystem-level requirements are passed on as targets to the second layer of optimization, and the second layer attempts to derive component-level specifications from the subsystem-level requirements derived in the first step. The second layer optimization utilizes component-level design variables and analysis models and attempts to minimize the difference between the targets transferred from the vehicle level and responses generated from the component-level analysis. An iterative loop is set up

with an objective to minimize the target/response consistency constraints (i.e., the targets at the vehicle level are constantly rebalanced to achieve a consistent and feasible solution). Figure 13 shows the ATC flow diagram used.

Ten different scenarios of vehicle handling dynamics are considered (see Table 1). The vehicle handling objective metrics from each scenario are grouped under four customer-specific brand attributes as described in Table 5. The fitness function at the first layer (vehicle-level) of the optimization framework is based on customer-relevant brand attributes and from market data. The design variables used in the first layer of the optimization framework can be grouped into three separate sub-systems — tires, suspension, and steering.

In the second layer of the optimization framework, the suspension sub-systems are analyzed using separate kinematics and compliance modules. The suspension kinematic characteristics are represented by eight design variables namely, suspension roll camber, roll steer, roll center height, mechanical trail, scrub radius, king pin inclination, caster angle, and anti-dive geometry. The suspension compliance characteristics are represented with three design variables: namely, suspension lateral force compliance steer, lateral force camber compliance and aligning moment compliance steer. The suspension kinematic characteristics are a function of suspension geometry, and the suspension compliance characteristics are a function of the suspension geometry and bushing stiffness.

In the proposed ATC optimization framework, a suspension geometry model and a suspension compliance model work separately to achieve the desired kinematics and compliance targets set at the first layer of the optimization framework. Note that both suspension kinematics and compliance models use suspension pickup points—three-dimensional spatial coordinates—as common design variables and hence are represented as linking variables in the ATC framework.

In the most general form, ATC problem can be represented as [notations and formulations adapted from Li et al., [5] and Tosserams et al., 46]

$$\min_{\bar{x}_{11}\ldots,x_{NM}} \sum_{i=1}^{N}\sum_{j=\varepsilon_i} f_{ij}(\bar{x}_{ij}) + \sum_{i=2}^{N}\sum_{j=\varepsilon_i} \pi(t_{ij} - r_{ij}) \tag{3}$$

For Augumented Lagrangian ATC Formulation:

$$\begin{aligned}
&\pi(t_{ij} - r_{ij}) = \lambda_{ij}^{T}(t_{ij} - r_{ij}) + ||w_{ij} \bullet (t_{ij} - r_{ij})||_2^2 \\
&s.t.\ g_{ij}(\bar{x}_{ij}) \le 0 \\
&h_{ij}(\bar{x}_{ij}) = 0 \\
&t_{ij} - r_{ij} = 0 \\
&where\ \bar{x}_{ij} = [\bar{x}_{ij}, t_{(i+1)k} \forall k \in C_{ij}] \\
&r_{ij} = a_{ij}(\bar{x}_{ij}) \forall j \in \varepsilon_i,\ i = 1,\ldots,N
\end{aligned} \tag{4}$$

Here, the system is decomposed into N levels with M elements each. The subscript ij represents the jth element of the system in the ith level. The variable f_{ij} represents the scalar objective function, and $g_{ij} \le 0$, $h_{ij} = 0$ are the inequality and equality constraints respectively. Local variables of element j are denoted by x_{ij} . The variable r_{ij}

is the response of element j calculated by analysis model a_{ij}. ε_i is the set of elements at level i, and C_{ij} is the set of children of element j. t_{ij} represents target variable created for each shared variable. π denotes the consistency constraint relaxation function. In the case of the Augmented Lagrangian (AL) method, applied to ATC formulation, the consistency constraint function, π, is formulated as a combination of the quadratic penalty function $||w_{ij} \bullet (t_{ij} - r_{ij})||_2^2, w = [w_{ij}, \forall i, j]$ and the Lagrangian function $\lambda_{ij}^T (t_{ij} - r_{ij}), \lambda = [\lambda_{ij}, \forall i, j]$.

Genetic Algorithms

Genetic Algorithms (GAs) are used as the principal optimization technique in this research. GA is a stochastic, evolutionary, non-deterministic search method that can help attain a global optimum solution. Every iteration of the optimization schedule in the ATC framework described above requires coordination between three separate GA functions. The first GA works to optimize the vehicle-level targets, and the other two GA's work towards optimization of suspension kinematics and compliances subsystem-requirements. A Matlab based GA function was applied in this research. The outline of the algorithm is described below [45]:

- The algorithm begins by generating a random initial population.
- The algorithm then creates a sequence of new populations by using the individuals in the current generation to create the next population. To create the new population, the algorithm performs the following steps:

a. It scores each member of the current population by computing its fitness value.
b. It scales the raw fitness scores to convert them into a more usable range of values.
c. It selects members, called parents, based on their fitness.
d. Some of the individuals in the current population that have lower fitness are chosen as *elite*. These elite individuals are passed to the next population.
e. It produces children from the parents. Children are produced either by making random changes to a single parent—*mutation*—or by combining the vector entries of a pair of parents—*crossover*.
f. It replaces the current population with the children to form the next generation.

- The algorithm stops when one of the stopping criteria is met.

At each layer of the optimization framework, *function tolerance* can be used as the principal stopping criterion for the genetic algorithm. Using *function tolerance* as the stopping criterion means that the genetic algorithm will run until the average relative change in the fitness function value over *stall generations* is less than the specified *function tolerance*. The *function tolerance* value was set to 1e-3 and *stall generations* were set to 50 at each layer of the GA-based framework.

From the initial trials with the optimization framework, it was found that using function tolerance as the sole stopping criterion for GAs at each layer, coupled with multiple iterations of the ATC framework, was computationally expensive for the vehicle handling design problem under consideration. This is because every iteration of the optimization schedule in the ATC framework requires coordination between three separate GA functions.

On careful analysis of the optimization problem, it was observed that the fitness value of the optimization function showed maximal changes during the first few generations of each GA evaluation. In an effort to improve the convergence times, the maximum number of generations for each GA function evaluation was used as a stopping criterion, in addition to the *function tolerance* criterion described above. The solutions obtained after this modification were found to be extremely 'close' to the solutions obtained from using *function tolerance* as the only stopping criterion, while having considerably improved overall convergence time.

CHAPTER FIVE

APPLICATIONS OF THE PROPOSED RESEARCH METHODOLOGY

In this chapter, six different case studies are conducted to demonstrate the applications of the proposed systems engineering framework for systematic design of the desired vehicle handling characteristics:

1. Conceptual Development of a RWD Coupe incorporating Brand Attributes.
2. Conceptual Development of a RWD Coupe for Maximum Performance.
3. Determination of Vehicle Handling Bandwidth to Support the Target Setting Process.
4. Replicating the Vehicle Characteristics of a Competitor Vehicle.
5. Selection of the best solution from a set of Pareto-optimal solutions obtained from Genetic Algorithms (GA) using Market Research Data – Subsystem-Level Optimization.
6. Handling sensitivity studies using Design-of-Experiments (DOE).

5.1 Case Study One

Conceptual Development of a RWD Coupe incorporating Brand Attributes.

Objectives and Scope of the Case Study

The overall objective of this case study is to apply the systems engineering framework to develop and tune the front suspension of a sporty rear wheel drive (RWD) coupe. Assume a case study where it is desired to develop different "flavors" of chassis setups incorporating the essence of various vehicle brands using one-and-the-same vehicle architecture. The case study explores a hypothetical scenario of developing a sporty RWD coupe for the BMW, MINI, Lexus, Toyota, and Volvo brand. To limit the scope of this case study, it is assumed that each team of engineers belonging to a particular vehicle brand can only redesign the steering system, front and rear tires, and front-axle suspension characteristics starting from a common baseline chassis setup.

Quantification of Vehicle Handling Characteristics

The handling characteristics are grouped and categorized with respect to various scenarios of vehicle handling (see Table 1 and Table 4). These include: steady-state handling, transient handling, on-center handling, emergency handling, parking, steering feedback, handling on different road surfaces, coupled dynamic cornering, disturbance sensitivity, and straight-line stability.

The geometric and inertial parameters for the sporty RWD coupe platform used as the starting (or reference) vehicle for this case study are shown in Table 7. The objective handling characteristics of this reference vehicle are illustrated in Table 8.

Table 7. Geometric and Inertial Parameters of Reference Vehicle.

Description	**Units**	**Reference Vehicle**
Vehicle (total) Mass	kg	1378
Front Un-sprung Mass	kg	97
Rear Un-sprung Mass	kg	94
Sprung Mass	kg	1187
Yaw Inertia (Whole Vehicle)	kg m^2	1936
Roll Inertia (Whole Vehicle)	kg m^2	392
Pitch Inertia (Whole Vehicle)	kg m^2	1946
Wheelbase, m	m	2.706
Track Width, m	m	1.499
Vehicle Width, m	m	1.684
Vehicle Height, m	m	1.407
Longitudinal Distance from Total CG to Front Wheels	m	1.261
Longitudinal Distance from Total CG to Rear Wheels	m	1.445
Longitudinal Distance from CG of Sprung Mass to Front Wheels	m	1.250
Longitudinal Distance from CG of Sprung Mass to Rear Wheels	m	1.456
Height of Vehicle (total) CG Above Ground	m	0.500
Height of Sprung Mass CG Above Ground, m	m	0.550
Height of Front Un-sprung Mass CG Above Ground	m	0.318
Height of Rear Un-sprung Mass CG Above Ground	m	0.318

Table 8. Handling Performance Metrics for Reference Vehicle.

Handling Domains	Objective Handling Metrics	Unit	Reference Vehicle (RWD)
Steady-State Handling (v=80 km/h)	Understeer Gradient	deg/G	1.197
	Yaw Rate Gain	1/sec	0.307
	Side-Slip Angle Gain	deg/G	-1.34
	Roll Angle Gain	deg/G	3.57
Transient Handling (v=80 km/h)	Yaw Rate Time Constant	ms	105
	Yaw Rate Damping Ratio	-	0.918
	Lateral Acceleration Phase Lag	deg	-43.4
	Roll Angle Overshoot	%	8.0
Steering Feedback (v=80 km/h)	Steering Torque Gain (per Steering Angle)	Nm/deg	0.308
	Steering Torque Feel (per Lateral Acceleration)	Nm/G	25.4
On-Center (v=80 km/h)	Steering Torque Time Lag (@ 0.2 Hz)	ms	63
Parking	Lock-to-Lock Steering Rotations	-	3.2
	Turning Circle Diameter	m	10.47
	Parking Static Torque	Nm	10.3
Disturbance Sensitivity (v=80 km/h)	Yaw Moment Sensitivity	deg/KN m-sec	2.301
Coupled Dynamics (v=80 km/h)	Yaw Rate Increment (Acceleration out of Turn)	%	3.54
Road Adaptability (v=80 km/h)	Yaw Rate Increment (Cornering on Rough Roads)	%	-1.95
Straight-Line Stability	Straight-Line Stability Index	Nm/N	1.518
	Pitch Gradient	deg/G	1.79
Emergency Handling (Roll Stability)	Static Stability Factor	-	1.499
	NHTSA Stars	-	5

Optimization Framework

The optimization framework used for this case study is based on the Analytical Target Cascading (ATC) methodology described in detail in the previous section. The framework works in a two-layer optimization schedule. The first layer is used to derive subsystem-level requirements from overall vehicle-level targets, and the second layer is used to derive component-level specifications from subsystem-level requirements derived in the first step. Genetic Algorithms (GAs) are used at each layer of the framework.

The objective function used in the first layer of optimization is based on customer relevant vehicle handling attributes and considers the relative brand attribute weights (see Table 2 and Table 3). Table 2 shows the customer ratings and brand attributes for five different brands: Volvo, Toyota, BMW, Lexus, and MINI from the AutoPacific 2013 New Vehicle Satisfactory Survey. Table 3 shows the relative brand attribute ranking derived from the market data and gives insight into the strategic focus for each brands.

The first step in the creation of the objective function for the optimization process requires calculation of handling attribute values from objective metrics for the reference vehicle using empirical relationships shown in Table 5.

Step One: Calculate attribute values from objective metrics for a reference vehicle.

Attributes (From objective metrics)	**Sporty**	**Fun to Drive**	**Comforting**	**Safe and Secure**
Reference Vehicle	**-0.231**	**-0.500**	**-0.500**	**-0.334**

The second step requires determination of the percentage difference in absolute ratings between the reference brand and the other brands considered in this case study (shown in Table 2).

Step Two: Determine percentage difference in absolute ratings between the reference brand and other brands.

Brand Attribute Rating (From Market Survey)					% Difference from Reference Brand			
Brands	**Sporty**	**Fun to Drive**	**Comforting**	**Safe and Secure**	**Sporty**	**Fun to Drive**	**Comforting**	**Safe and Secure**
BMW	**4.31**	**4.63**	**3.65**	**4.42**	**10.3**	**8.9**	**0.7**	**9.2**
MINI	**4.63**	**4.78**	**3.16**	**3.93**	**18.4**	**12.4**	**-12.9**	**-2.8**
Toyota	**3.29**	**3.96**	**3.83**	**4.23**	**-15.8**	**-6.9**	**5.8**	**4.6**
Lexus	**3.59**	**4.23**	**4.21**	**4.47**	**-8.1**	**-0.5**	**16.3**	**10.6**
Volvo	**3.64**	**4.07**	**3.80**	**4.71**	**-6.9**	**-4.3**	**4.7**	**16.6**
Reference	**3.91**	**4.25**	**3.62**	**4.04**	**0.0**	**0.0**	**0.0**	**0.0**

The third step requires calculation of “desired” attribute values for each brand by considering the attribute values for reference brand (step one) and the percentage difference from reference brand (step two).

Step Three: Calculate desired attribute values (optimization targets) for other brands using steps one and two.

Desired Attribute Values based on % Difference from Reference Brand				
Brands	**Sporty**	**Fun to Drive**	**Comforting**	**Safe and Secure**
BMW	**-0.207**	**-0.456**	**-0.497**	**-0.303**
MINI	**-0.188**	**-0.438**	**-0.565**	**-0.343**
Toyota	**-0.267**	**-0.534**	**-0.471**	**-0.318**
Lexus	**-0.250**	**-0.503**	**-0.419**	**-0.298**
Volvo	**-0.247**	**-0.521**	**-0.476**	**-0.278**

Once new "desired" attribute values for the different brands are created, the relative brand attribute weights (shown in Table 3) are used to create the final objective function.

Step Four: Use brand attribute weights as weighting factors in the optimization.

Brand Attribute Weights: Weighting Factors					
Brands	**Sporty**	**Fun to Drive**	**Comforting**	**Safe and Secure**	**Sum**
BMW	**0.253**	**0.272**	**0.215**	**0.260**	**1.000**
MINI	**0.280**	**0.290**	**0.191**	**0.239**	**1.000**
Toyota	**0.215**	**0.259**	**0.250**	**0.276**	**1.000**
Lexus	**0.218**	**0.256**	**0.255**	**0.271**	**1.000**
Volvo	**0.224**	**0.251**	**0.234**	**0.291**	**1.000**

Results from the Optimization Schedule

The objective of this case study was to derive multiple chassis configurations for a common RWD sporty coupe architecture by incorporating the essence of different vehicle brands. Figure 14 and Figure 15 shows a performance spider diagram comparing the handling performance attributes, expressed in terms of customers' subjective expectations for five different brands—Volvo, Toyota, BMW, Lexus, and MINI. The handling spider diagram is based on relationships described in Table 5 and uses a ranking scheme where a higher value on the spider diagram represents improvement in the handling attribute.

From Figure 14 it is observed that the MINI concept is clearly the best in terms of *Sporty* and *Fun-to-Drive* attributes, the Lexus concept is best in terms of *Comfort*, and the

Volvo concept is best in terms of *Safety*. Among the five vehicle concepts, MINI is the least *Safe* and *Comfortable*, and Toyota is the least *Sporty* and *Fun-to-Drive*.

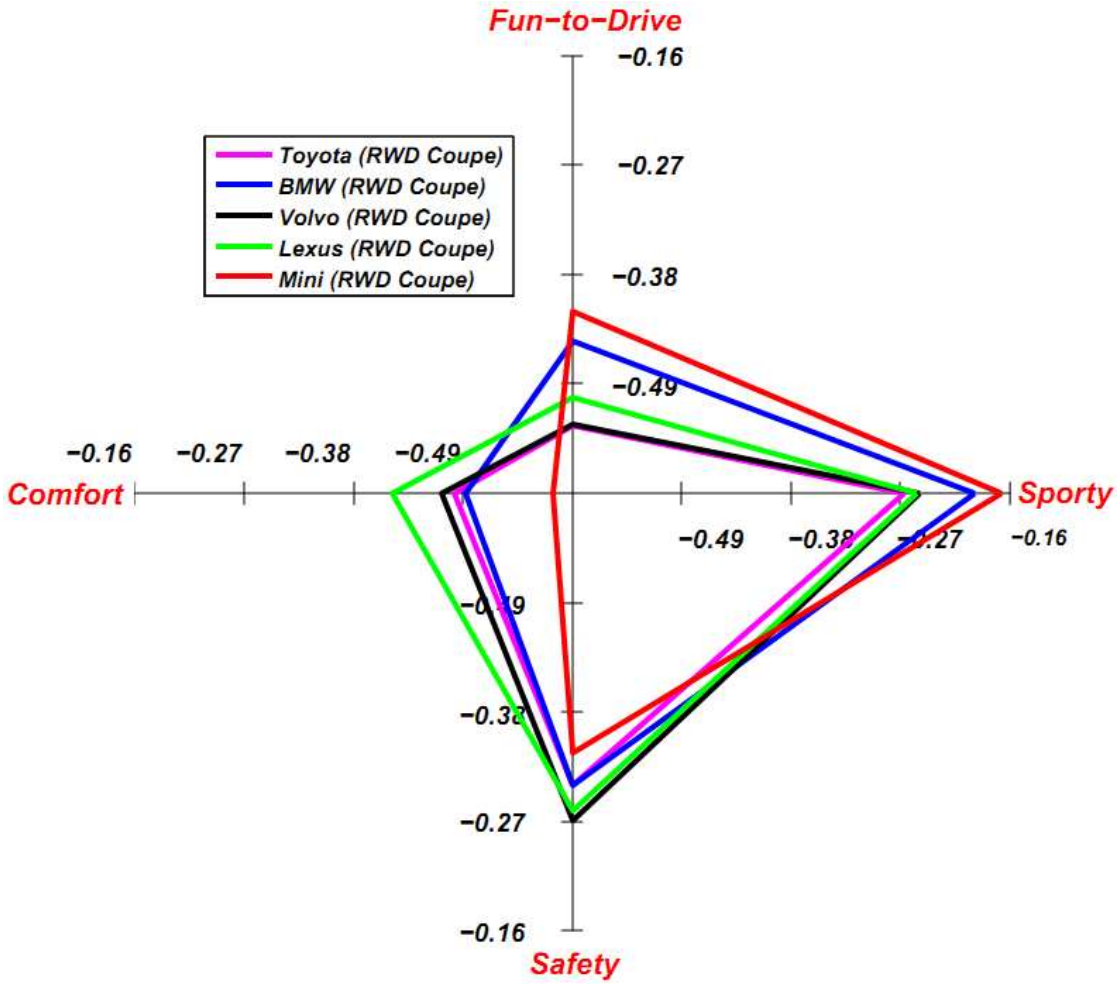

Figure 14. Vehicle Handling DNA Performance Spider Diagram & Performance Comparison, Higher Value on Handling Spider Diagram is Better (indicates improvement).

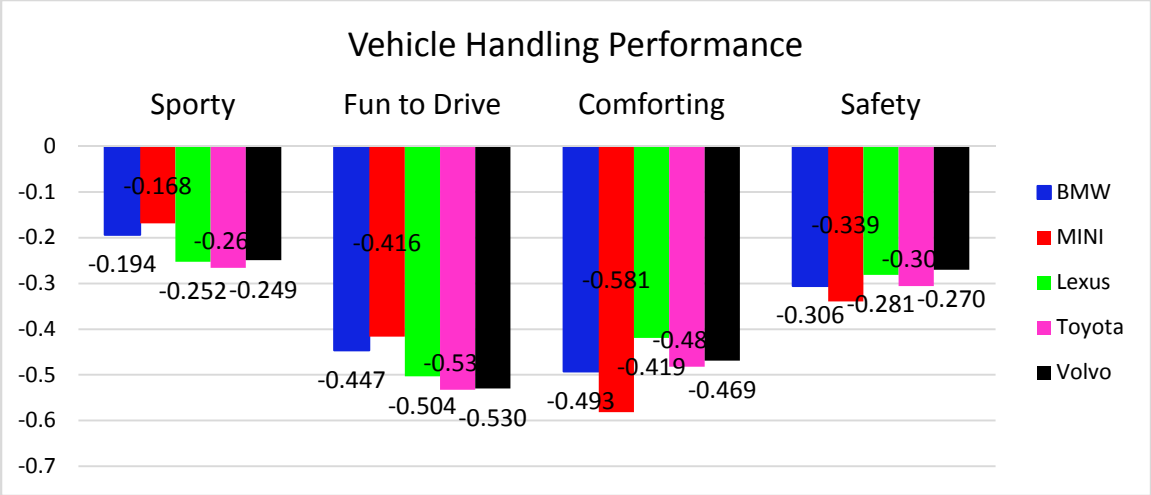

Figure 15. Vehicle Handling Attribute Chart. Higher (negative) Values Indicate Better Performance.

Table 9 compare the vehicle handling performance values for the five different configurations as an outcome of the optimization procedure. Among the five concepts derived from this case study, the MINI concept has the lowest understeer gradient and the highest yaw rate gain. The MINI concept also shows highest levels of steering torque gradients (wrt to lateral acceleration and steering angle), largest static parking torque value and requires least number of turns for lock-to-lock rotations. The MINI concept has the highest roll angle overshoot which is most probably the effect of side-slip angle and roll angle natural frequencies being very close to each other. This explains why the MINI concept is more *Sporty* and *Fun-to-Drive* than the other concepts but at the same time is least *Comfortable* and *Safe*.

Table 9. Comparison of Handling Performance Metrics for MINI, Lexus, BMW, Toyota and Volvo Concepts.

Handling Domains	Objective Handling Metrics	Units	MINI Concept	Lexus Concept	BMW Concept	Toyota Concept	Volvo Concept
Steady-State Handling (v=80 km/h)	Understeer Gradient	Deg/G	1.219	1.871	1.290	1.373	1.942
	Yaw Rate Gain	1/sec	0.304	0.237	0.296	0.292	0.270
	Side-Slip Angle Gain	Deg/G	-1.04	-1.82	-0.93	-1.34	-1.68
	Roll Angle Gain	Deg/G	4.30	1.74	3.16	4.82	2.17
Transient Handling (v=80 km/h)	Yaw Rate Time Constant	ms	95	110	91	105	108
	Yaw Rate Damping Ratio		0.943	0.918	0.968	0.924	0.903
	Lateral Acceleration Phase Lag	Deg	-36.7	-43.2	-33.7	-43.7	-42.1
	Roll Angle Overshoot	%	8.6	2.8	5.4	7.9	3.7
Steering Feedback (v=80 km/h)	Steering Torque Gain (per Steering Angle)	Nm/ deg	0.365	0.197	0.242	0.277	0.258
	Steering Torque Feel (per Lateral Acc.)	Nm/G	30.4	21.1	20.7	24.0	24.1
On-Center (v=80 km/h)	Steering Torque Time Lag (@ 0.2 Hz)	ms	47	73	42	61	65
Parking	Lock-to-Lock Steering Rotations		3.1	3.7	3.3	3.3	3.1
	Turn Circle Diameter	m	10.5	10.5	10.5	10.5	10.5
	Parking Static Torque	Nm	10.4	8.7	9.8	9.9	10.5
Disturbance Sensitivity (v=80 km/h)	Yaw Moment Sensitivity	Deg/ KN m-sec	2.101	2.436	2.02	2.26	2.34
Coupled Dynamics (v=80 km/h)	Yaw Rate Increment (Acceleration out of Turn)	%	3.76	4.44	3.72	3.85	4.86
Road Adaptability (v=80 km/h)	Yaw Rate Increment (Cornering on Rough Roads)	%	-1.96	-3.38	-2.47	-1.96	-2.89
Straight-Line Stability	Straight-Line Stability Index	Nm/N	1.497	1.474	1.503	1.469	1.501
	Pitch Gradient	Deg/G	1.94	1.45	2.77	1.59	2.30
Emergency Handling (Roll Stability)	Static Stability Factor	-	1.499	1.499	1.499	1.499	1.499
	NHTSA Stars	-	5	5	5	5	5

The BMW concept has the lowest magnitude of side-slip angle gain and is the most responsive among the other derived concepts. It has the least yaw rate time constant, lowest lateral acceleration phase lag and the least on-center time lag. It has the highest yaw rate damping ratio and least yaw moment sensitivity. The understeer gradient for the BMW concept is slightly higher than that of MINI but lower than any other concept, similarly, the yaw rate gain for the BMW concept is lower than that of a MINI but higher than any other concept. The BMW concept has the lower yaw rate increment during while accelerating out of a turn, lower roll angle overshoot and a lower yaw moment sensitivity than a MINI. Hence, the BMW concept represents a good balance between *Sporty*, *Fun-to-Drive* and *Safety* attributes.

Although, the Lexus concept is found to be the best in terms of *Comfort*, and the Volvo concept is found to be the best in terms of *Safety*, it is worth pointing out that the Volvo, Lexus and Toyota concepts were found to be very close to each other with respect to the different objective handling values.

The Lexus concept, as expected, has the least static parking torque value and the least steering torque gradient which minimizes the steering workload for the driver. However, this results in a vehicle that has the lowest yaw rate gain, highest side-slip angle gain, and a low yaw rate damping ratio. It is also the least responsive of all the concepts i.e., highest yaw rate time constant and on center delay, which also means that the vehicle is easy to drive, and forgiving in nature. The Lexus concept has the least roll and pitch angle gradient, and has the least roll angle overshoot. It is safe during split-mu

braking scenarios but is most sensitive to side-wind disturbances as indicated by high yaw moment sensitivity, and has a very high yaw rate increment during accelerating out of a turn scenario. This explains why the Lexus concept is the most *Comfortable* but not the most *Safest*. The Volvo concept has the largest understeer gradient indicating better yaw stability than any other concept derived from this case study. This is one of the most important factors explaining why the Volvo concept is the *Safest* among the others. It shows low values of rough road cornering index indicating better cornering stability over rough roads, low levels of roll angle overshoot indicating good roll stability, and low yaw moment sensitivity indicating better straight-line performance during side-wind disturbances. The Toyota concept on the other hand shows a very balanced set of attributes i.e., values of most of the objective metrics are found to be somewhere in between the best and worst of the five concepts.

One of the key strengths of the proposed methodology is that, for every vehicle concept derived through the optimization framework, the supporting subsystem- and component-level design variables are simultaneously determined, optimized and evaluated. The subsystem- and component-level design parameters are optimized considering realistic design and packaging constraints. In this case study, design variables for the three key chassis subsystems i.e., suspension, steering and tires, are derived for each of the five vehicle concepts —Volvo, Toyota, BMW, Lexus, and MINI. Detailed suspension component-level design specifications required to attain the suspension subsystem-level requirements are also derived.

Table 10. Comparison of Vehicle Subsystem-Level Design Variables.

Vehicle Design Variables				
Suspension Parameters				
Variables	Units	Reference Vehicle	BMW Concept	% Change
Roll Stiffness (Total)	Nm/deg	1,641	1,831	11.6
Roll Stiffness Distribution (Front)	%	65.3	50.8	-22.2
Roll Stiffness (Front)	Nm/deg	1,072	931	-13.2
Roll Stiffness (Rear)	Nm/deg	569	901	58.3
Front Wheel Rate (Suspension Stiffness, Front)	N/mm	26.60	16.59	-37.6
Rear Wheel Rate (Suspension Stiffness, Rear)	N/mm	18.40	12.45	-32.3
Roll Stiffness (sway bar, Front)	Nm/deg	573	606	5.7
Roll Stiffness (sway bar, Rear)	Nm/deg	129	656	408.9
Shock Damping (Front)	N-sec/mm	2,420	2,723	12.5
Shock Damping (Rear)	N-sec/mm	1,746	1,922	10.1
Lateral Force Compliance Steer (Front)	deg/N	-1.01E-04	-7.80E-05	-22.4
Lateral Force Compliance Steer (Rear)	deg/N	5.90E-06	5.90E-06	0.0
Lateral Force Camber Compliance (Front)	deg/N	1.18E-04	1.36E-04	15.4
Lateral Force Camber Compliance (Rear)	deg/N	6.35E-05	6.35E-05	0.0
Roll Camber (Front)	deg/deg	-0.620	-0.474	-23.5
Roll Camber (Rear)	deg/deg	-0.637	-0.637	0.0
Roll Steer (Front)	deg/deg	0.035	0.016	-54.4
Roll Steer (Rear)	deg/deg	-0.044	-0.044	0.0
Roll Center Height (Front)	mm	57.00	61.80	8.4
Roll Center Height (Rear)	mm	99.7	99.7	0.0
Anti-Dive Angle (Front)	deg	2.00	1.83	-8.4
Anti-Dive Angle (Rear)	deg	14	14	0.0
Steering Parameters				
Steering Ratio	-	16.4	17.3	5.5
Mechanical Trail	mm	30.00	24.72	-17.6
King Pin Inclination Angle	deg	12.39	9.98	-19.4
Caster Angle	deg	7.50	9.37	24.9
Scrub Radius	mm	34.00	28.43	-16.4
Aligning Torque Compliance Steer (Front)	deg/Nm	2.83E-04	2.53E-04	-10.6
Aligning Torque Compliance Steer (Rear)	deg/Nm	3.34E-04	3.34E-04	0.0
Tire Parameters				
Cornering Stiffness (Front, per tire)	N/deg	1,279	1,431	11.9
Cornering Stiffness (Rear, per tire)	N/deg	1,145	1,297	13.4
Cornering Stiffness Load Dependence Coefficient	a3	2,203	2,051	-6.9
BCD= a3 * sin (2 * atan (Fz ./ a4))	a4	11.21	8.80	-21.6
Camber Stiffness (Front, per tire)	N/deg	191.9	214.7	11.9
Camber Stiffness (Rear, per tire)	N/deg	171.7	194.6	13.4
Relaxation Length	mm	422.50	163.08	-61.4
Pneumatic Trail	mm	27.70	24.87	-10.2

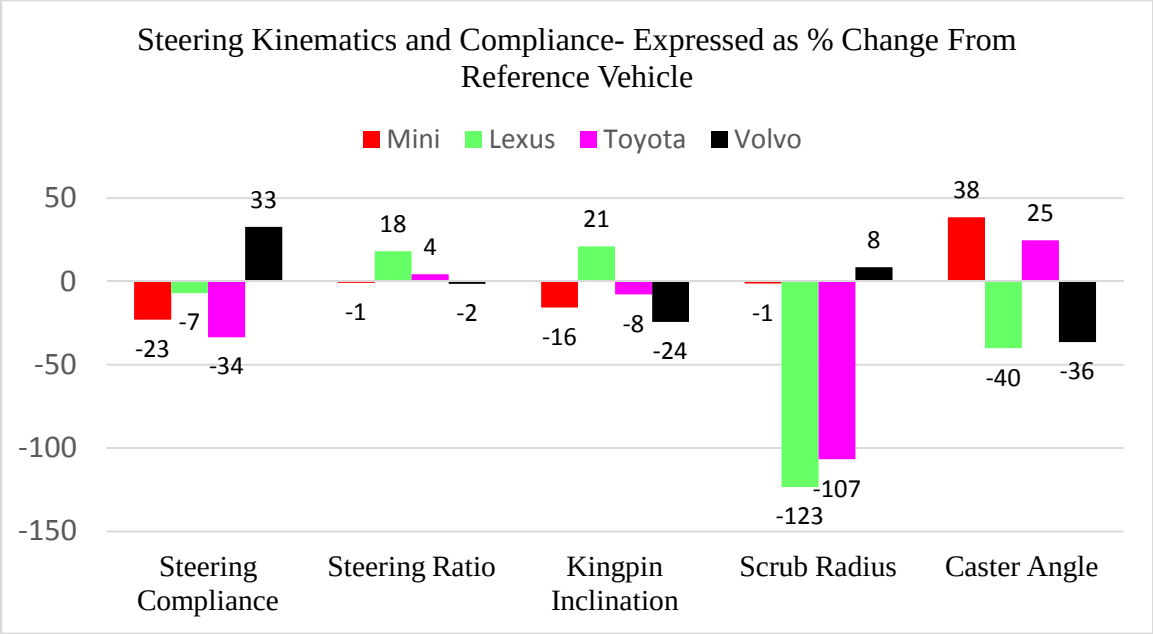

Figure 16. Comparison of Steering K&C.

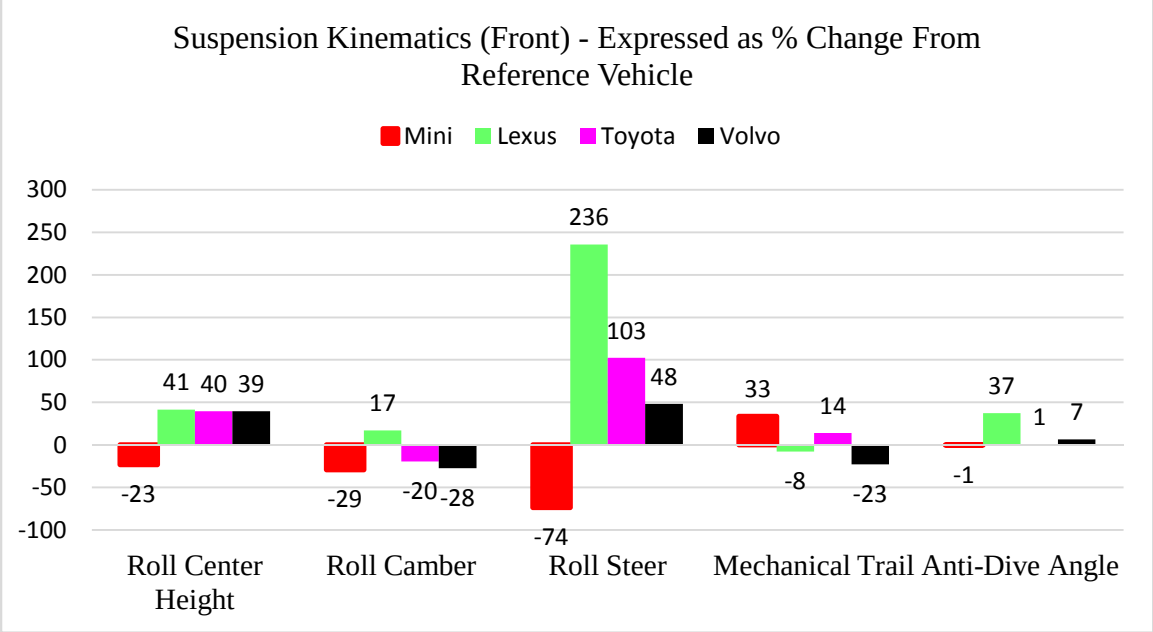

Figure 17. Comparison of Front Suspension Kinematics.

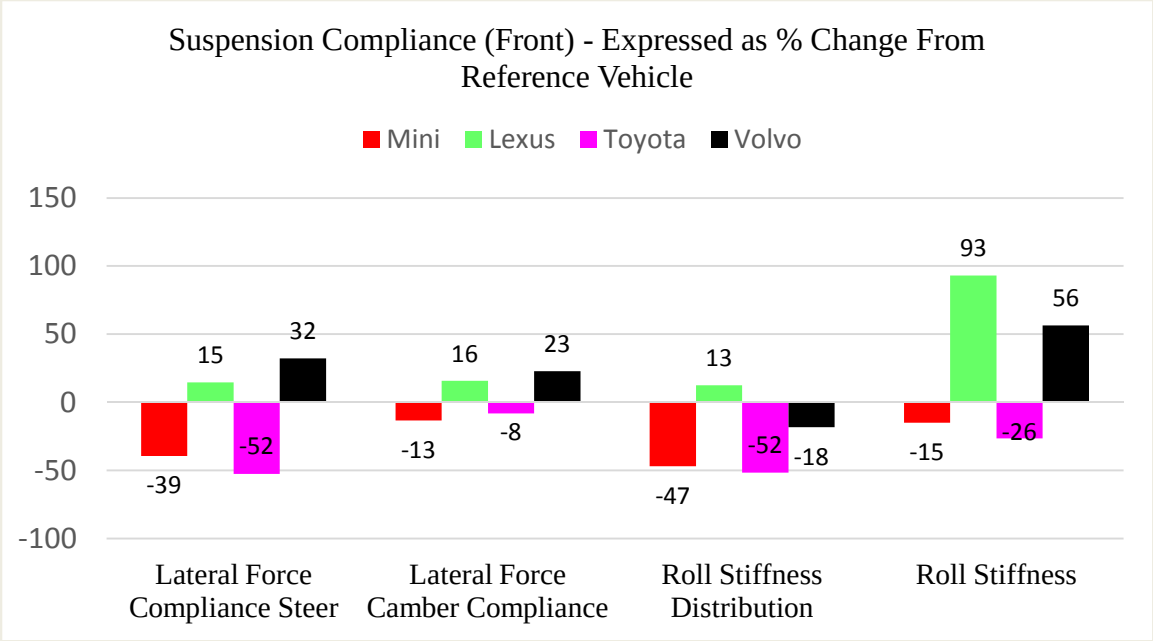

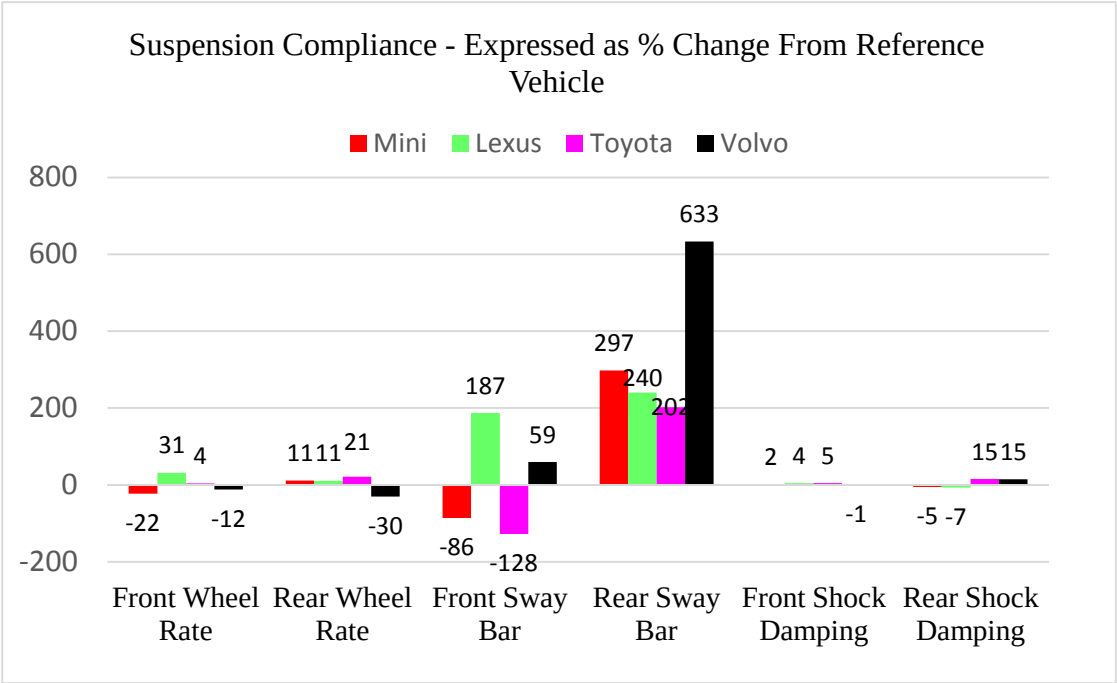

Figure 18. Comparison of Front Suspension Compliance.

Table 10 compares the subsystem-level design variables for the vehicle configuration (BMW concept) and the reference vehicle after applying the optimization. Figure 16, Figure 17, and Figure 18 show bar charts comparing the differences in the steering and suspension subsystem-level design variables derived from the optimization procedure for Lexus, MINI, Toyota, and Volvo concepts. Note that only front suspension design variables were independent for this case study.

Figure 19 shows the comparison of tire cornering stiffness characteristics for the five different concepts obtained from the optimized schedule. Note that both front and rear tires are assumed to have identical characteristics in this case study.

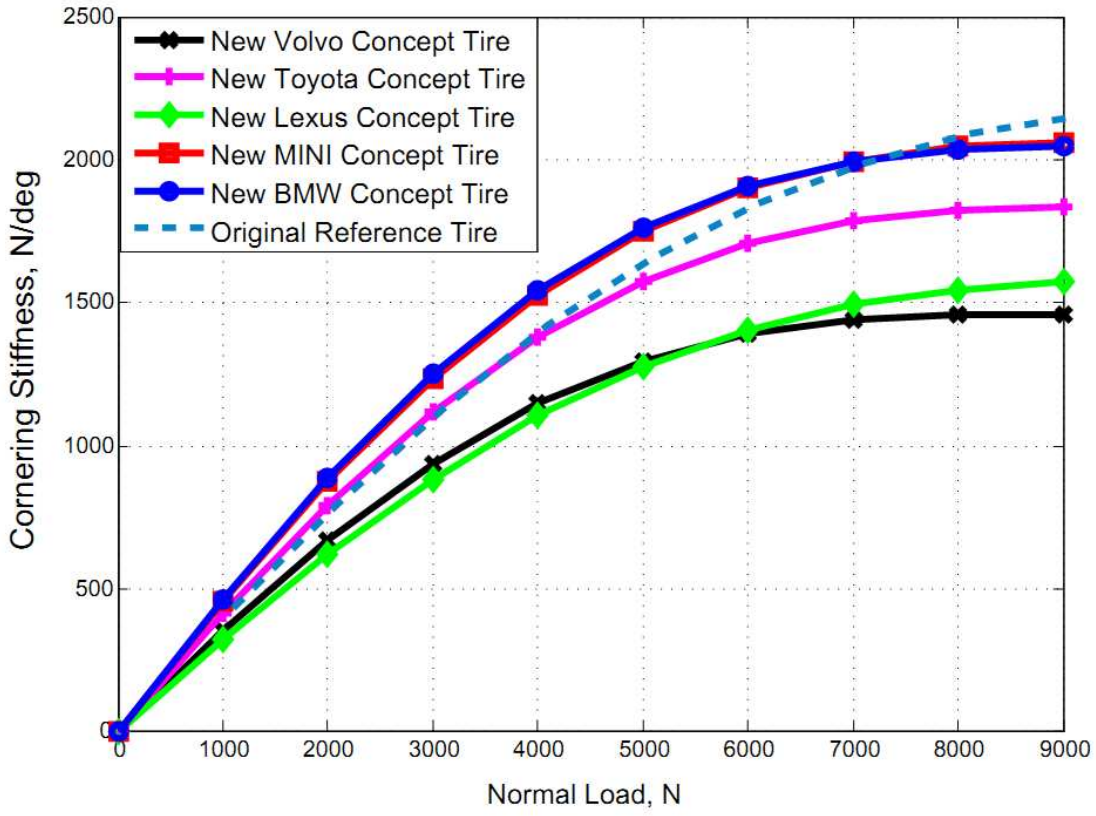

Figure 19. Tire Cornering Stiffness (N/deg) vs. Normal Load (N).

The suspension component-level specifications derived from the optimization schedule are shown next. The component-level specifications required to achieve the optimized subsystem-level kinematic and compliance coefficients are represented in terms of suspension spatial orientation (pick-up points) and suspension bushing stiffness.

Figure 20, Figure 22, and Figure 24 shows the optimized suspension geometry configuration (i.e., the re-designed suspension pick-up points). In this case study, only wheel-side points of suspension assembly were optimized i.e., only the front wheel knuckle was redesigned. Figure 21, Figure 23 and Figure 25 shows the suspension kinematic curves for the optimized suspension configurations. Table 11, and Figure 26 show the optimized bushing stiffness values obtained from the optimization schedule.

Conclusion

The case study described above demonstrates a unique method to integrate market research (and brand attribute weights) into the vehicle handling design process. The proposed method uses brand attribute information derived from market research for the development of vehicle-level targets, and guides the design direction of the chassis by the relative brand attributes weights. By using the market research inputs early on in the product development process, it was demonstrated that is possible to derive five different chassis setup configurations from one-and-the-same vehicle architecture. The systems engineering framework assured that vehicle-, subsystem- and component level specifications were systematically derived ensuring a consistent design solution accounting for realistic packaging constraints.

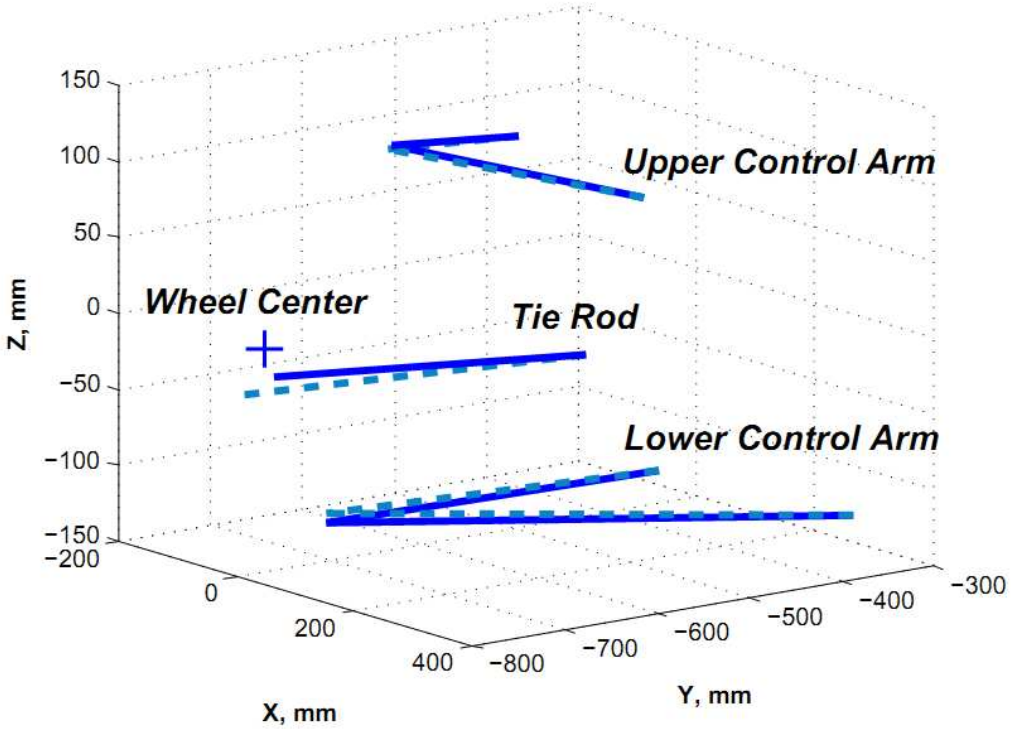

Figure 20. Optimized Suspension Geometry Configuration for Reference Vehicle & BMW Concept.

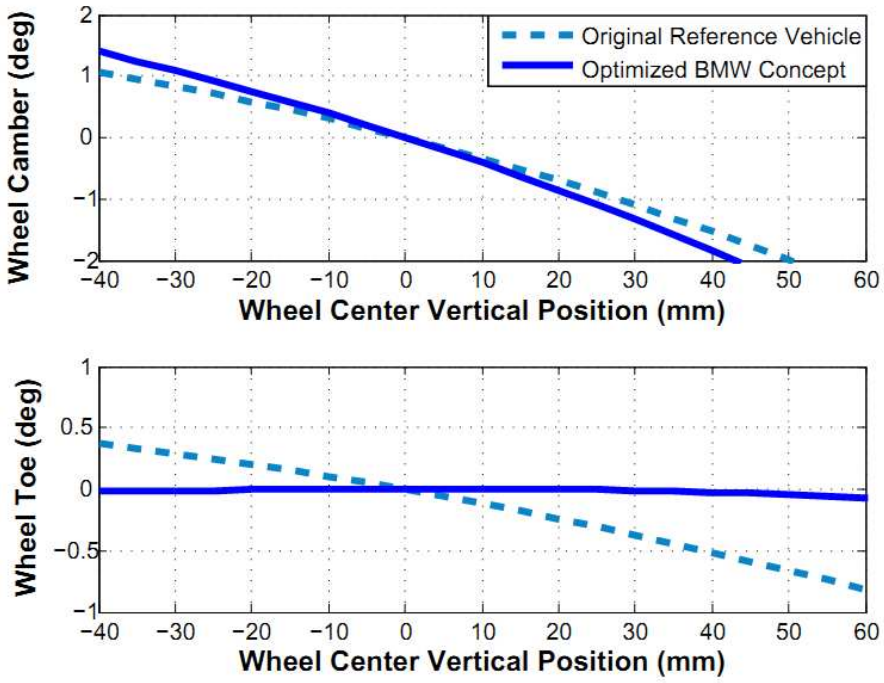

Figure 21. Optimized Suspension Kinematic Characteristics.

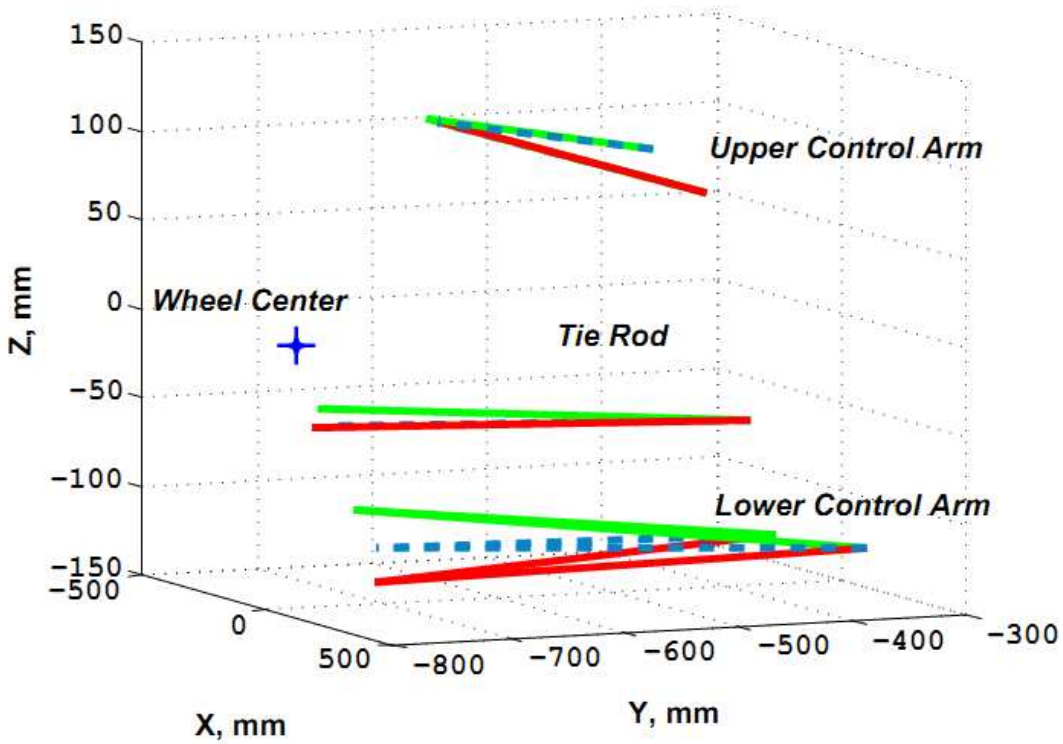

Figure 22. Optimized Suspension Geometry Configuration for Reference Vehicle, Lexus & MINI Concept.

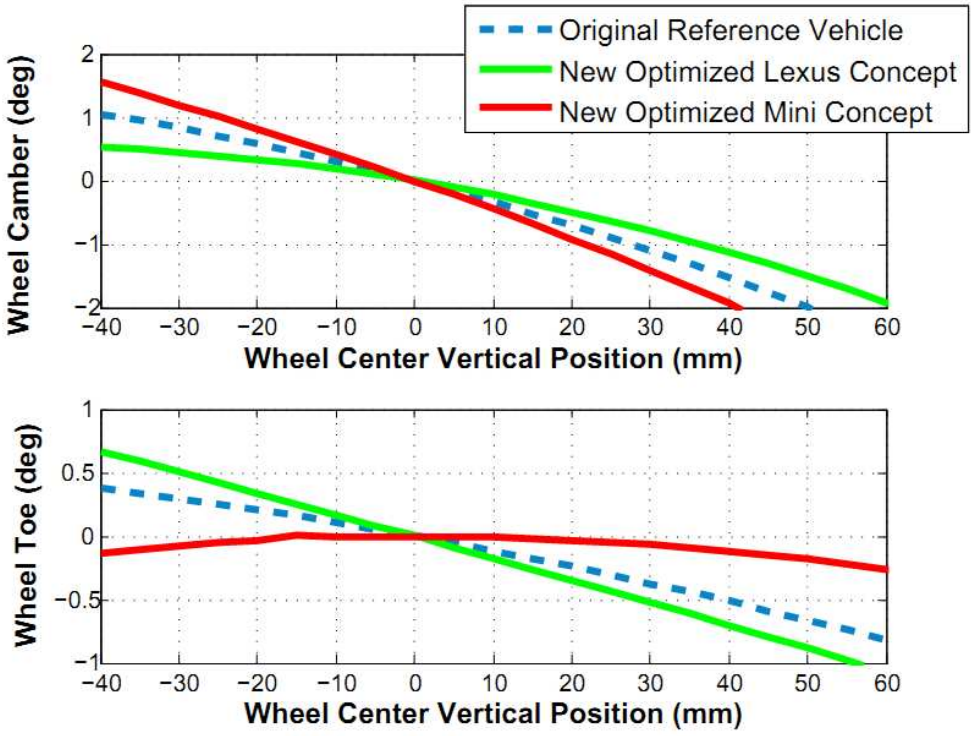

Figure 23. Optimized Suspension Kinematic Characteristics.

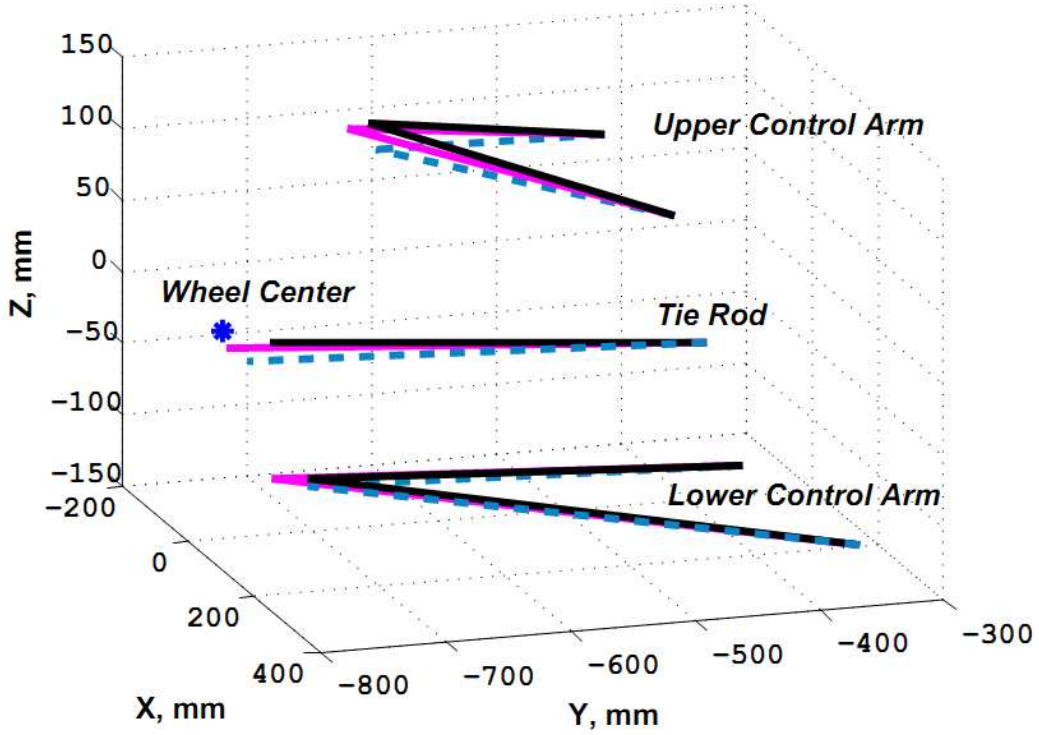

Figure 24. Optimized Suspension Geometry Configuration for Reference Vehicle, Toyota and Volvo Concepts.

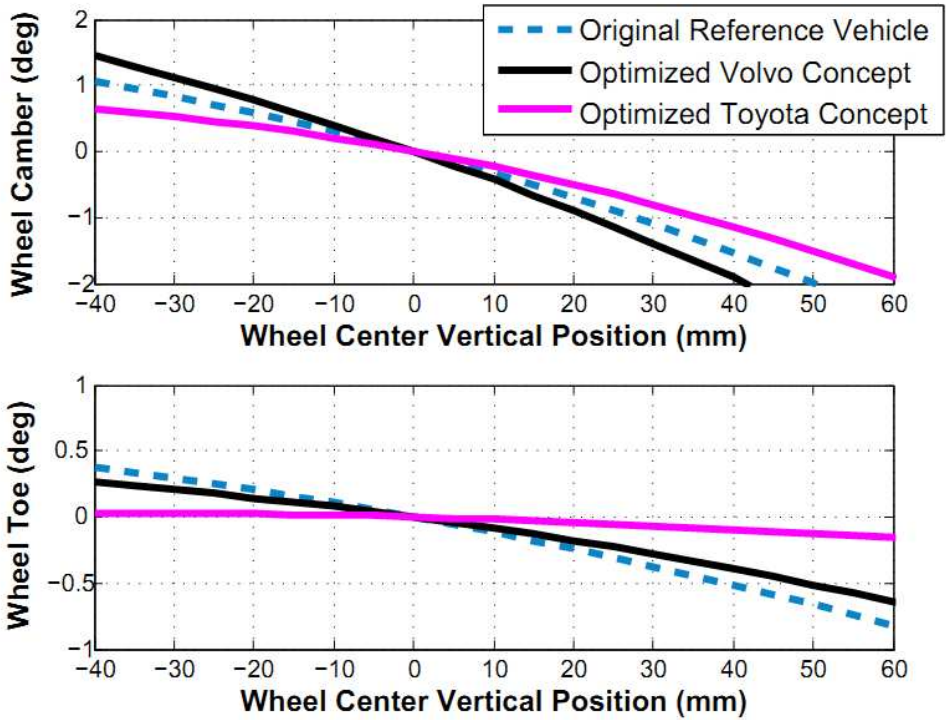

Figure 25. Optimized Suspension Kinematic Characteristics.

Table 11. Optimized Front Suspension Bushing Stiffness for Reference and BMW Concept.

Bushing Radial Stiffness (N/mm)			
	Reference Vehicle	Optimized-BMW Concept	% Change
Link 1 (Lower A Arm (F))	3,305	2,770	-16.2
Link 2 (Lower A Arm (R))	1,885	10,000	430.4
Link 3 (Upper A Arm (F))	7,831	3,983	-49.1
Link 4 (Upper A Arm (R))	3,531	1,310	-62.9
Link 5 (Tie Rod)	1.0E+09	1.0E+09	0

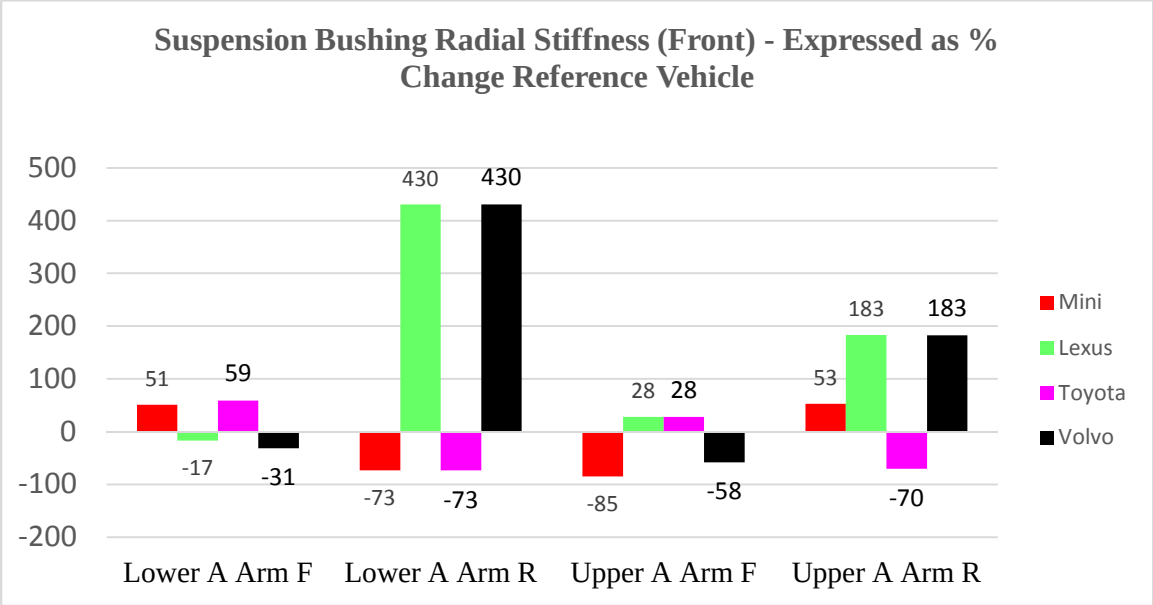

Figure 26. Front Suspension Bushing Stiffness.

5.2 Case Study Two

Conceptual Development of a RWD Coupe for Maximum Performance.

Objectives and Scope of the Case Study

The objective of this case study is apply the systems engineering chassis design framework to the conceptual design of a sporty RWD coupe to achieve maximum performance with respect to one of the four customer relevant vehicle attributes—*Sporty*, *Fun-to-Drive*, *Safety*, and *Comfort*. To limit the scope of this case study, it is assumed that the vehicle manufacturer can only redesign the steering system, front and rear tires, and front-axle suspension characteristics starting from a baseline chassis setup.

Optimization Framework

The objective fitness function used in the optimization schedule is setup for outright performance or maximum achievement of the handling attribute without considering the penalties suffered by the other attributes. The brand attribute weights used for this case study are shown below in Table 12.

Table 12. Brand DNA Weights used for deriving Maximum Performance Concepts.

Brand Weights – Trade-off Strategy					
Brands	Sporty	Fun-to-Drive	Comforting	Safe and Secure	SUM
Sporty	**0.7**	**0.1**	**0.1**	**0.1**	**1.0**
Fun-to-Drive	**0.1**	**0.7**	**0.1**	**0.1**	**1.0**
Comfort	**0.1**	**0.1**	**0.7**	**0.1**	**1.0**
Safety	**0.1**	**0.1**	**0.1**	**0.7**	**1.0**

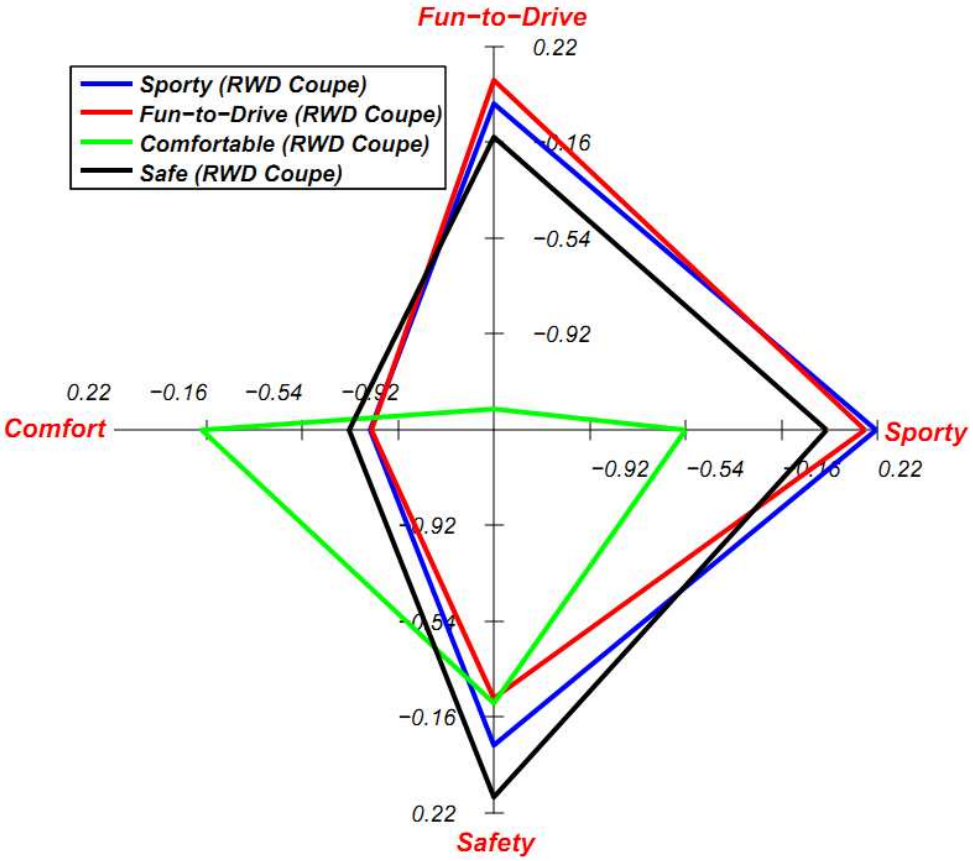

Figure 27. Vehicle Handling Attribute Diagram, Higher Value Indicates Improvement.

Results from the Optimization Scheme

Figure 27 shows a performance spider diagram comparing the handling attributes, expressed in terms of customers' subjective categories, for the four different concepts each representing maximum performance for —Sporty, Fun-to-Drive, Safety, and Comfort. The spider diagram is based on correlations described in Table 5 and uses a ranking scheme where a higher value on the spider diagram represents improvement in the handling attribute. From Figure 27 it is observed that each of the four concepts derived from the optimization schedule is maximum in terms of its respective handling attribute.

Table 13. Comparison of Handling Metrics for Maximum Performance Concepts.

Handling Domains	Objective Handling Metrics	Units	Sporty Concept	Fun-to-Drive Concept	Comfort Concept	Safe Concept
Steady-State Handling (v=80 km/h)	Understeer Gradient	deg/G	1.260	1.536	1.011	2.185
	Yaw Rate Gain	1/sec	0.368	0.350	0.276	0.310
	Side-Slip Angle Gain	deg/G	-0.30	0.11	-4.45	-0.47
	Roll Angle Gain	deg/G	1.55	1.54	1.55	1.63
Transient Handling (v=80 km/h)	Yaw Rate Time Constant	ms	75	66	176	80
	Yaw Rate Damping Ratio		0.990	1.000	0.947	0.962
	Lateral Acceleration Phase Lag	deg	-21.3	-15.9	-76.3	-23.2
	Roll Angle Overshoot	%	0.9	8.0	1.0	1.4
Steering Feedback (v=80 km/h)	Steering Torque Gain (per Steering Angle)	Nm/deg	0.606	0.564	0.182	0.467
	Steering Torque Feel (per Lateral Acc.)	Nm/G	41.7	40.8	16.7	38.2
On-Center (v=80 km/h)	Steering Torque Time Lag (@ 0.2 Hz)	ms	14	-2	217	16
Parking	Lock-to-Lock Steering Rotations		2.4	2.4	3.9	2.4
	Turn Circle Diameter	m	10.5	10.5	10.5	10.5
	Parking Static Torque	Nm	13.8	13.7	8.3	13.7
Disturbance Sensitivity (v=80 km/h)	Yaw Moment Sensitivity	Deg/KN m-sec	1.62	1.35	4.46	1.65
Coupled Dynamics (v=80 km/h)	Yaw Rate Increment (Acceleration out of Turn)	%	2.87	2.82	7.57	2.85
Road Adaptability (v=80 km/h)	Yaw Rate Increment (Cornering on Rough Roads)	%	-1.01	-1.89	0.00	0.01
Straight-Line Stability	Straight-Line Stability Index	Nm/N	1.482	1.504	1.433	1.496
	Pitch Gradient	Deg/G	1.21	1.21	1.40	2.30
Emergency Handling (Roll Stability)	Static Stability Factor	-	1.499	1.499	1.499	1.499
	NHTSA Stars	-	5	5	5	5

Table 13 compares the vehicle handling performance metrics for the four different configurations derived from the optimization procedure. From Table 13 it is observed that the *Fun-to-Drive* concept has the lowest magnitude of side-slip angle gain, in fact the *Fun-to-Drive* concept shows a positive value of side-slip angle gain whereas all the other derived concepts show negative values of side-slip angle gain. Consequently the *Fun-to-Drive* concept is the most responsive vehicle of all. It has the least yaw rate time constant, lowest lateral acceleration phase lag and the least on-center time lag. It also has the highest yaw rate damping ratio and least yaw moment sensitivity. However the *Fun-to-Drive* concept has the highest roll angle overshoot which is most probably the effect of an overlap of side-slip angle and roll angle natural frequencies. The *Sporty* concept, on the other hand, has the highest yaw rate gain and is only next to *Fun-to Drive* concept with respect to side-slip angle gain, yaw rate time constant, yaw rate damping ratio, and other transient handling metrics. The *Sporty* concept also has the highest steering torque gradients (wrt to lateral acceleration and steering angle).

The *Comfort* concept, as expected, has the least static parking torque value and the least steering torque gradient (wrt to lateral acceleration and steering angle), to minimize driver physical steering workload. But this results in a vehicle that has the least yaw rate gain, highest magnitude of side-slip angle gain, and the lowest yaw rate damping ratio. It is also the least responsive of all the other concepts i.e., it has the highest yaw rate time constant and on-center delay. The *Comfort* concept has the lowest straight-line stability margin indicating good straight-line stability during split-mu scenarios but shows highest yaw moment sensitivity and high yaw rate increment during

acceleration out of a turn. The *Safe* concept as expected has the highest understeer gradient indicating high yaw stability and has lowest rough road cornering index again indicating better cornering stability over rough roads. The *Safe* concept also shows very low levels of roll angle overshoot representative of good roll stability, and low yaw moment sensitivity implying better straight-line stability during side-wind disturbances.

As described earlier in this thesis, one the most important advantages of using an ATC based optimization framework for the vehicle handling design process is that, it always results in a consistent optimized configuration; meaning that the framework provides all the necessary subsystem and component-level design specifications required for realization of the optimized vehicle concept. The resulting subsystem and component-level specifications for the four concepts representing maximum performance for — *Sporty*, *Fun-to-Drive*, *Safety*, and *Comfort*—are described next.

Table 14 compares the subsystem-level design variables for the optimized vehicle configuration (Sporty concept) and the reference vehicle. Figure 28, Figure 29, and Figure 30 show bar charts comparing the differences in the subsystem-level design variables derived from the optimization procedure for the four optimized concepts. Note that only front suspension design variables were independent for this case study (i.e., only the front suspension was redesigned).

Table 14. Comparison of Vehicle Subsystem-Level Design Variables.

Vehicle Design Variables				
Suspension Parameters				
Variables	Units	Reference Vehicle	Sporty Concept	% Change
Roll Stiffness (Total)	Nm/deg	1,641	3,561	117.0
Roll Stiffness Distribution (Front)	%	65.3	32.1	-50.9
Roll Stiffness (Front)	Nm/deg	1,072	1,143	6.6
Roll Stiffness (Rear)	Nm/deg	569	2419	325.1
Front Wheel Rate (Suspension Stiffness, Front)	N/mm	26.60	39.87	49.9
Rear Wheel Rate (Suspension Stiffness, Rear)	N/mm	18.40	27.54	49.7
Roll Stiffness (sway bar, Front)	Nm/deg	573	361	-36.9
Roll Stiffness (sway bar, Rear)	Nm/deg	129	1,879	1356.5
Shock Damping (Front)	N-sec/mm	2,420	2,168	-10.4
Shock Damping (Rear)	N-sec/mm	1,746	2,095	20.0
Lateral Force Compliance Steer (Front)	deg/N	-1.01E-04	-5.10E-05	-49.2
Lateral Force Compliance Steer (Rear)	deg/N	5.90E-06	5.90E-06	0.0
Lateral Force Camber Compliance (Front)	deg/N	1.18E-04	9.33E-05	-20.9
Lateral Force Camber Compliance (Rear)	deg/N	6.35E-05	6.35E-05	0.0
Roll Camber (Front)	deg/deg	-0.620	-0.338	-45.5
Roll Camber (Rear)	deg/deg	-0.637	-0.637	0.0
Roll Steer (Front)	deg/deg	0.035	0.031	-12.3
Roll Steer (Rear)	deg/deg	-0.044	-0.044	0.0
Roll Center Height (Front)	mm	57.00	80.57	41.4
Roll Center Height (Rear)	mm	99.7	99.7	0.0
Anti-Dive Angle (Front)	deg	2.00	1.59	-20.6
Anti-Dive Angle (Rear)	deg	14	14	0.0
Steering Parameters				
Steering Ratio	-	16.4	12.3	-25.0
Mechanical Trail	mm	30.00	37.93	26.4
King Pin Inclination Angle	deg	12.39	10.28	-17.0
Caster Angle	deg	7.50	9.96	32.8
Scrub Radius	mm	34.00	-14.91	-143.8
Aligning Torque Compliance Steer (Front)	deg/Nm	2.83E-04	1.35E-04	-52.4
Aligning Torque Compliance Steer (Rear)	deg/Nm	3.34E-04	3.34E-04	0.0
Tire Parameters				
Cornering Stiffness (Front, per tire)	N/deg	1,279	1,520	18.8
Cornering Stiffness (Rear, per tire)	N/deg	1,145	1,349	17.9
Cornering Stiffness Load Dependence Coefficient	a3	2,203	3,071	39.4
BCD= a3 * sin (2 * atan (Fz ./ a4))	a4	11.21	10.59	-5.6
Camber Stiffness (Front, per tire)	N/deg	191.9	227.9	18.8
Camber Stiffness (Rear, per tire)	N/deg	171.7	202.4	17.9
Relaxation Length	mm	422.50	104.02	-75.4
Pneumatic Trail	mm	27.70	33.20	19.8

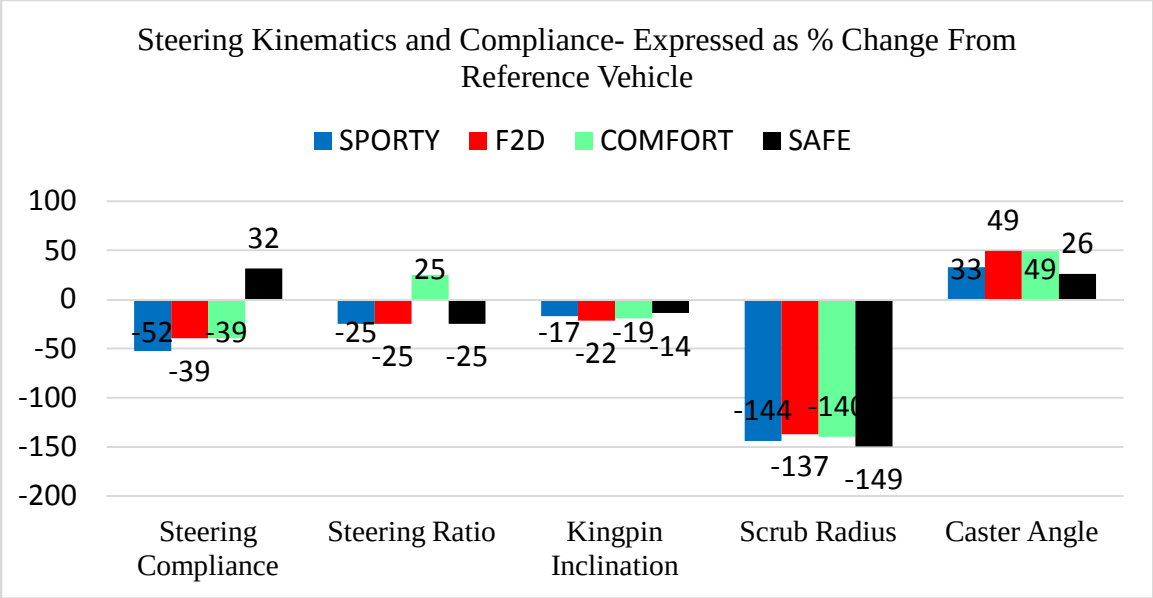

Figure 28. Comparison of Steering K&C Parameters.

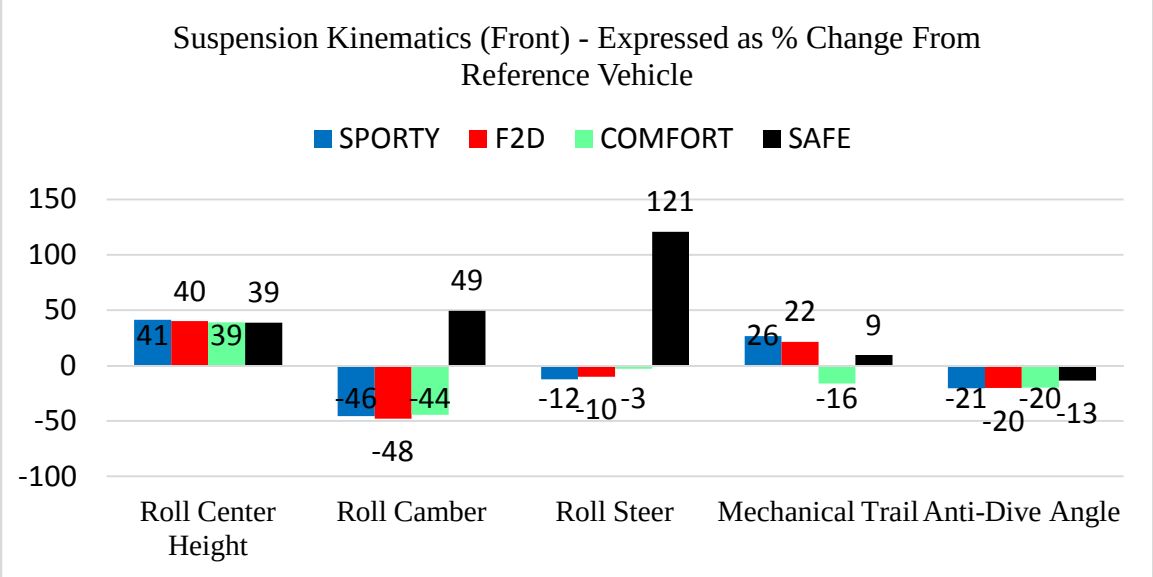

Figure 29. Comparison of Front Suspension Kinematics.

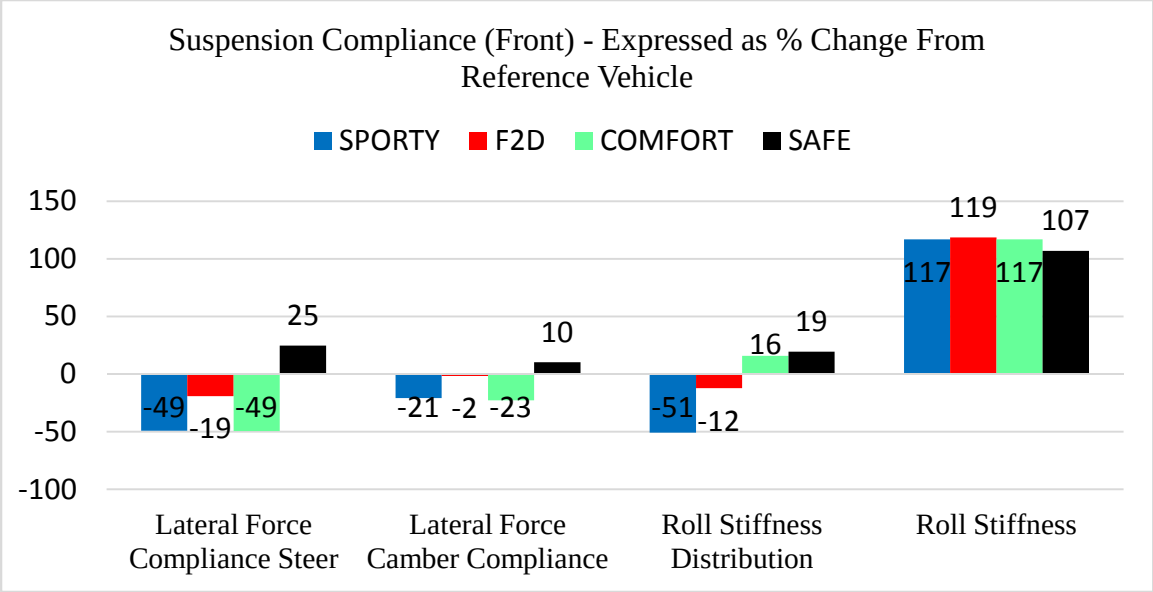

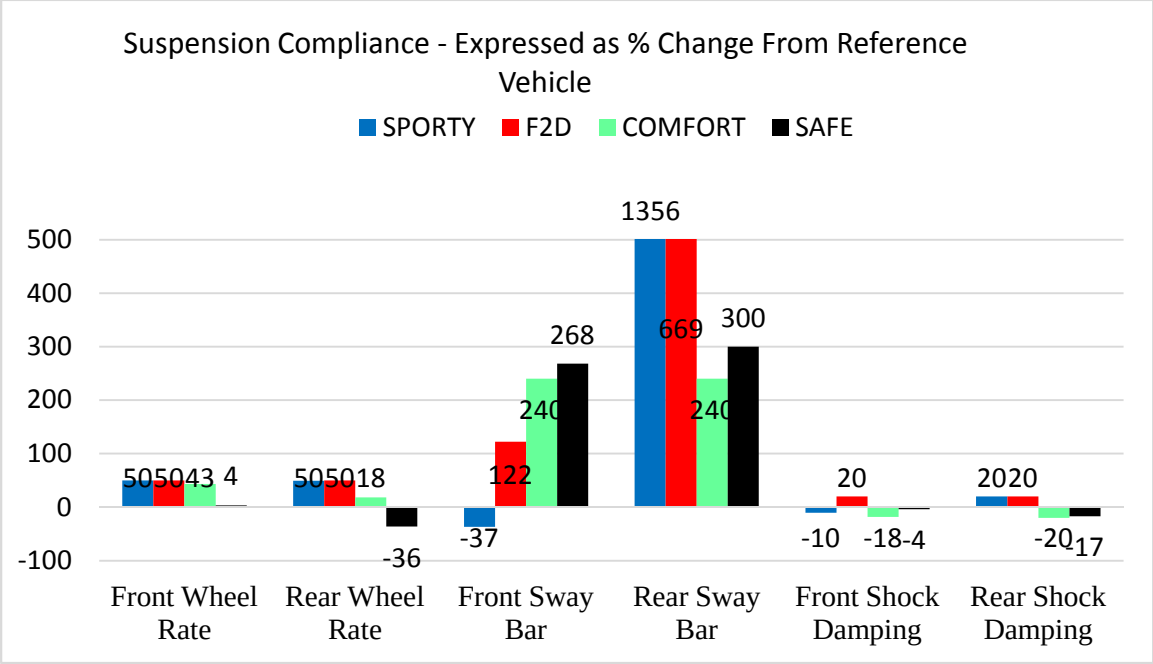

Figure 30. Comparison of Front Suspension Compliances.

Figure 31 shows the comparison of tire cornering stiffness characteristics for the five different concepts obtained from the optimized schedule. Note that both front and rear tires are assumed to have identical characteristics in this case study.

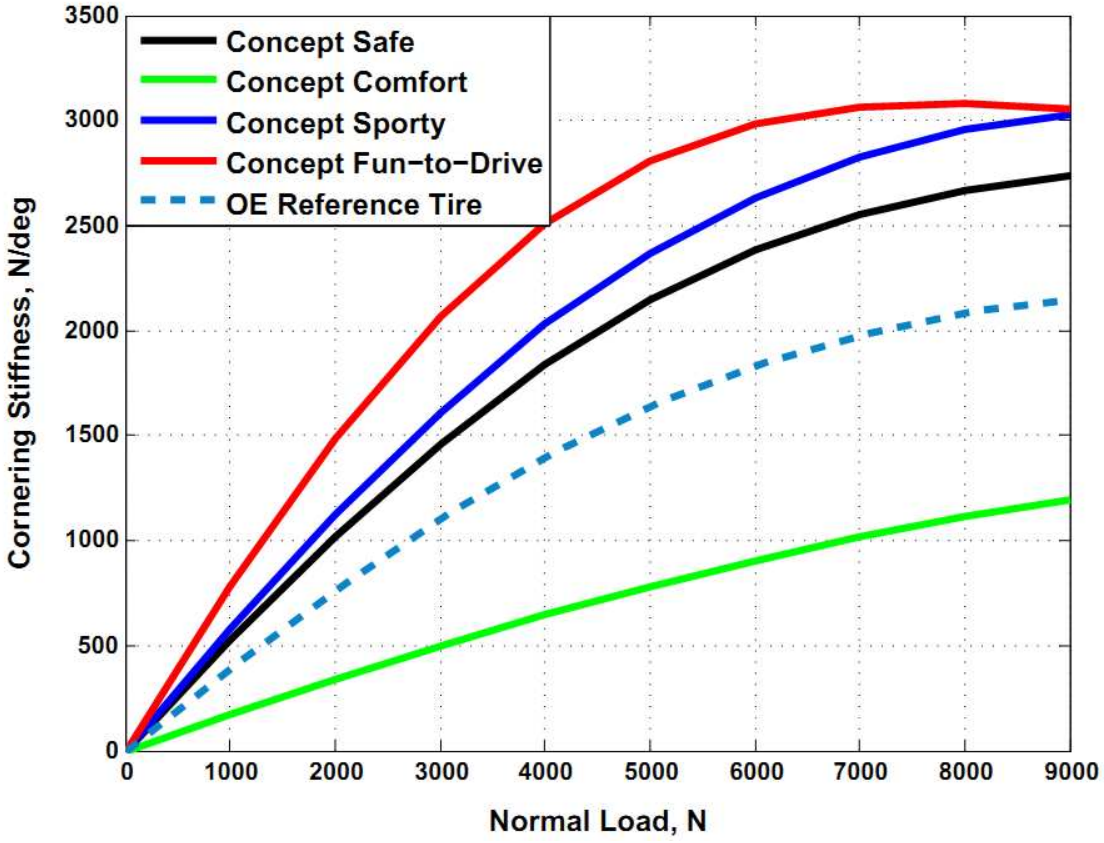

Figure 31. Tire Cornering Stiffness (N/deg) vs. Normal Load (N).

Figure 32 shows the optimized suspension geometry configuration (i.e., the re-designed suspension pick-up points). In this case study, only wheel-side points of suspension assembly were optimized i.e., only the front wheel knuckle was redesigned. Figure 33 shows the suspension kinematic curves for the optimized suspension configurations. Table 15, and Figure 34 shows the optimized bushing stiffness obtained from the optimization schedule.

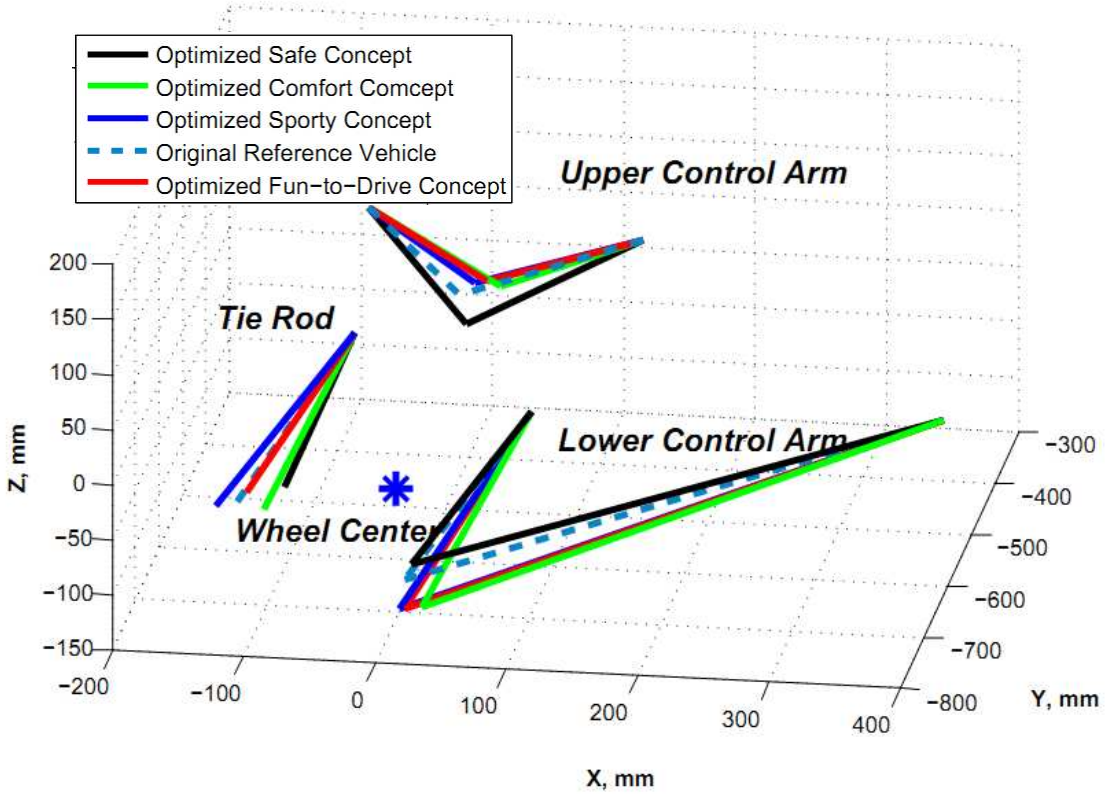

Figure 32. Optimized Suspension Geometry Configuration.

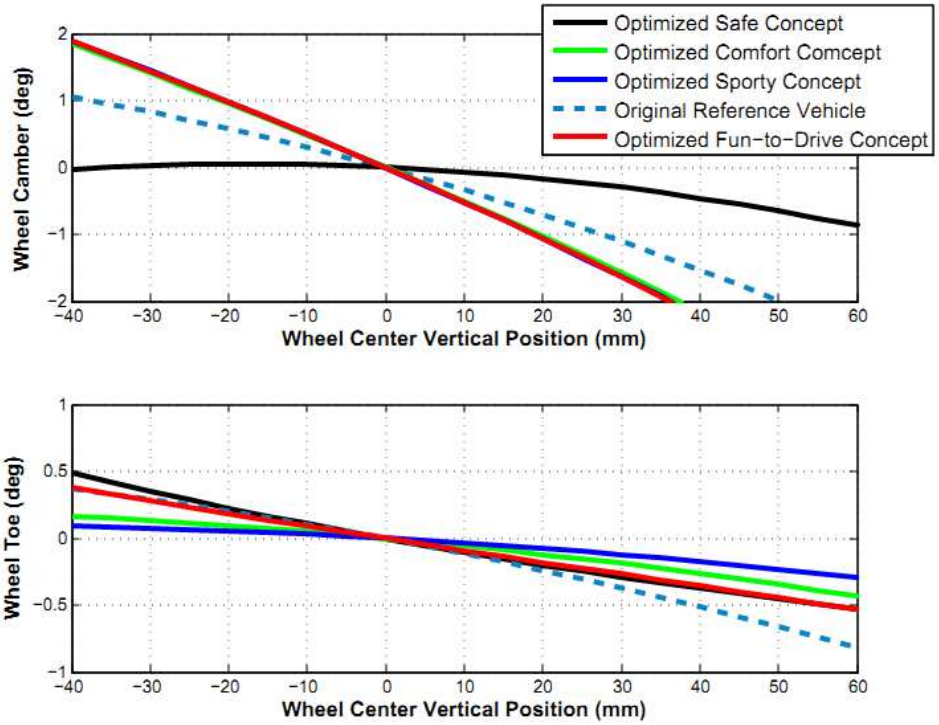

Figure 33. Optimized Suspension Kinematic Characteristics.

Table 15. Optimized Front Suspension Bushing Stiffness for Reference and Sporty Concept.

Bushing Radial Stiffness (N/mm)			
	Reference Vehicle	Optimized-Sporty Concept	% Change
Link 1 (Lower A Arm (F))	3,305	4,140	25
Link 2 (Lower A Arm (R))	1,885	559	-70
Link 3 (Upper A Arm (F))	7,831	9,857	26
Link 4 (Upper A Arm (R))	3,531	9,828	178
Link 5 (Tie Rod)	1.0E+09	1.0E+09	0

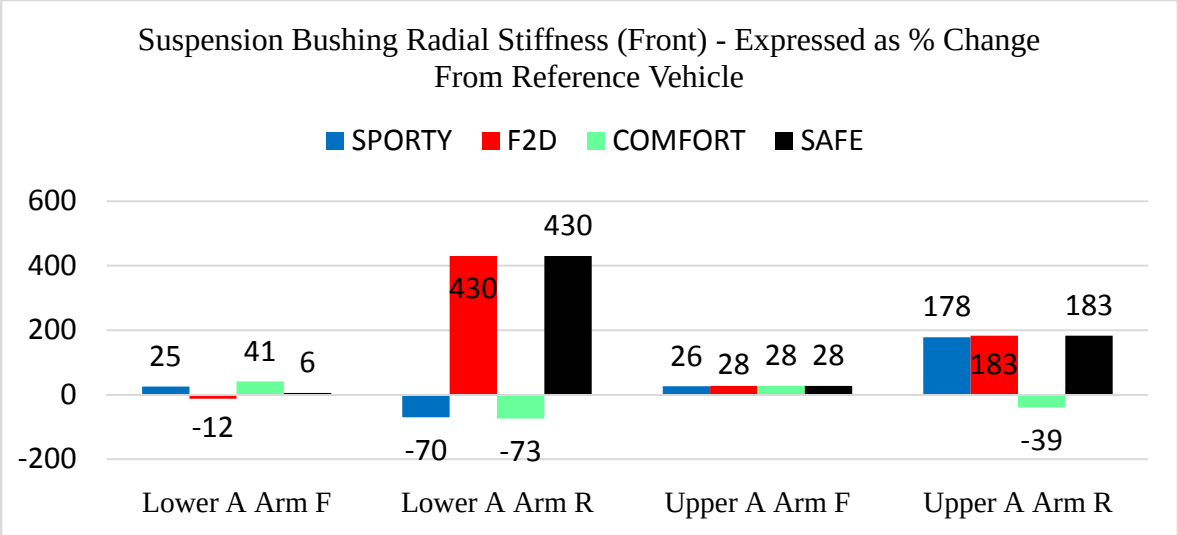

Figure 34. Front Suspension Bushing Stiffness.

Conclusion

In this case study, four concepts were derived from the same vehicle architecture representing maximum performance with respect to one of the four customer relevant vehicle attributes—*Sporty, Fun-to-Drive, Safety,* and *Comfort.* This case study demonstrates the application of the proposed systems engineering framework for aftermarket chassis suppliers; who are primarily interested in outright maximization of a specific customer relevant handling attribute without much consideration of the performance degradation of other attributes. This case study also demonstrates the usefulness of the proposed framework for exploration of the available design space during conceptual design. Knowledge of the maximum limits of achievable handling performance attributes can be very insightful for the chassis engineers and can greatly help in the handling design process.

5.3 Case Study Three

Determination of Vehicle Handling Bandwidth to Support the Target Setting Process.

As described in the earlier sections of this dissertation, the overall objective of this thesis is to develop a systematic processes and appropriate mathematical tools that can support vehicle definition during the concept development phase with the aim to reduce development time, increase early design maturity, resolve trade-offs, and balance solutions.

An important aspect of achieving these goals, is to assure that the higher-level targets set during the *Definition Phase* (see Figure 1) of the vehicle development process are realistic and achievable within the framework of limitations of fundamental physics, available technology, time, and cost. Traditional best-practice methods are heavily relying on benchmarking of competitor vehicles to develop vehicle-level targets. Competitive benchmarking may lead to products with performance levels that exceed customers' expectations and may lead to unnecessary engineering effort, higher product costs and weight, and can result in product performance that may not be perceived by the end-user.

Using the methodology described in this thesis, *Vehicle Handling Bandwidth Diagrams* are developed to help with the target-setting process. *Vehicle Handling*

Bandwidth Diagrams are indicators of the minimum and maximum limits of performance attributes achievable within realistic design constraints for a given chassis architecture.

A key consideration while creating the bandwidth diagrams is the way in which the trade-offs between the different customer relevant handling attributes are addressed. It is important to note that an Original Equipment Manufacturer (OEM) bandwidth diagram will be different from that of an aftermarket handling bandwidth diagram. In the case of OEM bandwidth diagrams, the balance among the attributes is more constrained than with an aftermarket setup since OEMs have to tailor their products to a large audience and cannot move the trade-offs to extreme levels of emphasizing one attribute (e.g. “sporty”) at the cost of another one (e.g. “comfort”). Most aftermarket chassis systems will emphasize certain performance attributes at the cost of others because it is the consumer’s intention to change the setup towards a particular direction.

In this research, two such handling bandwidth diagrams for a passenger car with sporty rear wheel drive (RWD) coupe architecture (see Table 7), are developed. Figure 35 shows the OEM handling bandwidth diagram, and Figure 36 shows the aftermarket handling bandwidth diagram.

The OEM handling bandwidth diagram shown in Figure 35 is created by considering the relative brand attribute ranking and brand essence information derived from the market data (see Table 2 and Table 3) and by the using same procedure described in Case Study 1. The OEM handling bandwidth diagram shown in Figure 35 is

developed considering the relative brand attribute ranking of five different OEM's—Volvo, BMW, Toyota, Lexus, and MINI.

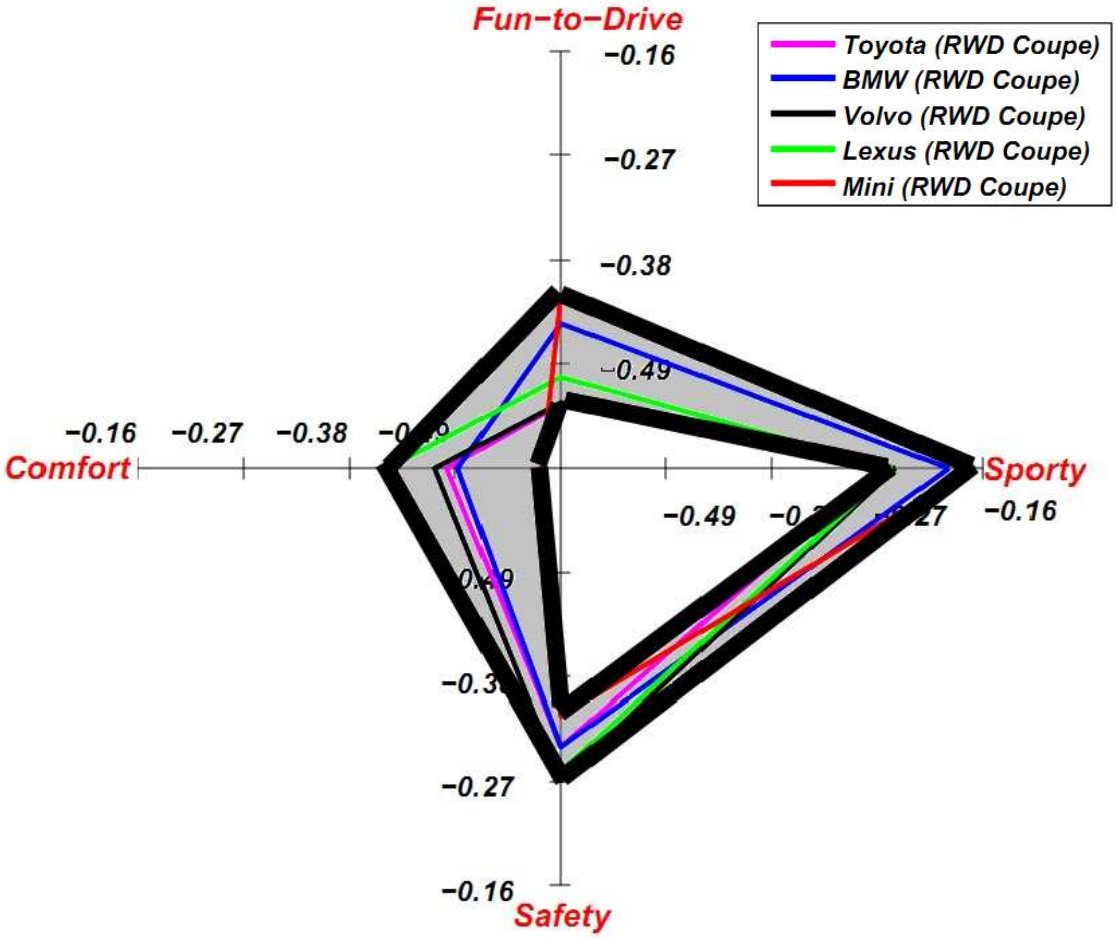

Figure 35. OEM Vehicle Handling Bandwidth Diagram (Based on Brand Attribute Ranking of five OEM's—Volvo, BMW, Toyota, Lexus, and MINI).

The aftermarket handling bandwidth diagram shown in Figure 36 is created for maximum performance/achievement of the handling attribute without considering the penalties suffered by the other attributes. The aftermarket diagram shown in Figure 36 is created by using the brand attribute weights shown in Table 12 and the procedure described in Case Study 2.

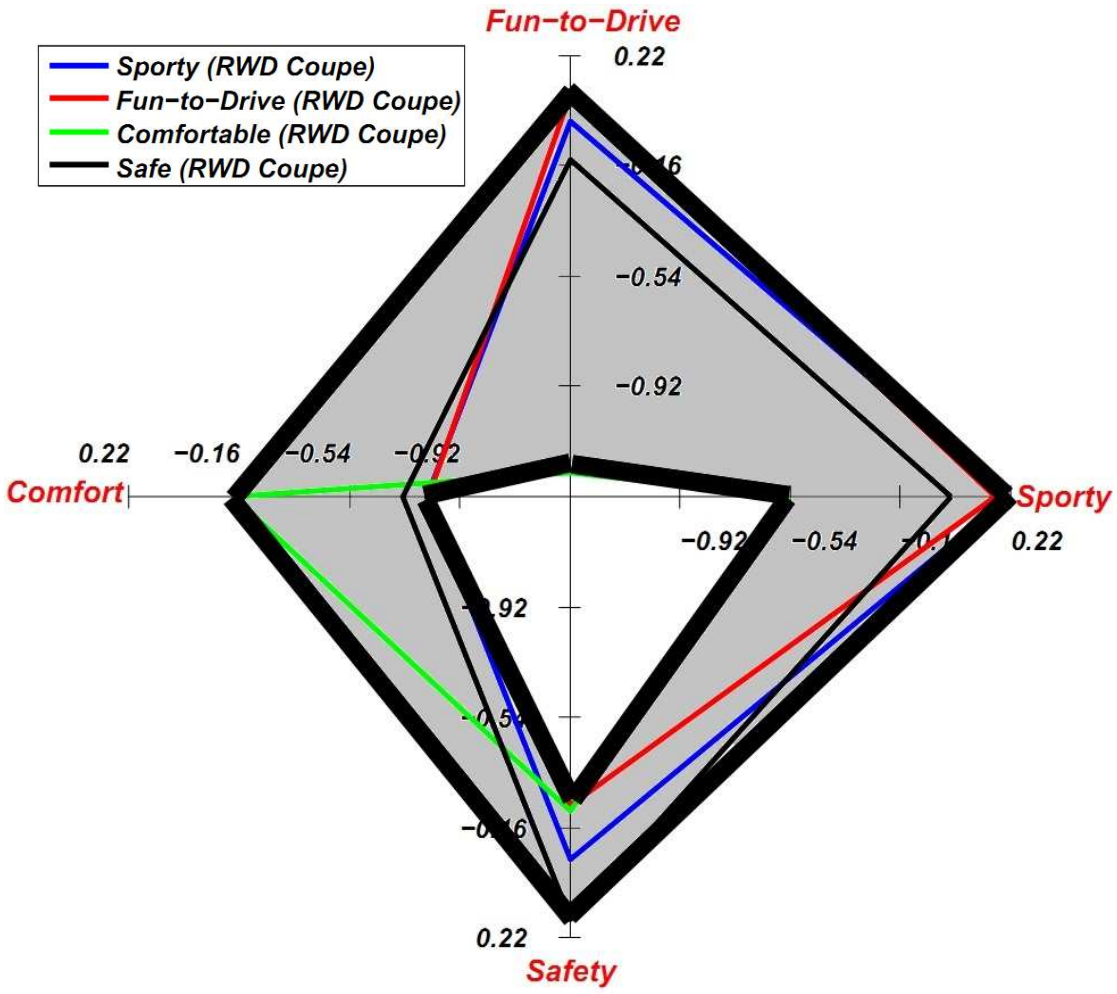

Figure 36. Aftermarket Vehicle Handling Bandwidth Diagram.

5.4 Case Study Four.

Replicating the Vehicle Characteristics of a Competitor Vehicle.

Objectives and Scope of the Case Study

This case study comprises of two competitor vehicles: vehicle A (compact FWD hatchback) and vehicle B (sporty RWD coupe). Assume that irrespective of having completely different vehicle architectures, these two vehicles are competitors of each other in the market. The overall objective of this case study is to explore if the framework developed for this research can be applied to such a scenario and if two vehicle with completely different architectures can be retuned to match each other's handling performance.

It is assumed that the manufacturer (or the chassis engineer) would like to redesign the chassis setup for vehicle B such that the new concept (say, optimized-vehicle B), handles similar to its competitor (or benchmark) vehicle A. It is also assumed that the vehicle manufacturer can only redesign the steering system, front and rear tires, and front and rear-axle suspension characteristics of vehicle B. In addition, the entire optimization schedule will be performed with realistic design constraints; for example, packaging constraints, which restricts drastic changes in suspension redesign. Specifically, only wheel-side points of suspension assembly were optimized i.e., only the wheel knuckle was redesigned.

Quantification of Vehicle Handling Characteristics

The handling requirements are grouped and categorized with respect to the various scenarios of vehicle handling. These include: steady-state handling, transient handling, on-center handling, emergency handling, parking, steering feedback, handling on different road surfaces, coupled dynamic cornering, disturbance sensitivity, and straight-line stability. Table 16 illustrates the differences in the handling characteristics of vehicle A (compact Front Wheel Drive (FWD) hatchback) and vehicle B (sporty Rear Wheel Drive (RWD) coupe), described with respect to the ten domains of vehicle handling.

As observed in Table 16, vehicle A "corners better" in steady-state conditions i.e., vehicle A has a lower overall understeer gradient, lower side-slip gain and higher yaw rate (and lateral acceleration) gain compared to vehicle B. Also, vehicle A rolls less during steady-state cornering conditions compared to vehicle B i.e., vehicle A has a lower roll angle gain. In terms of transient handling behavior, vehicle B is slightly more responsive (or agile) compared to vehicle A i.e., vehicle B has a lower yaw rate time constant and lower lateral acceleration phase lag @ 1 Hz. Although, vehicle B is more agile, its response is less damped (as seen from lower yaw rate damping ratio and higher roll angle overshoot). Lower damping is associated with poor controllability and poor course convergence capabilities.

Table 16. Handling Performance Metrics for Vehicle A and B.

Handling Domains	Objective Handling Metrics	Unit	Vehicle A (FWD)	Vehicle B (RWD)
Steady-State Handling (v=80 km/h)	Understeer Gradient	deg/G	0.727	1.197
	Yaw Rate Gain	1/sec	0.491	0.307
	Side-Slip Angle Gain	deg/G	-1.29	-1.34
	Roll Angle Gain	deg/G	2.39	3.57
Transient Handling (v=80 km/h)	Yaw Rate Time Constant	ms	113	105
	Yaw Rate Damping Ratio	-	0.994	0.918
	Lateral Acceleration Phase Lag	deg	-44.1	-43.4
	Roll Angle Overshoot	%	1.9	8.0
Steering Feedback (v=80 km/h)	Steering Torque Gain (per Steering Angle)	Nm/deg	0.391	0.308
	Steering Torque Feel (per Lateral Acceleration)	Nm/G	20.1	25.4
On-Center (v=80 km/h)	Steering Torque Time Lag (@ 0.2 Hz)	ms	86	63
Parking	Lock-to-Lock Steering Rotations	-	2.3	3.2
	Turn Circle Diameter	m	10.52	10.47
	Parking Static Torque	Nm	13.2	10.3
Disturbance Sensitivity (v=80 km/h)	Yaw Moment Sensitivity	deg/KN m-sec	3.327	2.301
Coupled Dynamics (v=80 km/h)	Yaw Rate Increment (Acceleration out of Turn)	%	-1.47	3.54
Road Adaptability (v=80 km/h)	Yaw Rate Increment (Cornering on Rough Roads)	%	-0.85	-1.95
Straight-Line Stability	Straight-Line Stability Index	Nm/N	1.197	1.518
	Pitch Gradient	deg/G	1.99	1.79
Emergency Handling (Roll Stability)	Static Stability Factor	-	1.416	1.499
	NHTSA Stars	-	4	5

With respect to steering feedback, vehicle A has a higher steering torque gradient (steering wheel torque per unit steering wheel angle) but a lower steering torque "feel" (steering wheel torque per unit lateral acceleration) compared to vehicle B. The higher steering torque gradient is indicative of "heavier" steering (increased steering torque workload) for vehicle A. The higher steering torque "feel" for vehicle B is representative of a more predictable and accurate off-center steering feedback. The on-center steering performance (particularly important at highway speeds and low lateral acceleration scenarios) is represented in this study with a metric of steering torque time lag at steering frequency of 0.2 Hz. Vehicle B has a lower steering torque time lag indicative of better on-center steering.

In terms of parking characteristics, vehicle A has higher static parking torque and a larger turn circle diameter (compared to vehicle B) but requires less steering wheel rotations (expressed in terms of Lock-to-Lock steering wheel rotations).

Coupled dynamic cornering, refers to vehicle handling behavior during coupled dynamic motions i.e., acceleration in a turn. Coupled dynamic cornering is expressed in terms of yaw-rate increment after the acceleration (or braking situation) while cornering. In Table 17, coupled dynamic cornering during acceleration-in-a-turn scenario for vehicle A and vehicle B is shown. Vehicle A has a negative yaw rate increment (after-before) indicating that the yaw rate decreases as the driver accelerates out of a corner, representative of an understeer response. Vehicle B on the other hand has a positive yaw rate increment (after-before) indicating that the vehicle yaw rate increases during

acceleration-in-a-turn scenario, representative of an oversteer response. This is a common difference between FWD (vehicle A) and RWD (vehicle B) vehicles. Road adaptability represents the cornering performance of the vehicle over different road surfaces. In this study, cornering over bumps (or rough road) is used as performance scenario. Rough road cornering is quantified with metric of yaw rate increment after transitioning to a rough road (from a smooth road). Both vehicles show a decrease in yaw rate values after entering rough roads, indicative of loss of cornering power on undulating surfaces. Vehicle B has lower (negative) yaw rate increment i.e., a larger loss of cornering power than vehicle A. Sudden loss of cornering power on entering rough roads can be related to loss of control issues during emergency handling situations.

Vehicle A is more sensitive to external side-wind disturbances than vehicle B, expressed in terms of heading angle sensitivity, which describes the heading angle change of the vehicle per unit external yaw moment disturbance. Vehicle A is more stable in a straight-line (indicated by lower straight-line stability factor) i.e., less prone to pull/drift and loss of control due to split mu acceleration/braking. Vehicle A pitches (squats/dives) more as indicated by the higher pitch gradient of the vehicle during straight-line acceleration/braking scenario. Emergency handling refers to vehicle handling performance during emergency or safety related scenarios such as obstacle avoidance maneuvers incorporating sudden severe lane changes. In this study, the primary focus is on evaluating the roll stability of the vehicle. Vehicle A has a lower static stability factor (SSF) than vehicle B, a lower SSF is indicative of higher roll instability. Vehicle B is rated 5 stars, and Vehicle A is rated 4 stars, according to NHTSA

(National Highway Transportation Safety Administration) 5 star ratings to represent roll over propensity. A higher star rating represents better roll stability.

Optimization Framework

A multi-scenario, multi-objective optimization framework was applied in this case study. The ATC optimization framework developed for this research works in a two-layer optimization schedule. Genetic Algorithms (GAs) [6], a type of evolutionary optimization algorithm, is used at each layer of the framework. The objective fitness function used in the first layer of the optimization schedule is setup to minimize any differences in objective handling metrics of vehicle A and vehicle B, so that vehicle B can attain the exact handling characteristics of vehicle A. The first layer then derives subsystem-level requirements from overall vehicle level targets. These subsystem-level requirements are passed on as *targets* to the second layer of optimization and the second layer attempts to derive component-level specifications from subsystem-level requirements derived in the first step. The second layer optimization utilizes component level design variables and analysis models and attempts to minimize the difference between the *targets* transferred from the vehicle level and *response* generated from the component level analysis. An iterative loop is set up with an objective to minimize the *target/response* consistency constraints i.e., the targets at the vehicle level are constantly rebalanced to achieve a consistent and feasible solution.

Results from the Optimization Process

The objective of the optimization process was to derive a new chassis configuration for vehicle B (called “optimized-vehicle B”) such that it has handling characteristics similar to those of vehicle A. The steering system, front and rear tires, and front and rear axle suspension characteristics were set as design variables in the optimization process.

Table 17 shows the final vehicle handling performance metrics for the optimized configuration obtained from this case study. From the Table 17, it is observed that the optimized-vehicle B has a lower understeer gradient, higher yaw rate gain, higher side-slip angle gain and lower roll angle gain compared to vehicle B. Hence, the optimized-vehicle B moves closer to Vehicle A in terms of steady-state cornering behavior.

The optimized-vehicle B shows higher steering torque gradient (wrt to steering angle) and lower steering torque gradient (wrt to lateral acceleration), and therefore moves closer to Vehicle A in terms of off-center steering feedback, as desired by the optimization schedule.

The optimized-vehicle B also shows increased levels of static parking torque, reduced number of rotations for steering full lock and increased steering turn circle diameter. This indicates that the optimized-vehicle B will show parking characteristics similar to vehicle A.

Table 17. Handling Performance Metrics for Vehicle A, B and Optimized-Vehicle B.

Handling Domains	Objective Handling Metrics	Units	Vehicle A	Vehicle B	Optimized - Vehicle B
Steady-State Handling (v=80 km/h)	Understeer Gradient	deg/G	0.727	1.197	0.990
	Yaw Rate Gain	1/sec	0.491	0.307	0.405
	Side-Slip Angle Gain	deg/G	-1.29	-1.34	-0.99
	Roll Angle Gain	deg/G	2.39	3.57	2.60
Transient Handling (v=80 km/h)	Yaw Rate Time Constant	ms	113	105	89
	Yaw Rate Damping Ratio		0.994	0.918	0.985
	Lateral Acceleration Phase Lag	deg	-44.1	-43.4	-33.8
	Roll Angle Overshoot	%	1.9	8.0	1.5
Steering Feedback (v=80 km/h)	Steering Torque Gain (per Steering Angle)	Nm/deg	0.391	0.308	0.316
	Steering Torque Feel (per Lateral Acc.)	Nm/G	20.1	25.4	19.8
On-Center (v=80 km/h)	Steering Torque Time Lag (@ 0.2 Hz)	ms	86	63	46
Parking	Lock-to-Lock Steering Rotations		2.3	3.2	2.6
	Turn Circle Diameter	m	10.52	10.47	10.5
	Parking Static Torque	Nm	13.2	10.3	12.6
Disturbance Sensitivity (v=80 km/h)	Yaw Moment Sensitivity	Deg/KN m-sec	3.327	2.301	2.115
Coupled Dynamics (v=80 km/h)	Yaw Rate Increment (Acceleration out of Turn)	%	-1.47	3.54	2.90
Road Adaptability (v=80 km/h)	Yaw Rate Increment (Cornering on Rough Roads)	%	-0.85	-1.95	-0.97
Straight-Line Stability	Straight-Line Stability Index	Nm/N	1.197	1.518	1.472
	Pitch Gradient	Deg/G	1.99	1.79	2.00
Emergency Handling (Roll Stability)	Static Stability Factor	-	1.416	1.499	1.499
	NHTSA Stars	-	4	5	5

The optimized-vehicle B improves its straight-line stability by lowering the straight-line stability index, reduces oversteer response (i.e., yaw-rate increase) during couple dynamics cornering and minimizes yaw-rate variations during rough road cornering. All these trends are in alignment with the goals set for the optimization i.e., to give vehicle B handling characteristics of vehicle A.

The transient handling response, on-center steering torque response lag, and yaw moment sensitivity are the three areas in which the optimization procedure fails to push the optimized-vehicle B in the desired direction. The optimized-vehicle B turns out to be much more responsive and agile than both vehicle A and vehicle B. The yaw rate time constant, lateral acceleration phase lag, and on-center steering torque time lag, decrease in magnitude and are lower than that of vehicle B. Similarly, the yaw moment sensitivity decreases lower than that of vehicle B and is not in line with the goal set in the optimization procedure.

The results of the case study indicates that the optimized-vehicle B can only partially attain the handling characteristics of vehicle A. There are three key reasons explaining this effect, firstly, the entire optimization schedule is performed with realistic design constraints; for example, packaging constraints, which restricts drastic changes in suspension redesign. Specifically, only wheel-side points of suspension assembly were optimized i.e., only the wheel knuckle was redesigned. Secondly, it is important to note that not all targets can be simultaneously achieved because of the inherent interdependence between conflicting handling requirements and objective metrics. For

example, in this case study, the optimized–vehicle B becomes less understeer in steady-state response and simultaneously becomes more responsive in transient scenarios. It was not possible to simultaneously make the vehicle less understeer and less responsive, while imposing the constraint of using the same tires on front and rear axle. Lastly, it should be noted that the two vehicles used for this case study belong to different vehicle platforms and have completely different architectures. They have different geometric and inertial properties which has some fundamental influence on the handling characteristics. Also, the fact that vehicle A is FWD and vehicle B is RWD is another major constraint which cannot be entirely compensated using the chassis optimization process.

As described in the previous case studies, the proposed system engineering framework ensures that the proposed vehicle-level solution can always be realized with feasible subsystem and component-level specifications. Table 18 compares the subsystem-level design variables for the optimized vehicle configuration (optimized-vehicle B) and the original vehicle (vehicle B).

Table 18. Optimized Vehicle Design Variables (Suspension, Steering and Tires).

Vehicle Design Variables				
Suspension Parameters				
Variables	Units	Vehicle B	Optimized -vehicle B	% Change
Roll Stiffness (Total)	Nm/deg	1,641	2,393	45.8
Roll Stiffness Distribution (Front)	%	65.3	79.6	21.9
Roll Stiffness (Front)	Nm/deg	1,072	1,904	77.6
Roll Stiffness (Rear)	Nm/deg	569	489	-14.1
Front Wheel Rate (Suspension Stiffness, Front)	N/mm	26.60	33.16	24.7
Rear Wheel Rate (Suspension Stiffness, Rear)	N/mm	18.40	19.17	4.2
Roll Stiffness (sway bar, Front)	Nm/deg	573	1,254	118.9
Roll Stiffness (sway bar, Rear)	Nm/deg	129	113	-12.4
Shock Damping (Front)	Nsec/mm	2,420	2,058	-15.0
Shock Damping (Rear)	Nsec/mm	1,746	1,511	-13.5
Lateral Force Compliance Steer (Front)	deg/N	-1.01E-04	-3.75E-05	-62.7
Lateral Force Compliance Steer (Rear)	deg/N	8.00E-06	-8.70E-07	-110.9
Lateral Force Camber Compliance (Front)	deg/N	1.18E-04	8.74E-05	-25.9
Lateral Force Camber Compliance (Rear)	deg/N	2.80E-05	2.76E-05	-1.2
Roll Camber (Front)	deg/deg	-0.620	-0.987	59.3
Roll Camber (Rear)	deg/deg	-0.637	-0.824	29.4
Roll Steer (Front)	deg/deg	0.035	0.050	44.4
Roll Steer (Rear)	deg/deg	-0.044	-0.009	-79.9
Roll Center Height (Front)	mm	57.00	29.10	-48.9
Roll Center Height (Rear)	mm	99.70	49.46	-50.4
Anti-Dive Angle (Front)	deg	2.00	2.35	17.5
Anti-Dive Angle (Rear)	deg	1.50	1.29	-14.0
Steering Parameters				
Steering Ratio	-	16.4	13.5	-17.8
Mechanical Trail	mm	30.00	14.73	-50.9
King Pin Inclination Angle	deg	12.39	17.81	43.8
Caster Angle	deg	7.50	5.67	-24.4
Scrub Radius	mm	34.00	-47.14	-238.6
Aligning Torque Compliance Steer (Front)	deg/Nm	2.83E-04	1.65E-04	-41.5
Aligning Torque Compliance Steer (Rear)	deg/Nm	1.06E-04	9.91E-05	-6.5
Tire Parameters				
Cornering Stiffness (Front, per tire)	N/deg	1,279	1,519	18.7
Cornering Stiffness (Rear, per tire)	N/deg	1,145	1,358	18.6
Cornering Stiffness Load Dependence Coefficient	a3	2,203	2,644	20.0
BCD= a3 * sin (2 * atan (Fz ./ a4))	a4	11.21	11.37	1.3
Camber Stiffness (Front, per tire)	N/deg	191.9	227.8	18.7
Camber Stiffness (Rear, per tire)	N/deg	171.7	203.7	18.6
Relaxation Length	mm	422.50	107.15	-74.6
Pneumatic Trail	mm	27.70	22.17	-20.0

Figure 37 shows the tire cornering stiffness characteristics obtained from the optimized schedule. Note that both front and rear tires are assumed to have identical characteristics in this case study.

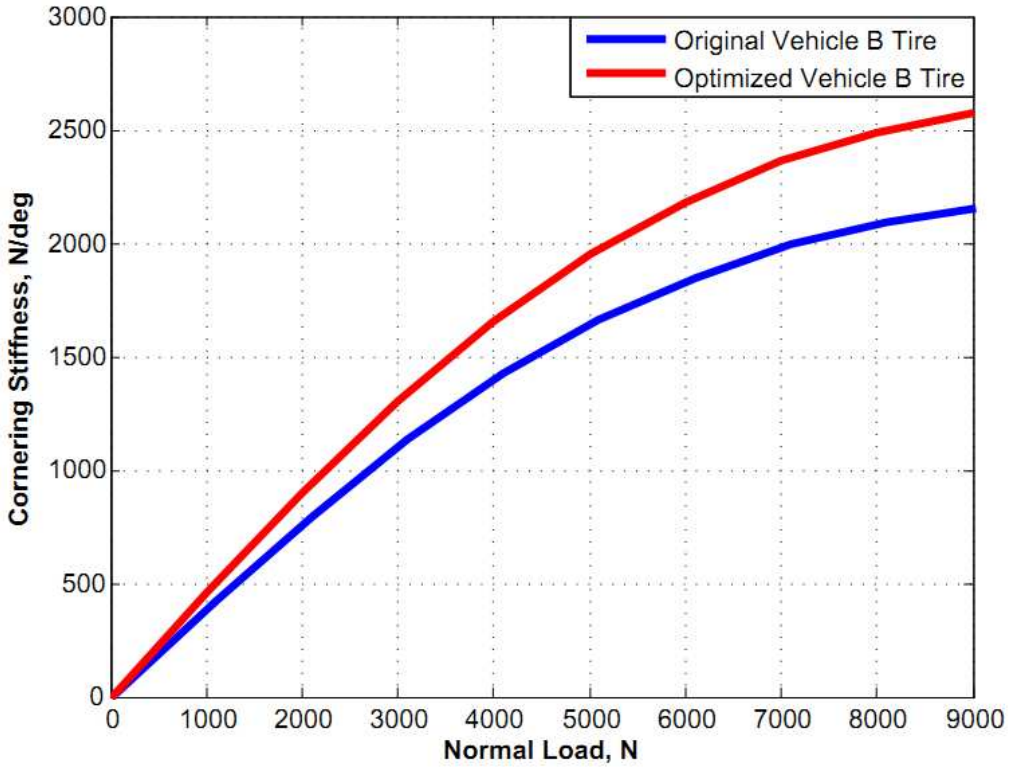

Figure 37. Tire Cornering Stiffness (N/deg) vs. Normal Load (N).

Figure 38 and Figure 40 show the optimized front and rear suspension geometry configurations (i.e., the re-designed suspension pick-up points). In this case study, only wheel-side points of suspension assembly were optimized i.e., only the wheel knuckle was redesigned. Figure 39 and Figure 41 show the front and rear suspension kinematic curves for the optimized suspension configurations. Table 19 and Table 20 show the optimized bushing stiffness obtained from the optimization schedule.

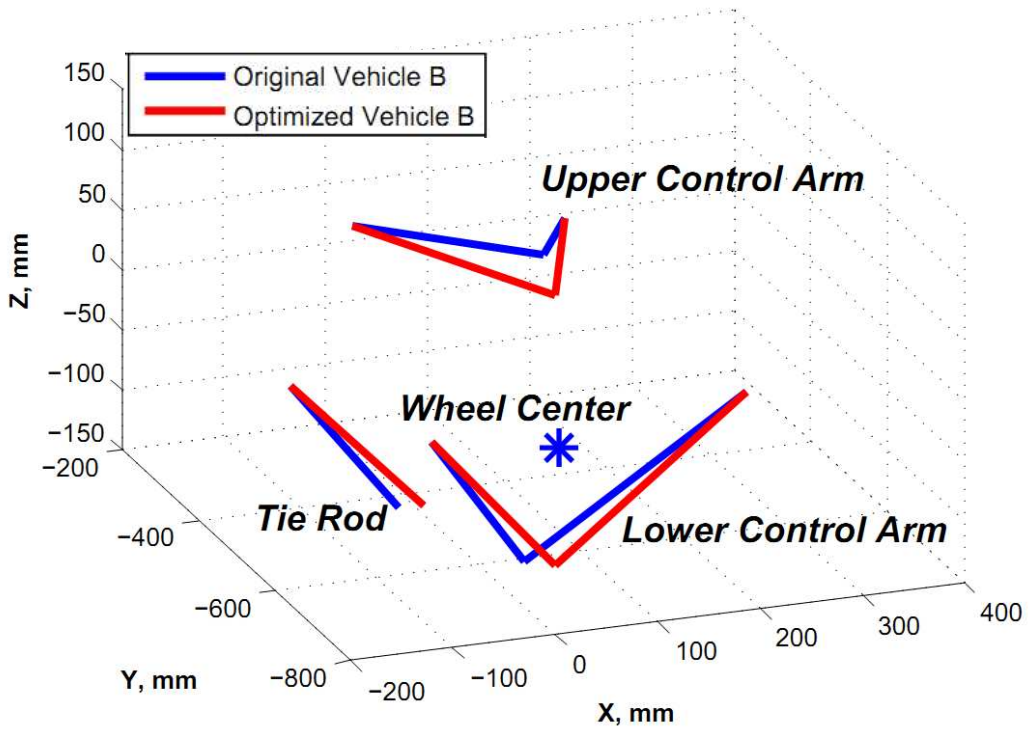

Figure 38. Optimized Front Suspension (Double Wishbone) Geometry Configuration for Vehicle B and Optimized-Vehicle B.

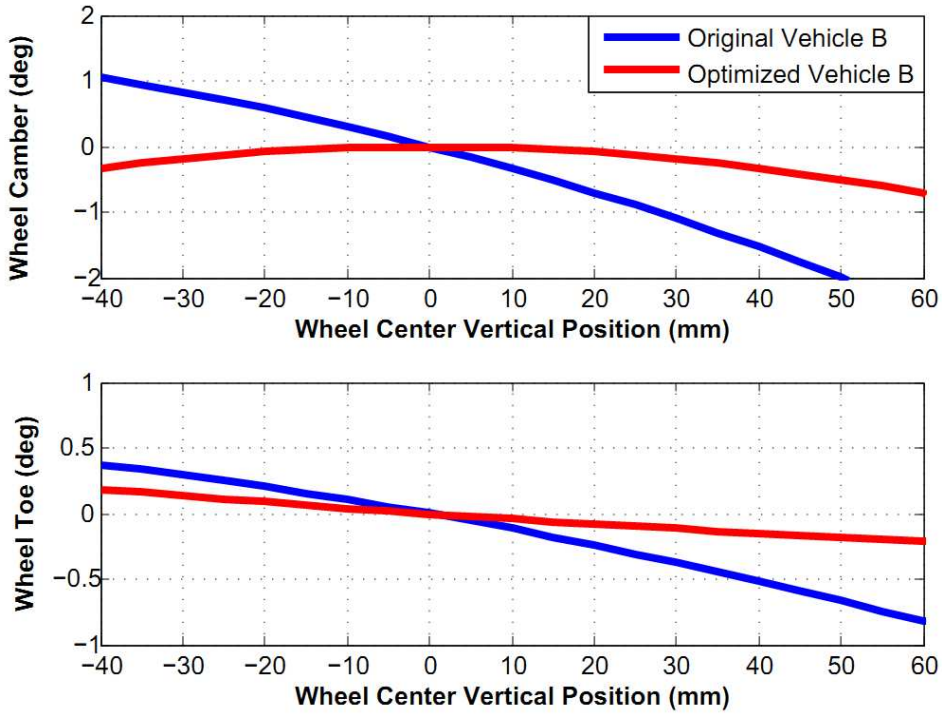

Figure 39. Optimized Front Suspension Kinematic Characteristics (Bump Steer, Bump Camber).

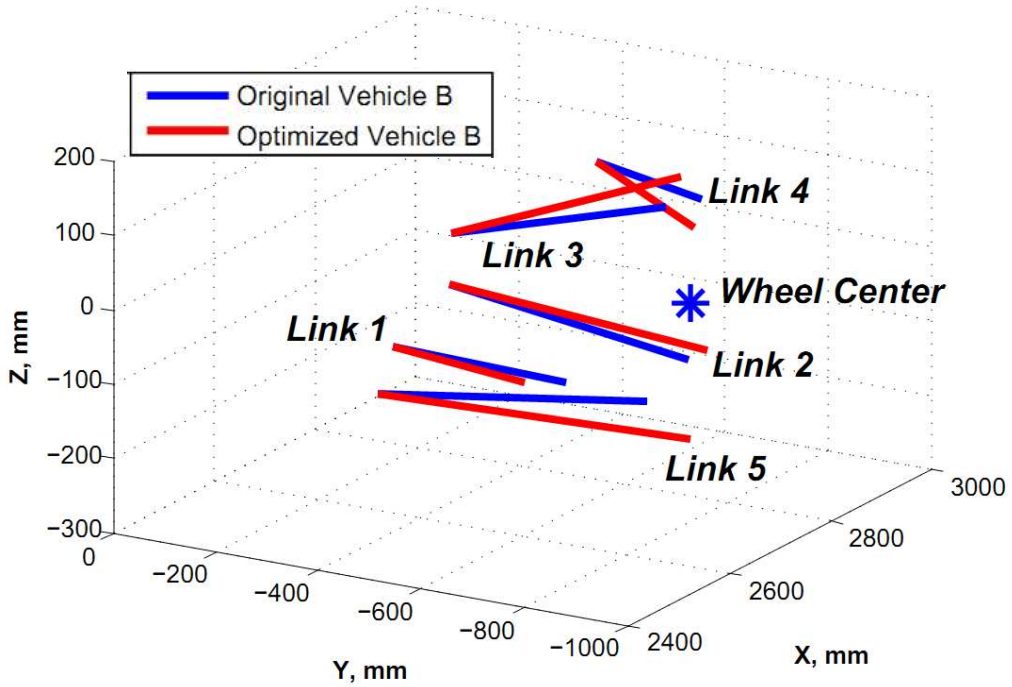

Figure 40. Optimized Rear Suspension (Five-Link) Geometry Configuration for Vehicle B and Optimized-Vehicle B.

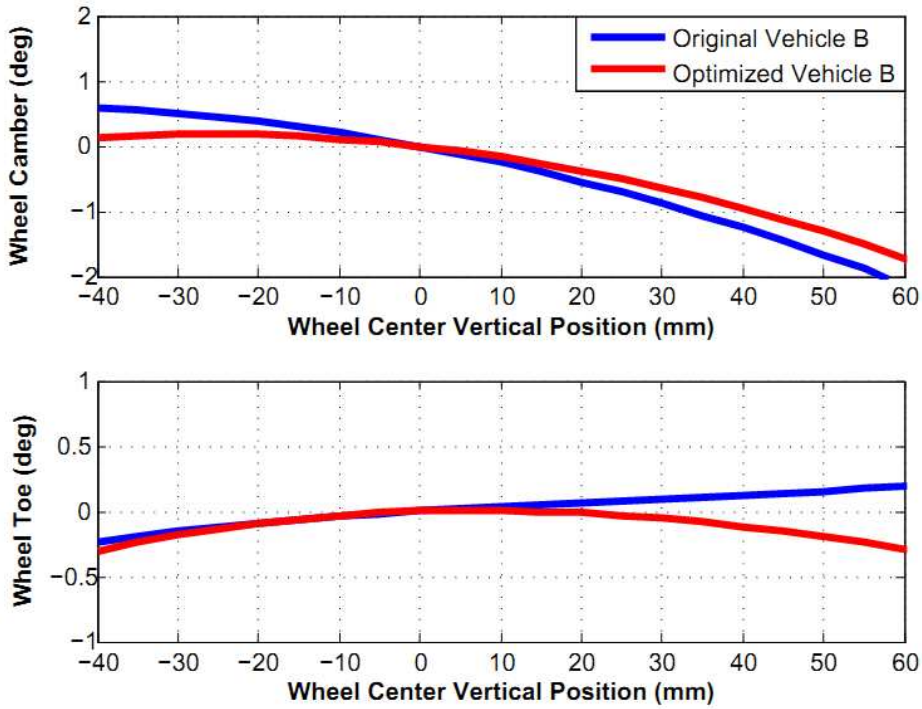

Figure 41. Optimized Rear Suspension Kinematic Characteristics (Bump Steer, Bump Camber).

Table 19. Optimized Front Suspension Bushing Stiffness.

Front Suspension-Bushing Radial Stiffness (N/mm)			
	Vehicle B	Optimized-Vehicle B	% Change
Link 1 (Lower A Arm (F))	3,305	5,126	55.1
Link 2 (Lower A Arm (R))	1,885	2,935	55.7
Link 3 (Upper A Arm (F))	7,831	1,801	-77.0
Link 4 (Upper A Arm (R))	3,531	9,741	175.8
Link 5 (Tie Rod)	1.0E+09	1.0E+09	0

Table 20. Optimized Rear Suspension Bushing Stiffness.

Rear Suspension-Bushing Radial Stiffness (N/mm)			
	Vehicle B	Optimized-Vehicle B	% Change
Link 1	10,000	5,397	-46.0
Link 2	10,000	10,000	0.0
Link 3	10,000	15,000	50.0
Link 4	10,000	15,000	50.0
Link 5	5,000	15,000	200.00

Conclusion

This case study demonstrates the application of the proposed handling design framework to scnerios where the intention of the chassis engineer is to exactly replicate the handling characterstics of a competetor vehicle. It is assusmed that the two vehicles under consideration have completely different geometric and inertial properties, and are based on different suspension and drivetrain architectures.

From the results, it is concluded that using the proposed optimization framework does not guarantee that all the optimization goals can be simulatenouly be achieved in every scenerio. The inherent inter-dependence between the different handling requirements, and objective metrics can sometimes result in a compromised vehicle design solution. Therefore users of this optimization framework must carefully understand the constraints imposed on the problem before expecting perfect results from the optimization program.

5.5 Case Study Five.

Selection of the Best Solution from a Set of Pareto-Optimal Solutions obtained from Genetic Algorithms.

Genetic Algorithm (GA) is used as the principal optimization technique in this dissertation. GA is a stochastic, evolutionary, non-deterministic search method, which can help attain globally optimum solution. There are several advantages of using Genetic Algorithms against traditional optimization methods because GAs:

Work with coding of the parameter set and search from a population of points, not a single point;

- Use objective function information, not derivatives;
- Use probabilistic transition rules, not deterministic ones;
- Work with a mix of continuous and discrete variables;
- Do not get trapped in local extremas.

The application of GAs to a multi-objective problem results in a set of Pareto-optimal solutions. Every Pareto-optimal solution should be equally acceptable [24]. Hence, the decision-maker has to make the choice of the final design solution from the Pareto-optimal set. The final selection must be based on information not contained in the objective function [26].

Goal Programming is one of the most commonly used methods for the selection of final design solutions from the Pareto-optimal set. In goal programming, the decision-

maker specifies an optimistic target, or *goal*, for the objective function to be attained. Any deviation from the target is then minimized [26]. A weighted sum approach, wherein the weighted sum of deviational variables is minimized, can be used at this stage. Although the weighted sum goal programming approach is easy to understand, the specifications of weighting coefficients and goals is a challenging task [26].

In this thesis, the use of brand essence information derived from a market survey data is recommended for specifications of weights and goals in the vehicle handling optimization process using goal programming based GAs.

To illustrate this process, a multi-objective GA-based vehicle handling optimization was setup. A sporty RWD coupe was used as the example vehicle for this case study. The geometric and inertial parameters of this example vehicle are shown in Table 21. To limit the scope of this case study, a subsystem-level vehicle handing optimization was performed with 20 different vehicle-level handling objectives and 21 subsystem-level design variables. The subsystem-level parameters used for this case study are shown in Table 22. Note that in this case study, only front suspension kinematics and compliance parameters were set as design variables along with other tire and steering system parameters. All the simulations were performed at a constant speed of 80 km/h using the vehicle dynamics models described in Appendix B.

Table 23 shows the list of vehicle handling objectives used for this case study and also specifies if the objective was minimized or maximized. The notations K1, K2 … K20 in Table 23 represent the normalized values of the objective metrics.

Table 21. Geometric and Inertial Parameters of Example Vehicle.

Description	**Units**	**Example Vehicle**
Vehicle (total) Mass	kg	1378
Front Un-sprung Mass	kg	97
Rear Un-sprung Mass	kg	94
Sprung Mass	kg	1187
Yaw Inertia (Whole Vehicle)	kg m^2	1936
Roll Inertia (Whole Vehicle)	kg m^2	392
Pitch Inertia (Whole Vehicle)	kg m^2	1946
Wheelbase, m	m	2.706
Track Width, m	m	1.499
Vehicle Width, m	m	1.684
Vehicle Height, m	m	1.407
Longitudinal Distance from Total CG to Front Wheels	m	1.261
Longitudinal Distance from Total CG to Rear Wheels	m	1.445
Longitudinal Distance from CG of Sprung Mass to Front Wheels	m	1.250
Longitudinal Distance from CG of Sprung Mass to Rear Wheels	m	1.456
Height of Vehicle (total) CG Above Ground	m	0.500
Height of Sprung Mass CG Above Ground, m	m	0.550
Height of Front Un-sprung Mass CG Above Ground	m	0.318
Height of Rear Un-sprung Mass CG Above Ground	m	0.318

Table 22. Sub-System Level Design Variable used for Subsystem-Level Optimization.

Vehicle Design Variables				
Suspension Parameters				
Variables	Units	Lower Bound	Nominal Value	Upper Bound
Roll Stiffness (Total)	Nm/deg	1,934	1,934	1,934
Roll Stiffness Distribution (Front)	%	0.30	0.65	0.80
Front Wheel Rate (Suspension Stiffness, Front)	N/mm	13.3	26.6	39.9
Rear Wheel Rate (Suspension Stiffness, Rear)	N/mm	9.2	18.4	27.6
Shock Damping (Front)	Nsec/mm	1,936	2,420	2,904
Shock Damping (Rear)	Nsec/mm	1,397	1,746	2,095
Lateral Force Compliance Steer (Front)	deg/N	-1.51E-04	-1.01E-04	-5.03E-05
Lateral Force Compliance Steer (Rear)	deg/N	5.90E-06	5.90E-06	5.90E-06
Lateral Force Camber Compliance (Front)	deg/N	9.44E-05	1.18E-04	1.42E-04
Lateral Force Camber Compliance (Rear)	deg/N	6.35E-05	6.35E-05	6.35E-05
Roll Camber (Front)	deg/deg	-0.929	-0.62	-0.310
Roll Camber (Rear)	deg/deg	-0.637	-0.637	-0.637
Roll Steer (Front)	deg/deg	0.017	0.035	0.052
Roll Steer (Rear)	deg/deg	-0.044	-0.044	-0.044
Roll Center Height (Front)	mm	39.9	57	79.8
Roll Center Height (Rear)	mm	99.7	99.7	99.7
Anti-Dive Angle (Front)	deg	0	2	3
Anti-Dive Angle (Rear)	deg	14	14	14
Steering Parameters				
Steering Ratio	-	12.3	16.4	20.5
Mechanical Trail	mm	24	30	36
King Pin Inclination Angle	deg	5.3	12.39	15.9
Caster Angle	deg	3.75	7.5	11.25
Scrub Radius	mm	-15.3	34	40.8
Aligning Torque Compliance Steer (Front)	deg/Nm	1.42E-04	2.83E-04	4.25E-04
Aligning Torque Compliance Steer (Rear)	deg/Nm	3.34E-04	3.34E-04	3.34E-04
Tire Parameters				
Cornering Stiffness Load Coefficient	a3	1,432	2,203	3,085
BCD= a3 * sin (2 * atan (Fz ./ a4))	a4	8	11.21	17
Relaxation Length	mm	100	222.5	300
Pneumatic Trail	mm	22.16	27.7	33.24

Table 23. List of Vehicle Handling Objectives.

Handling Domains	Objective Handling Metrics		Objective
Steady-State Handling	Understeer Gradient	K1	Minimize
	Yaw Rate Gain	K2	Maximize
	Side-Slip Angle Gain	K3	Minimize
	Roll Angle Gain	K4	Minimize
Transient Handling	Yaw Rate Time Constant	K5	Minimize
	Yaw Rate Damping Ratio	K6	Minimize
	Lateral Acceleration Phase Lag	K7	Minimize
	Roll Angle Overshoot	K8	Minimize
Steering Feedback	Steering Torque Gain (per Steering Angle)	K9	Minimize
	Steering Torque Feel (per Lateral Acceleration)	K10	Minimize
On-Center	Steering Torque Time Lag (@ 0.2 Hz)	K11	Minimize
Parking	Lock-to-Lock Steering Rotations	K12	Minimize
	Turn Circle Diameter	K13	Minimize
	Parking Static Torque	K14	Minimize
Disturbance Sensitivity	Yaw Moment Sensitivity	K15	Minimize
Coupled Dynamics	Yaw Rate Increment (Acceleration out of Turn)	K16	Minimize
Road Adaptability	Yaw Rate Increment (Cornering on Rough Roads)	K17	Minimize
Straight-Line Stability	Straight-Line Stability Index	K18	Minimize
	Pitch Gradient	K19	Minimize
Emergency Handling (Roll Stability)	Static Stability Factor	K20	Maximize

As mentioned previously, a GA-based optimization results in a set of Pareto-optimal solutions. The solutions can be visualized by plotting any two objective functions against each other. Figure 42 shows one such result wherein the objective metric of yaw rate gain is plotted against yaw rate time constant.

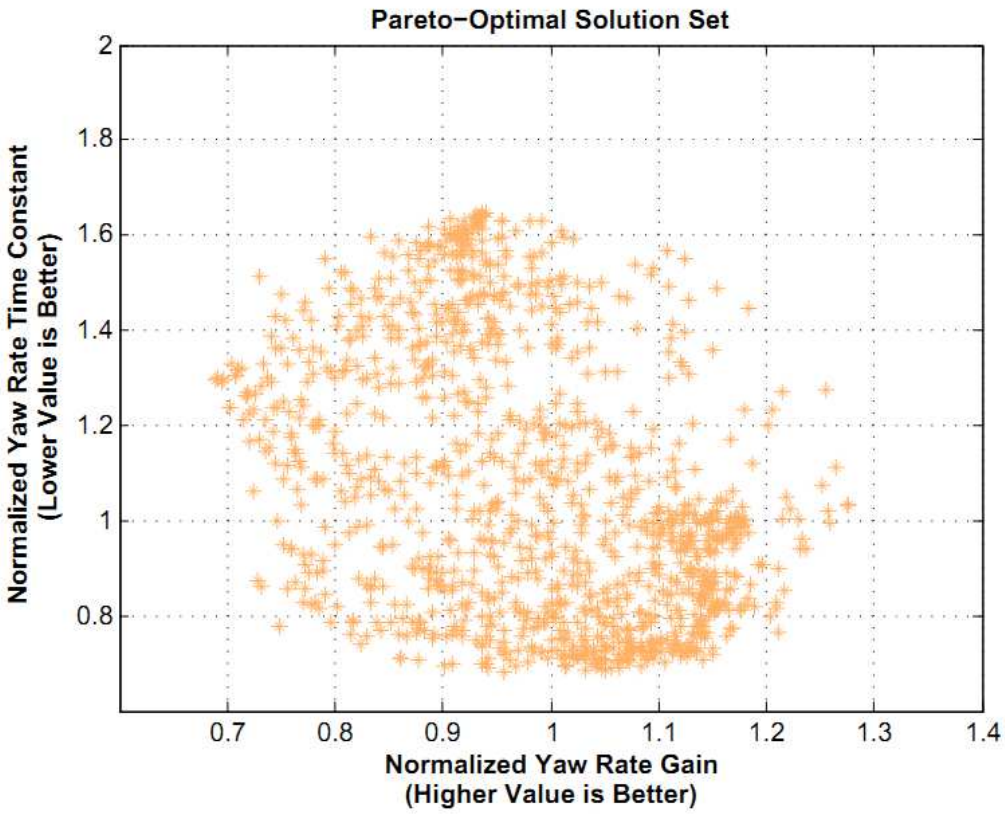

Figure 42. Pareto-optimal Solution set of Normalized Yaw Rate Gain vs. Normalized Yaw Rate Time Constant.

Using solutions from the Pareto-optimal solution set, the relevant vehicle handling attributes (i.e., Sporty, Fun to Drive, Safety, and Comfort) are calculated based on empirical correlations (shown in Table 5). For each Pareto-optimal solution, the four customer relevant handling attributes can be calculated using notations shown in Table 23.

SPORTY =(-K1+K2-K3-K4+K9+K10-K11+K16+K6-K5-K7-K8-K19)/13

FUN-TO-DRIVE= (-K5-K4-K4-K19-K3-K11+K6+K10)/8

COMFORT= (-K9-K10-K14-K12-K15-K13+K11+K5)/8

SAFETY= (K20+K1-K16-abs (K17)-K18-K8)/6

This results in a cloud of Pareto-optimal points expressed in terms of customer relevant vehicle handling attributes. The selection of the best solution is performed by using a weighted sum goal programming approach [26], where the goals and weights are derived from market analysis.

The weighted sum goal programming is shown in Equation 5.

$$min \sum w_i \left| f\left(x_i\right) - y_i \right|$$

$$w_i = Brand\ Attribute\ Weights;$$

$$y_i = Handling\ Attribute\ Targets\ or\ Goals\ (Desired);$$

$$f\left(x_i\right) = Handling\ Attributes\ Calculated\ (Achieved)$$

(5)

In this case, the goals are derived using the brand essence information shown in Table 2 and brand attribute weights shown in Table 3. Table 2 shows the absolute ratings and brand essence comparison results for Volvo, Toyota, BMW, Lexus, and MINI from the AutoPacific 2013 New Vehicle Satisfactory Survey. Table 3 shows the brand attribute weights derived from the marketing data and gives insight into the strategic directions for different brands.

The results of the goal programming approach will clearly help the decision-maker with the selection of the best solution from the Pareto-front. As an example, five different solutions were selected to represent Volvo, Toyota, BMW, Lexus, and MINI. The selected solutions are highlighted on Figure 43, Figure 44, Figure 45 and Figure 46. Among the five brand specific solutions derived in this case study, the MINI solution clearly represents the best performance in terms of *Sporty* and *Fun-to-Drive* attributes. The Volvo and the Lexus solutions leads the other brands in terms of *Safety* and *Comfort* attributes respectively. Among the five vehicle solutions, MINI is the least *Safe* and *Comfortable* and Toyota is the least *Fun-to-Drive*.

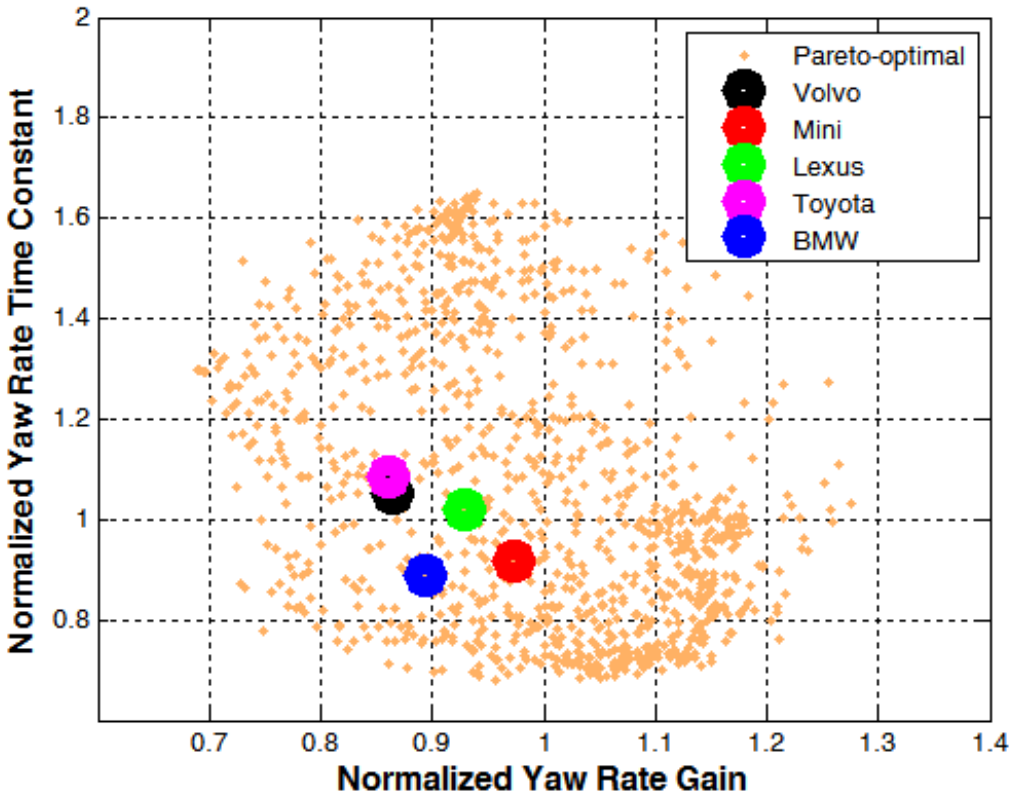

Figure 43. Pareto-optimal Solution Set for Yaw Rate Gain and Yaw Rate Time Constant.

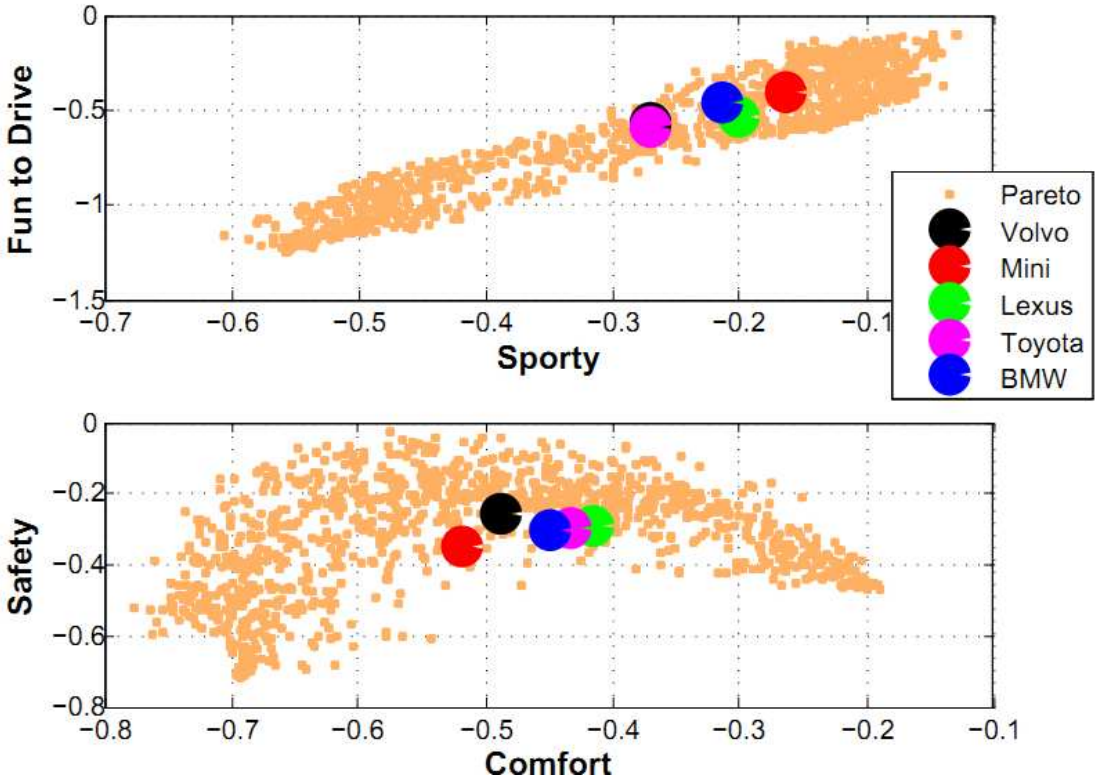

Figure 44. Pareto-optimal Solution Set for Sporty vs. Fun-to-Drive & Comfort vs. Safety.

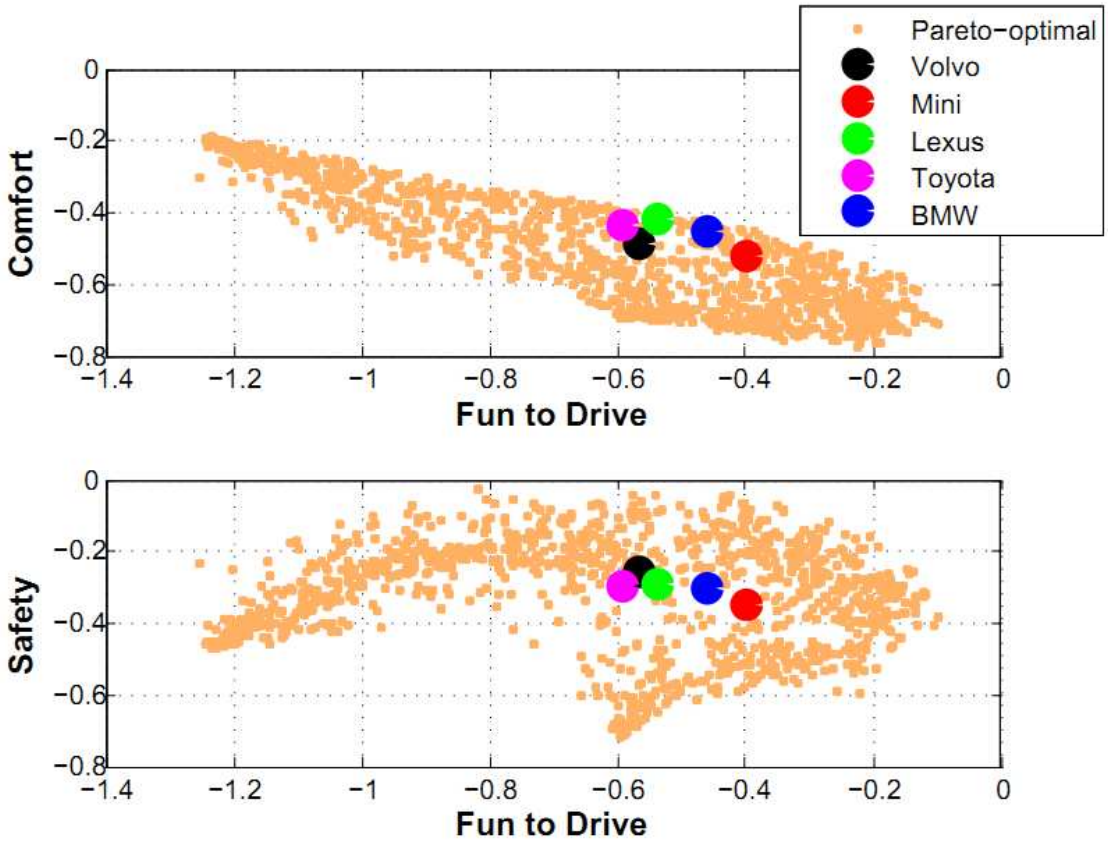

Figure 45. Pareto-optimal Solution Set for Fun-to-Drive vs. Safety & Comfort.

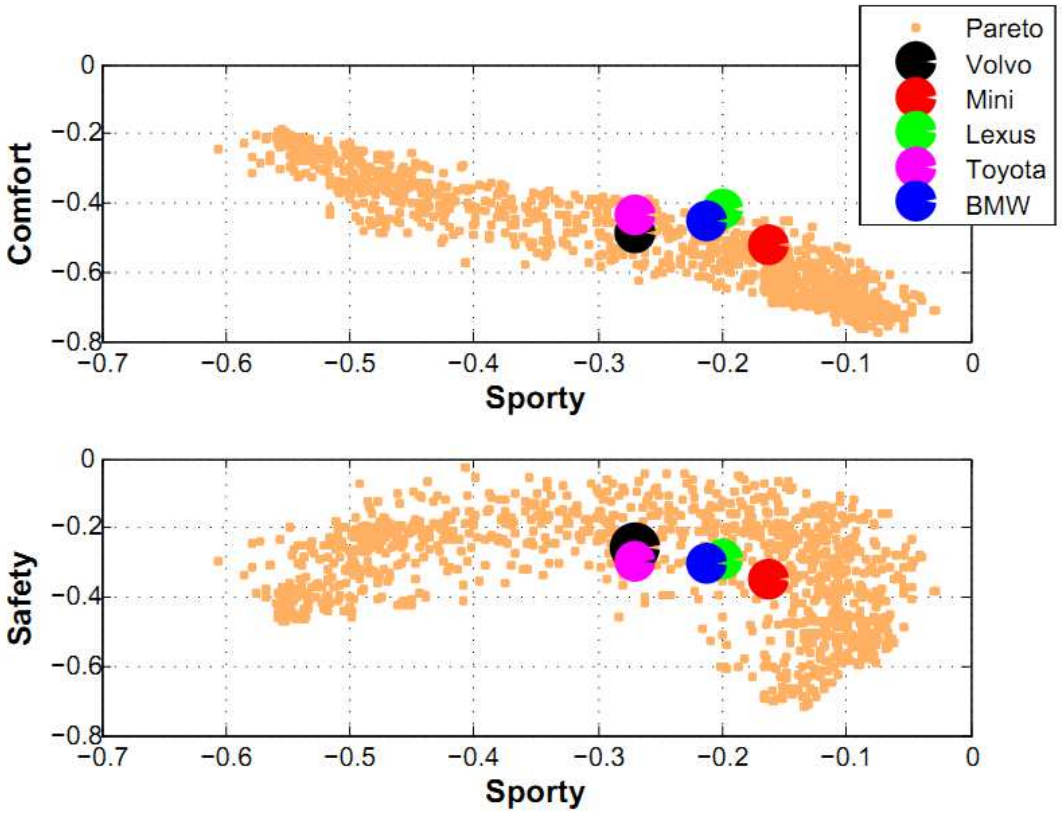

Figure 46. Pareto-optimal Solution Set for Sporty vs. Comfort & Sporty vs. Safety.

5.6 Case Study Six

Vehicle Handling Sensitivity Study Using Design of Experiments.

A Design of Experiments (DOE) coupled with global sensitivity analysis was conducted to better understand the sensitivities, dependencies, and trade-offs involved in vehicle handling design. The Sobol method [24] was used to create a quasi-random, low discrepancy design sequence for the DOE.

Global sensitivity analyses capture the effect of parameter variation on the system behavior when design variables are varied within broad ranges against the commonly used local sensitivity analysis [26]. The local sensitivity analysis based on a calculation of derivatives of the objective functions with respect to system parameters only describes the effect of small variation of the design parameters and provides a very limited insight into the design problem [26]. Also, note that a global sensitivity analysis will capture the effect of the simultaneous variation of several design parameters and hence is able to capture the inter-dependencies between the design parameters and objective functions more comprehensively.

The global sensitivity study performed in this research was used to explore the relationships between different handling objective metrics and is referred to as the *Target* vs. *Target* sensitivity study. All the simulations were performed for a sporty RWD coupe platform at a constant speed of 80 km/h using the vehicle dynamics models described in Appendix B. The geometrical and inertial parameters for the sporty RWD coupe platform

used for this case study are shown in Table 24. The subsystem-level parameters used for the DOE are shown in Table 25.

The Spearman Rank Correlation Coefficients (r_s) [26] were calculated between different objective functions or targets. The Spearman Rank Correlation Coefficient is calculated based on ranks of the individual components instead of their actual values and hence provides a robust estimation of global sensitivity. The rank correlation technique used in this research can cope with non-linear relationships and reports any correlations that exist between individual components [26].

Figure 47 and Figure 48 show the Spearman Rank Correlation Coefficient calculated between different handling objective metrics. Positive values of the correlation coefficient indicate direct correlations and negative values of the coefficient indicate inverse correlations. Values of correlation coefficient close to 1 (or -1) indicate strong direct (or inverse) correlations. All coefficients above value of 0.6 are highlighted in Figure 47 and Figure 48. Figure 47 shows the most important correlation results derived from this study.

From Figure 47, it is observed that the vehicle's side-slip angle gain (SSG) is one of the most important and influential objective handling metric. At vehicle speed of 80 km/h the nominal value of side-slip angle gain is found to be a negative number. Higher negative values (lower magnitudes) of side-slip angle gain (SSG) result in a vehicle which is more intuitive and *Fun-to-Drive* for the driver. Both vehicle's yaw rate time constant (YRTC) and lateral acceleration phase lag (LAPL) are strongly correlated with

side-slip angle gain (SSG). Note that LAPL is expressed as a negative value, indicating a lag, so higher values of LAPL indicate more responsive handling. Lower values of YRTC and higher values of LAPL are strong indicators of vehicle responsiveness or agility during transient handling scenarios and are correlated with higher values of SSG. The SSG, YRTC and LAPL are intern found to be correlated with steering torque time lag at 0.2 Hz, indicating that a responsive and agile vehicle will also have a fast responding steering torque response.

SSG is directly correlated with yaw rate damping ratio (YRDR) and inversely correlated with yaw moment sensitivity (YMS). This means that having a high (negative) side-slip angle gain is correlated with high yaw rate damping and low sensitivity to side-wind disturbances i.e., lower YMS. The SSG is directly correlated with roll angle overshoot (RAO) and inversely correlated with yaw rate increment during coupled dynamic scenarios (YRI-CD). The understeer gradient (USG) is found to be inversely correlated with the vehicle's yaw rate damping ratio (YRDR).

The yaw rate gain at the steering wheel (YRG) seems to be directly correlated with static parking torque (SPT) and steering torque gradient with respect to steering wheel angle (STG-SWA). The kinematic steering ratio seems to be dominant factor affecting these correlations.

More detailed results from the DOE based correlation study can be observed in Figure 48. The correlations provide a higher-level understanding of the trade-offs and sensitivities involved in vehicle handling design.

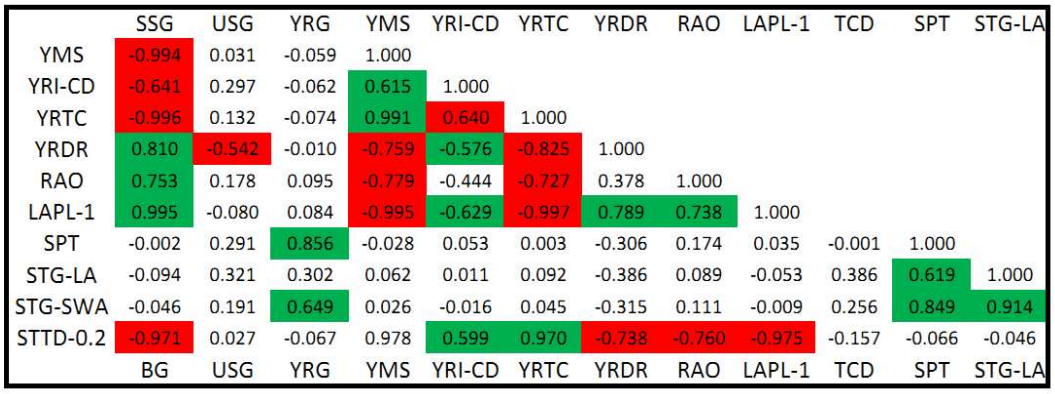

	SSG	USG	YRG	YMS	YRI-CD	YRTC	YRDR	RAO	LAPL-1	TCD	SPT	STG-LA
YMS	-0.994	0.031	-0.059	1.000								
YRI-CD	-0.641	0.297	-0.062	0.615	1.000							
YRTC	-0.996	0.132	-0.074	0.991	0.640	1.000						
YRDR	0.810	-0.542	-0.010	-0.759	-0.576	-0.825	1.000					
RAO	0.753	0.178	0.095	-0.779	-0.444	-0.727	0.378	1.000				
LAPL-1	0.995	-0.080	0.084	-0.995	-0.629	-0.997	0.789	0.738	1.000			
SPT	-0.002	0.291	0.856	-0.028	0.053	0.003	-0.306	0.174	0.035	-0.001	1.000	
STG-LA	-0.094	0.321	0.302	0.062	0.011	0.092	-0.386	0.089	-0.053	0.386	0.619	1.000
STG-SWA	-0.046	0.191	0.649	0.026	-0.016	0.045	-0.315	0.111	-0.009	0.256	0.849	0.914
STTD-0.2	-0.971	0.027	-0.067	0.978	0.599	0.970	-0.738	-0.760	-0.975	-0.157	-0.066	-0.046
	BG	USG	YRG	YMS	YRI-CD	YRTC	YRDR	RAO	LAPL-1	TCD	SPT	STG-LA

Figure 47. Results of Spearman-Rank Correlation Coefficients for Different Objective Functions.

	Vehicle Handling Metric (Target)	Units
SSG	Beta Gain-Side-slip Angle Gain	Deg/G
USG	Understeer Gradient	Deg/G
YRG	Yaw Rate Gain	Deg/sec/Deg
YMS	Yaw Moment Sensitivity	Deg/KN m-sec
YRI-CD	Yaw Rate Increment - Acceleration out of Turn	%
YRI-RRC	Yaw Rate Increment - Rough Roads	%
PG	Pitch Gradient	Deg/G
YRTC	Yaw Rate Time Constant	Sec
YRDR	Yaw Rate Damping Ratio	-
RAO	Roll Angle Overshoot	%
LAPL-1	Lateral Acceleration Phase Lag	Deg
TCD	Turning Circle Diameter	m
L2L	Lock-to Lock Steering Rotations	-
SPT	Static Parking Torque	Nm
STG-LA	Steering Torque Gradient per Lateral Acceleration	Nm/G
STG-SWA	Steering Torque Gradient per Steering Angle	Nm/Deg
STTD-0.2	Steering Torque Time Delay @0.2 Hz	Sec
SLSM	Straight Line Stability Index	Nm/N
RAG	Roll Angle Gain	Deg/G

	SSG	USG	YRG	YMS	YRI-CD	YRI-RRC	PG	YRTC	YRDR	RAO	LAPL-1	TCD	L2L	SPT	STG-LA	STG-SWA	STTD-0.2	SLSM	RAG
SSG	1.000																		
USG	-0.126	1.000																	
YRG	0.074	-0.164	1.000																
YMS	-0.994	0.031	-0.059	1.000															
YRI-CD	-0.641	0.297	-0.062	0.615	1.000														
YRI-RRC	0.004	-0.011	0.009	-0.001	-0.100	1.000													
PG	-0.002	0.008	-0.001	0.002	0.020	0.063	1.000												
YRTC	-0.996	0.132	-0.074	0.991	0.640	-0.015	-0.025	1.000											
YRDR	0.810	-0.542	-0.010	-0.759	-0.576	0.010	0.074	-0.825	1.000										
RAO	0.753	0.178	0.095	-0.779	-0.444	0.025	-0.103	-0.727	0.378	1.000									
LAPL-1	0.995	-0.080	0.084	-0.995	-0.629	0.011	0.019	-0.997	0.789	0.738	1.000								
TCD	0.001	0.031	-0.131	-0.006	0.022	0.075	-0.021	-0.002	0.007	-0.018	0.002	1.000							
L2L	-0.030	-0.072	-0.060	0.037	0.025	-0.070	0.000	0.028	0.030	-0.069	-0.033	-0.496	1.000						
SPT	-0.002	0.291	0.856	-0.028	0.053	0.022	-0.005	0.003	-0.306	0.174	0.035	-0.001	-0.150	1.000					
STG-LA	-0.094	0.321	0.302	0.062	0.011	0.085	-0.016	0.092	-0.386	0.089	-0.053	0.386	-0.298	0.619	1.000				
STG-SWA	-0.046	0.191	0.649	0.026	-0.016	0.065	-0.017	0.045	-0.315	0.111	-0.009	0.256	-0.260	0.849	0.914	1.000			
STTD-0.2	-0.971	0.027	-0.067	0.978	0.599	-0.015	-0.001	0.970	-0.738	-0.760	-0.975	-0.157	0.119	-0.066	-0.046	-0.064	1.000		
SLSM	0.087	0.015	-0.134	-0.090	-0.040	0.079	-0.022	-0.087	0.069	0.047	0.088	0.950	-0.522	-0.010	0.343	0.220	-0.231	1.000	
RAG	-0.021	0.091	-0.035	0.013	-0.007	-0.020	-0.012	0.041	-0.150	0.336	-0.059	-0.047	-0.027	-0.010	-0.033	-0.047	0.027	-0.043	1.000
	BG	USG	YRG	YMS	YRI-CD	YRI-RRC	PG	YRTC	YRDR	RAO	LAPL-1	TCD	L2L	SPT	STG-LA	STG-SWA	STTD-0.2	SLSM	RAG

Figure 48. Results of Spearman-Rank Correlation Coefficients for Different Objective Functions.

Table 24. Geometric and Inertial Parameters of Example Vehicle.

Description	Units	Reference Vehicle
Vehicle (total) Mass	kg	1378
Front Un-sprung Mass	kg	97
Rear Un-sprung Mass	kg	94
Sprung Mass	kg	1187
Yaw Inertia (Whole Vehicle)	kg m^2	1936
Roll Inertia (Whole Vehicle)	kg m^2	392
Pitch Inertia (Whole Vehicle)	kg m^2	1946
Wheelbase, m	m	2.706
Track Width, m	m	1.499
Vehicle Width, m	m	1.684
Vehicle Height, m	m	1.407
Longitudinal Distance from Total CG to Front Wheels	m	1.261
Longitudinal Distance from Total CG to Rear Wheels	m	1.445
Longitudinal Distance from CG of Sprung Mass to Front Wheels	m	1.250
Longitudinal Distance from CG of Sprung Mass to Rear Wheels	m	1.456
Height of Vehicle (total) CG Above Ground	m	0.500
Height of Sprung Mass CG Above Ground, m	m	0.550
Height of Front Un-sprung Mass CG Above Ground	m	0.318
Height of Rear Un-sprung Mass CG Above Ground	m	0.318

Table 25. Sub-System Level Design Variable used for DOE.

Vehicle Design Variables				
Suspension Parameters				
Variables	Units	Lower Bound	Nominal Value	Upper Bound
Roll Stiffness (Total)	Nm/deg	1,708	2,135	2,562
Roll Stiffness Distribution (Front)	%	0.30	0.65	0.80
Front Wheel Rate (Suspension Stiffness, Front)	N/mm	13.3	26.6	39.9
Rear Wheel Rate (Suspension Stiffness, Rear)	N/mm	9.2	18.4	27.6
Shock Damping (Front)	N-sec/mm	1,210	2,420	3,630
Shock Damping (Rear)	N-sec/mm	873	1,746	2,619
Lateral Force Compliance Steer (Front)	deg/N	-1.51E-04	-1.01E-04	-5.03E-05
Lateral Force Compliance Steer (Rear)	deg/N	2.95E-06	5.90E-06	8.85E-06
Lateral Force Camber Compliance (Front)	deg/N	5.90E-05	1.18E-04	1.77E-04
Lateral Force Camber Compliance (Rear)	deg/N	3.17E-05	6.35E-05	9.52E-05
Roll Camber (Front)	deg/deg	-0.929	-0.62	-0.310
Roll Camber (Rear)	deg/deg	-0.955	-0.637	-0.318
Roll Steer (Front)	deg/deg	0.017	0.035	0.052
Roll Steer (Rear)	deg/deg	-0.066	-0.044	-0.022
Roll Center Height (Front)	mm	28.5	57	85.5
Roll Center Height (Rear)	mm	49.85	99.7	149.55
Anti-Dive Angle (Front)	deg	0	2	3
Anti-Dive Angle (Rear)	deg	0	14	21
Steering Parameters				
Steering Ratio	-	12.3	16.4	20.5
Mechanical Trail	mm	15	30	45
King Pin Inclination Angle	deg	5.3	12.39	15.9
Caster Angle	deg	3.75	7.5	11.25
Scrub Radius	mm	-51	34	51
Aligning Torque Compliance Steer (Front)	deg/Nm	1.42E-04	2.83E-04	4.25E-04
Aligning Torque Compliance Steer (Rear)	deg/Nm	1.67E-04	3.34E-04	5.01E-04
Tire Parameters				
Cornering Stiffness Load Dependence Coefficient	a3	1,102	2,203	2,644
BCD= a3 * sin (2 * atan (Fz ./ a4))	a4	4	11.21	13
Relaxation Length	mm	100	222.5	300
Pneumatic Trail	mm	22.16	27.7	33.24

CHAPTER SIX

CONCLUSION AND SUMMARY

6.1 Summary of Dissertation

The overall focus of this research was to develop processes, methodologies, and tools that can support vehicle design during the conceptual development phase with the objective to reduce concept development time and increase early design maturity. In this thesis, vehicle handling—one of the key aspects of overall vehicle DNA—was researched in its totality.

A systems engineering methodology has been implemented using a simulation-based framework to address the challenges associated with the conceptual design of vehicle handling characteristics. The proposed methodology provides a comprehensive, multi-level, step-by-step, and top-down approach that links customer expectations to the final chassis component specifications and the validation of recommended design configurations.

The proposed simulation-based systems engineering framework integrates market research into the vehicle handling design process. Market research aimed towards understanding end-user preferences and expectations was used to develop insights regarding manufacturer's brand essence and relative importance of the various brand attributes. The framework was designed to accept inputs from market research, convert the market results to useful information to be used for creation of vehicle-level targets, and to guide the chassis design direction during the decision-making process.

To accelerate the vehicle handling design process a hybrid set of lower-order parametric models were developed and used in the simulation-based framework. Computationally efficient models with appropriate accuracy levels were developed and used to effectively connect, evaluate and optimize vehicle-, subsystem-, and component-level targets. To account for the interactions between various conflicting requirements and scenarios of vehicle handling, these easy-to-characterize, computationally inexpensive, and transparent, vehicle handling and chassis design models were linked to each other through a multi-objective and multi-scenario optimization scheme. Stochastic optimization algorithms coupled with design-of-experiments and sensitivity analyses were used to better understand the trade-offs and compromises involved in the chassis design process.

Lastly, the proposed systems engineering framework was implemented using a decomposition-based, Analytical Target Cascading (ATC) techniques [4]. ATC is an effective hierarchical, multi-level, and optimization-based design technique. It applies a decomposition approach in which the overall system is split into several subsystems that, are then solved independently and coordinated via target and response consistency constraints [5]. The framework works in a two-layer optimization schedule: the first layer is used to derive subsystem-level requirements from overall vehicle-level targets, and the second layer is used to derive component-level specifications from subsystem-level requirements derived in the first step. Genetic Algorithms (GA) are used at each layer of the framework. ATC assures a concurrent and consistent implementation of the proposed systems engineering approach.

Six case studies based on the proposed systems engineering methodology for the top-down design of vehicle handling characteristics were conducted in this dissertation. The first case study discusses the development of five different chassis configuration concepts relevant to five different OEM's based on their brand essence information. This case study demonstrates a unique method to integrate market research into the vehicle handling design process. The second case study describes a method to develop chassis configurations for aftermarket-modified vehicles. The aftermarket vehicles are often focused on outright performance with respect to one specific customer relevant attribute rather than well-balanced solution. The results of the two case studies led to the development of *Vehicle Handling Bandwidth Diagrams*. These diagrams are indicators of the minimum and maximum limits of performance attributes achievable within realistic design constraints for a given chassis architecture. These bandwidth diagrams were developed to be used in the initial vehicle target setting process and are described in the third case study. These diagrams will serve as a guideline for the chassis engineers, and will ensure that targets set during the early phases of the vehicle development program are realistic and achievable. The fourth case study describes the implementation of the proposed methodology in which the objective was to give a RWD sporty coupe the vehicle handling characteristics of a FWD hatchback. The results from this case study indicated that not all the optimization goals can always be achieved simultaneously. It showed that at times the inter-dependence and conflicts between the different handling attributes can lead to a compromised design solutions. This case study also indicated the need for proper consideration while imposing constraints in the optimization problem.

The fifth case study describes a formal method for the selection of the best solution from a set of Pareto-optimal solutions obtained from genetic algorithms (GA). A weighted goal programing based approach, which uses manufacturers brand essence information and relative brand attribute weights, is described in this case study. This proposed method will help the chassis engineers during selection of the final chassis setup solution. Finally, the sixth case study describes the results of a global sensitivity analyses performed using design of experiments (DOE). The global sensitivity study was used to develop insights on the sensitivities, dependencies, and trade-offs between different vehicle handling objective metrics.

6.2 Research Contributions

The fundamental research contributions of this dissertation are as follows:

- A simulation-based systems engineering framework, for conceptual design of vehicle handling dynamics that links customer expectations to the final chassis components specifications, was proposed and developed. The comprehensive systems engineering chassis design framework was implemented using the Analytical Target Cascading (ATC) technique.
- Computationally efficient models with appropriate levels of accuracy were developed to effectively connect, evaluate and optimize vehicle, sub-system, and component-level targets and accelerate the handling design process.
- The proposed framework provides a unique method to integrate market research into the vehicle handling design process. The framework uses brand essence information derived from market research for the development of vehicle-level targets, and guides the chassis design direction using relative brand attributes weights.
- From the market survey, four key attributes related to vehicle handling behavior—*Sporty, Fun-to-Drive, Safety,* and *Comfort*—were selected to associate the customer's perception of these attributes to various scenarios and objective metrics of vehicle handling. Empirical relationships were developed to associate these four key customer-relevant vehicle handling attributes with various handling objective metrics. These empirical relationships were used as the basis of the optimization framework.

- Based on the brand attribute information derived from the market research, a goal programming based approach for the selection of the best solution from a set of Pareto-optimal solutions obtained from genetic algorithms (GA) was proposed. The proposed weighted goal programing-based method will serve as a decision-making tool for the chassis engineers and will help during the selection of the final chassis setup solution.
- A concept of *Vehicle Handling Bandwidth Diagrams* was developed from the application of the proposed methodology. The bandwidth diagrams are indicators of the minimum and maximum limits of performance attributes achievable within realistic design constraints for a given chassis architecture. These diagrams are developed to ensure that higher-level targets set during the *Definition Phase* of the vehicle development process are realistic and achievable. Once the handling bandwidth diagrams are generated for a given chassis architecture they will serve as a guideline (and indicate boundaries) for the chassis engineers during the concept development phase. Information regarding the maximum and minimum limits of performance will enable the chassis engineers to explore the design space more effectively and efficiently, and will help towards reduction of concept development time.

6.3 Future Work

Several aspects of the research conducted can be addressed in future research:

- The Analytical Target Cascading (ATC) framework used in this research was implemented using the Augmented Lagrangian (AL) method. It would be interesting to investigate if by using other techniques from literature the computation cost associated with ATC implementation can be further reduced.
- The simulation framework can be further extended in several ways. For example, detailed component-level models representing other suspension and steering system architectures (i.e., MacPherson struts, solid axles, electric power steering etc.,) can be integrated into the simulation framework. More detailed tire models relevant for conceptual tire design can be added to the simulation framework.
- Metrics of cost and weight relevant to different chassis architectures and platforms can be included in the simulations to further help with the concept evaluation and decision-making process.
- The simulation framework can be extended to include the effects of active chassis control systems, for example, Electronic Stability Control (ESC).
- The simulation framework can be extended to integrate effects of other vehicle attributes (functions) such as, ride comfort, NVH, packaging, durability, etc.

APPENDICES

Appendix A.

Detailed Description of Vehicle Handling Domains.

Vehicle handling design engineering focuses on the development of tools and methods to quantify and qualify the directional behavior of a vehicle. The knowledge developed by studying vehicle handling design theory helps control and predict the response of a vehicle to different driver inputs during different driving scenarios.

Vehicle handling behavior can be comprehensively described by the different domains of vehicle handling: steady-state handling, transient handling, steering system feedback (which includes on-center and off-center steering performance), emergency or limit handling, parking, coupled dynamic cornering describing scenarios such as acceleration/braking while cornering, handling adaptability on different road surfaces, straight-line stability, drift/pull behavior during constant speed coasting, and disturbance sensitivity describing vehicles response to external agents such as side-winds, road roughness and road crown. These domains of vehicle handling are formulated considering the vehicle handling performance requirements of a driver during different scenarios of vehicle operation. The different domains of vehicle handling are described in detail in this section.

Steady-State Handling

Steady-state handling refers to the handling performance of a vehicle during steady-state cornering scenarios (i.e., cornering with constant speed and constant steer angle). During these scenarios, the vehicle travels in a steady-state circular motion along a fixed radius of curvature with a constant yaw velocity (heading angle velocity) and side-slip angle. The yaw velocity in these scenarios is simply the ratio of the vehicle's longitudinal velocity and radius of curvature of the turn.

Steady-state handling can be evaluated using the test procedures specified in International Organization for Standardization (ISO) 4138 [47]. ISO 4138 specifies open-loop test methods to determine the steady-state circular driving behavior of passenger cars [47]. The fundamental idea behind this test method is to bring the vehicle to a steady-state equilibrium with respect to speed, steering-wheel angle, and turn radius by driving the vehicle around a circular path and then holding one variable (i.e., speed, steering-wheel angle or turn radius) constant, varying the second and measuring the third. ISO 4138 specifies three methods for evaluating steady-state handling [47]:

-Method 1: *Constant-radius test method*. Here the vehicle is driven around a constant radius circle, vehicle speed is varied, and steering-wheel angle is measured. The recommended radius of the circular path is 100 m, with 40 m as the recommend lower value [47].

-Method 2: *Constant-steering wheel angle test method*. Here the driver steering wheel angle input is kept constant, speed is varied and radius is calculated from vehicle motion variables. The recommended value of steering wheel angle corresponds to the steering angle required to negotiate a circle of radius 30 m at low speeds.

-Method 3: *Constant-speed test method.* Here the vehicle speed is maintained constant, path radius is varied, and steering-wheel angle is measured (or, the steering wheel angle is varied and the radius is calculated from motion variables). ISO 4138 recommends a standard test speed of 100 km/h and also specifies that if other, multiple speeds are selected, they should be in increments of 20 km/h [47].

Theoretically, all test methods should produce equivalent steady-state results, but, in practice, the results obtained from the tests conducted with different combinations of speed, steer angle, and radius might differ due to non-linearities associated with the different vehicle subsystems (steering, suspension, tires, etc.).

Note that to ensure repeatability of test results it is always important to follow a strict set of standards with respect to test track conditions, wind velocity, test vehicle preparation guidelines, etc. ISO 1503-1 [48] specifies these general conditions for vehicle dynamics test measurements.

In this thesis, the following metrics will be used to represent the steady-state handling behavior of the vehicle: Understeer Gradient, Yaw Rate Gain, Lateral Acceleration Gain, Yaw Rate Linearity, Roll Gain, and Side-slip Angle Gain.

Understeer Gradient:

Understeer gradient is one of the most important metrics to quantify the steady-state cornering performance of a vehicle. It is expressed as the change in steering-wheel angle required to maintain a constant radius turn while increasing vehicle speed. It is calculated from the gradient of the steering wheel angle and lateral acceleration curve obtained during a steady-state circular driving maneuver described in ISO 4138 [47]. It is expressed in units of degrees per meter per second squared or degrees per G of lateral acceleration.

Vehicle behavior in a steady-state cornering scenario is a function of vehicle speed, steering-wheel angle, wheelbase, weight distribution, kinematics, and compliance characteristics of the steering, suspension, and tires. At low speeds (i.e., near-zero lateral accelerations), the path curvature of the vehicle is governed by the wheelbase and front-wheel steer angles. As vehicle speed increases, steady-state turning results in centrifugal forces, which further results in kinematic and compliance induced steer and camber angles. This effect can be lumped together and expressed in terms of effective cornering compliances (expressed in degrees per meter per second squared of lateral acceleration). Cornering compliances result in steer and slip angles in the front and rear of the vehicle, which eventually modify the low-speed path radius [47].

When the cornering compliances at the front axle are greater than at the rear, the radius of the path negotiated by the vehicle increases from the Ackermann condition and produces understeer. On the other hand, when the cornering compliances at the rear axle

are greater than at the front, the vehicle path radius reduces and eventually results in oversteer. The difference between the total front and rear cornering compliances is referred to as the understeer gradient [47].

Understeer gradient is also closely associated with the directional stability of the vehicle. Vehicles with a negative understeer gradient, or oversteered vehicles, are directionally unstable beyond a particular critical speed. For this reason, passenger cars are usually designed to have neutral or understeer characteristics. Understeer gradient is a clear indicator of the amount of steering-wheel angle input required by the driver while cornering. For understeer vehicles, the steering angle input increases with vehicle speed (or lateral acceleration) during steady-state cornering situations. The nominal range of understeer gradient is between -1 to 5 deg/G. Typical values of understeer gradient for a pick-up truck would be around 2-3 deg/G and, for a sporty hatchback, around 1-2 deg/G.

Yaw Rate Gain:

Yaw rate gain describes the sensitivity of a vehicle's yaw rate response to a driver's steering-wheel angle inputs and is expressed in units of degrees per second per degree. Yaw rate gain is an indicator of the change in heading angle response of the vehicle per unit steering wheel angle input by the driver; it is subjectively described as "heading easiness" [10]. Mimuro [10] suggests that a higher value of yaw rate gain is always subjectively preferable for the driver. Higher values of yaw rate gain are associated with lower understeer character (i.e., more neutral steer character) in the vehicle. It is important to note that extremely high values of yaw rate gain can lead to the

vehicle becoming oversteered, which might not be preferred by the drivers. Drivers often describe such vehicle with terms like “nervous,” “tail happy,” or “loose rear end”. Crolla [11] indicates that the values of the steady-state yaw rate gain metric should be within the range 0.12 – 0.2 (deg/sec)/deg to attain the best subjective ratings at 100 km/h. Weir and Dimarco [9] indicates an acceptable range of yaw rate gain for “expert” drivers to be between 0.2-0.4 (deg/sec)/deg and between 0.14 to 0.37 (deg/sec)/deg for “typical” drivers at 80 km/h.

Lateral Acceleration Gain:

Lateral acceleration gain describes the sensitivity of the vehicle's lateral acceleration response to the driver’s steering-wheel inputs and is expressed as meter per second squared per degree. This metric is closely related to the vehicle’s understeer gradient, as a higher value of lateral acceleration gain indicates lower understeer characteristics. In general, higher numerical value of lateral acceleration gain is subjectively more preferable.

Yaw Rate Linearity:

Yaw rate linearity describes the linearity of vehicle response during steady-state cornering maneuvers. This metric is often subjectively referred to as *Response Linearity*. It is defined as the ratio of yaw rate gain at different levels of lateral acceleration (i.e., 4 m/s^2 and 6 m/s^2). As the vehicle’s speed (and lateral acceleration) increases during a steady-state cornering scenario, centrifugal forces acting on the vehicle increase, which in

turn alter the understeer characteristics of the vehicle; this is due to the non-linear effects of weight transfer, kinematics, and compliance characteristics. This in turn affects vehicle response and path curvature during scenarios of increasing lateral accelerations. Drivers generally prefer a linear response from the vehicle, which means that drivers prefer a linear increase in yaw rate gain with increasing lateral acceleration during steady-state cornering scenarios.

Roll Gain:

Roll gain describes the sensitivity of the vehicle's roll angle response to lateral acceleration and is expressed as degrees per meter per second squared (or degrees per G). Roll gain for passenger cars is usually in the range of 1-5 deg/G. In general, lower values are preferable as the vehicle rolls less per unit lateral acceleration during cornering.

Sideslip Angle Gain:

Sideslip angle gain describes the sensitivity of the vehicle's sideslip angle response to lateral acceleration and is expressed in degrees per meter per second squared (or degrees per G). Lower values of sideslip angle gain are subjectively preferred by drivers. “Typically, ‘normal’ drivers prefer sideslip angle gain less than 6 deg/G as long as the variation of sideslip gain with lateral acceleration is linear” [49].

Transient Handling

Transient handling refers to a vehicle's cornering performance during dynamic scenarios involving rapid transitions and changes in yaw velocity, sideslip velocity and path curvature (e.g., transience during turn-entry and turn-exit situations).

Transient handling can be evaluated using the test procedures specified in ISO 7401 [50]. ISO 7401 specifies open-loop test methods for determining the transient response behavior of road vehicles. ISO 7401 recommends analyses in both time and frequency domains for the sufficient characterization of a vehicle's transient handling behavior. ISO 7401 describes the following test methods for evaluating transient handling:

Time Domain - Step input, Sinusoidal input

Frequency Domain - Random input, Pulse input, Continuous sinusoidal input

ISO 7401 recommends that at least one test from each time and frequency domain be performed for the characterization of a vehicle's transient handling behavior. In this thesis, the step input—from the time domain—and continuous sinusoidal input—from the frequency domain—are used to evaluate vehicle transient handling performance.

It is important to note that the characteristic values and metrics derived from the different test methods may not always be comparable because of non-linear vehicle behavior and differences in response to periodic and non-periodic input conditions [50].

ISO 7401 specifies that the transient handling test procedure shall be carried out in at least two loading configurations: minimum load conditions and maximum load condition. Minimum loading conditions consist of vehicle curb mass (ISO 1176 [51]), added to the masses of the driver and instrumentation. Maximum loading condition corresponds to the maximum authorized mass of the vehicle. More details on the distribution of mass in the vehicle can be found in ISO 2958 [52]. ISO 7401 [50] recommends a standard test speed of 100 km/h for the transient handling test maneuvers. ISO 1503 [48] specifies these general conditions for vehicle dynamics test measurements.

Step Steer Test:

In this test a vehicle is driven at a constant pre-defined test speed, followed by the rapid application of a step steering input to a preselected value; the input is then maintained at that value until the vehicle reaches a steady state. Steering wheel amplitude is selected in order to obtain a steady-state lateral acceleration at the end of the maneuver around 4 m/s^2 (i.e., around the linear range of vehicle handling).

ISO 7401 specifies the following performance metrics to be used in the analysis of step steer response of the vehicle:

Response time. The time required by the vehicle's response (yaw rate, lateral acceleration, roll, etc.) to first reach 90% of its steady-state value, measured from a reference time. Reference time is the time at which at the steering-wheel angle change reaches 50% of its final value.

Peak response time. The time required by the vehicle's response to reach its peak value, measured from the reference time.

Overshoot. The level of damping in the system, calculated as the ratio of the difference between the peak and steady-state values and steady-state value of the response variable.

Continuous Sinusoidal Steer Test:

In this test the vehicle is driven at a constant, pre-defined test speed, followed by application of a sinusoidal steering-wheel input with a pre-determined frequency and amplitude. Steering frequency is increased in steps covering a minimum frequency range of 0.2-2 Hz. Steering wheel amplitude is selected such that the steady-state lateral acceleration of 4 m/s^2 is achieved while driving at the defined test speed (100 km/h) around a constant radius circle. Lateral acceleration approximately up to 4 m/s^2 is regarded as the linear range of vehicle handling. It is particularly important to maintain the vehicle within the linear range of handling during the continuous sinusoidal steer test as the method of data analysis in the frequency domain—which is used for this test procedure—assumes the system's linear behavior.

ISO 7401 recommends the use of frequency response functions (e.g., gain and phase-angle functions) between the input—the steering-wheel angle—and the output variable—the yaw rate and lateral acceleration—for data analysis and presentation.

In this thesis, the following objective metrics will be used to quantify vehicles' transient handling behavior:

Time Domain Metrics from Step Steer Test: Yaw Rate Response Time, Yaw Rate, Overshoot, TB Factor or Vehicle Characteristics, Roll Rate Response Time, Roll Angle Overshoot.

Frequency Domain Metrics from Continuous Sinusoidal Steer Test: Lateral Acceleration Phase Lag at 1 Hz

Yaw Rate Response Time:

Yaw rate response time is defined as the time required by the vehicle's yaw rate response to first reach 90% of its steady-state value, measured from a reference time. Reference time is the time at which the steering-wheel angle change reaches 50% of its final value during a step steer maneuver. It is expressed in seconds. Yaw rate response time relates to the agility or responsiveness of the vehicle: the lower the yaw rate response time, the more agile and responsive the vehicle.

Yaw rate response time is regarded as a key factor in determining a driver's subjective perception of vehicle handling quality. Weir [9] suggests an upper bound (or a maximum value) for equivalent yaw rate time constant to be 0.3 seconds (and 0.27 sec) for expert (and typical) drivers at 80 km/h to achieve optimum vehicle characteristics of directional control. In this study, Weir [9] defines equivalent yaw rate time-constant as the inverse of the frequency at which the phase of the yaw rate transfer functions equals

45 degrees. It is important to understand that extremely low values of yaw rate response time might lead to the vehicle becoming overly responsive, which might not be subjectively preferred by the driver. Quantifying lower bounds for this metric needs further detailed investigation.

Yaw Rate Overshoot:

Yaw rate overshoot is defined as the ratio of difference in the peak value and steady-state value of yaw rate divided by the steady-state value of yaw rate during a step steer maneuver. It is described as a percentage, and lower values of yaw rate overshoot indicate high yaw rate damping, which is subjectively preferable for drivers.

TB Factor:

TB factor, also referred to as “vehicle characteristics” [Xia [12], Lincke [14], is defined as the product of steady-state side-slip angle and yaw rate peak response time during a step steer maneuver. It is expressed in units of degree-second. Lower values of TB factor indicate faster responses of the vehicle to drivers’ steering input. Lincke [14] found that lower values of TB factor correlate with higher subjective ratings by test drivers.

Lateral Acceleration Phase Lag at 1 Hz:

Lateral acceleration phase lag at 1 Hz is a key indicator of transient handling quality and represents the phase lag in the generation of lateral acceleration response. Mimuru [10] describes this criterion as “following controllability” and suggests that

lower values of this metric are subjectively preferred by drivers. Lower values of this metric also indicate higher vehicle responsiveness. Crolla [11] suggests that drivers' subjectively prefer vehicles with a lateral acceleration phase lag (at 1Hz) lower than or equal to 50 deg. and subjectively dislike vehicles with a lateral acceleration phase lag (at 1Hz) greater than 75 deg. Crolla's [11] results are based on frequency response functions derived from impulse inputs (described by ISO 7401 [50]) at 100 km/h for lateral acceleration levels up to 2 m/s^2.

Roll Rate Response Time

Roll rate response time is defined as the time required by the vehicle's roll rate response to first reach 90% of its steady-state value, measured from a reference time. Reference time is the time at which the steering-wheel angle change reaches 50% of its final value during a step steer maneuver. It is expressed in seconds. Roll rate response time relates to the *turn-in response* of the vehicle; in general, lower values of roll rate response time are preferred by drivers. Crolla [11] suggests an optimum range between approximately 0.3 and 0.45 seconds for a 2 m/s^2 step steer maneuver at 100 km/h. Crolla [11] further indicates that lower subjective ratings are achieved for values lower than 0.3 seconds and higher than 0.5 seconds.

Roll Overshoot:

Roll overshoot is defined as the ratio of difference between peak value and steady-state value of roll angle and the steady-state value of roll angle during a step steer

maneuver. It is described as a percentage, and lower values of roll overshoot (i.e., high roll damping) are subjectively preferred by drivers.

Steering Feedback

Steering feedback, or off-center steering *feel*, in this thesis refers to the steering torque response experienced by the driver while cornering during nominal driving scenarios—more specifically, sub-limit handling situations. Since the steering system happens to be the primary directional interface for the driver while controlling vehicle motion, the steering torque feedback through the steering system and its relationship with the driver's steering input and the vehicle's response (i.e., yaw rate or lateral acceleration) are key factors governing drivers' subjective perception of steering *feel* and overall handling quality.

Several different objective test maneuvers can be used to quantify a vehicle's steering system behavior. In this thesis, steering feedback will be quantified using a steady-state circle test (ISO 4138 [47]). ISO 4138 specifies open-loop test methods for determining the steady-state circular driving behavior of passenger cars. ISO 4138 describes the constant-speed test method, wherein the vehicle is driven at a constant speed, steering wheel angle is varied, and radius is calculated from motion variables. The standard test speed is 100 km/h. The steering torque feedback is measured along with the steering wheel angle input at different lateral acceleration levels.

The following objective metrics will be used to quantify steering feedback: Steering Torque Gradient, Steering Torque Linearity, and Steering Torque Feel.

Steering Torque Gradient

Steering torque gradient is defined as the slope of the steering wheel torque against steering wheel angle data obtained from a steady-state circle test. It is a measure of the stiffness felt by the driver during cornering and is often referred to as *steering stiffness*. It is expressed in units of Newton-meters per degree. High steering torque gradient indicates more feedback through the steering system but also implies an increased steering workload for the driver during cornering. Steering torque gradient describes the steering *feel* around the steering wheel center position. A typical value of steering torque gradient for a pickup truck with power assistance at 80 km/h at around 5 m/s^2 g's of lateral acceleration is approximately 0.05 Nm/deg. Steering torque gradient for a compact hatchback with power assist at 80 km/h at around 4 m/s^2 g's is approximately 0.1 Nm/deg.

Steering Torque Linearity

Steering torque linearity is defined as the ratio of steering wheel torque gradient at different levels of lateral acceleration (4 m/s^2 and 6 m/s^2). This is a measure of linearity in steering torque response.

Steering Torque Feel

Steering torque feel is defined as the slope of steering wheel torque against lateral acceleration obtained during a steady-state circle test. It is expressed in units of Newton-meter per meter per second squared. Norman [53] recommends an optimum value of 2.2 Nm/(m/s^2), and Mitschke [54] mentions an optimum value of 3.6 Nm/(m/s^2) for vehicles without power assistance. Jacksh [55] recommends a range of 1.5 to 3.6 Nm/ (m/s^2). Bartenheier [56] reports steering torque gradients of 22 vehicles with power assistance, indicating a range of 0.9 to 2.9 Nm/ (m/s^2). This generally indicates that the steering torque gradients of vehicles in the market today are considerably different from one another. This is related to the brand DNA of the manufacturers and individual preferences of the development engineers [57]. Typical values of steering torque gradient measured at 100 km/h around lateral acceleration of around 4 m/s^2 for a pick-up truck and compact hatchback are between 0.8 to 0.9 Nm/ (m/s^2) with power assistance.

On-Center Handling

On-center handling refers to the steering performance—the *feel* and *precision*—of the vehicle during nominal straight-line motion and/or while negotiation of large-radius, low-lateral acceleration turns at high speeds [58, 59]. It quantifies the steering response of the vehicle on and about the straight-ahead driving position and is an important aspect influencing the driver's subjective perception of the vehicle's overall handling quality, particularly during highway driving situations.

On-center handling analysis requires the evaluation of steering system response during low lateral accelerations maneuvers (around 1 to 2 m/s^2). On-center handling performance is affected by the parameters of the steering system, vehicle, and tires. In the low lateral acceleration environment of on-center handling, the steering system may well exhibit significant levels of non-linearity due to static friction, steering system lash, power boost, etc.

In general, the on-center handling quality is a function of three characteristics: steering activity, steering feel, and vehicle response [60, 53]. According to Farrer [60], "Excessive hand wheel activity, uninformative steering *feel* and imprecise vehicle response are all contributory factors to poor on-center handling".

ISO 13741 [58, 59] describes two methods to quantify on-center handling behavior, the Weave Test and Transition Test.

Weave Test:

This open-loop test procedure involves a sinusoidal steering input of 0.2 Hz (± 10%) at a constant vehicle speed of 100 km/h. The steering amplitude is adjusted to generate a zero-to-peak lateral acceleration of 2 m/s^2 (± 10 %) [58]. This on-center handling test or weave test was originally described by Norman [53] and Farrer [60].

Transition Test:

This open-loop test procedure involves a steering-wheel ramp input (i.e., an increase in amplitude with a nominally constant angular velocity). The steering input is applied with an angular velocity that increases smoothly from zero up to the nominally constant value (less than or equal to 5 degrees/second). The steering input is applied for a minimum duration of three seconds, until the lateral acceleration achieved by the vehicle reaches a minimum of 1.5 m/s^2 [59].

In this thesis, the weave test described by ISO 13741 will be used to quantify on-center handling performance. The following objective metrics can be used to quantify on-center handling performance: Steering Torque Deadband, Steering Torque Friction, Steering Torque Stiffness, Steering Torque Feel, Steering Torque Linearity, Steering Sensitivity, Yaw Rate Time Lag, Yaw Rate Deadband, Lateral Acceleration Deadband, Steering Work Load, and Steering Work Sensitivity.

Steering Torque Deadband

Steering torque deadband is the horizontal width of the hysteresis loop on the plot of steering-wheel torque (SWT) and steering-wheel angle (SWA), expressed in degrees. It is measured at zero SWT and is a measure of the torque deadband in the steering; furthermore, it quantifies the range of steering-wheel angle displacement about center steering during which the driver does not feel any torque feedback from the steering system. Lower values of torque deadband are preferred by the driver.

Steering Torque Friction

Steering torque friction is the vertical width of the hysteresis loop on the plot of steering-wheel torque (SWT) and steering-wheel angle (SWA), expressed in Newton-meters. It is measured at zero SWA and is proportional to the level of friction in the steering system. SWT at a lateral acceleration of 0 m/s^2 is also a measure of coulomb friction in the steering system. Lower values are preferable.

Steering Torque Stiffness

Steering torque stiffness is the steering torque gradient at zero steering-wheel angle (SWA), expressed in Newton-meter per degree. It is a measure of the stiffness felt by the driver when steering to the left or right [61]. This gradient can be understood as a measure of centering as well. According to Salaani [61, 62], “the better the centering, the better the driver can feel where the steering central position is”.

Steering Torque Feel

Steering torque feel is the steering torque gradient at zero lateral acceleration, expressed in Newton-meter per meter per second squared. This metric is related to *road feel* and *directional sense* [61]. Steering torque gradient at 1 m/s^2 is a measure of *road feel* just off of straight ahead [61].

Steering Torque Linearity

Steering torque linearity is the ratio of steering wheel torque gradient at 0 and 1 m/s^2 of lateral acceleration.

Steering Sensitivity

Steering sensitivity is defined as the gradient of the lateral acceleration against steering-wheel angle curve obtained from the weave test. It is expressed in units of meter per second squared per deg. A high value represents a vehicle subjectively rated to have a crisp feel [61]. A value of 7 m/s^2 / 100 deg is subjectively rated as desirable at 60 mph [61].

Yaw Rate Time Lag

Yaw rate time lag is the delay in seconds between steering input torque and yaw rate at 0.2 Hz of steering input during a weave test. This measure is related to steering system damping and friction. A wide hysteresis curve is the result of a long time delay [61]. Lower values are preferred.

Yaw Rate Deadband

Yaw rate deadband is the horizontal width of the hysteresis loop on the plot of yaw rate and hand wheel angle, expressed in degrees. It is measured at zero yaw rate and is a measure of yaw rate response deadband. Within the deadband zone, the vehicle does not respond to drivers' steering-wheel inputs and hence a lower value of deadband is subjectively preferable for drivers.

Lateral Acceleration Deadband

Lateral acceleration deadband is the horizontal width of the hysteresis loop on the plot of lateral acceleration and hand-wheel angle at zero lateral acceleration, expressed in units of degrees. It is a measure of lateral acceleration response deadband. Within the deadband zone, the vehicle does not respond to drivers' steering-wheel inputs and hence a lower value is preferred.

Steering Work Load

Steering work load is defined the area within the hysteresis loop of steering-wheel torque (SWT) and steering-wheel angle (SWA). It is calculated as the integral of the steering-wheel torque and steering-wheel angle during a complete cycle of the weave test. It is expressed in units of Newton-meter-degree. Lower steering workload is preferable.

Work = $\int T d\delta$; Where: T = SWT, Nm, and δ = SWA, deg.

Steering Work Sensitivity

Workload sensitivity is the slope of the plot of work difference and lateral acceleration at the steering wheel's center (for lateral acceleration within the plus and minus 0.05 g range). Work difference is calculated as an integral of the absolute value of steering-wheel torque (SWT) with respect to steering-wheel angle (SWA). It is expressed in units of Newton-meter-degree per meter per second squared. Lower values are preferred.

$$Work_d = \int | T | d\delta;$$

$$\text{Work Sensitivity} = \partial (Work_d) / \partial (ay) \text{ for } | ay | \leq 0.05 \text{ g.}$$

Emergency Handling

Emergency handling refers to vehicle handling performance during emergency- or safety-related scenarios and obstacle avoidance maneuvers such as severe high-speed lane changes. The primary focus here is on evaluating the yaw and roll stability of the vehicle.

Emergency handling behavior of the vehicle can be quantified based on objective handling test procedures governed by federal regulations, namely:

- Federal Motor Vehicle Safety Standard (FMVSS) 126 for yaw stability.
- National Highway Transportation Safety Administration (NHTSA) Fishhook for roll stability.

Yaw Stability

Yaw stability is governed by the Federal Motor Vehicle Safety Standard (FMVSS) 126 [63, 64]. FMVSS 126 requires all vehicles sold in the United States with a Gross Vehicle Weight Rating (GVWR) of less than 10,000 lbs (4,536 kg) and made after September 1, 2011 to include an Electronic Stability Control (ESC) system as standard equipment [63]. FMVSS 126 ensures, in part, that a particular vehicle with ESC meets the lateral responsiveness and lateral stability criteria that have been deemed as minimum standards for active prevention in various evasive maneuvers. These include single vehicle loss-of-control and run-off-the-road crashes, of which a significant portion result in rollover crashes. The dynamic performance requirements of FMVSS 126 require the

vehicle to be tested with a sequence of sine with dwell maneuvers using increasing steer amplitudes. Figure 49 and Figure 50 show the representative sine with dwell steering test input and a typical yaw rate response output during a FMVSS 126 maneuver. The metrics for vehicle performance are based on yaw rate levels at specific events during the maneuver, which are used as indicators of yaw stability and, at higher steer input values, lateral displacements of the Center of Gravity (CG) as indicators of overall handling responsiveness. The procedure requires that after the driver has taken the vehicle to 82 km/h, the accelerator pedal is released, and a steering robot initiates the steer inputs at 80 km/h. A flowchart for simulating the sine with dwell test series is shown—courtesy of Mechanical Simulation Incorporated—in Figure 51 [65].

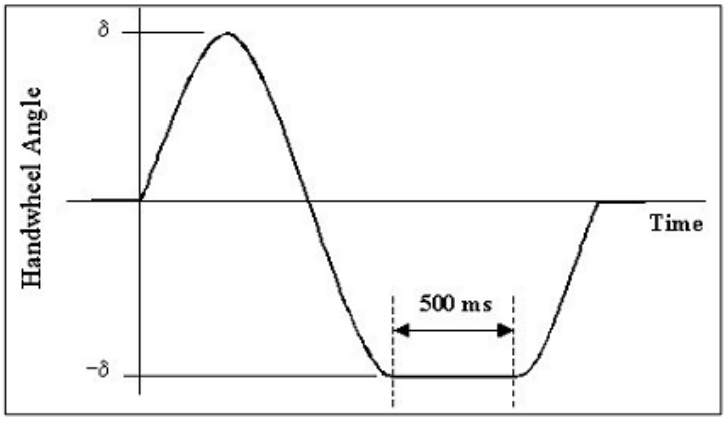

Figure 49. Sine with Dwell steering profile (p. 28 from TP-126-02 NHTSA FMVSS 126 [63]).

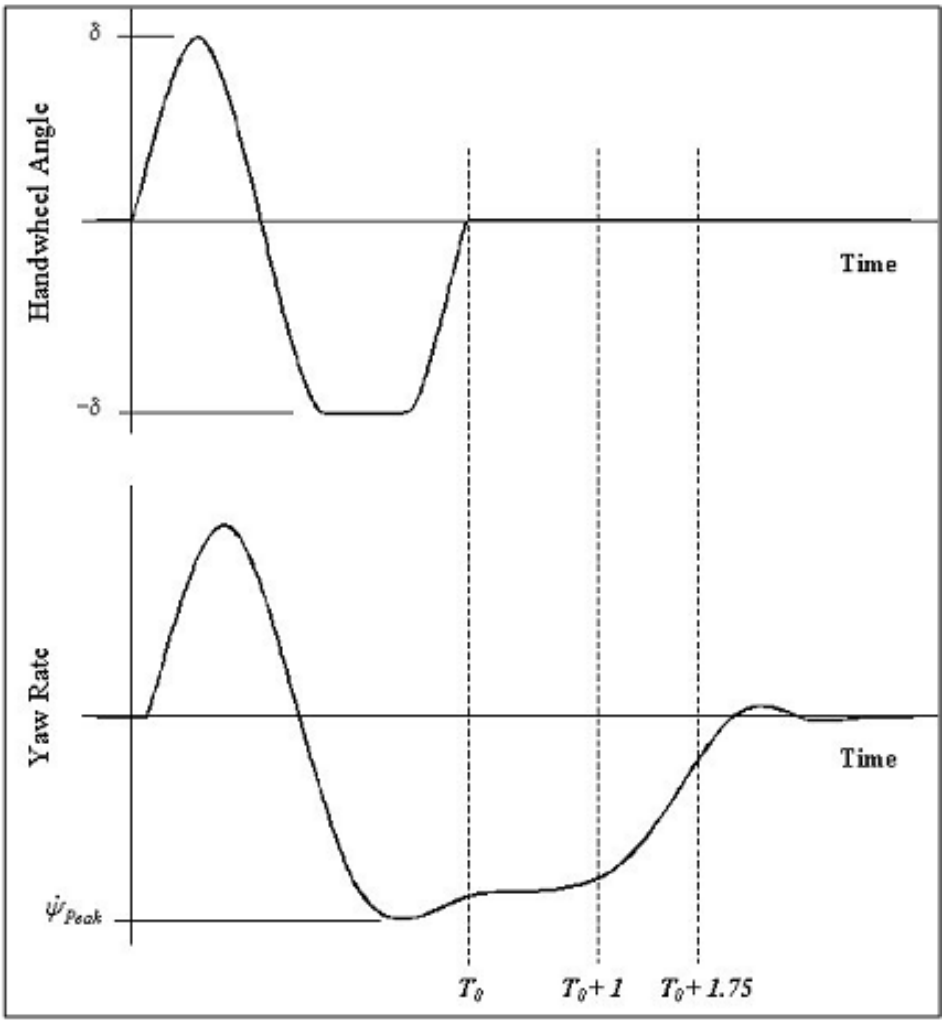

Figure 50. Steering Wheel Angle and Yaw Rate during Sine with Dwell Test

(p. 33 from TP-126-02 NHTSA FMVSS 126 [63]).

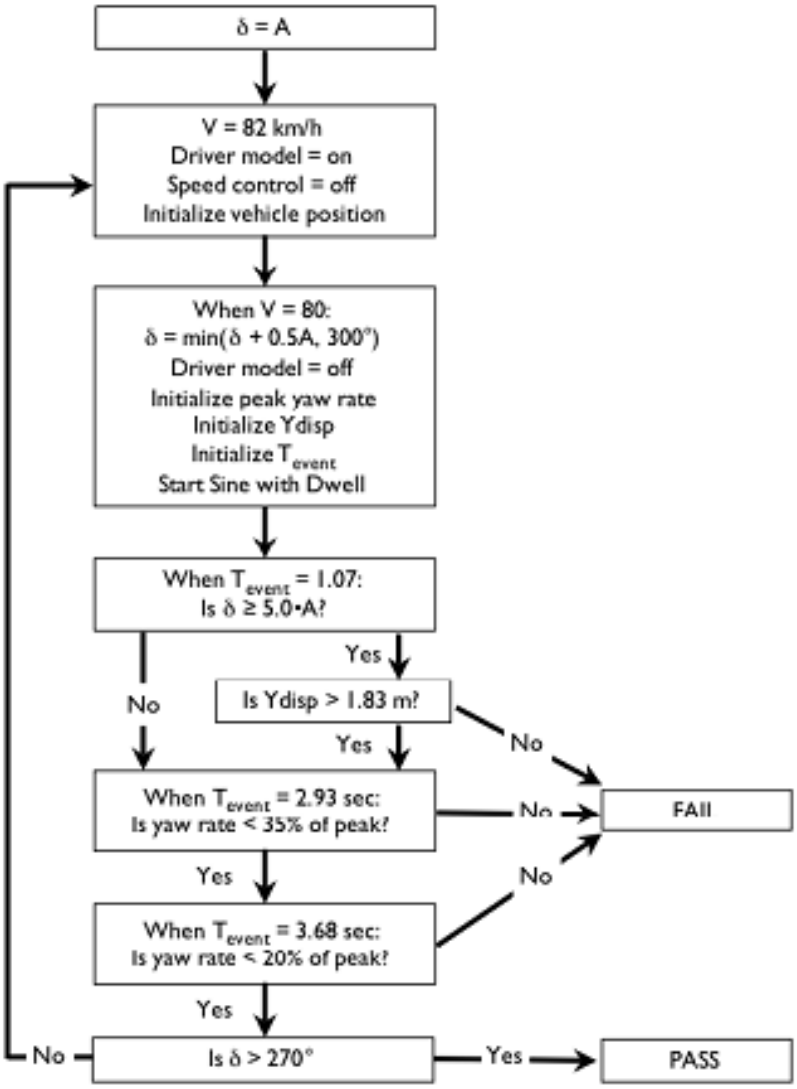

Figure 51. Flowchart for Sine with Dwell Test Series [65].

Roll Stability

Roll stability is evaluated using the NHTSA five-star ratings. The five-star ratings are based on the Static Stability Factor (SSF) and are defined as the ratio of half-track width, T/2, to center of gravity height, H, or SSF=T/2H. These ratings are based on a NHTSA's statistical model for the prediction of rollover rate per single-vehicle crash using both the vehicle's SSF measurement and its performance in the NHTSA fishhook maneuver with five-occupant loading [66]. These "5-Star" ratings are interpreted as "one star for a rollover rate greater than 40 percent; two stars, greater than 30 percent; three stars, greater than 20 percent; four stars, greater than 10 percent; five stars, less than or equal to 10 percent" [66]. Table 26 summarizes the NHTSA rollover ratings. The NHTSA also recommends the fishhook test as to quantify the rollover behavior of vehicles.

Table 26. NHTSA Rollover Ratings [66].

NHTSA 5 Star Ratings	SSF (=Track/2 CG Height)	Risk of Rollover / Rollover Rate per single-vehicle crash
*****	1.45 or more	< = 10 %
****	1.25 to 1.44	>10 %
***	1.13 to 1.24	> 20 %
**	1.04 to 1.12	> 30 %
*	1.03 or less	> 40 %

Figure 52 describes the steering-wheel angle profile for the NHTSA fishhook test. The vehicle is driven at a constant target speed while executing a steering maneuver as depicted in Figure 52. The steering wheel angles used for the test are based on the hand wheel angle required to attain 0.3 g's of lateral acceleration, resulting in different steering inputs for different chassis configurations. The numerical qualifier of this test equates the maximum speed at which the vehicle can successfully perform the maneuver (i.e. without simultaneously lifting two wheels or rolling over).

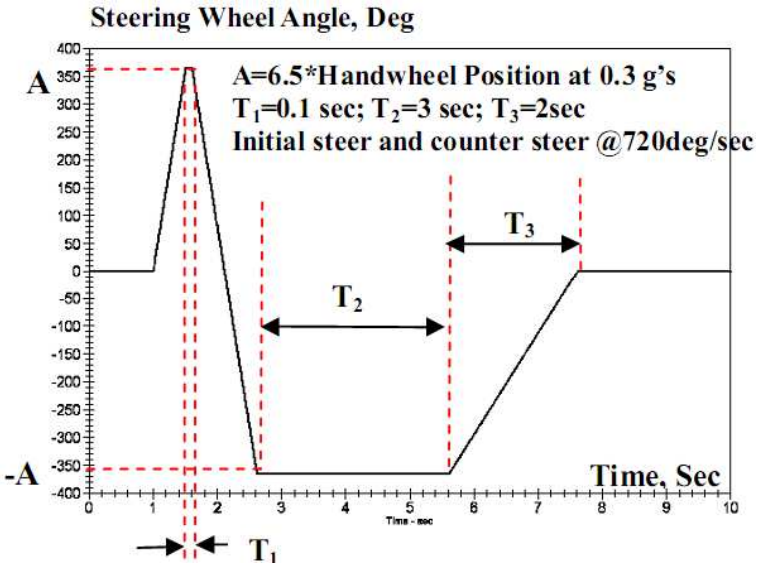

Figure 52. Steering Wheel Angle Profile for Fishhook Test.

Parking

This aspect of vehicle handling refers to the ease of vehicle maneuverability during low-speed, high-steer angle maneuvers typical of parking scenarios. The principal subjective criterion here is the ease of vehicle maneuverability at parking speeds and can be characterized by the objective metric of parking workload.

Parking workload is defined as the integral of steering torque and steering angle during a typical parking scenario. Parking workload is strongly affected by steering wheel rotations and steering torque during low-speed, high-steer angled situations, which in turn depends on factors such as steering geometry, steering ratio, power steering boost characteristics, wheelbase, turn radius and others.

A typical method for designing parking characteristics begins with understanding customer-relevant targets for vehicle turning radius and maximum steering wheel lock-to-lock turns or rotations. These targets are usually set at the beginning of the design cycle and are typically dependent on the vehicle's functional requirements (i.e., an urban mobility vehicle or long-distance cruiser). Given a target for the vehicle's turning radius and its wheelbase, it is possible to make a preliminary calculation, using the Ackerman steering principle, of the maximum hand wheel steer angle required for the vehicle to perform a typical low-speed turning maneuvers as shown in Figure 53.

Another important aspect here is the Ackermann steering geometry, which ensures that during low-speed, large-radius turns all steered wheels are aligned to be in

pure rolling conditions, without any slip angles or tire scrub, because the wheels are steered to track a common turn center. This is possible with a steering geometry where the left and right hand wheels are set up to give theoretically perfect steering at low speeds; this occurs when the tangents to the concentric circles about the turning center intersect on a line through the rear axle, as shown in Figure 54 [67].

With perfect Ackerman steering, the inner front wheel steers more than the outer front wheel. The chassis engineer can design the steering system to have the theoretical perfect, parallel, or reverse Ackermann, as shown in Figure 55. A perfect Ackermann is associated with advantages of minimum tire scrub, better tire-wear life, and low steering effort [49, 68]; however, in some racing applications reverse Ackermann is used because of its cornering performance advantages. For example, during high lateral acceleration scenarios—because of the load transfer effects—the inner wheel is lightly loaded compared to the outer wheel. With a perfect Ackermann steering, the inner wheel is forced to a higher slip angle, which can resulting in tire force saturation that drags the inside tire and eventually raises its temperature; this all can results in a loss of cornering performance.

The value of mean wheel steer angles calculated from the Ackermann formulations becomes a target for the packaging team during wheel envelope design. Also important is the selection of kinematic steering gear ratio which affects the number of steering wheel rotations (lock-to-lock), the magnitude of steering torque feedback and other aspects of vehicle handling (i.e., yaw rate gain).

The static parking torque feedback to the driver in vehicles without power steering primarily depends on the steering ratio, load on front wheels, front tire pressure, tire torsional stiffness, friction between tire and road surface, friction in the steering system, and steering geometry (wheel offset, caster, kingpin inclination) [68, 69]. For vehicles with power steering, the steering torque feedback is dominated by power steering boost characteristics.

In this thesis, the trade-offs involved with selection of steering ratio, power steering boost, and steering geometry, while balancing requirements of parking and other handling aspects, will be studied in sufficient detail to ensure that the 1st-order behavior is included. Sharp [69] and Dixon [70] recommend the following empirical model for estimation of static steering torques at parking speeds:

$$SST = \frac{\mu * F_v^{1.5}}{3 * P_i^{0.5} * K_{ST}} \tag{A.1}$$

SST = Static Steering Torque, Nm
F_v = Wheel Vertical Force, N
P_i = Inflation Pressure, Pa
μ = Coefficient of Limiting Friction
K_{ST} = Kinematic Steering Ratio

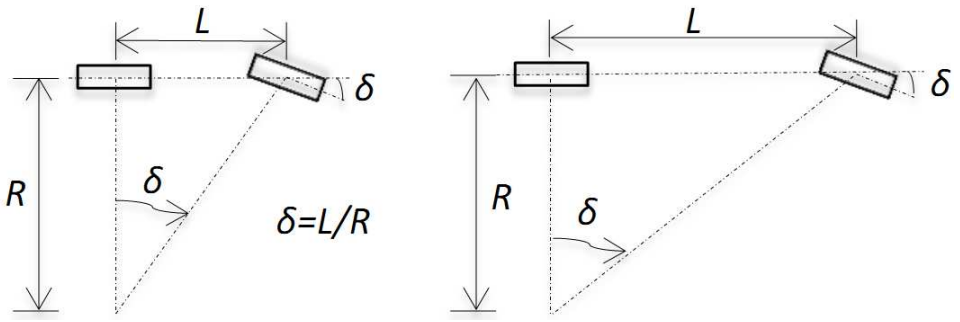

Figure 53. Ackermann Steering Angle during Low-Speed, Tight Turns [67].

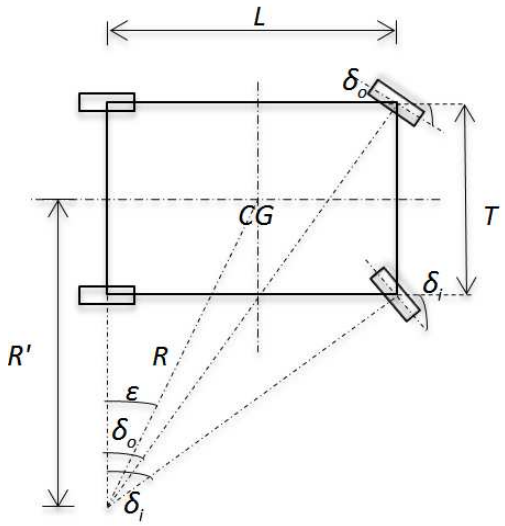

Figure 54. Ackermann Steering Geometry [67].

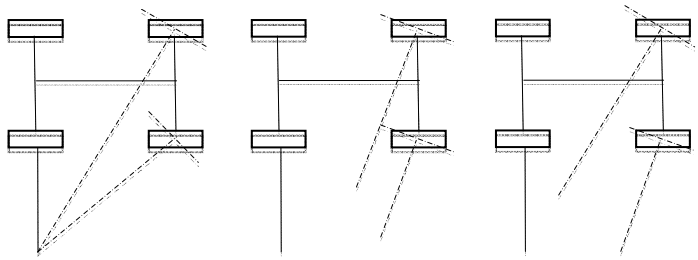

Figure 55. Ackermann Steering Geometry: Perfect, Parallel and Reverse Ackermann [67].

Road Adaptability

In this thesis, road adaptability refers to the vehicle's directional stability while cornering on different road surfaces such as uneven roads, curbs or bumps, and low friction surfaces.

Road irregularities result in dynamic wheel load variation at the tire-road interface. This wheel load variation results in a loss of the tire's cornering potential. The loss of cornering power can be divided into two parts: static loss and dynamic loss. Static loss can be attributed to the cornering stiffness dependence on normal loads, and the dynamic loss is attributed to the rate of change of relaxation on the wheel load [43]. This loss of cornering potential results in a reduction of lateral tire forces generated at the tire-road interface that affects the directional response of the vehicle. Low friction surfaces (i.e., wet road conditions) have a similar effect, reducing the overall lateral grip of the tire. Hence it is important to carefully evaluate the cornering behavior of the vehicle during these scenarios of changing road conditions.

The test procedure to measure and quantify vehicle's rough road cornering behavior involves bringing the vehicle into a steady-state cornering condition and then driving the vehicle over rough roads, or bumps, while cornering. Both steering wheel and throttle should be fixed *before* and *after* entering the rough surface. It is particularly important to maintain fixed inputs of steering wheel angle and throttle while performing this test procedure to ensure that the effect of road disturbances is differentiated against

other variables, such as, throttle lift-off understeer/oversteer and reduction of vehicle speed.

No ISO or SAE standards were found that describe a standard test procedure to test rough road cornering performance of vehicles. The fundamental challenge in having a standard test procedure to characterize rough road cornering performance lies in the fact that vehicle directional response is influenced by both wheel hop resonance and vehicle speed. If tests are done at an arbitrary fixed speed, wheel hop resonance bias might exist, and speed itself may become a bias if the test is conducted at different speeds. Bergman [71] highlights the complexity of formulating a consistent and practical test procedure to quantify rough road cornering performance. Bergman [71] presents detailed results from tests performed on real rough roads as well as test roads with equally spaced bumps, unequally spaced bumps, and a single bump. He also points out that the effect of a single bump on a vehicle's directional stability is very similar to that of randomly spaced bumps, making the single bump test relevant to real world conditions. Bergman's [71] results indicate a good correlation between subjective evaluation of vehicles on real rough roads with measurements during single bump tests. In this work, single bumps were made of rubber strips with trapezoidal cross section as shown in Figure 56. These tests were done at a speed of 48 km/h (30 mph) at 0.4 g lateral acceleration.

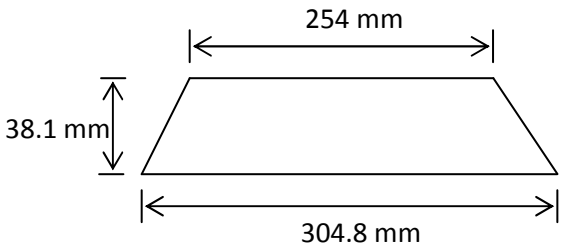

Figure 56. Cross-section of single bump used for rough road cornering [71].

As a vehicle corners over rough roads or bumps, its directional response can be studied for three different conditions: first, when the front wheels enter the bump and the rear wheels are still on the smooth surface;, second, when both front and rear wheels are on bumps; third, when the front wheels are leaving the bump, and the rear wheels are still on the bump. Past studies have suggested that drivers are particularly sensitive to the third phase of the maneuver (i.e., scenarios with reduction in rear grip).

Objective metrics that quantify a vehicle's cornering behavior over different road surfaces capture the changes in its yaw behavior as it transitions between different road surfaces.

Bergman [71] suggested this non-dimensional metric to quantify a vehicle's behavior while cornering over rough roads; it is called the Rough Road Cornering Index and is described in Equation A2. The Rough Road Cornering Index describes the difference in a vehicle's maximum and minimum yaw rate values while cornering on rough roads or bumps normalized with the steady-state yaw rate value prior to entering the bumps. A lower value on the Rough Road Cornering Index is preferable.

$$RRC = \frac{1}{\dot{\psi}_0}\left(\dot{\psi}_{max} - \dot{\psi}_{min}\right)$$

RRC = Rough Road Cornering Index (A.2)

$\dot{\psi}_0$ *= Steady state yaw rate at time prior to entering bump area, deg/sec*

$\dot{\psi}_{max}$ *= Max yaw rate at exit of bumps, deg/sec*

$\dot{\psi}_{min}$ *= Min yaw rate on the bumps, deg/sec*

Coupled Dynamic Cornering

Coupled dynamic cornering in this thesis refers to the vehicle's directional behavior in scenarios where cornering is coupled with other dynamic motions such as braking or acceleration. Braking or acceleration while cornering usually results in undesired yaw responses and changes in the vehicle's course. This vehicle response is not expected by the driver and clashes with the driver's intent to either increase or decrease vehicle speed without changing its heading direction. This unexpected vehicle behavior is a result of several factors: cornering capability decreases because of the traction or braking forces acting on the tires, a fore and aft weight transfer due to longitudinal acceleration affects the lateral force distribution around the vehicle, an unequal distribution of lateral forces and longitudinal forces around the vehicle causes destabilizing yaw moments, and the vehicle's understeer characteristics change because of the reduction of vehicle speed [71]. Extreme braking or acceleration during these maneuvers might lead to loss of steering control—front wheel lockup or saturation—or spin out—rear wheel lockup or saturation.

The test procedure to measure and quantify this aspect of vehicle handling involves cornering at a constant speed in a steady-state condition followed by the application or release of the brakes or throttle without applying corrective steering. ISO 7975 [72] specifies an open-loop test method for evaluating vehicle performance during braking-in-a-turn maneuvers. It specifies how the steady-state circular response of the vehicle is altered by a braking action alone. Here the vehicle is driven around a constant

radius circle (in a steady-state condition) followed by a sudden application of the brakes. The initial conditions are defined by constant longitudinal velocity and a circle of given radius. The steering wheel angle is held constant throughout the test. The recommended standard test speed is 81 km/h and on a circle of radius 100 m. The objective is to reach a steady-state lateral acceleration of 5 m/s^2 before application of the brakes. The steady-state lateral acceleration of 5 m/s^2 can also be achieved by using other combinations of test speeds (44 -114 km/h) and constant radius circles (30 -200 m). Several test runs can be performed with increasing levels of longitudinal acceleration until the wheels start to lock up. The minimum braking action should correspond to a mean longitudinal acceleration of 2 m/s^2 and should be increased by increments not more than 1 m/s^2. ISO 7975 specifies strict procedures for brake conditioning before starting the actual test. ISO 7975 recommends around 12 performance metrics expressed as ratios of the yaw rate, lateral acceleration, sideslip angle, and path curvature before and after the braking action. A similar test procedure to determine the effect of a sudden initiation of power-off condition (by release of the accelerator pedal) on a vehicle in a turn is described by ISO 9816 [73].

The objective metric to quantify a vehicle's directional behavior during these scenarios of coupled motions can be described in terms of change in the vehicle's yaw behavior due to brake or throttle application during steady-state cornering and is referred to as the *understeer angle increment*.

Bergman [71] presents this effective test criterion to quantify a vehicle's behavior during these scenarios called the *understeer angle increment* ($\Delta\delta_u$). This metric quantifies vehicle yaw rate response before and after brake or throttle application. Bergman [71] also presents results of subjective-objective correlation by using the metric understeer angle increment and suggests that the lower the value of normalized understeer gradient, the higher the subjective rating of the vehicle by test drivers.

$$\Delta\delta_u = \frac{L}{\ddot{x}}\left(\frac{\dot{\psi}}{V} - \frac{\dot{\psi}_0}{V_0}\right) \tag{A.3}$$

$\Delta\delta_u$ = *Understeer Angle Increment, deg/g*

$\dot{\psi}_0$ = *Steady state yaw rate prior to brake/acceleration application, deg/sec*

V_0 = *Steady state vehicle speed prior to brake/acceleration application, m/sec*

$\dot{\psi}$ = *Steady state yaw rate after brake/acceleration application, deg/sec*

V = *Steady state vehicle speed after brake/acceleration application, m/sec*

$\ddot{x}$ = *Longitudinal deceleration/acceleration, g*

L = *Wheelbase, m*

Straight-Line Stability

Straight-line stability, in this thesis, refers to the tendency of a vehicle to maintain stability and follow its intended path of travel during scenarios of straight-line braking, acceleration, and coasting. Straight-line stability is closely associated with both vehicle safety and driver comfort.

Vehicle stability during straight-line braking and acceleration on road surfaces with split-mu coefficients of friction is a key aspect of vehicle safety evaluated under the domain of straight-line stability. During a split-mu braking or acceleration scenario, the unequal forces acting on the vehicle result in a destabilizing moment around the vehicle's center of gravity and can result in a loss of stability. This tendency of the vehicle to lose control during these split-mu braking and acceleration scenarios is quantified using the metric of straight-line stability margin.

Driver comfort is related to the *pull* and *drift* behavior of a vehicle during vehicle straight-line motion. *Pull* is defined as the steering wheel torque required to keep the vehicle travelling on a straight-line path (i.e., fixed control mode) whereas *drift* is defined as the deviation of the vehicle from the straight-line path when the steering wheel is released (i.e., free control mode). Drift and pull behavior is most concerning to drivers while coasting on highways—a constant speed straight-line driving scenario. Driver comfort is also related to pitch characteristics—such as squat and dive—of the vehicle of the vehicle during straight-line braking and acceleration scenarios.

Vehicle straight-line stability is influenced by steering, suspension, and tire characteristics. Steering geometry (i.e., caster angle, kingpin inclination, scrub radius), suspension kinematics (i.e., bump steer, static alignment), suspension compliance (i.e., longitudinal force wheel center compliance), and tire characteristics (i.e., conicity, plysteer) all influence straight-line stability characteristics of the vehicle.

Note that vehicle straight-line pull and drift characteristics are also affected by external environmental disturbances such as side-winds, road unevenness, and road crown. In this thesis, vehicle straight-line behavior due to external environmental disturbances will be considered as a separate domain of vehicle handling and is described in the next section (see Disturbance Sensitivity).

Stability during Split-Mu Braking

ISO 14512 [74] describes an open-loop test method for determining vehicle reactions during a straight-line braking maneuver on a surface with a split coefficient of friction (e.g., a surface with a low coefficient of friction on one side). The initial condition for the test is driving in a straight-line at constant speed. The position of the steering wheel and accelerator are held as steady as possible in the initial state. As the vehicle enters the split-friction surface, the braking maneuver is initiated while the steering wheel is held fixed at its position. During the test, operating functions and vehicle responses are measured and recorded.

The recommended speed for straight-line driving before initiating the braking maneuver is 80 km/h. The yaw velocity at different mean longitudinal deceleration levels resultant from the braking action is used as the characteristic metric for this test. ISO 14512 mentions that that the maximum yaw acceleration at different longitudinal deceleration levels can also be used as a metric for this test.

In this thesis, the metric – *straight-line stability margin* – is used as a representative for straight-line stability during split-mu braking. *Straight-line stability margin* is a measure of vehicle's tendency to develop a destabilizing yaw moment while reacting to un-balanced longitudinal and lateral force inputs. Lower value of this indicates higher straight-line stability. Figure 57 and Equations A.4 and A.5 are used to derive the mathematical formulation for straight-line stability margin.

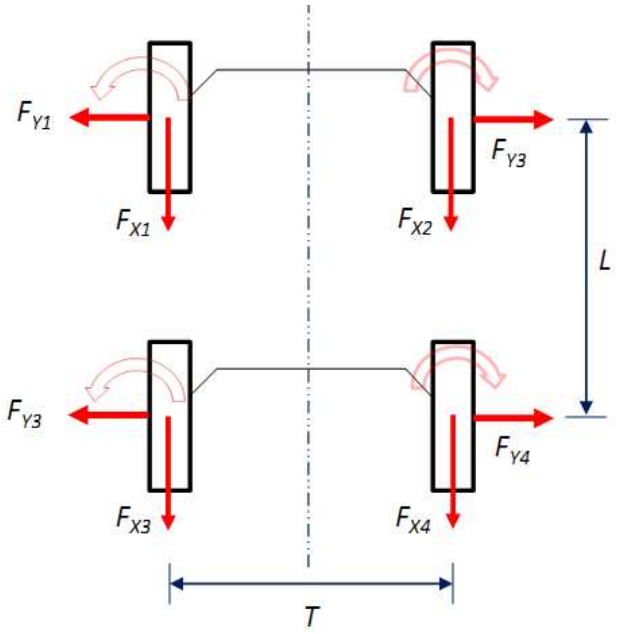

Figure 57. Longitudinal and Lateral Force Un-Balance acting on the Vehicle.

For Stability: $\sum M=0$

$$\Delta F_{xF}.(\frac{T}{2})+\Delta F_{YF}.(\frac{L}{2})+\Delta F_{xR}.(\frac{T}{2})+\Delta F_{YR}.(\frac{L}{2})=0$$
$$\Delta F_{xF}.\left[(\frac{T}{2})+C_{\alpha F}.LFCS_F.(\frac{L}{2})\right]+\Delta F_{xR}.\left[(\frac{T}{2})+C_{\alpha R}.LFCS_R.(\frac{L}{2})\right]=0 \quad \text{(A.4)}$$

SSM = Straight Line Stability Margin

$$=\frac{Moment(Nm)}{ForceUnbalance\_Front\ Axle(N)}$$

$$=\frac{M}{\Delta F_{XF}}=\left[\frac{T}{2}.(\frac{1}{P_{wf}})+(\frac{L}{2}).(C_{\alpha F}.LFCS_F+C_{\alpha R}.LFCS_R.(\frac{1-P_{wf}}{P_{wf}}))\right] \quad \text{(A.5)}$$

Assumption:

$W_f(axle) = P_{wf}*W$, $W_r(axle) = (1-P_{wf})*W$,

$$\Delta F_{xF}=\frac{P_{wf}}{(1-P_{wf})}\Delta F_{xR}$$

Front Axle Longitudinal Force Unbalance = $\Delta F_{xF}=F_{x1}-F_{x2}$

Rear Axle Longitudinal Force Unbalance = $\Delta F_{xR}=F_{x3}-F_{x4}$

Front Axle Lateral Force Unbalance = $\Delta F_{YF}=F_{Y1}-F_{Y2}=C_{\alpha F}.LFCS_F.\Delta F_{xF}$

Rear Axle Lateral Force Unbalance = $\Delta F_{YR}=F_{Y3}-F_{Y4}=C_{\alpha R}.LFCS_R.\Delta F_{xR}$

$C_{\alpha F}$, $C_{\alpha R}$ = *Front and Rear Cornering Stiffness per Tire(N/deg)*

$LFCS_F$, $LFCS_R$ = *Front and Rear Longitudinal Force Complaince Steer(Deg*

LFCS = +ve Number = Toe Out in Braking

W_f, *Wr (axle), = Weight on the Front and Rear Axle, N*

P_{wf} *=Percent Weight on the Front Axle*

W = Vehicle Weight, P_{wf} *= Ratio of Weight on the Front axle*

Pull and Drift

Different OEMs and tire suppliers have specific ways to access pull and drift behavior of a vehicle during coasting scenarios. No specific ISO/SAE standards were found related to test that quantify vehicular drift and pull behavior. However, Lee [75] and Oh [76] both indicate very similar methods for testing vehicular drift characteristics. Both papers suggest driving the vehicle at a constant speed of 80 km/h or 100 km/h in a straight line for some distance (control zone = 100 m), followed by the release of the steering wheel by the driver in the test zone (= 100 m). The amount of lateral movement of the vehicle in the test zone is used as a criterion to quantify vehicle drift behavior. In this same setup, if the driver applies a corrective steering to maintain the straight-line motion of the vehicle in the control zone, the residual steering torque applied by the driver can be used as a measurement of vehicle pull behavior [76].

The following objective metrics can be defined:

- *Pull.* The steering torque required by the driver to keep the vehicle on a straight-line path.
- *Drift*. The deviation of the vehicle from its intended straight-line path.

As described above, the pull and drift of the vehicle is mainly affected by two factors: *tire properties* and *suspension alignment*. With respect to tire properties, a vehicle's pull and drift issues result from the fact that the tire's lateral force and aligning moment are not centered at a zero slip angle (i.e., the tire produces a non-zero lateral force and aligning moment, even when the slip angle is zero).

Several researchers—Pottinger [77], Matlya [78], and Lee [75]—have contributed immensely in this area. Pottinger [77] and Matyja [78] found that vehicle pull occurs if aligning torque is non-zero at the slip angle where lateral force becomes zero or vice versa. The aligning torque at the slip angle (α1) where lateral force is zero is defined as the Residual Aligning Torque (RAT), and the lateral force at the slip angle (α2) where aligning torque becomes zero is called as the Residual Lateral Force (RLF). Pottinger [77] calls the angle difference (α1-α2) an Aligning Torque Static Phase (ATSP).

RAT, RLF, and ATSP in tires result from two main factors: *conicity* and *plysteer*. *Conicity* is defined as the component of lateral force produced by a tire rolling at a zero slip angle. It does not change directions when the rotational direction is changed but will change direction when the tire is reversed on the rim. Conicity in a radial tire is a result of the off-centering of top belts and is related to manufacturing tolerances [75]. *Plysteer*, on the other hand, is defined as the component of lateral force produced by a tire rolling at a zero slip angle, which changes directions when the rotational direction is changed but does not change directions when the tire is reversed on the rim. Plysteer is the result of pantographing of belts in a tire, comes from the fundamental physics of tire construction, and is designed very consistently into the tire. A typical value of plysteer force for a passenger car tire is around 300 N [79].

Disturbance Sensitivity

Disturbance sensitivity, in this thesis, refers to a vehicle's response sensitivity to external environmental force or displacement disturbances acting upon it. Typical examples of such disturbances include lateral side-winds, road crown, road roughness, and road irregularities.

A vehicle's response to road crown, or banking, can be evaluated by analyzing its response to a lateral force input acting at the CG (see Figure 58). The application of lateral forces can be studied with two cases: lateral force acting as an idealized step input or lateral force acting as an impulse input. On the same lines, a vehicle's reaction to side-wind disturbances can be evaluated with two ways: first, by assuming a constant speed lateral wind disturbance acting as a step input at the Aerodynamic Center (AC) of the vehicle; and second, by assuming a sudden lateral wind gust, or impulse input, acting at the Aerodynamic Center (AC) of the vehicle. In this thesis, a vehicle's disturbance sensitivity will be evaluated using an idealized step input acting at the CG of the vehicle to study its response to road crown, or banking, and by using an idealized step input acting at the AC of the vehicle to study response to lateral wind gusts.

A straight-line response to road roughness is another area that should be evaluated in order to analyze the vehicle's sensitivity to external disturbance.

ISO 12021 [80] specifies an open-loop test method to analyze the sensitivity of vehicles to lateral wind disturbances by using a wind generator. In this method, the vehicle is driven along a straight path, and its response to the crosswind input of a wind generator is measured while keeping the steering wheel in a fixed position. ISO 12021 specifies a standard test speed of 100 km/h. ISO 12021 proposes two methods for measuring lateral deviation of the vehicle.

- a direct method by means of direct measurement of the vehicle trail
- an indirect method by means of computation from measured vehicle motions

ISO 12021 gives well-defined guidelines for test track specifications and ambient weather conditions (e.g., wind velocity should be less or equal to 3 m/s). ISO 12021 specifies that this test procedure shall be carried out in at least two loading configurations: minimum load conditions and maximum load condition. Minimum loading conditions consist of vehicle curb mass [51] added to the masses of the driver and instrumentation. Maximum loading condition corresponds to the maximum authorized mass of the vehicle. More details on the distribution of mass in the vehicle can be found in ISO 2958 [52]. ISO 12021 [80] also specifies that the lateral wind generated by the wind generators should have an average velocity of 20 m/s ± 3 m/s (for an ambient wind condition of <1 m/s). The average wind velocity is calculated over the length of the wind zone and over the height of the test vehicle. The nominal length of the wind zone shall not be less than 15 m and should preferably be more than 25 m. More details on the specifications of this test can be found in ISO 12021 [80].

In addition to the lateral deviation metric, ISO 12021 also suggests an optional metric, defined as the pulse value of yaw velocity and lateral acceleration. ISO 12021 defines the pulse value as the average signal value during the time the signal exceeds 50% of peak value.

The objective metric to quantify a vehicle's sensitivity to road crown and side wind disturbances that will be used in this thesis is referred to as *understeer rate*.

Understeer rate [81] is defined as the ratio of a vehicle's resultant lateral acceleration due to external disturbance forces at CG to the input lateral acceleration (or, external disturbance force divided by vehicle mass).

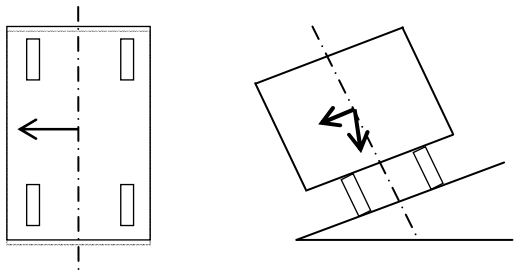

Figure 58. Disturbance Force at Vehicle CG due to Road Crown or Banking [83].

A simplistic 2 DOF (yaw velocity and lateral velocity) model can be used for the analyses of vehicle sensitivity to road crown. Equations determining vehicular motion with steer angle set to zero and lateral force acting at the center of gravity for a 2 DOF model are shown below.

$$Mv\frac{d\beta}{dt} + 2\left(C_{\alpha F}+C_{\alpha R}\right)\beta + \left\{Mv + \frac{2}{v}\left(aC_{\alpha F} - bC_{\alpha R}\right)\right\}r = Y \tag{A.6}$$

$$2\left(aC_{\alpha F}-bC_{\alpha R}\right)\beta + I\frac{dr}{dt} + \frac{2\left(a^2C_{\alpha F}+b^2C_{\alpha R}\right)}{v}r = 0 \tag{A.7}$$

By using the Laplace transformations, one can establish the transfer functions of sideslip angle and yaw rate with respect to the lateral disturbance input (Y). The steady-state values of sideslip angle and yaw rate in response to a step lateral force disturbance ($Y=Y_0$) at the CG is given by:

$$\beta = \frac{\left(a^2C_{\alpha F} + b^2C_{\alpha R}\right)Y_0}{2L^2C_{\alpha F}C_{\alpha R}\left[1-\frac{M\left(aC_{\alpha F}-bC_{\alpha R}\right)V^2}{2L^2C_{\alpha F}C_{\alpha R}}\right]} \tag{A.8}$$

$$r = \frac{-\left(aC_{\alpha F}-bC_{\alpha R}\right)vY_0}{2L^2C_{\alpha F}C_{\alpha R}\left[1-\frac{M\left(aC_{\alpha F}-bC_{\alpha R}\right)V^2}{2L^2C_{\alpha F}C_{\alpha R}}\right]} \tag{A.9}$$

Analysis using the above equations suggests that an oversteered vehicle is more sensitive to environmental disturbances as vehicle speed increases. Analyses of the vehicle's transient response in the presence of lateral wind disturbance can also be studied using Equations A6 and A7. Bergman [81] described the metric understeer rate U_R and defined it as

$$U_R = \frac{\ddot{Y}}{\ddot{Y}_0}$$

$\ddot{Y}$ = *Resultant Lateral Acceleration at CG due to Input Disturbance Force* Y_0 (A.10)

$\ddot{Y}_0$ = *Input Lateral Acceleration*

$$\ddot{Y} = \frac{\dfrac{-M\left(aC_{\alpha F} - bC_{\alpha R}\right)V^2}{2L^2 C_{\alpha F} C_{\alpha R}}}{\left(1 - \dfrac{M\left(aC_{\alpha F} - bC_{\alpha R}\right)V^2}{2L^2 C_{\alpha F} C_{\alpha R}}\right)} \frac{Y_0}{M} \tag{A.11}$$

$$\ddot{Y}_0 = \frac{Y_0}{M} \tag{A.12}$$

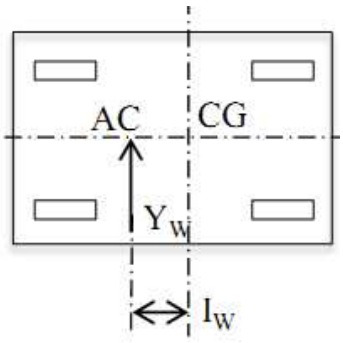

Figure 59. Lateral Force Disturbances by Side Winds [83].

A similar analysis technique can be used to assess vehicle directional stability during side wind disturbances. Because the lateral wind disturbance does not usually act at the CG of the vehicle, the acting point of lateral force (Y_W) is called the Aerodynamic Center (AC), as shown in Figure 59. Along with lateral force input, the influence of yaw

moment input ($N_W = I_W$ x Y_W) also needs to be analyzed. The equations of motion are shown below.

$$Mv\frac{d\beta}{dt} + 2\left(C_{\alpha F} + C_{\alpha R}\right)\beta + \left\{Mv + \frac{2}{V}\left(aC_{\alpha F} - bC_{\alpha R}\right)\right\}r = Y_W \tag{A.13}$$

$$2\left(aC_{\alpha F} - bC_{\alpha R}\right)\beta + I\frac{dr}{dt} + \frac{2\left(a^2C_{\alpha F} + b^2C_{\alpha R}\right)}{V}r = -I_W Y_W \tag{A.14}$$

An alternative performance metric commonly used to study a vehicle's directional stability in presence of side wind disturbances is called the *sensitivity coefficient* (S_W) and is defined as the steady-state lateral acceleration generated by the vehicle per unit lateral wind force. The equation for the *sensitivity coefficient* is below.

$$S_W = \frac{Vr}{Y_{W0}} = \frac{\left(l_N - I_W\right)\left(C_{\alpha F} + C_{\alpha R}\right)V^2}{2l^2C_{\alpha F}C_{\alpha R}\left(1 - \frac{M\left(aC_{\alpha F} - bC_{\alpha R}\right)V^2}{2L^2C_{\alpha F}C_{\alpha R}}\right)} \;;\quad l_N = \frac{-\left(aC_{\alpha F} - bC_{\alpha R}\right)}{\left(C_{\alpha F} + C_{\alpha R}\right)} \tag{A.15}$$

Appendix B.

Vehicle and Sub-System Level Models

In this thesis a simplified lower-order vehicle dynamics model which captures the behavior of the real-world naturalistic driving up to 0.3 -0.4 g's of lateral acceleration is used for the simulations.

The vehicle handling model used in this research is based on a three Degree-of-Freedom (DOF) vehicle model with roll, yaw, and lateral motion as the three degrees of freedom. This is coupled with a steering system model, which adds another DOF and accounts for steering system compliance between the road wheel and steering wheel.

The tire force model is based on Pacejka's Magic Formulae [43] and includes a simple transient tire side force model extension based on a first-order lag using the tire's relaxation length as the time constant. The influence of steering system compliance, suspension kinematics and compliance, weight transfer due to height of the center of gravity, roll stiffness, and centrifugal forces are included in the tire force calculations using effective axle cornering characteristics [43]. Such effective cornering characteristics include tire properties based on Pacejka's Magic Formulae, incorporate tire force dependency on slip angle and vertical load, and provide mechanisms for combined cornering and braking with tire force saturation.

The suspension elasto-kinematic characteristics are modeled using the suspension compliance matrix formulations described by Knapczyk [44].

Steady-State Vehicle Handling Model

Figure 60 and Figure 61 show the free body diagram (FBD) of the sprung and un-sprung mass of a vehicle during a steady-state cornering scenario. The equations of motion describing vehicle's behavior during steady-state cornering are described in this section.

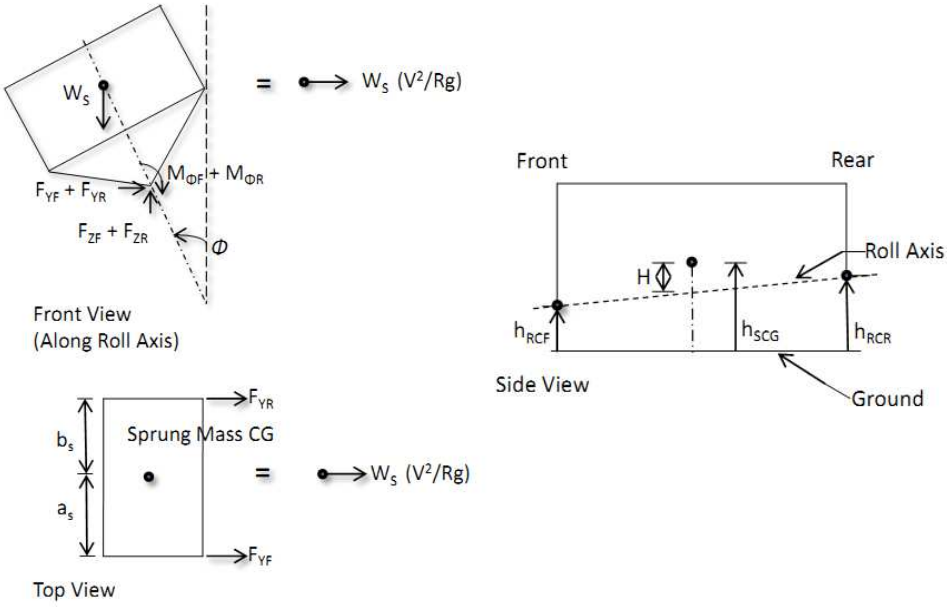

Figure 60. Vehicle Free Body Diagram of Vehicle Sprung Mass during Steady-State Handling Scenario.

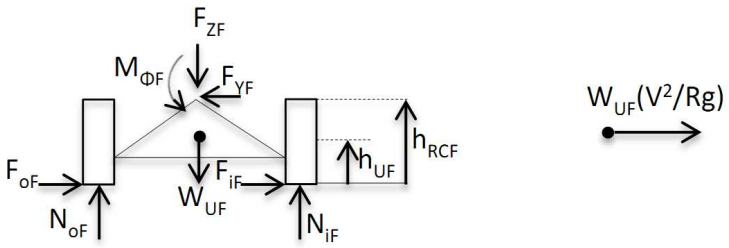

Figure 61. Vehicle Free Body Diagram of Vehicle Un-Sprung Mass during Steady-State Handling Scenario.

Equations B.1, B.3, and B.4 describe the roll moment, lateral force and yaw moment equilibrium during steady-state cornering. Equation B.7 describes the moment equilibrium for un-sprung masses and further helps derive the formulations for vertical loads experienced by the four tires during a steady-state cornering scenario (see Equation B.8, B.9, B.10 and B.11).

Roll Moment Equation:

$$\sum M_X = - W_S \, H \sin\Phi + M_{\Phi F} + M_{\Phi R} = W_S \frac{V^2}{Rg} H\cos\Phi \tag{B.1}$$

For small Φ

$$\left(K_{\Phi F} + K_{\Phi R} - W_S H\right)\Phi = W_S \frac{V^2}{Rg} H \tag{B.2}$$

5

Lateral Force Equation:

$$\sum F_Y = F_{YF} + F_{YR} = W_s \frac{V^2}{Rg} \tag{B.3}$$

Yaw Moment Equation:

$$\sum M_Z = F_{YR}\, b_S - F_{YF}\, a_S = 0 \tag{B.4}$$

$$\begin{aligned} &F_{YF} = \frac{b_S}{a_S} F_{YR}; \\ &\left(\frac{b_S}{a_S} + 1\right) F_{YR} = W_s \frac{V^2}{Rg}; \\ &F_{YR} = \frac{a_S}{L} W_s \frac{V^2}{Rg}; F_{YF} = \frac{b_S}{L} W_s \frac{V^2}{Rg}; \end{aligned} \tag{B.5}$$

$$F_{ZF} = W_S \frac{b_S}{L}; F_{ZR} = W_S \frac{a_S}{L}; \tag{B.6}$$

The normal load at each tire can be found by calculating the summation of moments about the outside tire (see Figure 61),

$$\sum M = W_{UF} \frac{T}{2} - N_{iF} T + F_{ZF} \frac{T}{2} - F_{YF} h_{RCF} - M_{\Phi F} = W_{UF} \frac{V^2}{Rg} h_{UF} \tag{B.7}$$

$$N_{iF} = \frac{1}{2}\left(W_{UF} + \frac{W_S b_S}{L}\right) - \frac{V^2}{Rg}\left[W_S \frac{b_S}{L} \frac{h_{RCF}}{T} + W_S \frac{H}{T} \frac{K_{\Phi F}}{K_{\Phi F} + K_{\Phi R} - W_S H} + W_{UF} \frac{h_{UF}}{T}\right] \tag{B.8}$$

$$N_{oF} = \frac{1}{2}\left(W_{UF} + \frac{W_S b_S}{L} \right) + \frac{V^2}{Rg}\left[W_S \frac{b_S}{L}\frac{h_{RCF}}{T} + W_S \frac{H}{T}\frac{K_{\Phi F}}{K_{\Phi F} + K_{\Phi R} - W_S H} + W_{UF}\frac{h_{UF}}{T} \right] \quad \text{(B.9)}$$

$$N_{iR} = \frac{1}{2}\left(W_{UR} + \frac{W_S a_S}{L} \right) - \frac{V^2}{Rg}\left[W_S \frac{a_S}{L}\frac{h_{RCR}}{T} + W_S \frac{H}{T}\frac{K_{\Phi R}}{K_{\Phi F} + K_{\Phi R} - W_S H} + W_{UR}\frac{h_{UR}}{T} \right] \quad \text{(B.10)}$$

$$N_{oR} = \frac{1}{2}\left(W_{UR} + \frac{W_S a_S}{L} \right) + \frac{V^2}{Rg}\left[W_S \frac{a_S}{L}\frac{h_{RCR}}{T} + W_S \frac{H}{T}\frac{K_{FR}}{K_{FF} + K_{FR} - W_S H} + W_{UR}\frac{h_{UR}}{T} \right] \quad \text{(B.11)}$$

Nomenclature:

F_{iF}, F_{0F} = Lateral Forces Front (inside and outside), N
N_{iF}, N_{0F} = Vertical Forces Front (inside and outside), N
$K_{\Phi F}, K_{\Phi R}$ = Roll Stiffness (Front and Rear), Nm / deg
$M_{\Phi F}, M_{\Phi R}$ = Roll Moment (Front and Rear), Nm

W_S = Sprung Weight, N
$W_{UF,} W_{UR}$ = Front and Rear Un - Sprung Weight, N

L = Wheelbase, m
T = Trackwidth, m
a_S = Distance of Front axle from CG, m
b_S = Distance of Rear axle from CG, m
h_{UF}, h_{UR} = Height of Front and Rear Un - Sprung Mass CG, m
h_{RCF}, h_{RCR} = Height of Front and Rear Roll Center, m
h_{SCG} = Height of Sprung Mass CG, m
H = Height of Sprung Mass CG above Roll Axis, m

Understeer Gradient (Kus)

$$K_{US} = K_{Tires} + K_{LLT} + K_{RollCamber} + K_{RollSteer} + K_{LFCS} + K_{ATCSF} + K_{ATLPT} \quad \text{(B.12)}$$

$$K_{Tires} = \frac{W_F}{C_{Eff,aF}} - \frac{W_R}{C_{Eff,aR}} \quad \text{(B.13)}$$

K_{US} = *Total Understeer Gradient, Deg/g*
$C_{Eff,aF}$ =*Front Effective Cornering Stiffness, N/deg*
$C_{Eff,aR}$ =*Rear Effective Cornering Stiffness, N/deg*

K_{Tires} = *Understeer Gradient due to Tires (Static Cornering Stiffness), Deg/g*
K_{LLT} = *Understeer Gradient due to Weight Transfer, Deg/g*
$K_{RollCamber}$ = *Understeer Gradient due to Suspension Roll Camber, Deg/g*
$K_{RollSteer}$ = *Understeer Gradient due to Suspension Roll Steer, Deg/g*
K_{LFCS} = *Understeer Gradient due to Lateral Force Compliance Steer, Deg/g*
K_{ATCSF} = *Understeer Gradient due to Aligning Torque Compliance Steer, Deg/g*
K_{ATLPT} = *Understeer Gradient due to Pneumatic Trail, Deg/g*

$$K_{Tires} = \frac{W_F}{C_{aF}} - \frac{W_R}{C_{aR}} \quad \text{(B.14)}$$

W_F =*Weight on Front Axle, Per Wheel, N*
W_R =*Weight on Front Axle, Per Wheel, N*
C_{aF} = *Per Tire Cornering Stiffness at Front Axle, N/deg*
C_{aR} = *Per Tire Cornering Stiffness at Rear Axle, N/deg*

$$K_{LLT} = \frac{W_F}{C_{aF}}\left(\frac{C_2 . \Delta F_{ZF}^2}{C_{aF}}\right) - \frac{W_R}{C_{aR}}\left(\frac{C_2 . \Delta F_{ZR}^2}{C_{aR}}\right) \quad \text{(B.15)}$$

C_2 = *Cornering Stiffness vs. Normal Load Coefficient*
ΔF_{ZF} = *Weight Transfer, N*

$$K_{RollCamber} = -\left(\left(\frac{C_{gF} . K_{gF}}{C_{aF}} \right) - \left(\frac{C_{gR} . K_{gR}}{C_{aR}} \right) \right) . K_f \quad \text{(B.16)}$$

K_f = *Roll Gain, deg/g*

C_{gF} = *Per Tire Camber Stiffness at Front Axle, N/deg*

C_{gR} = *Per Tire Camber Stiffness at Front Axle, N/deg*

K_{gF} = *Roll Camber at Front Axle, deg/deg*

K_{gR} = *Roll Camber at Rear Axle, deg/deg*

$$K_{RollSteer} = \left(e_F - e_R \right) . K_f \quad \text{(B.17)}$$

e_F = *Roll Steer at Front Axle, deg/deg*

e_R = *Roll Steer at Rear Axle, deg/deg*

$$K_{LFCS} = 2.(W_R . A_R - W_F . A_F) \quad \text{(B.18)}$$

A_F = *Lateral Force Compliance Steer at Front Axle, deg/N*

A_R = *Lateral Force Compliance Steer at Rear Axle, deg/N*

$$K_{ATCSF} = 2.W_F . K_{SCF} . (L_{PT} + L_{MT}) - 2.W_R . K_{SCR} . (L_{PT}) \quad \text{(B.19)}$$

K_{SCF} = *Aligning Torque Compliance Steer at Front Axle, deg/Nm*

K_{SCR} = *Aligning Torque Compliance Steer at Rear Axle, deg/Nm*

L_{PT} = *Pneumatic Trail, m*

L_{MT} = *Mechanical Trail, m*

$$K_{ATLPT} = \left(\frac{W . L_{PT}}{2.L} \right) . \left(\frac{C_{aF} + C_{aR}}{C_{aF} . C_{aR}} \right) \quad \text{(B.20)}$$

L = *Wheelbase, m*

Yaw Rate Gain (YRG)

$$YRG=\left(\frac{V/L}{1+K_{us}.\left(\frac{(180/\pi)}{L.g}\right)}\right) \tag{B.21}$$

YRG = YawRateGain, 1/sec
K_{us} = Overall Understeer Gradient, Deg/G
V = Vehicle Speed, m/sec
L = Wheelbase, m
g = Acceleration due to gravity, G

Side-Slip Gradient (SS-GR)

$$SS\text{-}GR=\left(\frac{1-\frac{m}{2L}\frac{a}{bC_{Eff,\,aR}}V^2}{1-\frac{m}{2L^2}\frac{aC_{Eff,\,aF}-bC_{Eff,\,aR}}{C_{Eff,\,aF}C_{Eff,\,aR}}V^2}\right)\frac{b}{L} \tag{B.22}$$

$SS\text{-}GR$=Side-Slip Gradient wrt Road Wheel Angle, Rad/Rad
$C_{Eff,\,aF}$=Front Effective Cornering Stiffness, N/rad
$C_{Eff,\,aR}$=Rear Effective Cornering Stiffness, N/rad

Roll Gain (RG)

$$RG=\left(\frac{W_S.H}{K_{\Phi F}+K_{\Phi R}-W_S.H}\right) \tag{B.23}$$

RG = Roll Gain, Deg/G
$K_{\Phi F}$=Front Roll Stiffness, Nm/Deg
$K_{\Phi R}$=Rear Roll Stiffness, Nm/Deg

Transient Vehicle Handling Model

The three degree-of-freedom vehicle handling model described in the previous section is used for analyzing transient handling scenarios. Detailed derivations and discussions of the model are given in [82]. Equations B.24, B.25 and B.26 show the lateral force, yaw moment and roll moment equilibrium equations during a transient cornering scenario.

Linearized Equations of Motion:

Lateral Force Equation:

$$m*V_x*\dot{\beta} - m_s*H*\ddot{\varphi} + m*V_x*r = F_{YF} + F_{YR} \tag{B.24}$$

Yaw Moment Equation:

$$I_z*\dot{r} + I_{xz}*\ddot{\varphi} = a*F_{YF} - b*F_{YR} \tag{B.25}$$

Roll Moment Equation:

$$(I_x + m_s*H^2)*\ddot{\varphi} + I_{xz}*\dot{r} + k_\varphi*\varphi + b_\varphi*\dot{\varphi} = m_s*H*V_x*\dot{\beta} + m_s*g*H*\varphi + m_s*H*V_x*r \tag{B.26}$$

Nomenclature:

I_Z = *Yaw Moment of Inertia of Total Vehicle, Kgm*^{2}

I_{ZS} = *Yaw Moment of Inertia of Sprung Mass,Kgm*^{2}

I_X = *Roll Moment of Inertia of Total Vehicle, Kgm*^{2}

I_{XZ} = *Yaw-Roll Product of Inertia, Kgm*^{2}

I_Y = *Pitch Moment of Inertia of Total Vehicle, Kgm*^{2}

V_X = *Longitudinal Velocity, m/s*

V_Y = *Lateral Velocity, m/s*

β = *Side-Slip Angle, deg*

φ = *Roll Angle, deg*

r =*Yaw Rate, deg/sec*

m_S = *Sprung Mass, Kg*

$m_{UF,}$ m_{UR} = *Front and Rear Un-Sprung Mass, Kg*

H = *Height of Sprung Mass CG above Roll Axis, m*

k_Φ = *Total Roll Stiffness, Nm/deg*

$k_{\Phi F}$,$k_{\Phi R}$ = *Roll Stiffness (Front and Rear), Nm/deg*

b_Φ = *Total Roll Damping, Nm-sec/deg*

$b_{\Phi F}$,$b_{\Phi R}$ = *Roll Stiffness (Front and Rear), Nm-sec/deg*

Steering System Model

Figure 62 shows the steering system model used in this research. In this model [83, 84, 85], a rotating body equivalent to steering wheel is connected to another rotating body equivalent to the front wheels. The moment of inertia of the steering wheel and the front wheel (assembly) are represented by I_H and I_S respectively. The two bodies are connected via a rotating steering shaft equivalent to the steering wheel shaft and gearbox with spring constant K_S. The damping friction at the steering wheel shaft and kingpin is represented by damping coefficient C_H and C_S respectively. The rotational angle of the steering wheel converted around the kingpin (represented by α) and actual front wheel steer angle (represented by δ), form the 2 DOF of the torsional vibrational steering system model. Note that I_S and C_S, are representative of both front (left and right) wheels. T_H represents the hand wheel torque and T_S represents the moment around the kingpin.

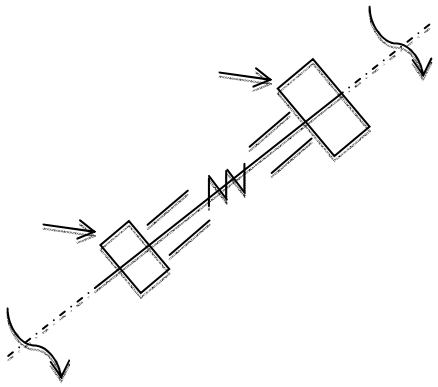

Figure 62. Free Body Diagram of the Steering Model used for predicting Steering Torque Feedback [adapted from Abe [83]].

$$I_H\left(\frac{d^2\alpha}{dt^2}\right)+C_H\left(\frac{d\alpha}{dt}\right)+K_S\left(\alpha-\delta\right)=T_H \tag{B.27}$$

$$I_S\left(\frac{d^2\delta}{dt^2}\right)+C_S\left(\frac{d\delta}{dt}\right)+K_S\left(\delta-\alpha\right)=M_K \tag{B.28}$$

$$M_K = -(F_{ZFL}+F_{ZFR})d\sin(\phi_K)\sin(\delta) + (F_{ZFL}-F_{ZFR})d\sin(\phi_C)\cos(\delta) + \ldots$$
$$\ldots (F_{YFL}+F_{YRL})r(\tan(\phi_C)) + (F_{XFL}-F_{XFR})d + (M_{ZFL}+M_{ZFR})\cos\left(\sqrt{(\phi_K{}^2+\phi_C{}^2)}\right) \tag{B.29}$$

$$T_H=K_S\left(\alpha-\delta\right) \tag{B.30}$$

Nomenclature:

T_H = *Steering Wheel Torque*
M_K = *Aligning Moment at SteerAxis*

K_S = *Steering Stiffness Stiffness*
θ_{SW} = α = *Steering Wheel Angle*
δ = *Road Wheel Angle*

F_{ZFL}, F_{ZFR} = *Front Tire Vertical Force Left and Right*
F_{YFL}, F_{YFR} = *Front Tire Lateral Force Left and Right*
F_{XFL}, F_{XFR} = *Front Tire Longitudinal Force Left and Right*
M_{ZFL}, M_{ZFR} = *Front Tire Aligning Moment Left and Right*
M_{KL}, M_{KR} = *Moment about Kingpin Axis Left and Right*

L_{PT} = *Pneumatic Trail*
L_{MT} = *Mechanical Trail*
ϕ_C = *Caster Angle*
ϕ_K = *Kingpin Inclination*
d = *Scrub Radius*
K_{ST} = *Steering Ratio*
I_s = *Steering Wheel Moment of Inertia*

Tire Model

The tire force model used in this research is based on Pacejka's Magic Formulae [43] and includes a simple transient tire side force model extension based on a first-order lag using the tire's relaxation length as the time constant. Equation B.31 shows the Pacejka Magic Formula expressing the relationship between the lateral force, slip angle and normal load on the tire and Equations B.32 and B.33 show the influence of tire relaxation length in the tire model. Figure 63 and Figure 64 show the lateral force (against slip angle at different normal loads) and cornering stiffness (against normal load) curves generated using the Pacejka Magic Formula for P 205/50 R 15 tire at 2.1 bars.

$$F_Y = D * \sin\left(C * \operatorname{atan}\left(B * phi \right) \right) + SV \tag{B.31}$$

$phi = (1 - E) * (delta + SH) + E / B. * \operatorname{atan} (B. * (delta + SH))$

$D = Peak\ Factor = (a1 * Z + a2) * Z$

$BCD = Cornering\ Stiffness = (a3 * \sin (2 * \operatorname{arctg} (Z / a4))) * (1 - a5 * |gamma|)$

$B = Stiffness\ Factor = BCD / (C * D)$

$C = Shape\ Factor = a0$

$E = Curvature\ Factor = a6 * Z + a7$

$SH = Horizontal\ Shift = a8 * gamma + a9 * Z + a10$

$SV = Vertical\ Shift = (a112 * Z + a111) * Z * gamma + a12 * Z + a13,$

F_Y = Lateral Force, Z = Normal Load, Delta = Slip Angle, Gamma = Camber Angle

a0…a13 are parameters that characterize the influence of normal load and slip angle on generation of Lateral Forces.

Equations B. 32 and B. 33 describe the influence of relaxation lengths as first order time lag on the lateral force generated by the tire.

Transient Tire Model – Relaxation Length Effect

$$\dot{F}_{YF} = \left(\left(-1/R_v\right) F_{YF}\right) + \left(\left(C_{aF}/R_v\right)*\delta_F\right) - \left(\left(C_{aF}/R_v\right)*\left(V_y/V_x\right)\right) - \left(\left(C_{aF}/R_v\right)*\left(r*a/V_x\right)\right) \tag{B.32}$$

$$\dot{F}_{YR} = \left(-1/R_v\right) F_{YR} + \left(C_{aR}/R_v\right)*\left(b*r/V_x\right) - \left(C_{aR}/R_v\right)*\left(V_y/V\right) \tag{B.33}$$

$$R_v = RL/V_x, \quad RL = Relaxation\ Length \tag{B.34}$$

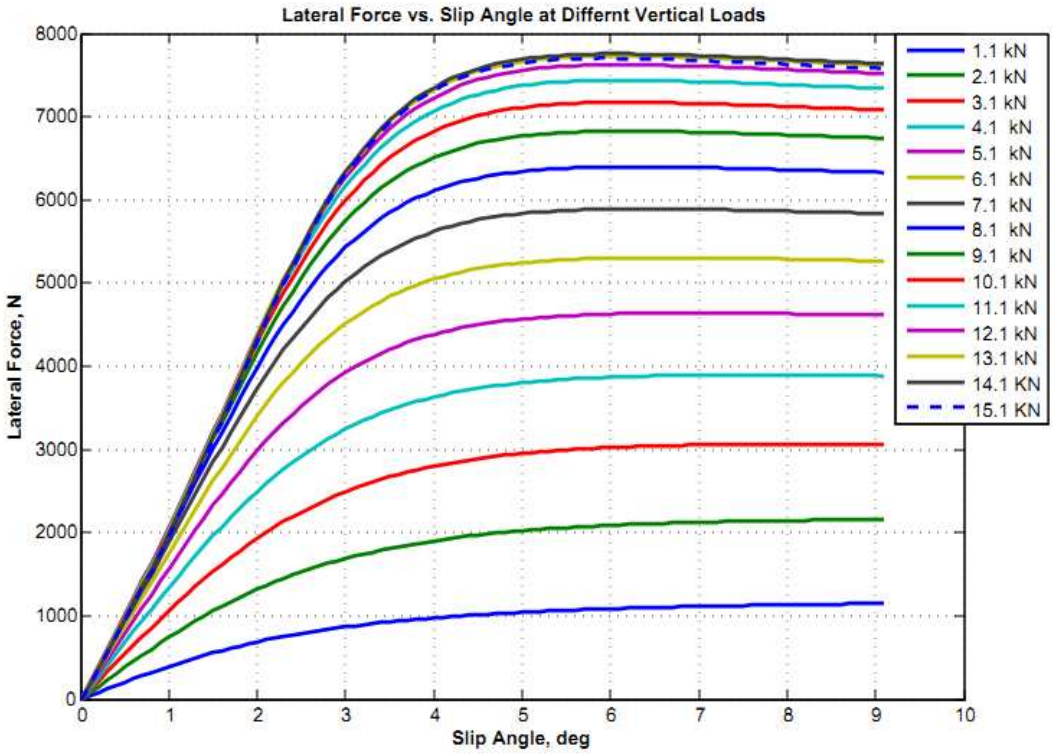

Figure 63. Lateral Force vs. Slip Angle at different Normal Load for 205/45 R17

P = 2.1 bar.

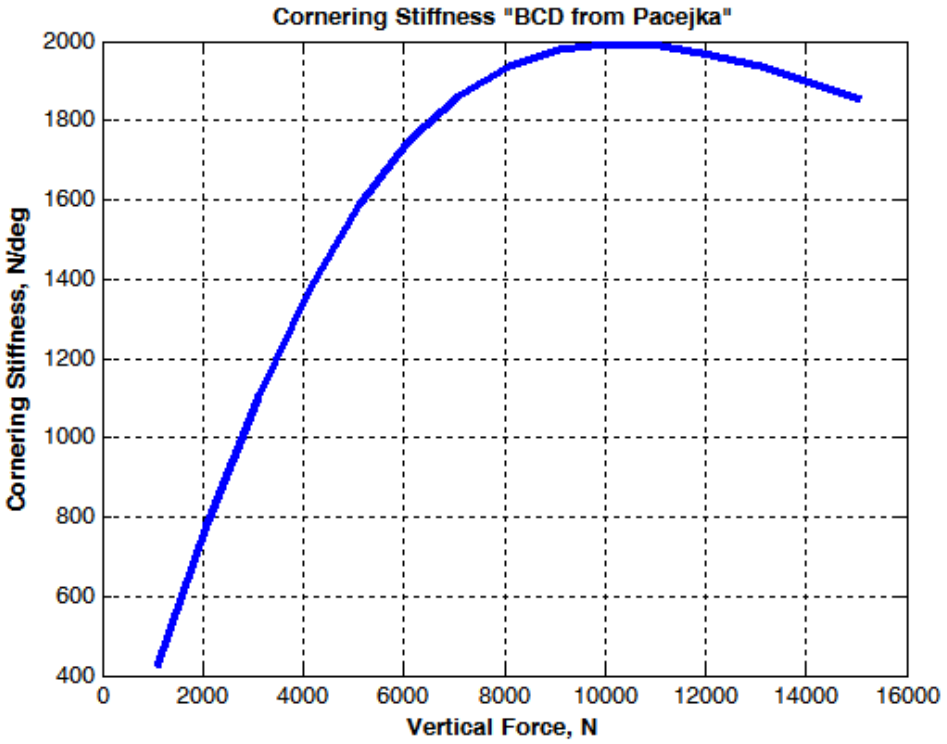

Figure 64. Cornering Stiffness vs. Normal Load for 205/45 R17 P = 2.1 bar.

In this thesis, the effect of traction/braking force on overall lateral force capability of the tire is simulated using the Equation B.35 from Pacejka [43]. The main effect of introduction of longitudinal force is the reduction of the maximum side force that can be generated from the tire. This phenomenon is often explained using the concept of traction ellipse [43] for a tire.

$$C_{F\alpha}\ (\mu, F_z, F_x) = \varphi_{xa}\ (C_{F\alpha}(F_z) - 0.5\,\mu\,F_z) + 0.5\,(\mu\,F_z - F_x)$$

$$\varphi_{xa} = \left\{1 - \left(\frac{F_x}{\mu F_z}\right)^n\right\}^{1/n} \quad ;\ n=2\text{-}8,\ \text{more or less curved}\ C_{F\alpha}\ \text{vs.}\ F_x\ \text{characterstics}\ ; \tag{B.35}$$

Equation B.35 describes the effect of longitudinal force (FX) on the cornering stiffness of tire and assumes that the friction coefficient (μ) is the same for longitudinal and lateral direction. The parameter 'n' in Equation B.35, describes the interaction of longitudinal and lateral forces for different tires. Figure 65 and Figure 66 depict the influence of the parameter 'n' on lateral cornering stiffness of a representative tire.

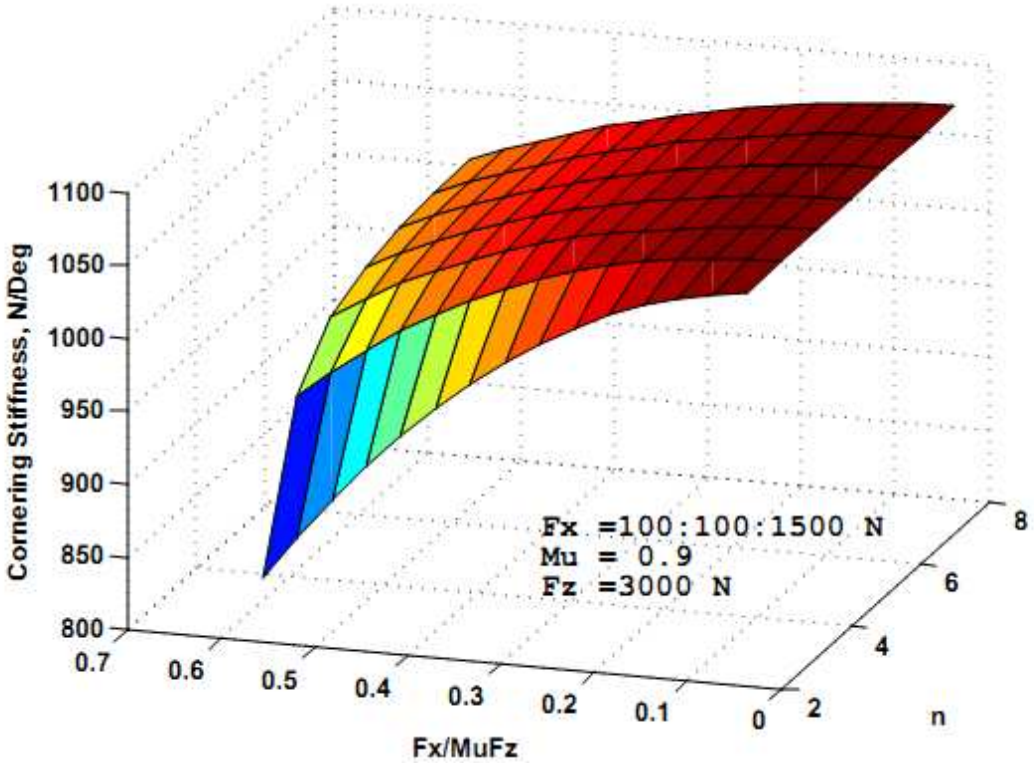

Figure 65. Effect of Tractive Forces on Cornering Stiffness.

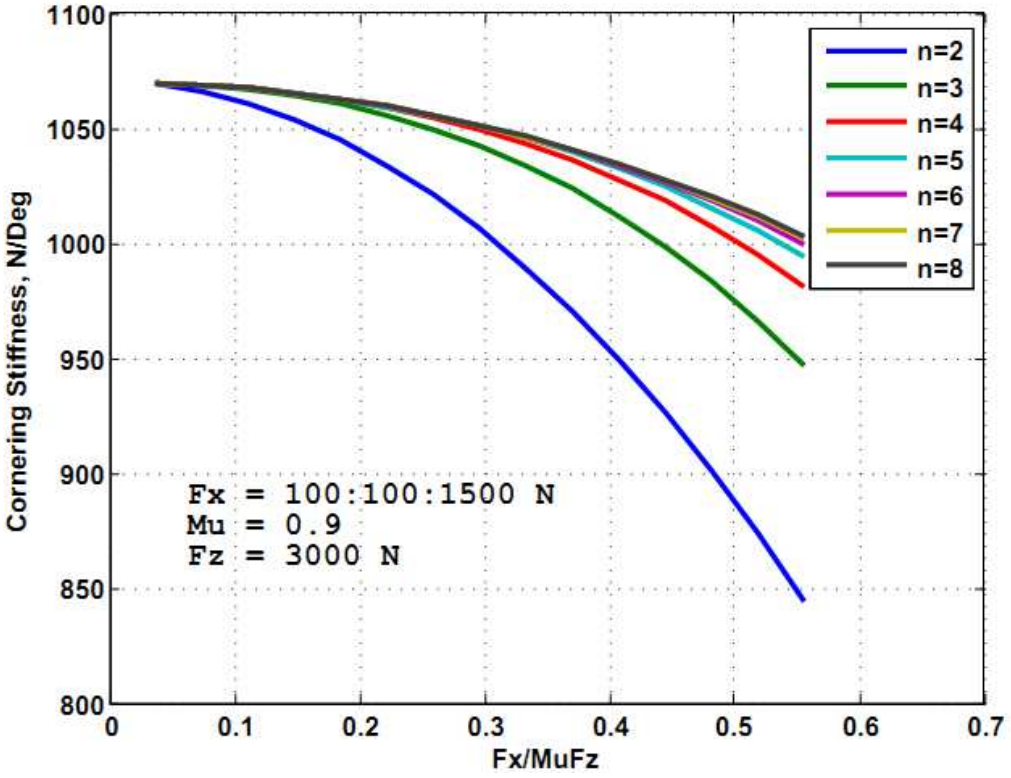

Figure 66. Effect of Tractive Forces on Cornering Stiffness.

Suspension Model

In this research, a quasi-static model of an independent suspension system, described by Kanspsky [44], is used for the elasto-kinematic analysis. The independent five links suspension system shown in Figure 67, consists of the following elements: rigid wheel carrier, suspension spring, tire spring, ideal kinematic joints, and compliant joints (bushings). The wheel carrier with six degrees of freedom (DOF) is supported with respect to the base on seven compliant links, i.e., the five suspension links (K_1–K_5), the main spring (K_S), and the tire (K_T).

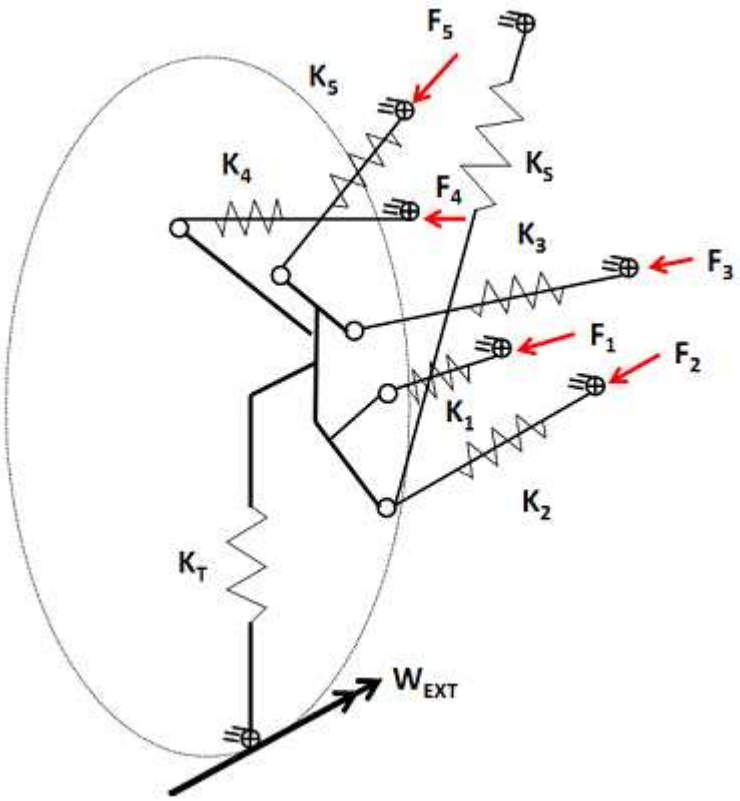

Figure 67. Free Body Diagram of a Five Link Independent Suspenion.

Each suspension link is modelled as a two force member with spherical connection joints at each end which constrain the motion of the wheel carrier relative to car body. The suspension links are represented by equivalent longitudinal stiffness resulting from radial stiffness of the elastomeric bushing in the suspension.

Below are some of the assumptions relevant to this model,

- The motion of the suspension links is assumed to be quasi-planar.
- The suspension motion is represented by small displacements of the suspension links.
- The suspension links are in tension or compression state only i.e., the model cannot represent suspension types where the links are loaded in bending/shear/torsion.
- No interaction between left and right side of the car axle.

If an arbitrary force system is applied to the wheel carrier, it must be in equilibrium with the link's tensile forces. The distribution of forces within the links depends on the orientation of the links in space and thus can be represented using Plucker coordinates. Figure 68 shows the plucker coordinate representation of a line in space.

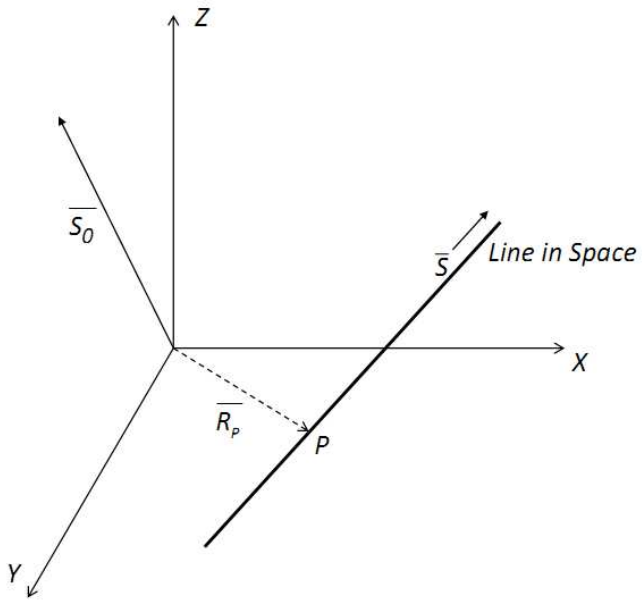

Plucker Line Coordinates: $\begin{pmatrix} \overline{S} \\ \overline{S_o} \end{pmatrix}$

$$\text{Unit Vector: } \overline{S} = \begin{pmatrix} l \\ m \\ n \end{pmatrix}$$

$$\overline{S_0} = \overline{Rp} \times \overline{S} = \begin{pmatrix} p \\ q \\ r \end{pmatrix}$$

Figure 68. Plucker Coordinates of a Line in Space.

$\overline{S}$ *represents the unit vector along the line in space represented by its directional cosines l, m, and n,*

$\overline{S_0}$ *represents the moment of the unit vector* $\overline{S}$ *about the origin,*

l, m, n, p, q, and r, represent the plucker co-ordinates of a line in space.

For an external force system (wrench) applied at the wheel center, following static equilibrium hold true:

$$W_i = F_i \begin{pmatrix} l_i \\ m_i \\ n_i \\ \hline p_i \\ q_i \\ r_i \end{pmatrix} \tag{B.36}$$

W_i represents the external forces and moments acting on the wheel carrier, F_i represents the linear (tensile/compressive) forces acting in the suspension links, and l_i, m_i, n_i, p_i, q_i, and r_i, represent the plucker coordinates of the links in space.

$$\begin{aligned} Wext &= \left(Px, Py, Pz, Mx, My, Mz\right)^T \\ F &= \left(F_1\ F_2\ F_3\ F_4\ F_5\ F_6\ F_7\right)^T \end{aligned} \tag{B.37}$$

$$\begin{bmatrix} l_1 \ldots l_7 \\ m_1 \ldots m_7 \\ n_1 \ldots n_7 \\ p_1 \ldots p_7 \\ q_1 \ldots q_7 \\ r_1 \ldots r_7 \end{bmatrix}_{6\times 7} \begin{bmatrix} F_1 \\ F_2 \\ F_3 \\ F_4 \\ F_5 \\ F_6 \\ F_7 \end{bmatrix}_{7\times 1} = - \begin{bmatrix} Px \\ Py \\ Pz \\ Mx \\ My \\ Mz \end{bmatrix}_{6\times 1} \tag{B.38}$$

Px, Py, Pz, Mx, My and Mz represents the external forces and moments in x, y and z directions. F_1, $F_2 \ldots F_5$ represents the forces in the five suspension links, F6 represents the force acting on the main suspension spring and F7 represents the force acting along the tire spring.

$$[F] = - [J]^{-1} [Wext]$$

$$J = \begin{bmatrix} l_1 \ldots. l_7 \\ m_1 \ldots. m_7 \\ n_1 \ldots. n_7 \\ p_1 \ldots. p_7 \\ q_1 \ldots. q_7 \\ r_1 \ldots. r_7 \end{bmatrix} = \textit{Suspension Jacobian Matrix} \tag{B.39}$$

Consider an arbitrary twist (*T*) is applied at the wheel carrier,

$T = [\varepsilon_x, \varepsilon_y, \varepsilon_z; \delta_{ox}, \delta_{oy}, \delta_{oz}]$

$\varepsilon_x, \varepsilon_y, \varepsilon_z$ = *Rotation*

$\delta_{ox}, \delta_{oy}, \delta_{oz}$ = *Translation*

To accommodate the twist (T) acting on the wheel carrier, the suspension links deflect in space, and this results in a small change in length of the suspension links, ΔL,

$$\begin{pmatrix} \Delta L_1 \\ \Delta L_2 \\ \Delta L_3 \\ \Delta L_4 \\ \Delta L_5 \\ \Delta L_6 \\ \Delta L_7 \end{pmatrix} = \begin{bmatrix} l_1 \; m_1 \; n_1 \; p_1 \; q_1 \; r_1 \\ \ldots\ldots \\ \ldots\ldots \\ \ldots\ldots \\ \ldots\ldots \\ \ldots\ldots \\ l_7 \; m_7 \; n_7 \; p_7 \; q_7 \; r_7 \end{bmatrix} \begin{pmatrix} \delta_{ox} \\ \delta_{oy} \\ \delta_{oz} \\ \varepsilon_x \\ \varepsilon_y \\ \varepsilon_z \end{pmatrix} \tag{B.40}$$

$$[\Delta L] = [J^T] \left[\frac{\overline{\delta o}}{\overline{\varepsilon}} \right] \tag{B.41}$$

Assuming linear stiffness of the suspension links, main suspension spring and tire spring,

$$F_i = K_i . \Delta l_i$$

$$K = \begin{bmatrix} K_1 & 0 & 0 & 0 & 0 & 0 \\ 0 & K_2 & 0 & 0 & 0 & 0 \\ 0 & 0 & K_3 & 0 & 0 & 0 \\ 0 & 0 & 0 & K_4 & 0 & 0 \\ 0 & 0 & 0 & 0 & K_5 & 0 \\ 0 & 0 & 0 & 0 & 0 & K_S \\ 0 & 0 & 0 & 0 & 0 & K_T \end{bmatrix} \quad \text{(B.42)}$$

K_1, K_2, K_3, K_4, K_5 represent the radial stiffness of the suspension links, K_S represents the main suspension spring stiffness and K_T represents the tire radial stiffness.

$$[\frac{\overline{\delta o}}{\varepsilon}] = [J^T]^{-1} [\Delta L] \quad \text{(B.43)}$$

$$[Wext] = - [J] [F] \quad \text{(B.44)}$$

$$\begin{aligned} [Wext] &= - [J] [K] [\Delta L] \\ &= - [J] [K] [J^T] [\frac{\overline{\delta o}}{\varepsilon}] \end{aligned} \quad \text{(B.45)}$$

$$[Kwheel] = [J] [K] [J^T] = Suspension\ Stiffness\ Matrix$$

$$[Wext] = - [Kwheel] [\frac{\overline{\delta o}}{\varepsilon}] \quad \text{(B.46)}$$

$$[\overline{\frac{\delta o}{\varepsilon}}] = -inv[Kwheel][Wext] \tag{B.47}$$

Equation B.47 represents the elasto-kinematic orientation of the wheel resulting from an external wrench (force-moment system) acting at the wheel center.

Appendix C.

Vehicle Model Validation

In this dissertation, a simplified lower-order vehicle dynamics model which captures the behavior of the real-world naturalistic driving up to 0.3 -0.4 g's of lateral acceleration is used for the simulations. The vehicle dynamics model was validated with data from real world physical testing of vehicles on proving grounds. Validation results for a 1991 Mazda Miata, 2010 Ford Focus and an aftermarket modified six-inch lifted 2010 F-150 are shown in this section. All the vehicles were tested for a step steer maneuver at around 80 km/h. The steering wheel angle input was adjusted for each vehicle to achieve around 0.4 g's of lateral acceleration (the linear range of vehicle handling).

Figure 69 shows the steering wheel angle and vehicle speed input used for Mazda Miata. Figure 70 and Figure 71 show the validation results in terms of yaw rate, lateral acceleration and roll angle for the Mazda Miata.

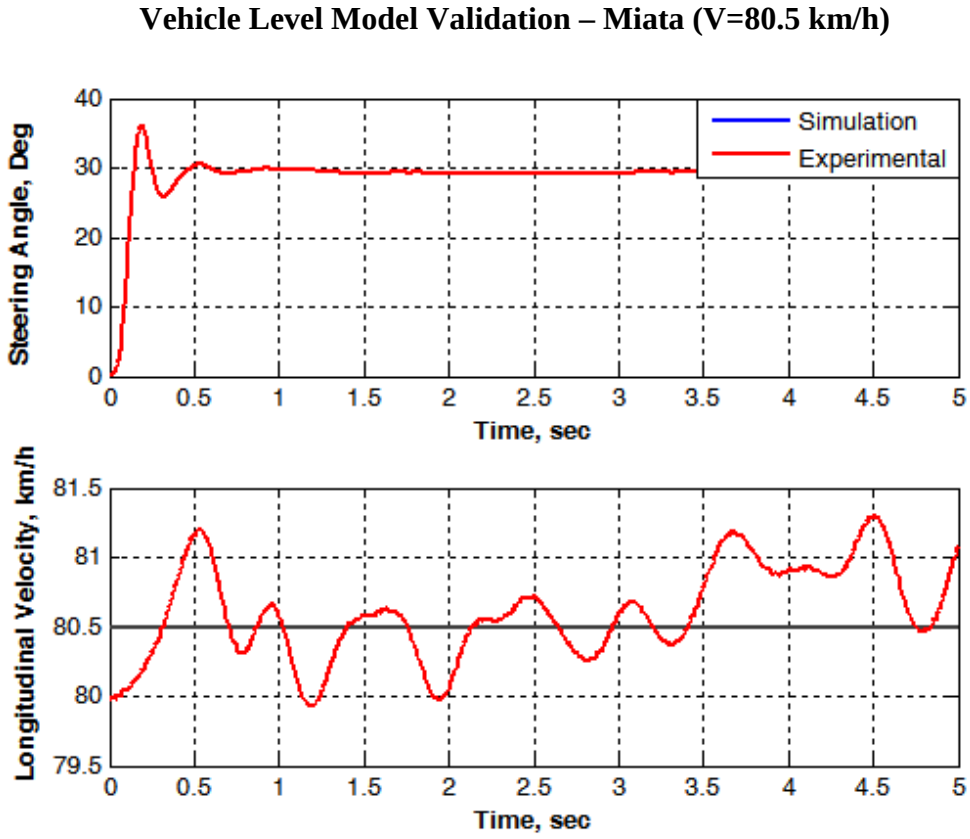

Figure 69. Steering Wheel Angle and Vehicle Speed Input for Model Validation.

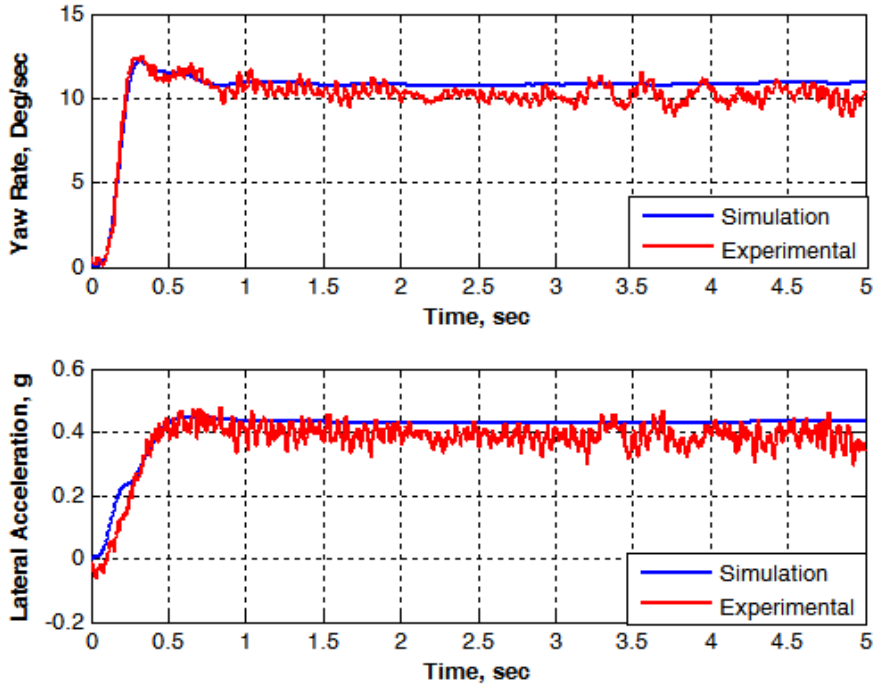

Figure 70. Steering Wheel Angle and Vehicle Speed Input for Model Validation.

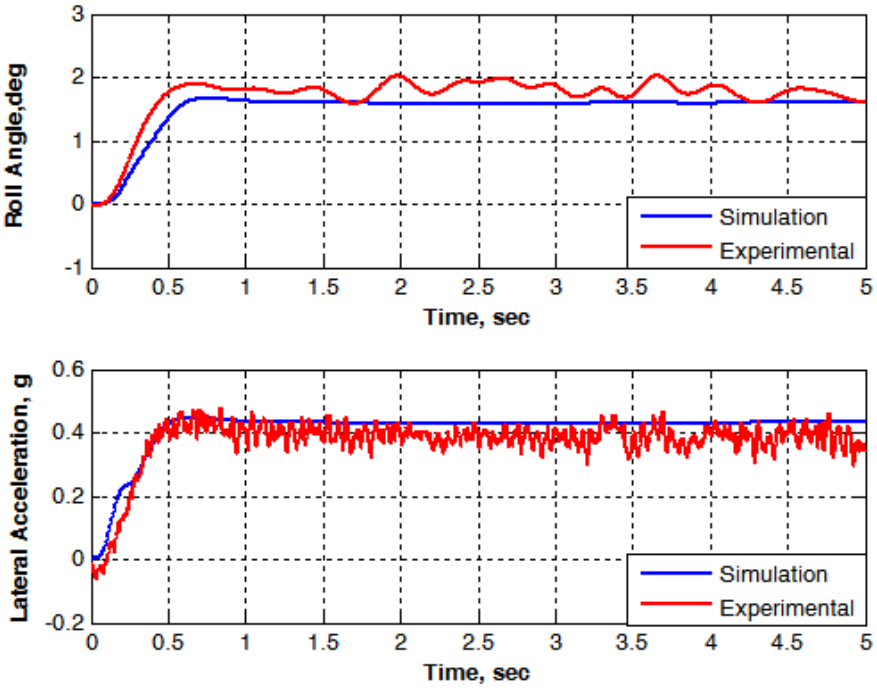

Figure 71. Comparison of Roll Angle and Lateral Acceleration for Model Validation.

Figure 72 shows the steering wheel angle and vehicle speed input used for Ford Focus. Figure 73 show the validation results in terms of yaw rate, and lateral acceleration for the Ford Focus.

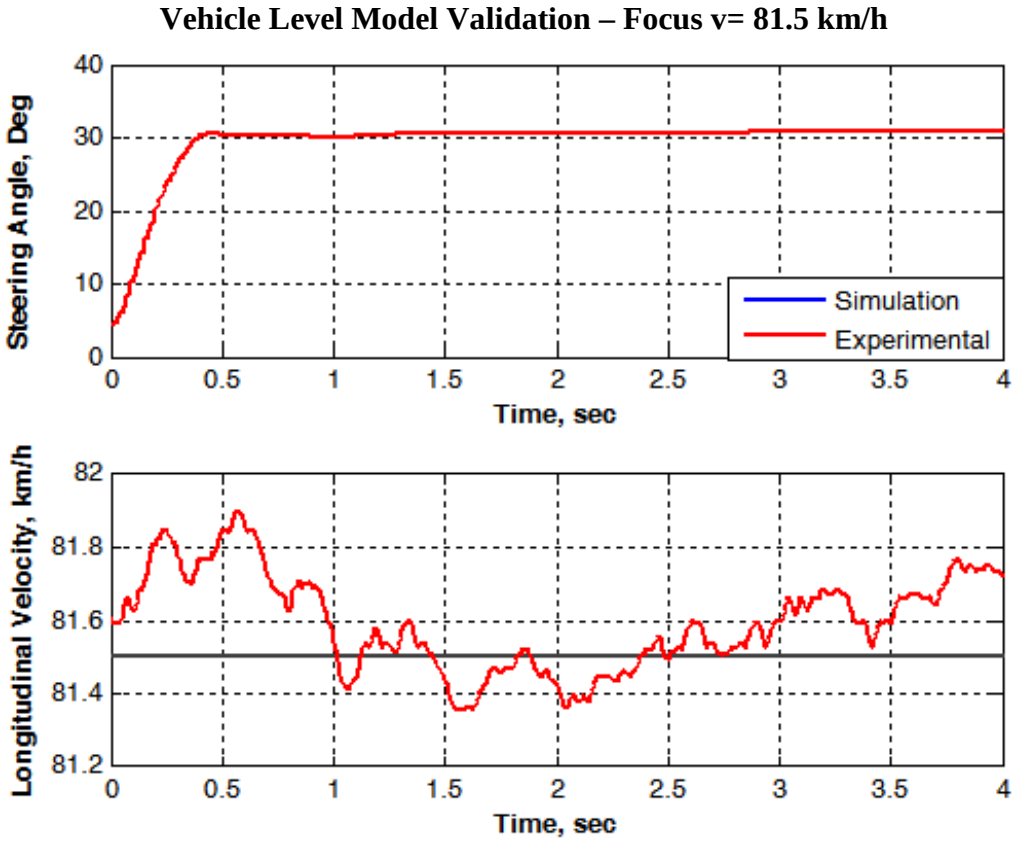

Figure 72. Steering Wheel Angle and Vehicle Speed Input for Model Validation.

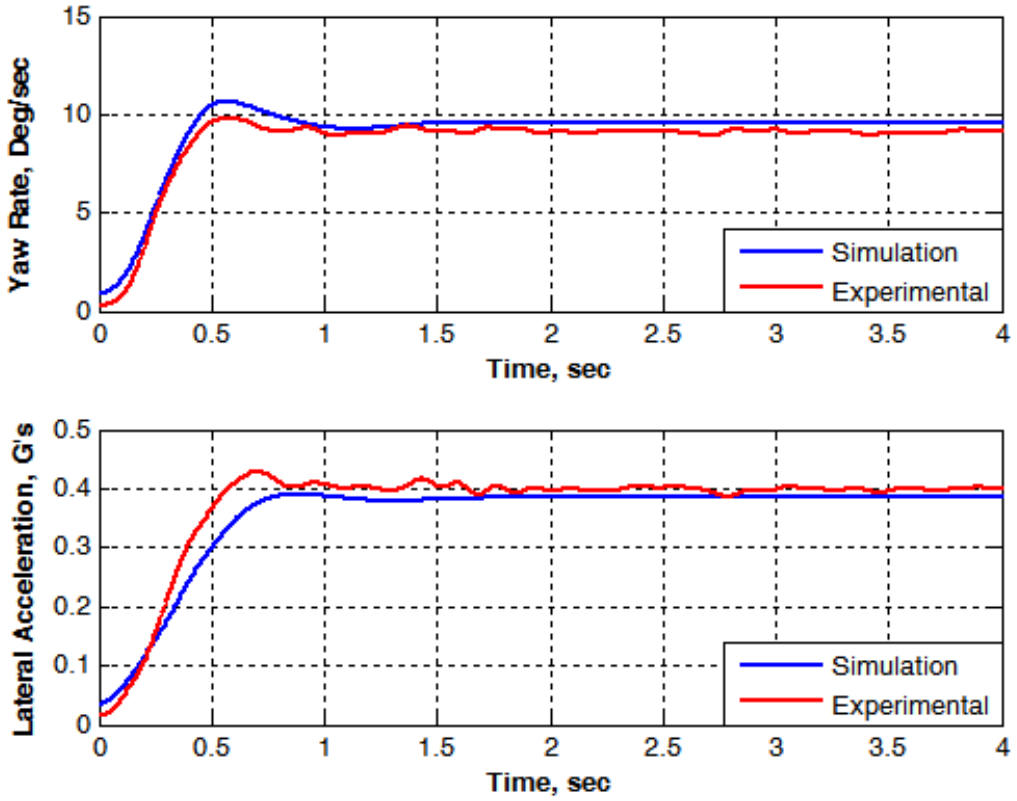

Figure 73. Comparison of Yaw Rate and Lateral Acceleration for Model Validation.

Figure 74 shows the steering wheel angle and vehicle speed input used for modified F-150. Figure 75 and Figure 76 show the validation results in terms of yaw rate, lateral acceleration and roll angle for the aftermarket modified F-150.

Vehicle Level Model Validation – Modified F-150 (v=84 km/h)

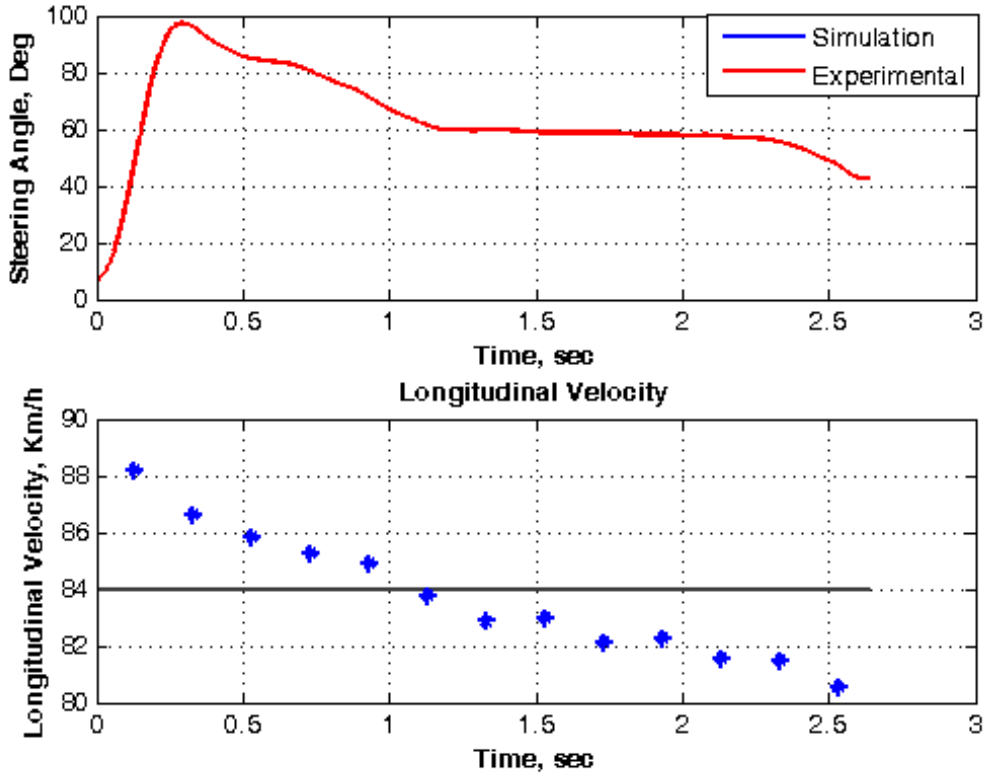

Figure 74. Steering Wheel Angle and Vehicle Speed Input for Model Validation.

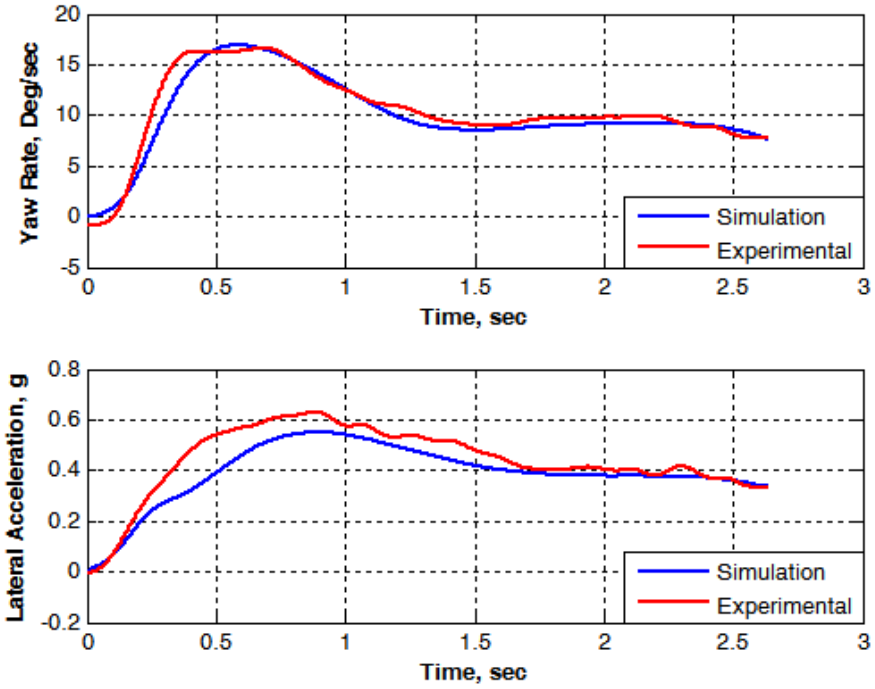

Figure 75. Comparison of Yaw Rate and Lateral Acceleration for Model Validation.

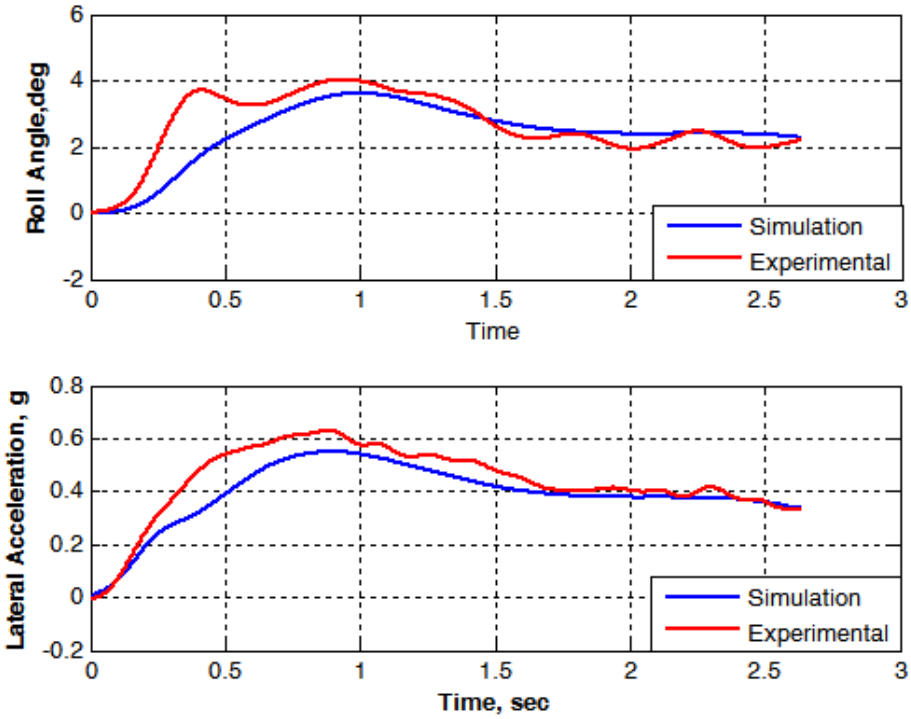

Figure 76. Comparison of Roll Angle and Lateral Acceleration for Model Validation.

REFERENCES

1. Venhovens, P.J., “Automotive Systems Overview,” AuE 881 Lecture Notes, Department of Automotive Engineering, Clemson University, USA, 2012.
2. Mau, R., “Hybrid Lower Order Modelling for Conceptual Vehicle Design,” Ph.D. Thesis, Department of Automotive Engineering, Clemson University, USA, 2013.
3. Crolla, D. A., “Vehicle dynamics-theory into practice,” Automobile Division Chairman’s Address, IMechE, 1995.
4. Kim, H.M., Rideout, D.G., Papalambros, P.Y., and Stein, J.L., "Analytical Target Cascading in Automotive Vehicle Design," *ASME Journal of Mechanical Design*, 125(3):474-480, 2003.
5. Li, Y., Lu, Z., and Michalek, J., “Diagonal Quadratic Approximation for Parallelization of Analytical Target Cascading,” *ASME Journal of Mechanical Design*, 130(5):051402, 2008.
6. Deb, K., “Multi-Objective Optimization Using Evolutionary Algorithms,” (John Wiley and Sons, New York, 2001).
7. Bergman, W., “Considerations in determining vehicle handling requirements,” SAE Technical Paper 690234, 1969.
8. Bergman, W., “Correlation between vehicle tests and subjective evaluation,” Ford Motor Company, State of the Art of Objective Procedures for Testing Vehicle Handling, 1978.
9. Weir, D., and DiMarco, R.J., “Correlation and evaluation of driver/vehicle handling data,” SAE Technical Paper 780010, 1978.

10. Mimuro et al, “Four Parameter Evaluation Method of Lateral Transient Response,” SAE Technical Paper 901734, 1990.
11. King, R. P., Crolla, D. A., Ash, H. A. S and Whitehead, J., “Identification of subjective-objective vehicle handling links using neural networks for the foresight vehicle,” SAE Technical Paper 2002-01-1126, 2002.
12. Xia, X., and Willis, J.N., “The effect of tire cornering stiffness on vehicle linear handling performance,” SAE Technical Paper 950313, 1995.
13. Chen, D., “Subjective and Objective Vehicle Handling Behavior,” Ph.D. Thesis, School of Mechanical Engineering, The University of Leeds, 1997
14. Lincke, W., Richter, B. and Schmidt, R., “Simulation and measurement of driver vehicle handling performance,” SAE Technical Paper 730489, 1973.
15. Good, M.C., “Sensitivity of Driver-Vehicle performance to vehicle characteristics revealed in open-loop tests,” *Vehicle System Dynamics: International Journal of Vehicle Mechanics and Mobility*, 6(4): 245-277, 1977.
16. McRuer, D., and Klein, R., “Effect of Automobile Steering Characteristics on Driver-Vehicle Performance for Regulation Tasks,” SAE Technical Paper 780778, 1978.
17. Venhovens, P.J., Hazare, M.A., “Setting Vehicle Handling Engineering Targets based on Driver’s Preferences, Abilities and Limitations,” Proceeding of the 11th International Symposium on Advanced Vehicle Control, AVEC 12, Seoul, South Korea, August 2012.
18. Horiuchi, S. and Yuhara, N., “An Analytical Approach to the Prediction of Handling Qualities of Vehicles With Advanced Steering Control System Using Multi-Input

Driver Model," *ASME Journal of Dynamic Systems, Measurement and Control*, 122(3):490-497, 2000.

19. Ishio, J., Ichikawa, H., Kano, Y., and Abe, M., "Vehicle-handling quality evaluation through model-based driver steering behavior," *Vehicle System Dynamics*, 46(1):549-560, 2008.
20. Haghiac, H., Haque, I. and Fadel, G. "An assessment of a genetic algorithm-based approach for optimizing multi-body systems with applications to vehicle handling performance," *Int. J. Vehicle Design*, 36(4): 320-344, 2004.
21. Scarlat, G., Haque, I., Fadel, G. and Schuller, J. "A modified Monte-Carlo approach to simulation-based vehicle design with multiple objectives and multiple scenarios," SAE Technical Paper 2002-01-1186, 2002.
22. Chakravartula S., Haque, I. and Fadel, G., "A modified Monte-Carlo simulation approach to heavy vehicle design for good dynamic performance in multiple scenario," Heavy Vehicle Systems, *A Special Issue of the Int. J. of Vehicle Design*, 10(1.2): 112-143, 2005.
23. Chandramoulli, T., "Application of simulated annealing for optimization of the lateral dynamics behavior of an automobile," M.S. Thesis, Department of Mechanical Engineering, Clemson University, 2002.
24. Miano, C., Gobbi. M., and Mastinu, G., "Multi-Objective Optimization of the Handling Performances of a Road Vehicle: A Fundamental Study on Tire Selection," *ASME Journal of Mechanical Design*, 126(4): 687, 2004.

25. Schuller, J., Haque, I., and Eckel, M., “An Approach for Optimization of Vehicle Handling Behavior in Simulation,” *Journal of Dynamics of Vehicles on Roads and Tracks, Vehicle Systems Dynamics,* Supplement 37:24-37, 2002.
26. Mastinu, G., Gobbi, M., and Miano, M. “Optimal Design of Complex Mechanical Systems- With Applications to Vehicle Engineering,” (Springer Science & Business Media, 2006).
27. Benedetti, A., Farina, M., Gobbi, M., “Evolutionary multi-objective industrial design: the case of a racing car tire-suspension system, *IEEE Transactions on Evolutionary Computations*, 10(3):230-244, 2006.
28. Gobbi, M., Mastinu, G. and Doniselli, C., “Optimizing a car chassis,” *Vehicle System Dynamics*, 32(2–3), 149–170, 1999.
29. Gobbi, M. and Mastinu, G., “Global Approximation – Performance Comparison of Different Methods with an Application to Road Vehicle Engineering,” *Proceedings of IMECE, Innovations in Vehicle Design and Development*, 101:15-24. 1999.
30. Guarneri, P., Rocca, G., Gobbi, M., “A neural-network-based model for the dynamic simulation of the tire/suspension system while traversing road irregularities,” *IEEE Transactions of Neural Networks*, 19(9):1549, 2008.
31. Choi, L. B., et al., “The Optimization of Automotive Suspension System Considering Multidisciplinary Design Requirements,” SAE Technical Paper 2009-01-1239, 2009.
32. MSC. ADAMS view, MSC Corporation, 2005.
33. PIAnO User's Manual, FRAMAX INC., 2008.

34. Li, L., et al., “Optimization of Suspension Elastomeric Bushing Compliance under Constraints of Handling, Ride and Durability,” SAE Technical Paper 2010-01-0721, 2010.

35. Li, M., et al., “Parameters Sensitivity Analysis and Optimization for the Performance of Vehicle Handling,” SAE Technical Paper 2007-01-3573, 2007.

36. Mehdi, S.M., et al., “Optimization of Vehicle Steering Linkage With Respect to Handling Criteria Using Genetic Algorithm Methods,” SAE Technical Paper 2005-01-3499, 2005.

37. Fujita, k., et al., “Design optimization of multi-link suspension system for total vehicle handling and stability,” *The American Institute of Aeronautics and Astronautics*, AIAA-98-4787, 1998.

38. Guarneri, P., Gobbi, M., and Papalambros, P.Y., “Efficient multi-level design optimization using analytical target cascading and sequential quadratic programming,” *Journal: Structural and Multidisciplinary Optimization*, 44(3), 351-362, 2011.

39. Fadel, G.M., Haque, I., Blouin, V.Y., and Wiecek, M.M., “Multi-criteria Multi-scenario Approaches in the Design of Vehicles,” Proceedings of 6th World Congresses of Structural and Multidisciplinary Optimization, Rio de Janeiro, Brazil, 2005.

40. Gobbi, M., Haque, I., Papalambros, P. Y. and Mastinu, G., “Optimization and integration of ground vehicle systems,” *Vehicle System Dynamics*, 43(6):437-453, 2005.

41. Austin, T.E., “Why Have a Systems Engineering (SE) Capability for Automotive Product Development? - Questions and Answers,” SAE Technical Paper 2007-01-0782, 2007.
42. AutoPacific New Vehicle Satisfaction Survey, 2013.
43. Pacejka, H., “Tire and Vehicle Dynamics Second Edition,” (SAE International Warrendale, 2005).
44. Knapczyk, J., and Dzierz□ek, S., "Displacement and force analysis of five-rod suspension with flexible joints,” *ASME J. Mech. Des.*, 117(4):532–538, 1995.
45. MATLAB, Global Optimization Toolbox, Genetic Algorithm, Release 2014a, The MathWorks, Inc., Natick, Massachusetts, United States.
46. Tosserams, S., Etman, L. F. P., and Rooda, J. E., “An Augmented Lagrangian Relaxation for Analytical Target Cascading Using the Alternating Directions Method of Multipliers,” *Struct. Multidiscip. Optim.*, 31(3):176–189, 2006.
47. International Standards Organization, “Passenger cars — Steady-state circular driving behavior -Open-loop test methods,” ISO 4138, 2004.
48. International Standards Organization, “Road vehicles - Vehicle dynamics test methods,” ISO 15037-1, 2006.
49. Law, E.H., “Ground Vehicle Dynamics,” ME 653, Lecture Notes, Department of Mechanical Engineering, Clemson University, USA, 2010.
50. International Standards Organization “Road vehicles -Lateral transient response test methods - Open-loop test methods,” ISO 7401, 2011.

51. International Standards Organization “Road vehicles -- Masses -- Vocabulary and codes,” ISO 1176, 1990.
52. International Standards Organization “Passenger cars -- Mass distribution,” ISO 2958, 1973.
53. Norman, K. D, “Objective Evaluation of On-center Handling Performance,” SAE Technical Paper 840069, 1984.
54. Mitschke M., Wallentowitz H., "Vehicle Dynamics Fourth Edition,” (Springer, New York, 2004).
55. Jaksch F., O., "Driver-Vehicle Interaction with Respect Steering Controllabity,” SAE Technical Paper 790740, 1979.
56. Bartenheier T., "Potential of a driver and driving condition dependent steering wheel torque characteristics,” *VDI Fortschritt-Berichte*, 12(854), VDI-Verlag, Dusseldorf, 2004.
57. Pfeffer, P.E., Harrer, M., “On-Centre Steering Wheel Torque Characteristics during Steady State Cornering,” SAE Technical Paper 2008-01-0502, 2008.
58. International Standards Organization, “Road vehicles — Test method for the quantification of on-center handling Part 1: Weave test,” ISO 13674-1, 2010.
59. International Standards Organization, “Road vehicles — Test method for the quantification of on-center handling Part 2: Transition test,” ISO 13674-2, 2006.
60. Farrer, D. G., “An Objective Measurement Technique for the Quantification of On-center Handling Quality,” SAE Technical Paper 930827, 1993.

61. Salaani, M. K., Heydinger, G. J., and Grygier, P. A., "Experimental Steering Feel Performance Measures," SAE Technical Paper 2004-01-1074, 2004.

62. Dettki, F., "A Test Method for the Quantification of On-center Handling with Respect to Cross-Wind," *Journal of Automobile Engineering, Proceedings of the Institution of Mechanical Engineers*, 216(4):259-266, 2002.

63. US DOT NHTSA, "TP-126-02 Laboratory Test Procedure for Federal Motor Vehicle Safety Standard 126, Electronic Stability Control Systems," FMVSS 126, Nov. 2008.

64. Federal Register, Vol. 72, No. 66, April 6, 2007, pp. 17310-17315, Part 571.126.

65. Mike Sayers and Phil Mather, "FMVSS 126 Electronic Stability Test and CarSim: Technical Memo," Mechanical Simulation Corporation, www.carsim.com, 2011.

66. U.S. Department of Transportation National Highway Traffic Safety Administration, 49 CFR Part 575; Docket No. NHTSA-2001- 9663; Notice 3; RIN 2127-AI81; Consumer Information; New Car Assessment Program; Rollover Resistance.

67. Milliken W. F., and Milliken D.L., "Race Car Vehicle Dynamics", (SAE International, Warrendale, 1995).

68. Wong, J.Y., "Theory of Ground Vehicles Third Edition," (John Wiley & Sons, New Jersey, 2001).

69. Sharp, R.S., and Granger, R., "On car steering torque at parking speeds," *Proceedings of the Institution of Mechanical Engineers, Part D: Journal of Automobile Engineering*, 217(2):87-96, 2003.

70. Dixon, J., C., "Tires, Suspension and Handling, Second Edition," (SAE International Warrendale, 1996).

71. Bergman, W., “Measurement and Subjective Evaluation of Vehicle handling,” SAE Technical Paper 730492, 1973.
72. International Standards Organization, “Passenger cars - Braking in a turn -Open-loop test method,” ISO 7975, 2006.
73. International Standards Organization, “Passenger cars — Power-off reaction of a vehicle in a turn - Open-loop test method,” ISO 9816, 2006.
74. International Standards Organization “Road vehicles — Passenger cars — Straight-ahead braking on surfaces with split coefficient of friction — Open-loop test method.” ISO 14512, 1999.
75. Jung-Hwan Lee, “Analysis of Tire Effect on the Simulation of Vehicle Straight Line Motion,” *Vehicle System Dynamics: International Journal of Vehicle Mechanics and Mobility*, 33(6): 373-390, 2000.
76. Oh, S., H., Cho, Y.H., and Gim, G., “Identification of A Vehicle Pull Mechanism,” SAE Technical Paper 2000-05-0253, 2000.
77. Pottinger, M.G., “Tire/Vehicle Pull: An Introduction Emphasizing Plysteer Effects,” Tire Science and Technology, TSTCA, 18(3):170-190, 1990.
78. Matyja, F.E., “Steering Pull and Residual Aligning Torque,” Tire Science and Technology, TSTCA, 15(3):207-240, 1987.
79. Rhyne, T., “Tire Mechanics,” AuE 829, Lecture Notes, Department of Automotive Engineering, Clemson University, USA, 2010.
80. International Standards Organization “Road vehicles — Sensitivity to lateral wind - Open-loop test method using wind generator input,” ISO 12021, 2010.

81. Bergman, W., “Bergman gives new meaning to under-steer and over-steer,” *SAE Journal*, 73(12):36 1965.

82. Gerdes, C.J., Gadda, D. C., and Laws, S.M., “Frequency Characteristics of Vehicle Handling: Modeling and Experimental Validation of Yaw, Sideslip, and Roll Modes to 8 Hz,” Proceeding of the 8th International Symposium on Advanced Vehicle Control, AVEC 06, Taipei, Taiwan, August 2006.

83. Abe, M., “Vehicle Handling Dynamics: Theory and Application,” (Elsevier, UK, 2009).

84. Chrstosa, J. P., & Heydinger G. J., “Inclusion of Steering System Freeplay in Open-Loop Vehicle Dynamic Simulations,” *Vehicle System Dynamics: International Journal of Vehicle Mechanics and Mobility*, 20 (Supplement 1):99-113, 1992.

85. Katzourakis, I. D., “Driver Steering Support Interfaces Near the Vehicle’s Handling Limits,” Ph.D. Thesis, Technical University of Delft, The Netherlands, 2012.